CANADIAN THESES ON MICROFICHE

THÈSES CANADIENNES SUR MICROFICHE

National Library of Canada
Collections Development Branch

Canadian Theses on
Microfiche Service

Ottawa, Canada
K1A 0N4

Bibliothèque nationale du Canada
Direction du développement des collections

Service des thèses canadiennes
sur microfiche

NOTICE

The quality of this microfiche is heavily dependent upon the quality of the original thesis submitted for microfilming. Every effort has been made to ensure the highest quality of reproduction possible.

If pages are missing, contact the university which granted the degree.

Some pages may have indistinct print especially if the original pages were typed with a poor typewriter ribbon or if the university sent us an inferior photocopy.

Previously copyrighted materials (journal articles, published tests, etc.) are not filmed.

Reproduction in full or in part of this film is governed by the Canadian Copyright Act, R.S.C. 1970, c. C-30. Please read the authorization forms which accompany this thesis.

AVIS

La qualité de cette microfiche dépend grandement de la qualité de la thèse soumise au microfilmage. Nous avons tout fait pour assurer une qualité supérieure de reproduction.

S'il manque des pages, veuillez communiquer avec l'université qui a conféré le grade.

La qualité d'impression de certaines pages peut laisser à désirer, surtout si les pages originales ont été dactylographiées à l'aide d'un ruban usé ou si l'université nous a fait parvenir une photocopie de qualité inférieure.

Les documents qui font déjà l'objet d'un droit d'auteur (articles de revue, examens publiés, etc.) ne sont pas microfilmés.

La reproduction, même partielle, de ce microfilm est soumise à la Loi canadienne sur le droit d'auteur, SRC 1970, c. C-30. Veuillez prendre connaissance des formules d'autorisation qui accompagnent cette thèse.

THIS DISSERTATION
HAS BEEN MICROFILMED
EXACTLY AS RECEIVED

LA THÈSE A ÉTÉ
MICROFILMÉE TELLE QUE
NOUS L'AVONS REÇUE

Canada

NL 339 (r. 85/09)

THE UNIVERSITY OF ALBERTA

ANALYSIS OF ATMOSPHERIC AEROSOL COMPOSITION

by-

FRED JAMES HOPPER

(C)

A THESIS

SUBMITTED TO THE FACULTY OF GRADUATE STUDIES AND RESEARCH

IN PARTIAL FULFILMENT OF THE REQUIREMENTS FOR THE DEGREE

OF DOCTOR OF PHILOSOPHY

IN

METEOROLOGY

DEPARTMENT OF GEOGRAPHY

EDMONTON, ALBERTA

FALL 1986

Permission has been granted to the National Library of Canada to microfilm this thesis and to lend or sell copies of the film.

The author (copyright owner) has reserved other publication rights, and neither the thesis nor extensive extracts from it may be printed or otherwise reproduced without his/her written permission.

L'autorisation a été accordée à la Bibliothèque nationale du Canada de microfilmer cette thèse et de prêter ou de vendre des exemplaires du film.

L'auteur (titulaire du droit d'auteur) se réserve les autres droits de publication; ni la thèse ni de longs extraits de celle-ci ne doivent être imprimés ou autrement reproduits sans son autorisation écrite.

ISBN 0-315-32595-X

THE UNIVERSITY OF ALBERTA

RELEASE FORM

NAME OF AUTHOR FRED JAMES HOPPER

TITLE OF THESIS ANALYSIS OF ATMOSPHERIC AEROSOL COMPOSITION

DEGREE FOR WHICH THESIS WAS PRESENTED DOCTOR OF PHILOSOPHY

YEAR THIS DEGREE GRANTED FALL 1986

Permission is hereby granted to THE UNIVERSITY OF ALBERTA LIBRARY to reproduce single copies of this thesis and to lend or sell such copies for private, scholarly or scientific research purposes only.

The author reserves other publication rights, and neither the thesis nor extensive extracts from it may be printed or otherwise reproduced without the author's written permission.

(SIGNED) F. J. Hopper

PERMANENT ADDRESS:

15 Amelia St.

Paris, Ontario

N3L 1Z2

DATED Sept 1 1986

THE UNIVERSITY OF ALBERTA

FACULTY OF GRADUATE STUDIES AND RESEARCH

The undersigned certify that they have read, and recommend to the Faculty of Graduate Studies and Research, for acceptance, a thesis entitled ANALYSIS OF ATMOSPHERIC AEROSOL COMPOSITION submitted by FRED JAMES HOPPER in partial fulfilment of the requirements for the degree of DOCTOR OF PHILOSOPHY in METEOROLOGY.

Robert B. Olthoff

Supervisor

Gerald W. Sadler

O. P. Reimelt

Keith D. Hage

Edward D. Dawson

Leonard A. Barrie

External Examiner

Date August 25, 1986

Abstract

Techniques of factor analysis are reviewed, particularly with regard to analysis of the chemical composition of atmospheric aerosols. The methods most frequently used were found to be lacking in some respects, and improvements in the scaling of the original data and in the method of rotation are described.

Application of these modified procedures to two separate data sets gave mixed results. Analysis of the chemical composition of cloud particulates gave poor results, most likely due to the inappropriateness of the linearly-additive model of factor analysis for this system. Results from an analysis of the chemical composition of aerosols collected in an urban area were found to be consistent with an independent study of the data. The factor scores were found to be very useful for apportioning the partial mass contributions from various source types, and for depicting trends and cycles in the source strengths. Problems of factor analysis, both in general and with respect to aerosol data, are discussed.

The literature on Arctic haze is surveyed briefly. Factor analysis of aerosol composition data from Alert, Mould Bay, and Igloolik, collected from July 1980 to May 1983, gave results generally consistent with other studies. The omission of the total mass of each aerosol sample prevented the scaling of the aerosol source profiles and source strengths to physical units. The normalized factors and scores were used for comparison with simultaneous meteorological data.

Three factors were found to be common to all three Arctic stations: marine (sea salt), crustal, and a general anthropogenic component. A fourth factor was found at Mould Bay and Igloolik which had features similar to both the sea salt and anthropogenic components. The interpretation of this factor as a real aerosol source is questionable. Another analysis of winter concentrations showed the appearance of a unique bromine factor at each station in late winter.

The normalized factor scores revealed that the dominant components have characteristic annual cycles. Comparison with meteorological data indicated that cyclonic activity in the Barents Sea region, combined with the presence of a Siberian anticyclone, was

likely responsible for rapid increases in the anthropogenic aerosol component at Alert during December and January. Some chemical and meteorological evidence is discussed which suggests that the maximum in aerosol concentrations during late winter and spring is composed of two similar overlapping cycles, but the results are inconclusive.

Table of Contents

Chapter		Page
1.	Introduction	1
2.	Factor Analysis Methodology	5
	2.1 FA Research Design	8
	2.2 Blind Factor Analysis	11
	2.3 Problems with FA Methods	15
3.	Target Factor Analysis	18
	3.1 Data Preprocessing	22
	3.2 Missing Data	24
	3.3 Number of Factors	26
	3.4 Target Rotation	29
	3.5 Source Scaling	31
	3.6 Errors in the Source Profiles	33
	3.7 Summary of the TFA Procedure	34
	3.8 Variations of the TFA Procedure	36
4.	Examples of Factor Analysis of Atmospheric Data	38
	4.1 TFA of Cloudwater Data	40
	4.2 TFA of Urban Aerosol Data	50
	4.3 Summary	66
5.	Arctic Haze - Introduction	68
	5.1 Data	81
6.	TFA of Arctic Aerosol Data	86
	6.1 Arctic1 - Factors	96
	6.2 Arctic1 - Scores	106
	6.3 Arctic2 - Factors	116
	6.4 Arctic2 - Scores	128
	6.5 Element Ratios	132

7. Arctic Aerosols and Meteorology 141

7.1 Conjectures 176

8. References 181

9. Appendix A 199

10. Appendix B 203

List of Tables

Table		Page
3.1	FA analysis modes	20
3.2	Values of the Exner function	28
4.1	Cloudwater sample descriptions	41
4.2	Cloudwater sample concentrations	42
4.3	Cloudwater eigenvalue calculations	44
4.4	Cloudwater target and final vectors	46
4.5	Urban aerosol concentration data	53
4.6	Urban aerosol eigenvalue calculations	54
4.7	Urban aerosol factors	56
4.8	Urban aerosol source profiles	57
4.9	Relative composition of similar sources	59
4.10	Observed and predicted TSP	65
5.1	Arctic aerosol composition data	82
6.1	Arctic1 variable statistics	90
6.2	Arctic2 variable statistics	93
6.3	Arctic1 eigenvalue calculations for Alert	97
6.4	Arctic1 eigenvalue calculations for Mould Bay	98
6.5	Arctic1 eigenvalue calculations for Igloolik	99
6.6	Arctic1 test and refined vectors for Alert	101
6.7	Refined Arctic1 aerosol source profiles	103
6.8	Arctic1 scaled source profiles	108
6.9	Arctic2 eigenvalue calculations for Alert	119
6.10	Arctic2 eigenvalue calculations for Mould Bay	121
6.11	Arctic2 eigenvalue calculations for Igloolik	123
6.12	Arctic2 aerosol source profiles	126
6.13	Comparison of Arctic1 and Arctic2 components	127

List of Figures

Figure — Page

2.1 Hypothetical observed and modelled $SO_4^{=}$ concentrations 6

2.2 Flow diagram for FA research design 9

3.1 The data cube 19

4.1 Location map of the Edmonton area 51

4.2 Time series of aerosol source strengths 61

4.3 Time series of related meteorological data 62

4.4 Frequency of reduced visibilities at YXD during cold spells 63

5.1 Sulphate concentrations in the Canadian Arctic 70

5.2 Logarithms of sulphate concentrations 71

5.3 Sulphate concentrations at Igloolik and Ny Alesund 72

5.4 Map of the Arctic region 73

5.5 Map of Canada and the Canadian Arctic 74

5.6 Monthly TSP concentrations in Canadian cities 75

5.7 Absorptivity of atmospheric aerosols 78

5.8 Hourly averages of the aerosol scattering coefficient 84

6.1 Availability of concentration data at Alert 87

6.2 Availability of concentration data at Mould Bay 88

6.3 Availability of concentration data at Igloolik 89

6.4 Source strengths for the Alert factors (Arctic1) 109

6.5 Source strengths for the Mould Bay factors (Arctic1) 110

6.6 Source strengths for the Igloolik factors (Arctic1) 111

6.7 Normalized factor scores at Alert (Arctic1) 112

6.8 Normalized factor scores at Mould Bay (Arctic1) 113

6.9 Normalized factor scores at Igloolik (Arctic1) 114

6.10 Cross-correlations for Arctic1 scores 117

6.11 Normalized factor scores at Alert (Arctic2) 129

Figure Page

6.12 Normalized factor scores at Mould Bay (Arctic2) 130

6.13 Normalized factor scores at Igloolik (Arctic2) 131

6.14 The Al(ICP)/Fe(ICP) ratio 134

6.15 The Al(NAA)/Fe(ICP) ratio 136

6.16 Enrichment factors for Mn and V at Alert 137

6.17 XMn, XV, and XMn/XV at Alert 138

6.18 XMn versus XV at Alert 139

7.1 Temperatures at the 90 kPa level at Alert 142

7.2 Daily totals of global solar radiation 143

7.3 LWE at Arctic stations 144

7.4 LWE spectra 145

7.5 LWE and sulphate concentrations 147

7.6 Mean monthly vertical profiles of temperature 148

7.7 Mean monthly vertical profiles of zonal wind speed 149

7.8 Mean monthly vertical profiles of meridional wind speed 150

7.9 Mean monthly vertical profiles of horizontal sensible heat flux H 151

7.10 Mean monthly vertical profiles of horizontal latent heat flux 152

7.11 Time series of potential temperature at Alert 154

7.12 Boundary layer characteristics at Alert 155

7.13 PVS and the anthro factor scores at Alert 156

7.14 Surface weather map for 80/12/08 158

7.15 Surface weather map for 80/12/15 159

7.16 Surface weather map for 80/12/18 160

7.17 Surface weather map for 80/12/21 161

7.18 Surface weather map for 80/12/28 162

7.19 Surface weather map for 82/01/08 164

7.20 Surface weather map for 82/01/12 165

Figure Page

7.21 Surface weather map for 82/01/14 166

7.22 Surface weather map for 82/04/23 168

7.23 Surface weather map for 82/04/26 169

7.24 Surface weather map for 82/04/29 170

7.25 Surface weather map for 82/04/30 171

7.26 Surface weather map for 82/05/03 172

7.27 Anthro factor scores and the 95 kPa heat flux at Alert 175

7.28 Mean surface pressure (kPa) in January 177

7.29 Mean surface pressure (kPa) in April 178

1. Introduction

The problem which eventually defined itself was this: given a data matrix X_{m*n}, where the rows represent m aerosol samples, each of which has been analyzed for the concentrations of n chemical species[1], what is the most efficient way of extracting meaningful information from the data? When the product $m*n$ is on the order of several thousand, then an element by element examination of X_{m*n} is tedious, expensive, and likely to be misleading, because larger structures or patterns in the data may be overlooked.

Multivariate statistical methods offer a solution to this problem. But this answer is not clear-cut because there are many different inferential statistical methods which could be applied, and choices and assumptions must be made with each method. Factor analysis[2] was the technique selected here because it appeared to address the main goal of an analysis of aerosol composition data: what are the underlying sources (factors) which have contributed to the observed variability in the concentrations of the different chemical species? Other statistical methods have been applied to such data, including multiple linear regression, cluster analysis, and multiple discriminant analysis, but these have not been considered here. Even with factor analysis, which seemed the most appropriate method, there was still a degree of forcing of the statistical model to fit an independent physical concept. More precisely, the statistical method was not drastically changed but the results were interpreted in terms of aerosol source profiles (the factors) and aerosol source strengths (the factor scores).

Chapter 2 reviews FA basics, particularly with regard to application to aerosol composition data. Studies using FA techniques are being reported more and more frequently, but it often seems that FA has been employed as some sort of objective analysis method. This is certainly encouraged by the wide availability of statistical computer packages, which make it very easy to use FA as a 'black box': data are fed in at one end, and the correct and

---

[1] 'Chemical species' refers to both individual elements (eg., sulphur S, lead Pb) and ions (eg., sulphate $SO_4^{=}$, nitrate NO_3^{-}), since many aerosol data sets are a mixture of elemental and ionic concentrations.

[2] Factor analysis (FA) is assumed to include the classical factor analytical models, where the communalities of the variables must be estimated, plus eigenvector/components analysis.

meaningful answers appear quickly and painlessly at the other end.

Consideration of the goals of an analysis of aerosol data led to a rejection of the usual FA methods. Two points seemed particularly important for such data: (1) appropriate scaling of the original data so that the relative proportions of the chemical species in each sample are preserved, and (2) rotation of the abstract or 'raw' factors to a physically-significant set of factors. Existing knowledge of the aerosol sources can be incorporated into the analysis at the rotation stage. By using a 'flexible' rotation method, instead of one which satisfies some abstract mathematical criteria, suspected patterns in the data matrix can be tested. This contrasts with the interpretation of factors derived from the usual FA methods: the factor with the highest loadings for sodium and/or chlorine, for example, is automatically labelled marine or sea salt.

The new procedure for the analysis of aerosol composition data is outlined in Chapter 3. It is based largely on the Target Factor Analysis method of Hopke (1981) and co-workers. Where possible, it has been simplified. It has also been expanded because aerosol data are frequently from successive samples in a monitoring program, and trends and cycles in aerosol concentrations can be very important. Thus the factor scores can be as significant as the factors themselves. There are problems with the method too, and since this is only the second independent application of Target Factor Analysis to atmospheric aerosol data, it should not be expected that all these problems have been overcome here. Different approaches were tried, which may seem unusual. For instance, much of the FA literature discusses criteria for determining the proper number of significant factors to retain, since FA theory is incomplete on this point. The most influential criteria used here was the 'interpretability' of the factors, which can be defined only loosely: if a factor looks physically reasonable, and it (or the associated scores) can be related to other data, or it has been derived from the same variables in another data set, then keep the factor at least temporarily. This is not to imply that the selection of the number of factors was completely arbitrary. A number of tests were calculated which have been suggested as being capable of doing this, but there was always a degree of judgement involved when the tests did not agree as to the appropriate number of factors.

Target Factor Analysis is tested with two separate data sets in Chapter 4. Analysis of urban aerosol composition data gave results consistent with the original interpretation of the data in a summary report, and also revealed additional information. The method failed with the other data set because, it is believed, the linearly-additive model (a basic assumption of FA) was not valid for such data.

Chapter 5 briefly reviews the subject of Arctic haze. The reason for developing the TFA procedure was to be able to do an analysis of composition data from aerosol samples collected in the Canadian Arctic. The analysis and results are described in Chapter 6 while Chapter 7 attempts to tie together the ideas presented earlier.

Using real data to test an analysis procedure, and then drawing conclusions from an analysis of the same data with the same procedure, is not the most 'scientific' approach. There are inadequacies at all levels of this study, beginning with the terminology used. 'Factors', 'vectors', and 'components' are all used somewhat loosely and may be applied to the same quantities at different times, although the terms should denote a trend from the abstract (factors) to the physically-significant (components of the aerosol). In a similar vein, 'aerosol' is the predominant term used here although 'particulate matter' is probably more appropriate.

In many respects this thesis is flawed because nothing is 'proved' or 'disproved'. Nor are there any startling new discoveries, theoretical or experimental. Verification of the results of TFA was less than conclusive, and depended mainly on being able to show that the results were consistent with other data or with other studies. Even the calculation of correlations between variables and data sets presented difficulties. With one of the computer packages used, three command lines would have been sufficient to calculate over a dozen different statistical tests of correlation, from the usual normal-distribution tests to non-parametric tests to rank correlation tests. In the end, these tests were not used (although a few cross-correlations were calculated to depict general relationships; they should be interpreted very cautiously). There were two reasons for this. First, the assumptions for using the various tests could rarely be satisfied. Second, for the Arctic data it was found that all of the tests were biased by the predominant annual cycle in the aerosol and meteorological data;

correlations or anti-correlations on a time-scale of a few weeks were simply 'swamped' by the effects of this common climatological feature. Perhaps filtering and/or cross-spectrum analysis could be used, but that would require forcing a number of irregular time series to fit a common sampling period. Instead, extensive use was made of graphical presentations of these series, relying on a visual, somewhat subjective, estimation of correlations and common trends.

It is readily acknowledged that many things have been treated less thoroughly than they deserved. This was very much an interdisciplinary, exploratory study, and a much too-ambitious one. It was necessary to try to combine statistics, geochemistry, air pollution, meteorology, and Arctic climatology, without the time or resources to become an 'expert' in any one subject. And some things had to be dropped; it would have been interesting to make a comparison of aerosol optical and chemical data in the Arctic, but this would have been a major project in itself. It is hoped that this study will at least help to suggest or encourage other work.

2. Factor Analysis Methodology

The application of FA techniques to a data set represents a rather important philosophical decision on the part of the analyst. It is the result of a realization, perhaps implicit, of the deficiencies of the existing theory or knowledge of the system that produced the data. This is the normal state of affairs in a subject like psychology where the end results, such as observations of human behaviour or decision-making, are likely to be the product of a large number of ill-defined, ambiguous, and/or time-varying processes. Thus, it is not surprising that the origins of FA lie in the early attempts of psychologists to identify the most important underlying factors which contribute to the final observed entities.

This notion can be carried further by contrasting the use of statistical methods in general (*a posteriori* analysis) with modelling studies (*a priori* analysis). There is not always a clear separation between the two, since the development of a particular theory (culminating in the formation and application of some sort of model) may well rely on previous statistical analysis to identify variables or processes which are significant (must be included in the model) or insignificant (can be excluded from the model). Similarly, statistical analyses of data sets are certainly influenced by the analyst's knowledge of the system processes, if only in biasing the selection of variables to include in the analysis.

Fig. 2.1 is a simple example of the practical consequences of these different approaches. The figure shows the concentrations of SO_4^{2-} which might be observed in five Hi-Vol samples of atmospheric particulate matter from each of three monitoring sites. Also shown are the results from a model which, perhaps based on knowledge of source strengths and air parcel trajectories, attributed the SO_4^{2-} at the measuring sites to two separate sources. The calculated contributions of these sources are indicated. Faced with such a set of observed concentrations, the honest factor analyst would admit that an analysis should not be performed on the data; the SO_4^{2-} concentrations at each site are fully described by a single parameter, the mean value. On the other hand, the modeller could legitimately claim that the model is exceptionally good and fully explains the observations.

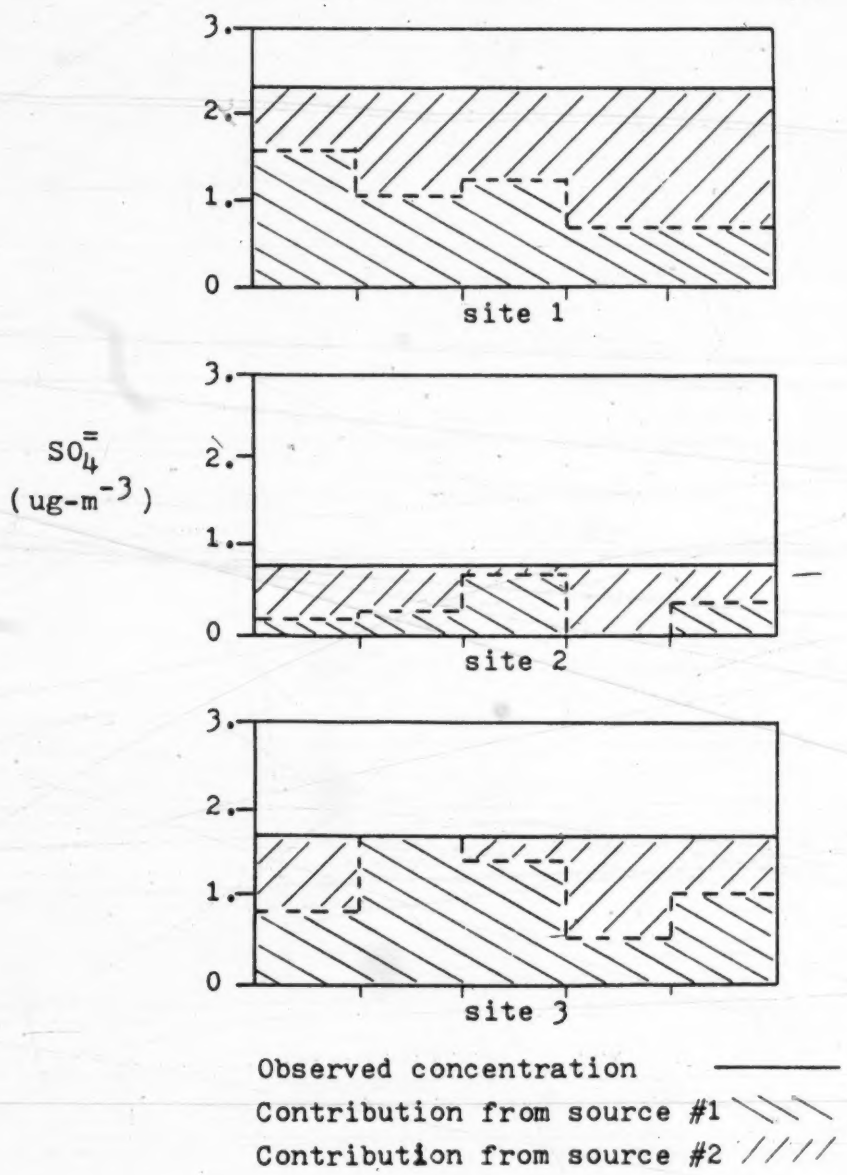

Fig. 2.1 Hypothetical observed and modelled $SO_4^{=}$ concentrations. There are three monitoring sites, and five samples from each site. Only two sources are assumed to contribute to the observed $SO_4^{=}$ concentrations. The fraction contributed by each source to each sample, as might be derived from modelling calculations, is indicated.

This example was admittedly 'cooked', but serves to illustrate the essential difference: since FA begins by analyzing the original data, it is constrained by the information contained in the observations. The *a priori* analysis is also constrained, but by physical and meteorological laws; the actual observed concentrations may be completely ignored until the final step, model verification. Both approaches can be used to advantage in scientific study. The selection of one or the other depends largely on how well-known are the details of the system which produced the set of observations.

A review of papers on the analysis of atmospheric aerosol composition, particularly those dealing with large sets containing many chemical species, suggested that the combination of source uncertainties, meteorological variability (transport and removal), and transformation processes is, at least at present, a system where the general principles are adequately known but the details are still vague. This is particularly true for aerosol samples from remote areas. Prospero et al. (1983), in a review of the global atmospheric aerosol cycle which highlighted the complexities of this particular system, stated that

> "At present, we do not have a good understanding of the global cycles of most elements and of their global budgets because of the dearth of data on the large-scale distribution of these species and their temporal variability. Data are scarce for most remote regions. Few measurements exist for very large areas of Asia, South America, Africa, and the polar regions. Over the oceans there are almost no data for vast areas in the Indian Ocean, the South Atlantic, and much of the Pacific, especially the South Pacific. These ocean regions alone constitute well over half of the earth's surface."

They made the same point later in regard to sampling of aerosols:

> "... the timing and the spatial distribution of the measurements should be small in comparison to the characteristic scales for the respective variations. At present, the dispersion of pollutants over microscale and mesoscale regions is much better understood than transport over larger distances."

There seems reasonable justification for adopting an *a posteriori* approach with such data.

The remainder of this chapter describes the principles of FA, with an emphasis on traditional or classical methods. These are the methods most frequently encountered in the literature since they are the best developed and they are widely available. Indeed, the standard computer statistical packages such a BMDP (Dixon, 1983) and SPSSx (Anon., 1986) are programmed to use these procedures as the default. It takes some effort to devise better methods.

2.1 FA Research Design

Factor analysis of a data set is much more involved than the selection and application of a factor model. It is a multi-step process, the final results being dependent on the techniques used at each step. Thus it is appropriate to consider FA as a problem in research design. Such a view was advocated by Rummel (1970) and Joreskog et al. (1976). Fig. 2.2 is an outline of the major steps involved (adapted from Rummel, 1970).

The heart of any FA procedure is the linearly-additive model. Consider the data matrix $\mathbf{X}_{m*n}$ where the rows represent m different aerosol samples, each of which was analyzed for n different chemical species. If the chemical species are conservative and are not involved in any chemical reactions or removal processes, then the observed concentration of the j^{th} species in the i^{th} sample is exactly equal to the individual contributions from all p sources of the chemical species:

$$x_{ij} = s_{i1}f_{1j} + s_{i2}f_{2j} + \ldots + s_{ik}f_{kj} + \ldots + s_{ip}f_{pj} \qquad (2.1)$$

Here, the elements f_{kj} are the source concentrations of the chemical species (in units of milligrams per gram of particulate matter) and the s_{ik} elements represent the particulate matter per unit volume contributed by the k^{th} source at the sample collection site.

Repeating Eqn. 2.1 for all m samples gives a set of equations which can be expressed succinctly in matrix form:

$$\mathbf{X}_{m*n} = \mathbf{S}_{m*p}\mathbf{F}^{\dagger}_{p*n} \qquad (2.2)$$

The row vectors of the $\mathbf{F}^{\dagger}_{p*n}$ matrix represent the concentration profiles of each of the p sources, and the $\mathbf{S}_{m*p}$ matrix contains the amount per unit volume in each sample from each

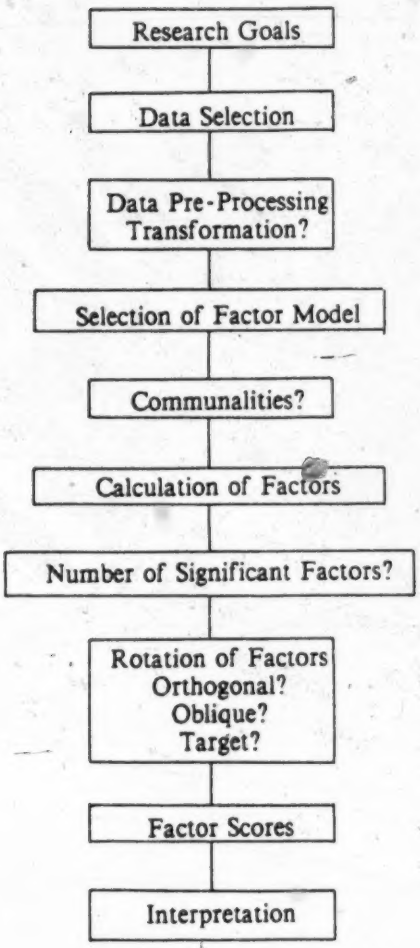

Fig. 2.2 Flow diagram for FA research design.

individual source. In FA terminology, $\mathbf{F}^{\dagger}_{p*n}$ is the transpose of the factor loading matrix and $\mathbf{S}_{m*p}$ is the factor score matrix. More commonly, a centered and/or scaled data matrix $\mathbf{Z}_{m*n}$ is used instead of the original data matrix.

The assumption of a conservative chemical species is a condition which is best satisfied by samples from urban areas with an averaging time (sample collection time) of one to several days; the aerosol characteristics, both physical and chemical, are still closely related to the processes which produced the aerosol (Prospero et al., 1983). This assumption is not restrictive because the linearly-additive model is a reasonable first approximation to any collective sample which is time- and volume-averaged, such as an aerosol sample collected in a Hi-Vol sampler. In applying the model to aerosol samples from remote areas, however, it must be realised that the source profiles (rows of the $\mathbf{F}^{\dagger}_{p*n}$ matrix) may not represent individual sources, such as particular regions or industrial processes, but might only indicate 'prototypical' sources which appear as the end products of the combined effects of many separate sources and transformation reactions. This is an unresolved question which will be discussed later in conjunction with the results of an analysis of some aerosol composition data.

The ultimate goal of FA is to decompose the data matrix $\mathbf{X}_{m*n}$ into the two component matrices on the right hand side of Eqn. 2.2. Inextricably linked with this goal is the determination of the minimum dimension of the component matrices. In other words, the rank r of the data matrix must be found, where r is the

> "order of the largest matrix with non-zero determinant formed by deleting rows and columns from the original matrix" (Rummel, 1970).

Equivalent definitions of the rank are also possible (Horst, 1965; Harman, 1967; Joreskog et al., 1976). The functional importance of rank is to place an upper limit on the number of factors p which are significant

$$p \leq r \leq min(m,n) \tag{2.3}$$

but the exact number must be derived by other means. More than p factors can be calculated, up to $min(m,n)$, but $(min(m,n)-p)$ of these factors must be attributed to noise in the system (realised as observational errors, measurement errors, etc.).

Most FA studies attempt to determine the true value of p, but the use of FA methods with aerosol composition data emphasizes the point that p can be, at best, an approximation. The number of possible sources which may contribute to the concentration of a chemical species in a sample is very large, much greater that either m or n is ever likely to be. Thus the determination of the p factors which adequately represent the observed concentrations is made within a factor space already truncated to the dimensions m,n by the practicalities of aerosol sampling.

2.2 Blind Factor Analysis

Rummel (1970) gives a thorough discussion of each of the stages depicted in Fig. 2.2. Classical or traditional FA methods assume that little is known about the underlying factors, so this sort of analysis will be referred to as BFA (blind factor analysis). Typically, the first step in BFA is to standardize each column of $\mathbf{X}_{m*n}$. The minor product moment of the column standardized data matrix $\mathbf{Z}_{m*n}$ gives the correlation matrix

$$\mathbf{R}_{n*n} = \frac{1}{m}\mathbf{Z}^{\dagger}_{n*m}\mathbf{Z}_{m*n} \tag{2.4}$$

where the † superscript indicates the transpose of the matrix. (It is assumed that $n < m$.) While this is by far the most common approach, there are four related matrices which could be used. Rozett and Petersen (1975) describe these as

1. Correlation about the mean ($\mathbf{R}_{n*n}$; Eqn. 2.4)
2. Correlation about the origin (not centered,normalized)
3. Covariance about the mean (centered,not normalized)
4. Covariance about the origin (not centered, not normalized)

It is $\mathbf{R}_{n*n}$, or one of the other three product moment matrices, which is the actual starting point for the decomposition calculations.

BFA usually uses one of two factor models in the next step. The terminology varies considerably. The first model will be called PCA (principal components analysis; components analysis; eigenvector analysis) and is described by

$$\mathbf{Z}_{m*n} = \mathbf{S}_{m*p}\mathbf{F}^{\dagger}_{p*n} \tag{2.5}$$

that is, the same as Eqn. 2.2 but for a column standardized data matrix. The second most common factor model is PFA (principal factor analysis; common factor analysis; true factor analysis; classical factor analysis; factor analysis)

$$\mathbf{Z}_{m^*n} = \mathbf{S}_{m^*p}\mathbf{F}^{\dagger}_{p^*n} + \mathbf{S}_{m^*p}\mathbf{E}_{p^*n} \tag{2.6}$$

where $\mathbf{E}_{m^*n}$ is an error matrix whose elements are unique residuals not explained by the p common factors in the system.

There are striking differences between PCA and PFA. The former makes no assumptions regarding the variance observed in the data matrix; a solution is derived which attempts to explain all of the variance. The solution is found by calculating the n eigenvalues of the system, starting from the characteristic equation

$$\begin{aligned} | \mathbf{R}_{n^*n} - l_n\mathbf{I}_{n^*n} | &= \mathbf{O}_{n^*n} \\ | \mathbf{R}_{n^*n} - \mathbf{L}_{n^*n} | &= \mathbf{O}_{n^*n} \end{aligned} \tag{2.7}$$

where $\mathbf{L}_{n^*n}$ is a diagonal matrix with the n scalar eigenvalues as its elements. Once the eigenvalues are found, the n associated eigenvectors $\mathbf{q}_n$ can be calculated from

$$| \mathbf{R}_{n^*n} - \mathbf{L}_{n^*n} | \, \mathbf{q}_n = \mathbf{O}_{n^*n} \tag{2.8}$$

or, with the normalized eigenvectors arranged as columns in the matrix $\mathbf{Q}_{n^*n}$

$$\begin{aligned} \mathbf{R}_{n^*n}\mathbf{Q}_{n^*n} &= \mathbf{Q}_{n^*n}\mathbf{L}_{m^*m} \\ \mathbf{R}_{n^*n} &= \mathbf{Q}_{n^*n}\mathbf{L}_{n^*n}\mathbf{Q}^{-1}_{n^*n} \\ \mathbf{R}_{n^*n} &= (\mathbf{Q}_{n^*n}\mathbf{L}^{1/2}_{n^*n})\,(\mathbf{L}^{1/2}_{n^*n}\mathbf{Q}^{-1}_{n^*n}) \end{aligned} \tag{2.9}$$

The matrix $\mathbf{Q}_{n^*n}$ is square orthonormal such that

$$\mathbf{Q}^{\dagger}_{n^*n} = \mathbf{Q}^{-1}_{n^*n}$$

$$\mathbf{Q}_{n^*n}\mathbf{Q}^{\dagger}_{n^*n} = \mathbf{Q}^{\dagger}_{n^*n}\mathbf{Q}_{n^*n} = \mathbf{I}_{n^*n}$$

so

$$\mathbf{L}_{n^*n} = \mathbf{Q}^{\dagger}_{n^*n}\mathbf{R}_{n^*n}\mathbf{Q}_{n^*n}$$

and

$$\mathbf{R}_{n^*n} = \mathbf{F}_{n^*n}\mathbf{F}^{\dagger}_{n^*n}$$

where

$$\mathbf{F}_{n^*n} = \mathbf{Q}_{n^*n}\mathbf{L}^{1/2}_{n^*n} \tag{2.10}$$

Two important properties of the eigenvalues are:

1. Trace $\mathbf{L}_{n^*n}$ = trace $\mathbf{R}_{n^*n}$; that is, the sum of the eigenvalues equals the sum of the elements in the diagonal of $\mathbf{R}_{n^*n}$.

2. The number of non-zero eigenvalues equals the rank r of $\mathbf{R}_{n^*n}$.

With real data, it is almost always possible to calculate $r = n$ eigenvalues but $(n - p)$ of these are due to system or observational errors. Similarly, the n eigenvectors form a set of linearly independent (orthogonal) basis vectors which completely span the n-dimensional space, but only p eigenvectors are really necessary to describe the significant portion of the data.

By contrast, PFA attempts to derive the significant factors which account for only the common variance in the data. The residual or unique variance ($\mathbf{E}_{p^*n}$ in Eqn. 2.6), containing both variable-specific and system error contributions, is not accounted for by the derived factors. A major problem arises because the communalities (or uniquenesses) are not known before-hand, but must be derived during the analysis. Typically, the diagonal elements of $\mathbf{R}_{n^*n}$ are replaced by the squared multiple correlation (SMC) of the variable, the matrix is factored, and new communalities are calculated from the derived factors. These new communality estimates are inserted into the diagonal of $\mathbf{R}_{n^*n}$, and the procedure is repeated until the communality estimates converge.

Derivatives of PFA have been developed but these are less commonly used. The principal ones are Image Factor Analysis (Guttman, 1953), Canonical Factor Analysis (Rao, 1955), Alpha Factor Analysis (Kaiser and Caffrey, 1965), and Maximum Likelihood Factor Analysis (Lawley, 1943). Rummel (1970) makes a detailed comparison of these factor models, which have interesting, and useful, properties. But BFA usually relies on the PCA or PFA models.

Once the raw factor loading matrix $\mathbf{F}_{n^*n}$ has been derived, a decision must be made as to the number of the factors p which are significant. Except for a couple of the lesser-known factor models, there are no objective analytic procedures which can be used to calculate p. BFA procedures typically invoke Guttman's Weakest Lower Bound, the 'eigenvalue-one' criterion, which states that all factors associated with eigenvalues greater than 1.0 are significant (Rummel, 1970); but it does not say anything about the significance of factors with eigenvalues less than 1.0. Rummel (1970) winds up his discussion of the problem with eight 'rules of thumb' which can be used to decide on the number of significant factors.

The factoring methods used in BFA produce a set of factors which are mutually orthogonal. The set is not unique, however, as there are an infinite number of sets which can be derived by rotating the raw factor loading matrix $\mathbf{F}_{n^*p}$. In contrast to the number of factors problem, there are methods available for determining the 'best' rotation to apply to $\mathbf{F}_{n^*p}$ in order to meet some sort of analytical criterion. A frequently used method is Varimax, which attempts to maximize the variance of the squared factor loadings. This is an orthogonal rotation so that the final set of factors are still uncorrelated. Varimax was developed by Kaiser (1958) to meet the goal of simple structure; that is, the rotated solution should have these characteristics (Rummel, 1970):

1. Each variable is closely associated with one (preferably) or a few factors.
2. The number of variables correlated with a factor is minimized.
3. Each factor accounts for about the same magnitude of variance.
4. Each factor is identified with a cluster of interrelated variances.

A common mistake in BFA is to apply the number of significant factor criteria (whatever it may be) to the unrotated factor loading matrix. It is not at all unusual to find a couple of factors with eigenvalues between 0.5 and 1.0. Application of Guttman's Weakest Lower Bound would discard these factors as insignificant. If, however, they are retained and a Varimax rotation is used, the final rotated solution frequently has all eigenvalues greater than 1.0. Indeed, the rotation attempts to distribute the variance fairly evenly among the factors, in accordance with the simple structure criteria, even though the unrotated factor loading matrix might have indicated that a smaller number of factors were significant.

With the PCA model, it is possible to calculate an exact solution for $\mathbf{S}_{m^*p}$ once the rotated factor loading matrix has been found:

$$\mathbf{X}_{m^*n} = \mathbf{S}_{m^*p}\mathbf{F}^{\dagger}_{p^*n}$$

$$\mathbf{X}_{m^*n}\mathbf{F}_{n^*p} = \mathbf{S}_{m^*p}\mathbf{F}^{\dagger}_{p^*n}\mathbf{F}_{n^*p}$$

$$\mathbf{X}_{m^*n}\mathbf{F}_{n^*p}(\mathbf{F}^{\dagger}_{p^*n}\mathbf{F}_{n^*p})^{-1} = \mathbf{S}_{m^*p}$$

therefore

$$\mathbf{S}_{m^*p} = \mathbf{X}_{m^*n}\mathbf{F}_{n^*p}\mathbf{L}^{-1}_{p^*p}$$

since $$\mathbf{F}^{\dagger}_{p^*n}\mathbf{F}_{n^*p} = \mathbf{L}_{p^*p} \qquad (2.11)$$

where $\mathbf{L}_{p^*p}$ is a diagonal matrix with elements equal to the significant eigenvalues of the unrotated factor loading matrix. This does not work for the PFA model, and it is necessary to use regression methods with the factor loadings as independent variables.

The two final steps in Fig. 2.2 will be discussed later. The most important point to be made now is that if BFA, or in general any FA method, is being used to derive factors for comparison with another set of factors, then using the same factor model does not provide a sufficient basis for a meaningful comparison. Rather, it is necessary that the two analyses use the same methods at each step in Fig. 2.2. This was the problem faced by Hopper (1984); a comparison with the results of Heidam (1981) was only feasible by following the same methodology.

2.3 Problems with FA Methods

The description of BFA mentioned some of the problems of using FA methods, such as the difficulty in determining the number of factors. In simplest terms, FA methodology is technically underdeveloped. Thus the analyst relies on 'rules of thumb' rather than applying a demonstrably sufficient analytical criterion. Matalas and Reiher (1967) prepared a critique of PFA methods, with additional comments on PCA and rotation methods as well. Some of their comments regarding PFA were (Matalas and Reiher, 1967):

1. There are several inherent indeterminacies in the PFA model (communalities, number of factors, rotation); choices must be made which are often subjective.
2. Little is known of the sampling properties of the factor loadings.
3. The factors are not directly observable or expressible in terms of the observed variables.
4. The interpretation of the factors as the 'cause' of the observations is not implicit in the PFA model, but is imposed by the analyst.
5. It is difficult to use the results of PFA in other analytical studies.

On the other hand, Matalas and Reiher (1967) describe PCA as a 'self-contained' method which, despite the superficial similarity to the PFA model, has quite different aims. The most significant advantage of PCA is that the communality problem is avoided; it really doesn't matter whether or not the underlying probability distributions of the variables are known (as long as they are reasonably well-behaved). The principal components (the PCA factors) are mathematical devices which describe the observed system, but they have no physical interpretation (according to Matalas and Reiher, 1967).

The use of FA methods with aerosol samples raises other difficulties. Prominent among these is the effect of serial correlations between the samples. A typical situation is the analysis of m samples from a continuous monitoring program. The concentrations in sample i are related to the observed concentrations in sample i-1. The elements of the correlation matrix $\mathbf{R}_{n*n}$ are not the true correlation coefficients between the n chemical species consistent with statistical random sampling. Nor is it possible to avoid the problem by calculating $\mathbf{R}_{m*m}$, the correlations between samples rather than elements, because now the elements of $\mathbf{R}_{m*m}$ are affected by the inter-elemental correlations. Whichever method is chosen, the elements of the correlation matrix $\mathbf{R}$ are biased estimates of the true correlations, and all subsequent analyses performed on this matrix inherit this bias (Redman and Zinsmeister, 1982).

Another concern in FA, one which tends to be overlooked, is the scale dependence of the factor model. Of all the models described or mentioned here, only Canonical Factor Analysis and Alpha Factor Analysis produce results which are truly invariant of scale (Rummel, 1970). As an example, consider the use of the PFA model with aerosol composition data where the columns of the $\mathbf{X}_{m*n}$ matrix contain the measured concentrations of the n chemical species. Some of these species may be in the parts per million range, while others are expressed as micrograms per cubic meter. Still others may have concentrations in ranges which are an order of magnitude larger or smaller. These scale differences will only proportionally change the results of a factor analysis with a scale-independent model; if a column of $\mathbf{X}_{m*n}$ is multiplied by 0.001 to convert from parts per billion to parts per million, the results of the analysis will be within a scalar multiple (x1000) of the results obtained without the pre-analysis

conversion. This is, in general, not true for scale-dependent models such as PCA and PFA. Scale-independence might be achieved by using the correlation matrix as the starting point for the calculations, but then one must consider the possible consequences of calculating product-moment correlations from variables which may have non-normal distributions.

3. Target Factor Analysis

There is nothing to prevent the application of BFA methods to aerosol composition data or any other meteorological data set, except the realization that there might be a better approach. As a matter of fact, an analysis of the correlation matrix formed from a column-standardized data matrix has the important advantage of removing the physical units from each variable. Thus it is possible to form X_{m*n} from a miscellaneous collection of chemical data, physical data (eg., aerosol size and light-scattering properties), meteorological variables, etc., and to apply BFA methods to explore the data space and see 'what falls out'. Such an approach may be of use in uncovering qualitative correlations between variables which would otherwise have been obscured or overlooked, but it is at odds with the research design concept of Rummel (1970) and others.

This chapter describes an FA procedure expressly for the analysis of composition data such as the chemical composition of atmospheric aerosol samples, but it has other applications. With a well-defined goal, it is possible to select a method at each step of Fig. 2.2 which will maximize the information available at the end of the analysis; moreover, outside knowledge of the system can be incorporated into part of the analysis, although it is at the expense of the 'objectivity' of FA methods which is often cited as a main advantage. The procedure also remains close to the original data. Several previous studies have been reviewed which used BFA methods with aerosol composition data, but by the time a distribution transformation (usually logarithmic) was applied, and the variables were standardized, and the eigenvalues were found with a PFA model, and the factor scores were calculated by a multiple linear regression model, it was not certain that the physical meaning of the results was anywhere near the interpretation of Eqn. 2.1 presented earlier.

This type of analysis falls under the general heading of Q-mode FA, while the BFA methods of Chapter 2 are usually (but not always) R-mode analyses. The various modes arise from the concept of the data cube, originally outlined by Cattell (1952). Fig. 3.1 shows the data cube for an aerosol sampling problem, where there might be several monitoring sites continuously collecting samples over a period of time. FA is a two-dimensional analysis;

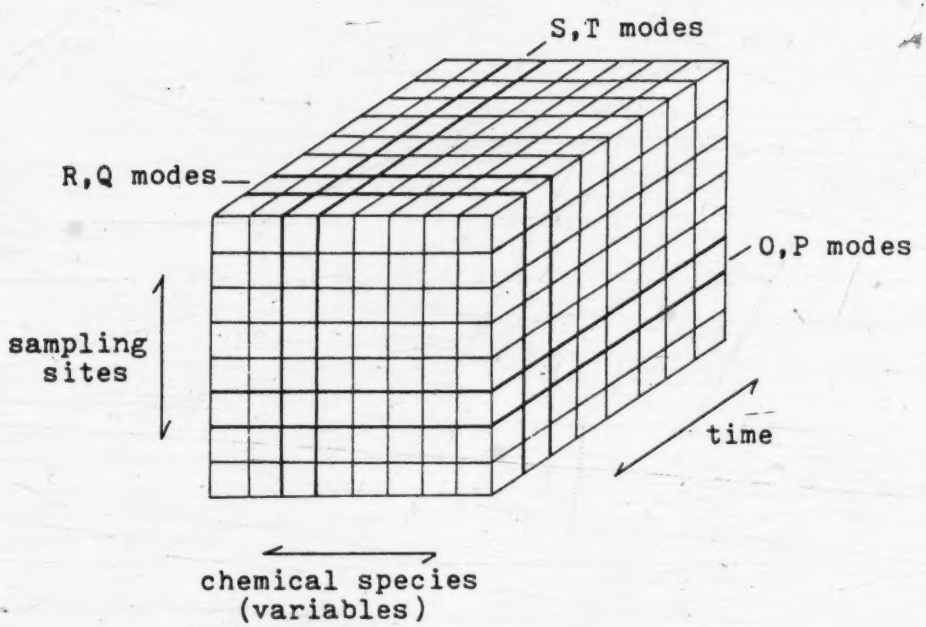

Fig. 3.1 The data cube.

because the data cube can be sliced three ways, and each slice has two distinct row-column arrangements, there are six possible modes of analysis (Table 3.1). The BFA methods could have been interpreted as either R-mode or P-mode, depending on whether the samples (rows of $\mathbf{X}_{m*n}$) were from different sites at the same time, or from the same site at different times.

Table 3.1 FA analysis modes. A data matrix is a slice of the data cube with one of the parameters held constant. The other two parameters form either the rows or columns of the data matrix.

Mode	Rows	Columns	Constant
R	samples from different sites	chemical species	time
Q	chemical species	samples from different sites	time
O	chemical species	samples from differrent times	sampling site
P	samples from different times	chemical species	sampling site
S	samples from different sites	samples from different times	chemical species
T	samples from different times	samples from different sites	chemical species

Q-mode analysis attempts to decompose

$$\mathbf{Z}_{m*n}\mathbf{Z}^{\dagger}_{n*m} \tag{3.1}$$

while R-mode analysis starts with

$$\mathbf{Z}^{\dagger}_{n*m}\mathbf{Z}_{m*n} \tag{3.2}$$

where $\mathbf{Z}_{m*n}$ represents the scaled data matrix. Thus R-mode analyzes the correlation between variables (concentrations of chemical species), while Q-mode analyzes the correlation between samples. There is some confusion in the literature over the best method to use in any given case, and also regarding the relationship between the results of Q-mode and R-mode analyses. For instance, Rozett and Petersen (1975) compared Q-mode and R-mode analyses of mass

spectra for each of the four product moment matrices. Table VI of Rozett and Petersen (1975) shows identical results from both R-mode and Q-mode analyses, using an untransformed data matrix (ie., covariance about the origin) as the starting point. More recently, Hwang et al. (1984) made a comparison of Q-mode and R-mode analyses, using real atmospheric aerosol data. They suggested that the two modes produced equivalent results with most of their data sets although R-mode may be slightly more sensitive and hence capable of resolving a weak factor into two separate factors. Heidam and Kronberg (1985) criticized that work, pointing out that the equivalence can be proven only if the PCA model is used and if the same matrix is used in the initial step; the empirical equivalence found by Hwang et al. (1984) may not be true in general.

The equivalence of the positive eigenvalues of Q-mode $\mathbf{Z}_{m^*n}\mathbf{Z}^{\dagger}_{n^*m}$ and R-mode $\mathbf{Z}^{\dagger}_{n^*m}\mathbf{Z}_{m^*n}$ is rather important. The basic structure concept of a data matrix ('singular value decomposition', Joreskog et al., 1976) states that

$$\mathbf{Z}_{m^*n} = \mathbf{V}_{m^*r}\mathbf{L}_{r^*r}\mathbf{U}^{\dagger}_{r^*n} \tag{3.3}$$

where r is the rank of $\mathbf{Z}_{m^*n}$, $\mathbf{V}^{\dagger}_{r^*m}\mathbf{V}_{m^*r} = \mathbf{I}_{r^*r}$, and $\mathbf{U}^{\dagger}_{r^*n}\mathbf{U}_{n^*r} = \mathbf{I}_{r^*r}$; that is, the columns of $\mathbf{V}_{m^*r}$ and $\mathbf{U}_{n^*r}$ are orthonormal. The matrix $\mathbf{L}_{r^*r}$ is a diagonal matrix with positive elements which are the singular values of $\mathbf{Z}_{m^*n}$. The Eckart-Young theorem (Eckart and Young, 1936; Johnson, 1963) describes the relationships between these component matrices. Summarizing from Joreskog et al. (1976)[3]:

1. The major product moment of $\mathbf{Z}_{m^*n}\mathbf{Z}^{\dagger}_{n^*m}$ has r positive eigenvalues (squares of the singular values) and $(m - r)$ zero eigenvalues; the columns of $\mathbf{V}_{m^*r}$ are the corresponding eigenvectors.
2. The minor product moment $\mathbf{Z}^{\dagger}_{n^*m}\mathbf{Z}_{m^*n}$ has r positive eigenvalues (squares of the singular values) and $(n - r)$ zero eigenvalues; the columns of $\mathbf{U}_{n^*r}$ are the corresponding eigenvectors.
3. The positive p eigenvalues of $\mathbf{Z}^{\dagger}_{n^*m}\mathbf{Z}_{m^*n}$ are the same as those of $\mathbf{Z}_{m^*n}\mathbf{Z}^{\dagger}_{n^*m}$, and are related by:

[3]If $(r - p)$ factors can be considered physically insignificant, then the dimension r of these matrices is reduced to p.

$$\mathbf{V}_{m^*r} = \mathbf{Z}_{m^*n}\mathbf{U}_{n^*r}\mathbf{L}^{-1}_{r^*r}$$
$$\mathbf{U}_{n^*r} = \mathbf{Z}^{\dagger}_{n^*m}\mathbf{V}_{m^*r}\mathbf{L}^{-1}_{r^*r} \qquad (3.4)$$

Both Hwang et al. (1984) and Heidam and Kronberg (1985) were aware of the Eckart-Young theorem but disagreed on two points. The first concerned the importance of using the same initial matrix. Since one of the first steps of the usual R-mode (Q-mode) procedure is to standardize the columns (rows) of the data matrix, the product moment matrices will be different because of the different scaling functions. The second point of disagreement arose due to confusion over the matrix decomposition with the PFA model; it has not been shown that the usual methods for estimating communalities will give the same results (within a simple matrix transformation operation) starting from $\mathbf{Z}_{m^*n}\mathbf{Z}^{\dagger}_{n^*m}$ or $\mathbf{Z}^{\dagger}_{n^*m}\mathbf{Z}_{m^*n}$.

The PCA model forms the basis of the method to be used here with the atmospheric aerosol composition data. Not only does it avoid the problem of estimating communalities, but the matrix decomposition gives the basic structure of the data matrix $\mathbf{X}_{m^*n}$ regardless of whether $\mathbf{Z}_{m^*n}\mathbf{Z}^{\dagger}_{n^*m}$ or $\mathbf{Z}^{\dagger}_{n^*m}\mathbf{Z}_{m^*n}$ is examined. The main disadvantages of the PCA model which remain to be dealt with are the scale-dependence, the number of significant factors, and the rotation to apply to the factor loading matrix.

3.1 Data Preprocessing

All of the data sets to be described were obtained from elsewhere. None were collected with the intention of applying FA methods, nor was there any opportunity for input as to sampling sites, sampling procedures, nor the chemical species which were to be measured.

The first steps of this procedure are the same as those listed by Joreskog et al. (1976) under the heading 'Imbrie Q-mode analysis'. The scaling procedure seems to have originated with Imbrie and Purdy (1962) who were concerned with the chemical analysis of geological samples, as was Joreskog et al. (1976). The rotation techniques have been refined by Malinowski and Howery (1980) for studies in chemistry, and they have been most recently applied by Hopke and co-workers for use with atmospheric aerosol samples (Alpert and Hopke, 1980; Hopke, 1981; Alpert and Hopke, 1981; Roscoe and Hopke 1981a, 1981b; Liu

et al., 1982; Hwang et al., 1984).

Since the aim of the analysis is to profile the constituent sources of the aerosol according to chemical composition, the most important information is the relative proportion of each of the elements in each sample (Q-mode FA). Joreskog et al. (1976) recommended the use of Imbrie and Purdy's (1962) 'index of proportional similarity', also known as cosine theta:

$$\cos\ \theta_{ij} = \frac{\sum_{j=1}^{n} x_{ij}\ x_{kj}}{\{\sum_{j=1}^{n} x_{ij}\} \sum_{j=1}^{n} x_{kj}^{2}\ \}^{1/2}} \qquad (3.5)$$

$i=1,2,....m \qquad\qquad k=1,2,....m$

This is just the cosine of the angle between each pair of row vectors of the data matrix $\mathbf{X}_{m^*n}$. Cosine theta ranges from zero (orthogonal vectors; no similarity) to a value of 1.0 (parallel vectors; identical samples, within a constant multiplier). Computing cosine theta for all possible combinations of samples gives the association matrix $\mathbf{H}_{m^*m}$.

The association matrix can be calculated in another way, one which is more in line with the usual FA terminology described earlier, and with the terminology of Hwang et al. (1984), Rozett and Petersen (1975), and Malinowski and Howery (1980):

$$\mathbf{H}_{m^*m} = (\mathbf{D}^{-1/2}_{m^*m}\mathbf{X}_{m^*n})\ (\mathbf{X}^{\dagger}_{n^*m}\mathbf{D}^{-1/2}_{m^*m}) \qquad (3.6)$$

$\mathbf{D}_{m^*m}$ is a diagonal matrix with elements equal to the row sum of squares of the data matrix $\mathbf{X}_{m^*n}$. In the parlance of factor analysts, the association matrix is equivalent to a Q-mode analysis of the covariance about the origin.

If $m > n$, as usually happens, then the matrix $\mathbf{H}_{m^*m}$ will be very large and the computation of the eigenvalues will be rather expensive. The computations are also unnecessary since only a maximum of $p \leq n < m$ eigenvalues can be significant. This is where the Eckart-Young theorem has a very practical value, since the eigenvalues of

$$G_{n*n} = (D^{-1/2}_{m*m} X^{\dagger}_{n*m})\,(X_{m*n} D^{-1/2}_{m*m}) \qquad (3.7)$$

can be calculated instead of using H_{m*m}; the positive eigenvalues of Eqn. 3.7 are the same as those of Eqn. 3.6 (Joreskog et al., 1976).

All of these product moment matrices are real and symmetric, and finding the eigenvalues does not present much difficulty.[4] It is also possible to operate on the data matrix directly and calculate the sub-matrices S_{m*p} and $F^{\dagger}_{p*n}$ without finding the eigenvalues of any product moment matrix. Appendix A is a *FORTRANVS program to do this, based on the Basic Structure Single Factoring algorithm of Horst (1965). It was proven by Horst (1965) that the method is both a rank reduction solution[5] and a basic structure solution,[6] so the method will ultimately give the same results as the more common eigenvalue decomposition of the product moment matrix. A numerical example of this equality is given by Horst (1965).

3.2 Missing Data

The Basic Structure Single Factoring Method is convenient and economical in some instances, but would require extensive modifications with data sets where missing data are a problem. This problem also arises when product-moment eigenvalue methods are used, but it is slightly easier to devise alternative procedures. The problem of missing data is one which has tended to be overlooked. In an aerosol monitoring program, the number of samples for which there is a complete set of element concentrations available depends on the sensitivity of chemical analysis method. If trace elements such as heavy metals are included, there may be many samples where the concentrations are below the sensitivity of the chemical analysis method (or 'bdl', below detection limits). Treating these samples as missing data will

---

[4]Various 'canned' software programs, such as routine EIGRS in the IMSL mathematical package (Anon., 1979), were tested, as well as the eigenvalue routines in the BMDP (Dixon, 1983) and SPSSx (Anon., 1986) packages by entering the FA routines with a pre-calculated product moment matrix. No significant differences were found.

[5]A factor loading vector and the corresponding factor score vector are derived simultaneously at each stage; the major product of these vectors subtracted from the residual data matrix reduces the rank by exactly 1.

[6]Each basic structure factor accounts for the maximum variance in the matrix from which it was calculated.

introduce a systematic error and bias the subsequent FA by weighting those samples which have all concentrations above the detection limits, possibly completely ignoring those samples where the concentrations of one or more chemical species are 'bdl'.

Such is the case, unfortunately, when BFA methods are implemented using the default values of a statistical software package. If any variable is coded as missing or 'bdl', the default procedure is to delete the entire case or sample from the analysis. Alternatives exist. The mean value of the non-missing cases could be substituted for all the missing values of a variable; this is only valid for true missing values, not for 'bdl' values. Or product moment calculations can be carried out using means and variances from all available data for each element; again, this introduces a bias towards complete samples which are those with higher concentrations. Or the data set could be split into two (or more) sets, which are separately analysed and later compared.

There are no fixed guidelines on how to cope with 'bdl' values. The method suggested here is to select a comprehensive data set, that is, one including as many variables as possible without introducing an exorbitant number of 'bdl' values, certainly $< 5\%$ of the product of m and n. The product moment matrix can be calculated (Eqn. 3.7) using the non-missing, non-'bdl' values, and the partial products of terms with one or both values 'bdl' are set to zero. This has the practical, and desirable, effect of biasing the elements of the product-moment matrix G_{n*n} according to the pattern of each pair of row vectors. For instance, the dot products of

$$\mathbf{x} = (\ .183,\ .365,\ \text{bdl},\ .913\ )$$
$$\mathbf{y} = (\ .267,\ .535,\ \text{bdl},\ .802\ )$$

$$\mathbf{x} = (\ .707,\ \text{bdl},\ .707,\ \text{bdl}\ )$$
$$\mathbf{y} = (\ \text{bdl},\ .707,\ \text{bdl},\ .707\ )$$

are 0.976 and 0.0, respectively, which agrees with the intuitive appraisal that the first two vectors have both pattern and magnitude similarity while the second pair are perfectly uncorrelated. This is, of course, equivalent to setting 'bdl' values equal to zero. The validity of this assumption depends on the actual sensitivity of the chemical analysis method (ie., the cut-off level at which the element concentrations are labelled 'bdl'). If the detection limits are

low, then classifying 'bdl' values as functionally equivalent to zero is a reasonable approach. But if the opposite is true, then that variable should be excluded from the analysis or be used to divide the data into two sets which are analyzed separately.

3.3 Number of Factors

The common methods for determining the number of significant factors, used extensively by social scientists, are described in standard texts such as those by Harman (1967) and Rummel (1970). The more recent applications of FA methods to the physical sciences have sparked a number of advances. The main reason for this lies in the nature of the raw observations, which are physical quantities that (usually) can be rigidly defined and can be measured with a known precision. Malinowski and Howery (1980) summarized several tests for factors which are based on the experimental error in the data. In general, there is less emphasis on the significance of individual eigenvalues (abstract mathematical quantities), and more concern with the physical interpretability of the data and results.

The keystone for the newer approach is the 'reproducibility' of the PCA model. With all $p = n$ factors, the product of the factor score and factor loading matrices is $\mathbf{S}_{m*p}\mathbf{Y}^{\dagger}_{p*n} = \mathbf{X}_{m*n}$. Factors can be extracted successively until all of the non-error variance has been included. The remaining data then have a variance equal to the experimental error in the original data, and may be ignored.

There are problems with this approach too. The actual error or uncertainty in the data should be known reasonably well and should not be just a limit error, such as is expressed by the statement "the element concentrations are believed to be accurate to better than ±50%". The error analysis methods would tend, in this case, to ignore data which are really significant. And there is still ambiguity in some of the tests as to just what is significant and what is negligible.

The multiple-test method seems to be the safest one, and it was used here. Several tests are calculated for each value of p. When two or more tests indicate the same number of significant factors, the analyst will justifiably have more confidence in the results. But as often

happens, the choice remains unclear and there is still a certain degree of subjectivity involved. One very simple way to circumvent (not overcome) the problem is to consider the selection of p factors as a testing of the consequences of this number of factors.

The tests used here were:

1. VAR - percent of the total variance in the data associated with each eigenvalue.
2. CPV - cumulative percent variance, which is equal to the cumulative total of the p VAR values.
3. SCR - scree test, or percent of the total variance remaining in the residual data matrix.
4. IME - imbedded error, a measure of the difference between the pure data and the factor analysis reproduced data.
5. IND - Malinowski Indicator function; the physical meaning of this parameter is uncertain, but it has been claimed to give good results (Malinowski and Howery, 1980). It is defined as:

$$IND = \frac{1}{(n-p)^2} \cdot \left\{ \frac{\sum_{p+1}^{n} \lambda}{m(n-p)} \right\}^{1/2}$$

where λ_j is the j^{th} eigenvalue. A minimum in this function (when it exists) is assumed to indicate the correct number of factors.

6. RSD - residual standard deviation, approximately equal to the difference between the pure data and the raw experimental data.
7. XNR - the Exner function, a measure of the deviations between the raw data set and the data reproduced with only p factors (Exner, 1966).

The tests are described in detail by Malinowski and Howery (1980). The calculations can be simplified considerably by noting that, for Q-mode analysis of the covariance about the origin, the sum of all the eigenvalues is equal to m. Some of these tests (CPV, IME, RSD) require a knowledge of the true experimental error in the data in order to make a comparison. Others (VAR, XNR) require assigning some sort of critical value which corresponds to the boundary between pure data and error. SCR and IND are mathematical functions which may

change abruptly at the transition from significant data to errors or negligible data.

Of all these tests, the Exner function was found to be the most reliable. It also required the most computations, since the data set is re-calculated *n* times. It was derived by Exner (1966) specifically for additive data, and gives a direct measure of the deviation between the original and re-constructed data matrices:

$$XNR = \{ \frac{\sum_i \sum_j (x_{ij} - x'_{ij})^2}{\sum_i \sum_j (x_{ij} - \bar{x})^2} \cdot \frac{mn}{(mn - p)} \}^{1/2} \qquad (3.8)$$

where the x_{ij} are the elements of the original data matrix, the x'_{ij} are the elements of the data matrix re-calculated with *p* factors, and $\bar{x}$ is the grand mean of all the x_{ij}. By assuming that the deviations $(x_{ij} - x'_{ij})$ have a normal distribution, Exner (1966) described how the t-test can be used to judge the appropriate theory which, for FA studies, is the hypothesis that *p* is the true number of significant factors. Table 3.2 is a rough guide for acceptable values of XNR. A value of XNR $\sim<0.1$ was judged to be acceptable with most of the aerosol data here.

Table 3.2 Values of the Exner function.

XNR	Quality of Fit
0.02	very good agreement
0.1	good
0.2	fair
0.5	upper limit for acceptability
>0.5	unacceptable

3.4 Target Rotation

While Varimax and other rotation methods will satisfy the appropriate analytic criteria, there is no reason to suppose that such criteria have physical significance. Moreover, it would be unusual to have no idea of some of the sources of atmospheric aerosol which might be important at a monitoring site; at the very least one should expect a crustal component derived from wind-blown dust and soil. Any existing knowledge of the chemical profiles of major aerosol sources can be incorporated into the analysis at the rotation stage. Once an acceptable number of factors is found, then the factor loading matrix $\mathbf{F}_{n^*p}$ can be rotated to a best fit with known or hypothesized factors. This also provides a way of testing the significance of an hypothesized source profile, since the factor space is, in effect, being searched for that vector. If the suspected source is not identified with one of the p factors, then the rotation will produce a best fit vector which is dissimilar from the original target vector.[7]

Given the unrotated factor loading matrix $\mathbf{F}_{n^*p}$ and the hypothesized factor loading matrix $\mathbf{Y}^{\ddagger}_{n^*p}$ composed of columns which are the suspected aerosol source profiles, then the goal is to find the transformation matrix $\mathbf{T}_{p^*p}$ such that

$$\mathbf{F}_{n^*p}\mathbf{T}_{p^*p} = \mathbf{Y}^{\ddagger}_{n^*p} + \mathbf{D}_{n^*p} \tag{3.9}$$

where $\mathbf{D}_{n^*p}$ is a matrix of fitting errors. Pre-multiplying by $\mathbf{F}^{\dagger}_{p^*n}$ gives:

$$\mathbf{F}^{\dagger}_{p^*n}\mathbf{F}_{n^*p}\mathbf{T}_{p^*p} = \mathbf{F}^{\dagger}_{p^*n}\mathbf{Y}^{\ddagger}_{n^*p} + \mathbf{F}^{\dagger}_{p^*n}\mathbf{D}_{n^*p} \tag{3.10}$$

If $\mathbf{D}_{n^*p}$ is uncorrelated with $\mathbf{F}_{n^*p}$:

$$\mathbf{F}^{\dagger}_{p^*n}\mathbf{D}_{n^*p} = \mathbf{O}_{p^*p}$$

$$\mathbf{F}^{\dagger}_{p^*n}\mathbf{F}_{n^*p}\mathbf{T}_{p^*p} = \mathbf{F}^{\dagger}_{p^*n}\mathbf{Y}^{\ddagger}_{n^*p}$$

$$\mathbf{T}_{p^*p} = (\mathbf{F}^{\dagger}_{p^*n}\mathbf{F}_{n^*p})^{-1}\mathbf{F}^{\dagger}_{p^*n}\mathbf{Y}^{\ddagger}_{n^*p}$$

or

$$\mathbf{T}_{p^*p} = \mathbf{L}^{-1}_{p^*p}\mathbf{F}^{\dagger}_{p^*n}\mathbf{Y}^{\ddagger}_{n^*p} \tag{3.11}$$

The transformation matrix $\mathbf{T}_{p^*p}$ gives the best fit matrix $\mathbf{Y}_{n^*p}$, in a least squares sense (Rummel, 1970; Alpert and Hopke, 1980), of the factor loading matrix $\mathbf{F}_{n^*p}$ to the target

---

[7]The target and derived factors are most easily manipulated as vectors. Some measures of vector similarity are (Rummel, 1970):

- visual (subjective)
- root mean square coefficient
- coefficient of congruence

matrix $\mathbf{Y}^{\ddagger}_{n^* p}$. That is,

$$\mathbf{F}_{n^* p}\mathbf{T}_{p^* p} = \mathbf{Y}_{n^* p} \tag{3.12}$$

The least squares nature of the target rotation is demonstrated in Appendix B. The column vectors of $\mathbf{Y}_{n^* p}$ may still be orthogonal, depending on the rotation. More likely, $\mathbf{T}_{p^* p}$ will be an oblique rotation so that the orthogonality of the columns of $\mathbf{Y}_{n^* p}$ is not preserved.

The method of target rotation is more commonly called Procrustean transformation[1] by social scientists (Hurley and Cattell, 1962; Mulaik, 1972). Either a complete target rotation matrix $\mathbf{Y}^{\ddagger}_{n^* p}$ can be specified, or else individual vectors can be tested (recommended by Malinowski and Howery, 1980, and Alpert and Hopke, 1980). The procedure suggested here is to first use a Varimax rotation on $\mathbf{F}_{n^* p}$ to give $\mathbf{F}^{\ddagger}_{n^* p}$; this has the advantage of making the preliminary identification of the suspected factors (crustal, sea salt, industrial sources) somewhat easier. Target rotation can then be applied to $\mathbf{F}_{n^* p}$ (or $\mathbf{F}^{\ddagger}_{n^* p}$, which is really the same as $\mathbf{F}_{n^* p}$) with individual test vectors in order to refine the source profiles. A final operation on the factor loading matrix is necessary in order to remove the effects of the variable weights from the source profiles; this can be done simply by multiplying the factor loading matrix by $\mathbf{W}^{-1}_{n^* n}$. The result is a matrix of vectors which are the relative concentrations of the chemical species in each of the p sources.

If the factor score matrix $\mathbf{S}_{m^* p}$ was already derived from Eqn 2.11, then an inverse rotation must be applied to it in order to preserve the basic model:

$$\mathbf{S}_{m^* p} = (\mathbf{Z}_{m^* n}\mathbf{F}_{n^* p}\mathbf{L}^{-1}_{p^* p})\,(\mathbf{T}^{\dagger}_{p^* p})^{-1} \tag{3.13}$$

since $$\mathbf{Z}_{m^* n} = \mathbf{S}_{m^* p}(\mathbf{T}^{\dagger}_{p^* p})^{-1}(\mathbf{F}_{n^* p}\mathbf{T}_{p^* p})^{\dagger}$$

Otherwise, the factor scores can be calculated directly from $\mathbf{Y}_{n^* p}$

$$\mathbf{S}_{m^* p} = \mathbf{Z}_{m^* n}\mathbf{Y}_{n^* p}\mathbf{P}^{-1}_{p^* p} \tag{3.14}$$

where $\mathbf{P}_{p^* p} = \mathbf{Y}^{\dagger}_{p^* n}\mathbf{Y}_{n^* p}$ is the matrix of correlations between the p factors. This matrix arises when the dot products of the columns of $\mathbf{Y}_{n^* p}$ are not zero (oblique factors). Then the PCA model becomes

[1]Procrustes was a bandit in Greek mythology whose victims were strapped to a bed and had their legs cut off or stretched to fit the length of the bed.

$$\mathbf{Z}_{m^*n} = \mathbf{S}_{m^*p}\mathbf{Y}^{\dagger}_{p^*n} \tag{3.15}$$

and the matrix $\mathbf{Y}_{n^*p}$ is called the primary pattern matrix. Eqn. 2.10 becomes:

$$\mathbf{R}_{n^*n} = \mathbf{Y}_{n^*p}\mathbf{P}_{p^*p}\mathbf{Y}^{\dagger}_{p^*n} \tag{3.16}$$

In the orthogonal case, $\mathbf{P}_{p^*p}$ would be an identity matrix.

The factor scores can also be calculated from the original data matrix $\mathbf{X}_{m^*n}$ instead of the scaled and weighted data matrix $\mathbf{Z}_{m^*n}$ in Eqn. 3.13. While the scaling matrix $\mathbf{V}_{m^*m}$ can be by-passed, the variable weights contained in the $\mathbf{W}_{n^*n}$ matrix must be added to the calculations for the factor scores. Now if, instead of $\mathbf{L}_{p^*p} = \mathbf{F}^{\dagger}_{p^*n}\mathbf{F}_{n^*p}$, the weighted matrix

$$\mathbf{L}_{p^*p} = \mathbf{F}^{\dagger}_{p^*n}\mathbf{W}^{-1}_{n^*n}\mathbf{F}_{n^*p} \tag{3.17}$$

is used, then Eqn. 3.13 becomes:

$$\mathbf{S}_{p^*p} = \mathbf{X}_{n^*p}\mathbf{F}_{n^*p}\mathbf{L}^{-1}_{p^*p}(\mathbf{T}^{\dagger}_{p^*p})^{-1} \tag{3.18}$$

Post-multiplication of Eqn. 3.18 by $\mathbf{Y}^{\ddagger}_{p^*n} = (\mathbf{F}_{n^*p}\mathbf{T}_{p^*p})^{\dagger}$ will show that the PCA model $\mathbf{X}_{m^*n} = \mathbf{S}_{m^*p}\mathbf{F}^{\dagger}_{p^*n}$ has been transformed only by a rotation. If all factors were retained ($p = n$), then the original data could be re-calculated exactly from $\mathbf{S}_{m^*p}$ and $\mathbf{Y}^{\dagger}_{p^*n}$.

3.5 Source Scaling

The rotated factor solution gives the best fit of the hypothetical source profiles to the actual data, but there is one more parameter which must be calculated if the PCA model is to be used to determine the actual source strengths in accordance with the physical interpretation assigned to Eqn. 2.1. The factor loading and factor score matrices contain only the relative profiles and source contributions. This is a major advantage of FA methods, since it is the reason why binary, normalized, or even measured absolute source concentration profiles can be tested. It still remains, however, to determine the scaling parameters (represented by elements of the diagonal matrix $\mathbf{A}_{p^*p}$) such that:

$$\mathbf{X}_{m^*n} = (\mathbf{S}_{m^*p}\mathbf{A}_{p^*p})(\mathbf{A}^{-1}_{p^*p}\mathbf{Y}^{\dagger}_{p^*n}) \tag{3.19}$$

This can be done quite easily if the total mass of each sample (TSP, or Total Suspended Particulates) is known. Hopke et al. (1980) and Alpert and Hopke (1981) used multiple linear regression (MLR), with TSP as the dependent variable and the p relative source contributions

(columns of S_{m*p}) as the independent variables. The MLR coefficients can then be used to scale the factor loadings and the factor scores to physically realistic units.

This method of determining the scaling vector is simple and straight-forward, but it is only valid with an important assumption. It seems unlikely that an aerosol sample could ever be analyzed for the concentrations of all of the constituent elements; much of the mass is likely to be due to elements sueh as oxygen and nitrogen. For instance, the crustal component in the sample will contain elements such as Si, Al, Fe, etc., as oxides, but the analytical methods used will only give the concentrations of these elements. The result is that the sum of all the measured element concentrations is less than the TSP value. This does not prevent the use of the TSP-MLR method for determining the scaling parameters, as long as it can be assumed that the fraction of the total mass which is actually measured from each component is a constant. If, say, the measured Si, Al, and Fe concentrations represent the crustal component in the aerosol samples, then the TSP-MLR method is valid if these elements are always a fixed proportion of the total mass from the crustal source.

This assumption is not unique to FA methods. It would seem to be a necessary assumption for the interpretation of any set of composition data where the total mass of the sample has not been partitioned into all of its elemental components.

Source scaling is, in a sense, the last step in the return journey from somewhat abstract mathematics to the physical world. There are a number of stops along the way, however, where it is possible to check that the results conform to a physical interpretation. For instance, application of the linearly-additive model of Eqn. 2.1 to aerosol sources does not admit negative terms in the chemical profiles of the aerosol sources (the factors), nor in the source strengths for each sample (the factor scores). But the PCA model is not constrained to give only positive elements in F_{n*p} and S_{m*p}, as is readily seen by an examination of any of the raw factor loading matrices of later chapters.

This constraint on the factor loadings was added as part of the target rotation phase. Rotated vectors with large negative elements were assumed to be a signal that the test vector (and the product vector) were not factors representing aerosol sources. The negative elements

were replaced by zero, and a new target rotation tried. In most cases, a stable refined vector with only a few small negative elements could be derived in several iterations. When this did not happen, the hypothetical source type was rejected.

No constraint of this sort could be applied during the calculation of the factor scores, since these are already fixed by the original data and the selected factors. Negative scores were arbitrarily replaced by zero, which will be interpreted as the absence of a mass contribution from the corresponding source in those samples. This substitution was made after examining the scores in order to determine that most of the scores for each factor were greater than zero; otherwise, the factor was rejected.

Source scaling, when it could be used, provided a third check on the physical significance of the factors. The scaling was expected to give aerosol profiles which were 'reasonable looking'; that is, concentrations of major elements were on the order of 100 mg-g^{-1}, and the sum of all elements was less than 1000 mg-g^{-1}. Furthermore, the regression model TSP = $\sum_{i=1}^{p} a_i S_i$.) was assumed; a calculation with a regression model of the form TSP = $a_0 + \sum_{i=1}^{p} a_i S_i$.) should show the constant term to be small. If not, or if the scaled aerosol source profiles were physically unreasonable, then this was an indication of a major problem with the selected set of factors.

3.6 Errors in the Source Profiles

This is perhaps the weakest part of TFA. It is not clear how all of the uncertainties involved will propagate through the many steps of the TFA procedure. Roscoe and Hopke (1981b) devised a method which partitioned the differences between the raw data and the data re-constructed with *p* factors, but this method is still only an approximation.

The errors in the factor loadings (source profiles) are estimated here by a simplified form of the Roscoe and Hopke (1981b) approach. An average error vector e_n is calculated for each of the *n* variables from

$$e_n = \{\frac{1}{m}\sum_{l} (x_{ij} - x'_{ij}) \}^{1/2} \qquad (3.20)$$

where the x_{ij} and x'_{ij} are the elements of the raw and re-constructed data matrices,

respectively. The average error for each variable is divided among the p factors by multiplying by:

$$\frac{\{\mathrm{diag}(\mathbf{L}^{-1}_{p^*p})\}^{1/2}}{\{\mathrm{trace}(\mathbf{L}^{-1}_{p^*p})\}} \tag{3.21}$$

where $$\mathbf{L}_{p^*p} = \mathbf{Y}^{\dagger}_{p^*n}\mathbf{W}_{n^*n}\mathbf{Y}_{n^*p}$$

That is, the errors in the elements of the factor loading matrix $\mathbf{Y}_{n^*p}$ are:

$$\sigma_{n^*p} = \mathbf{e}_n \frac{\{\mathrm{diag}(\mathbf{L}^{-1}_{p^*p})\}^{1/2}}{\{\mathrm{trace}(\mathbf{L}^{-1}_{p^*p})\}} \tag{3.22}$$

Errors in the factor scores are assumed to be only due to fitting errors from the multiple linear regression.

3.7 Summary of the TFA Procedure

Following is the step-by-step procedure for Target Factor Analysis of a data set which is composed of the concentrations of chemical species in a number of individual samples.

1. Form the data matrix $\mathbf{X}_{m^*n}$.

   Each of the n columns of the matrix is a vector representing the measured concentrations of the j^{th} species. Each row is a vector of species concentrations in each sample. Variables (chemical species) or samples with more than ~5% of the values 'bdl' should be omitted.

2. Multiply each column of $\mathbf{X}_{m^*n}$ by a weighting factor, if necessary.

   If a variable is more, or less, significant than the others, then the weighting factor can be selected accordingly. This is particularly useful when the analytical uncertainties in the measured concentrations are different for the chemical species. Otherwise, weights should be used which will give roughly the same range (order of magnitude) of values in each column.

3. Normalize each row of the weighted data matrix to unit length.

   This normalization will give equal weight to each sample and still preserve the

relative proportions of the chemical species in each sample.

4. Calculate the minor product moment matrix $\mathbf{R}_{n^*n}$:

$$\mathbf{R}_{n^*n} = (\mathbf{V}^{-1/2}_{m^*m}\mathbf{X}_{m^*n}\mathbf{W}_{n^*n})^{\dagger}(\mathbf{V}^{-1/2}_{m^*m}\mathbf{X}_{m^*n}\mathbf{W}_{n^*n})$$

The diagonal matrix $\mathbf{W}_{n^*n}$ contains the weighting factors applied in Step 2. $\mathbf{V}_{m^*m}$ is a diagonal matrix with elements equal to the row sum of squares of the weighted data matrix $\mathbf{X}_{m^*n}\mathbf{W}_{n^*n}$ from Step 3.

5. Calculate the eigenvalues and eigenvectors of $\mathbf{R}_{n^*n}$.

The scaled eigenvector matrix is the raw factor loading matrix $\mathbf{F}_{n^*n}$.

6. Apply several tests for the significance of the factors, and discard insignificant factors. Factors which are clearly insignificant according to all tests should be dropped.

If the tests do not all indicate the same number p of significant factors, retain the larger number. Alternatively, select an arbitrary number of factors which are sufficient to profile the major sources.

7. Use a Varimax rotation to find an approximate orthogonal simple structure matrix.

Consider again the tests for the significance of the factors and drop any insignificant factors.

8. Construct and test individual source profile vectors $\mathbf{y}^{\ddagger}_{n}$.

In the absence of any other information, binary test vectors can be used which have elements equal to 0 or 1. Use the results of each least squares rotation of $\mathbf{F}_{n^*p}$ to refine the test vector, and repeat the target rotation until the calculated best fit vector has converged to a stable profile $\mathbf{y}_n$. The stability can be checked by varying the elements of $\mathbf{y}_n$ slightly, and doing another target rotation. If the vector is stable (ie., associated with a well-defined cluster of variables), then the small changes in the test vector have no effect and the calculated best fit vector $\mathbf{y}_n$ will not change.

9. Collect the p refined vectors into the rotated factor loading matrix $\mathbf{Y}_{n^*p}$.

The associated rotation vectors form the columns of the rotation matrix $\mathbf{T}_{p^*p}$. Compute the factor correlation matrix $\mathbf{P}_{p^*p} = \mathbf{Y}^{\dagger}_{p^*n}\mathbf{Y}_{n^*p}$. Factors which are

highly correlated (~> 0.9) may really represent the same source, within a scaling factor. Unless there is additional information to justify retaining these factors, such as previous knowledge of the actual sources, or possibly a difference in a unique 'marker' element for different sources, then only one of these should be kept.

10. The corresponding factor score matrix can be calculated from Eqn. 3.18.

    Use multiple linear regression to find the p scaling parameters for the sources. If the regression calculations are made with TSP in ug-m^{-3} then the individual source contributions (in units of ug-m^{-3}) are equal to $S_{m*p}A_{p*p}$, and the source concentration profiles (mg-g^{-1}) are equal to 1000 x $Y_{n*p}A^{-1}_{p*p}$.

3.8 Variations of the TFA Procedure

The TFA procedure outlined in this chapter was designed specifically for aerosol source apportionment from composition data. Many modifications and extensions are possible; one such procedure will be described for the analysis of data from large air quality networks.

The Inco stack at Sudbury is one of the largest point sources of sulphur compounds in the world. Yet initial analysis of precipitation chemistry data from a monitoring network in the Sudbury basin revealed no significant change in acidic deposition during a nine-month shut-down of the refining operations; only after an effort was made to determine background levels, and amounts transported into the region, could a 10% - 20% reduction in acidic deposition be identified (comments by M. Lusis during a panel discussion on air quality monitoring networks, reported in Pierce et al., 1982, p. 445-446). Meteorological variability and the small local contribution from the 380 m stack were cited as possible causes for this.

It would be interesting to perform an eigenvalue analysis of monthly CANSAP[9] precipitation chemistry data (time versus station,distance), and then attempt a target rotation of the factor score matrix to a record of monthly emission data for the Inco operations. This assumes that there would be sufficient variability in the emissions data within the CANSAP

[9]CANSAP: Canadian Network for Sampling Precipitation (AES, 1978-1983)

sampling period to permit an identification of the Inco component. If so, then the rotation would give the best estimate (in a least squares sense) of the response of the system to the variation in the source strength. There are several considerations which may make this approach unsuccessful, however, such as the rather large uncertainties associated with CANSAP data (Barrie and Sirois, 1982) and the use of monthly average data, but it seems like a worthwhile experiment.

In a similar vein, there is a great deal of similarity between the linearly-additive models of FA and the atmospheric 'transfer matrix' model of Young and Shaw (1986), which may be of use in devising national control strategies (Shaw, 1986).

4. Examples of Factor Analysis of Atmospheric Data

Applications of FA methods to meteorological data sets seem to have originated with Lorenz (1956; cited by Barry and Perry, 1973). Craddock and Flintoff (1970) outlined the use of eigenvectors to describe the spatial structure of meteorological fields. Statistical considerations on the use of the PCA model (eigenvector method; empirical orthogonal functions), including tests for the significance of factors, have been discussed by Essenwanger (1976), Preisendorfer and Barnett (1977), and Buell (1975). A few examples of recent studies of FA methods in meteorology, which illustrate the diversity of the possible applications, are the papers by Essenwanger (1975), Schickedanz (1977), Blasing (1975), LeDrew (1980), and Pitchford and Pitchford (1985). These have mostly used the principal-component/empirical orthogonal-function approach to analyze a spatial correlation matrix, using procedures which fall under the heading of BFA.

BFA methods have been applied frequently to aerosol composition data from urban areas, beginning with Blifford and Meeker (1967). Other examples are the studies by Hopke et al. (1976), Gaarenstroom et al. (1977), Gatz (1978), Parekh and Husain (1981), and Tanner and Leaderer (1982). BFA methods have also been applied to aerosol composition data from remote areas such as Antarctica (Boutron and Martin, 1980; Shaw, 1983a), Alaska (Shaw, 1983a; Lowenthal and Rahn, 1985), the Canadian Arctic (Hopper, 1984), and Greenland (Heidam, 1981, 1982, 1984, 1985). The Antarctic study of Boutron and Martin (1980) and the study by Shaw (1983a) were somewhat different. Instead of collecting atmospheric aerosols on a filter, Boutron and Martin (1980) analyzed the composition of surface snow samples. Shaw (1983a) used surface and airborne impactors to collect aerosol samples, and then analyzed individual particles with a scanning electron microscope equipped with an energy dispersive X-ray spectrometer. His results describe the composition of individual particles, not the bulk sample.

TFA methods have been used with aerosol data from urban areas by Henry (1977), Hopke et al. (1980), Alpert and Hopke (1980, 1981), Hopke (1981), Liu et al. (1982), Roscoe and Hopke (1981a, 1981b), and Hwang et al. (1984). With a few small differences, the TFA

procedure described in Chapter 3 is the same as that developed by Hopke and co-workers. Henry's (1977) method is not exactly the same as the Hopke TFA method, but the differences are in the technical details rather than the overall approach, so it is reasonable to consider his method a forerunner of the Hopke TFA procedure. Some interesting discussions of the problems of using BFA, TFA, and FA methods in general with atmospheric aerosol samples, can be found in the comments of Hopke (1982), Redman and Zinsmeister (1982), and Heidam and Kronberg (1985).

The development and application of TFA methods for urban aerosol samples was stimulated in large part because of the potential for use as a receptor-oriented aerosol source apportionment model. TFA has several points in common with the more familiar chemical element balances (CEB) of Friedlander (1973), Gatz (1975), Kowalczyk et al. (1978), and Macias and Hopke (1981). The linearly-additive model of Eqn. 2.1 and Eqn. 2.2 is assumed to be valid, and source profile vectors are constructed for each of the p major aerosol sources in the area. A sub-set of the chemical species is formed by selecting elements which are strongly associated with only one or two of these sources.[10] These marker elements should also be "well-measured, relatively non-volatile, and sensitive to variations in the strengths of specific components" (Kowalczyk et al., 1978). A least-squares fit of the concentrations of the marker elements to the measured concentrations gives the fractional mass from each of the p sources.

The TFA procedure does much the same thing, with two important exceptions. The source profile vectors are, in a sense, compared to the actual or 'realizable' factors derived from the eigenvalue decomposition portion of the calculations. Or the factor space can be searched via the target rotation, and the best source profiles extracted and refined. In either case, relative source strengths (the factor scores) are found simultaneously, and need only be scaled by the TSP-MLR coefficients.

There have been no published applications of TFA methods to aerosol samples from remote areas.

---

[10]A sub-set of chemical species must be used because the problem is over-defined; that is, there might be n different elemental concentrations known, but there are only p ($< n$) major sources known/assumed/postulated.

4.1 TFA of Cloudwater Data

This data set is composed of the concentrations of six elements (silver, iron, manganese, magnesium, potassium, sodium) and three anions (chloride, nitrate, sulphate) observed in cloud droplets. The samples were collected by a cryogenic impactor mounted on an aircraft during a co-operative experiment in August 1983 between the Desert Research Institute and the Alberta Hail Project (Stone and Warburton, 1984). Most of the samples were collected in the Hail Project target area in south-central Alberta, although several were also collected downwind of a ground-based seeding network near Lethbridge. Both seeded (with AgI) and non-seeded clouds were sampled, the latter samples usually obtained during an initial 'background' pass through the target cloud. The main goal of the experiment was to evaluate the use of the observed silver concentration as a cloud-seeding signature.

Full details of the chemistry portion of the experiment are given by Stone and Warburton (1984). Typically, sample volumes of ~5 - 20 cm^3 were accumulated during each pass through a cloud, with an integrating time of 2 - 20 minutes. Table 4.1 and Table 4.2 describe the samples and list the measured concentrations (copied from the report by Stone and Warburton, 1984). The instrumental uncertainties (upper limits) of the analytical procedures were 5% for the anions, 20% for Ag, and 10% for the other elements.

The major conclusions from the experiment were (Stone and Warburton, 1984):

1. The difference in the Ag concentration between the seeded and non-seeded clouds was statistically significant. The background (non-seeded) Ag concentration was low and relatively stable, ~$(36.6 \pm 10.) \times 10^{-12}$ g - ml^{-1}.
2. There were no significant differences between seeded and non-seeded clouds in the remaining species concentrations.
3. The Ag concentration was linearly proportional to the mean ice crystal concentration ($r^2 = 0.69$) (both seeded and non-seeded clouds).
4. Ag concentrations were at the background level in clouds sampled downwind of the ground-based seeding network.

These data are from a complex mixed-phase system, so one would not expect the simple

Table 4.1 Cloudwater sample descriptions.

ID #	Date	Collection Time (GMT)	Cloud	Seed?	Volume (ml)	Sample Appearance	Code
1	83/08/08	2313-2326	A	yes	10.5	clear rime	1
2	83/08/08	2342-2352	B	yes	13.9	clear rime	1
3	83/08/08	2407-2418	C	yes	-0-	sample lost	
4	83/08/08	2447-2455	D	yes	9.9	rime+particulates	3
5	83/08/14	2107-2108	A	no	5.4	clear rime	
6	83/08/14	2113-2127	A	yes	8.8	clear rime	
7	83/08/14	2135-2136	B	no	4.0	clear rime	
8	83/08/14	2138-2149	B	yes	9.5	clear rime	
9	83/08/14	2209-2220	C	yes	7.8	clear rime	2
10	83/08/15	2155-2206	A	yes	-0-	sample lost	3
11	83/08/15	2213-2215	B	no	6.3	rime+particulates	
12	83/08/15	2219-2222	B	yes	8.4	clear rime	1
13	83/08/15	2224-2227	B	yes	8.0	clear rime	
14	83/08/15	2231-2233	C	no	6.5	clear rime	
15	83/08/15	2236-2238	C	yes	8.7	rime+particulates	
16	83/08/15	2242-2244	C	yes	9.5	clear rime	
17	83/08/15	2306-2316	D	yes	4.2	clear rime	1
18	83/08/15	2326-2329	E	no	6.2	clear rime	1
19	83/08/15	2331-2338	E	yes	8.2	clear rime	1
20	83/08/16	2042-2044	A	no	5.6	clear rime	
21	83/08/16	2046-2048	A	yes	7.7	rime+particulates	
22	83/08/16	2051-2053	A	yes	8.4	clear rime	2
23	83/08/16	2104-2106	B	no	18.1	clear rime	
24	83/08/16	2112-2113	B	no	8.3	clear rime	
25	83/08/16	2122-2124	C	no	9.4	clear rime	
26	83/08/16	2127-2132	C	no	17.1	rime+particulates	
27	83/08/16	2152-2156	D	yes	20.1	clear rime	2
28	83/08/16	2200-2206	D	yes	22.5	clear rime	
29	83/08/17	2242-2247	A	yes	7.4	opaque rime	
30	83/08/17	2258-2301	B	no	14.3	clear rime	
31	83/08/17	2306-2310	B	yes	7.2	rime+particulates	
32	83/08/17	2314-2319	B	yes	11.8	rime+particulates	
33	83/08/17	2323-2329	B	yes	5.8	particulates	
34	83/08/17	2359-2404	C	no	15.8	clear rime	
35	83/08/17	2406-2411	C	no	16.1	clear rime	
36	83/08/18	2235-2242	A	yes	6.9	clear rime	4
37	83/08/18	2247-2255	B	yes	9.5	rime+particulates	4
38	83/08/18	2257-2302	B	yes	7.3	rime+particulates	4
39	83/08/18	2304-2314	B	yes	19.2	rime+particulates	4
40	83/08/18	2324-2330	C	yes	5.5	clear rime	4

1 inaccurate volume measurement
2 known outlier
3 operational cloud base seeding mode
4 seeding by ground generators 100km upwind of sampled clouds

Table 4.2 Cloudwater sample concentrations. The concentrations are in 10^{-9} g-ml^{-1}, except for Ag which has concentration units of 10^{-12} g-ml^{-1}.

ID #	Ag	Na	Mg	Fe	Mn	K	Cl^-	NO_3^-	$SO_4^{=}$
4	36.6	147.6	474.8	15.6	27.8	106.8	58.7	333.4	537.1
5	56.8	369.2	661.7	28.3	25.7	142.1	74.1	356.3	985.7
6	33.4	967.9	353.0	186.7	52.2	1073.6	49.7	354.1	469.6
7	37.3	304.2	485.3	25.9	37.6	144.7	64.3	365.1	307.2
8	53.7	223.8	105.0	49.4	17.2	129.5	75.9	442.6	782.3
11	36.0	395.7	486.6	153.5	32.5	215.5	114.6	925.3	708.7
12	66.9	284.6	362.0	21.5	30.9	167.0	111.4	1029.3	728.4
13	46.4	258.3	668.2	65.4	41.4	175.2	114.9	962.9	1648.4
14	41.2	280.8	416.6	216.2	32.0	185.7	173.4	1103.1	986.2
15	83.3	267.3	208.6	107.0	8.0	114.8	80.3	712.7	709.5
16	54.2	492.7	376.0	172.1	18.4	285.3	99.7	955.0	435.1
17	111.5	399.6	490.0	177.3	40.9	328.0	243.3	3510.0	3210.0
18	30.1	187.2	465.9	65.5	18.2	167.7	129.9	1117.9	932.6
19	69.0	289.7	411.8	50.9	33.6	256.4	223.3	2534.0	1961.0
20	64.2	191.6	77.1	26.5	8.2	89.4	108.1	782.1	689.7
21	76.2	805.2	242.4	62.9	17.4	153.2	45.9	679.7	982.3
23	40.8	240.6	112.1	31.1	17.7	115.6	43.8	776.2	772.1
24	43.9	353.8	229.1	40.2	28.1	208.7	43.5	826.4	978.2
25	36.1	441.5	915.8	14.6	53.2	302.9	54.4	952.0	4215.0
26	38.3	190.0	293.1	27.0	17.6	124.6	53.9	926.0	1092.0
28	72.1	200.4	272.1	157.9	34.4	249.4	62.0	858.5	433.5
29	60.5	201.3	23.3	8.1	5.4	125.6	85.5	131.2	178.9
30	44.1	248.0	83.2	44.3	12.7	189.9	35.6	477.3	430.2
31	89.8	161.3	59.0	29.2	16.7	97.1	49.4	679.0	718.0
32	79.7	421.3	200.8	17.0	20.1	340.3	51.5	364.4	407.4
33	91.9	306.3	70.5	28.5	18.2	111.7	55.7	791.7	553.1
34	27.3	210.3	93.4	68.2	10.5	128.6	35.3	675.1	1235.5
35	26.6	134.2	106.6	75.7	15.1	68.5	28.8	806.5	1183.1
36	26.0	848.2	132.2	101.7	24.8	482.0	120.0	888.4	950.1
37	34.7	334.8	46.5	20.2	2.5	178.5	96.8	540.8	427.1
38	29.3	236.0	450.8	24.8	43.2	402.6	102.8	526.0	1974.0
39	29.3	129.6	215.1	32.9	33.4	107.7	130.4	807.6	993.2
40	26.6	392.4	266.3	33.3	24.5	329.4	153.1	1204.1	404.1

particle-source interpretation of Eqn. 2.1 to be valid. Nevertheless, it is an interesting data set on which the TFA methods can be tested.

Samples which were flagged in Table 4.1 as having a known outlier were deleted. The remaining thirty-three samples were combined into a single data matrix. Weights of 1.0 were assigned to all elements except Ag (weight = 0.5) because the emphasis was on the unperturbed cloudwater chemistry. A comparison with CANSAP data (AES, 1978-1983) for August 1983 shows that the mean concentrations of Na, Mg, K, Cl^-, NO_3^-, and SO_4^{2-} in the cloudwater samples are similar to the concentrations in precipitation reaching the ground. For this comparison, sodium, magnesium, and potassium are assumed to be present solely as cations. It should be emphasized that the CANSAP data are from composite precipitation samples collected during the month, while these cloudwater concentrations are averages from thirty-three samples of (usually) non-precipitating clouds. And the CANSAP samples may be contaminated, because soil and organic matter were visible in the samples.

	ppn	Na^+	Mg^{2+}	K^+	Cl^-	NO_3^-	SO_4^{2-}
CANSAP							
Rocky Mountain House	0.8	1.43	0.47	0.82	1.68	1.33	2.71
Coronation	1.8	0.09	0.15	0.13	0.14	1.90	2.61
CLOUDWATER							
mean		0.33	0.30	0.22	0.09	0.86	1.00
σ		0.20	0.21	0.18	0.05	0.63	0.83
maximum		0.97	0.92	1.07	0.24	3.51	4.22
minimum		0.13	0.02	0.07	0.03	0.13	0.18

(precipitation in cm.; all concentrations in $mg\text{-}l^{-1}$)

Table 4.3 displays the results of the eigenvalue calculations. [11] Both the Scree test and

[11]Only the lower left triangle of symmetric matrices will be shown.

Table 4.3 Cloudwater eigenvalue calculations.

Data set dimensions:	33	9						
Variable (column) weights:								
Ag	Na	Mg	Fe	Mn	K	Cl^-	NO_3^-	$SO_4^{=}$
0.5	1.0	1.0	1.0	1.0	1.0	1.0	1.0	1.0
Initial product moment matrix:								
0.026								
0.233	3.052							
0.142	1.806	2.110						
0.034	0.452	0.344	0.126					
0.014	0.166	0.155	0.030	0.014				
0.143	1.943	1.167	0.314	0.114	1.445			
0.065	0.672	0.470	0.109	0.042	0.425	0.217		
0.429	4.786	3.751	0.962	0.333	3.001	1.361	12.103	
72.4	98.4	100.0	68.1	91.2	93.8	77.9	100.0	100.0
Total variance (covar0):								
0.026	3.052	2.110	0.126	0.014	1.445	0.217	12.103	13.908
Eigenvectors (columns):								
0.128	-0.041	-0.008	0.023	-0.026	-0.042	0.014	0.067	-0.004
1.472	-0.818	-0.347	0.213	-0.220	0.038	-0.003	-0.003	0.000
1.175	-0.161	-0.316	-0.777	-0.008	-0.002	-0.007	0.000	-0.001
0.272	-0.098	0.034	-0.027	0.064	0.099	0.162	0.002	0.000
0.102	-0.024	-0.019	-0.032	0.013	-0.001	-0.004	0.011	0.030
0.931	-0.627	-0.274	0.144	0.297	-0.026	-0.024	0.001	-0.001
0.397	-0.107	0.013	0.011	-0.043	-0.199	0.080	-0.014	0.001
3.366	-0.173	0.859	-0.052	0.007	0.006	-0.017	-0.000	-0.000
3.621	0.728	-0.487	0.178	0.010	0.002	0.004	-0.000	-0.000
Eigenvalues:								
29.114	1.670	1.272	0.708	0.144	0.053	0.034	0.005	0.001
Significance tests for eigenvalues:								
#	EIGEN	VAR	CPV	SCR	IME	IND	RSD	XNR
1	29.114	88.22	88.22	11.776	0.040	0.00190	0.1213	0.4393
2	1.670	5.06	93.28	6.716	0.046	0.00200	0.0979	0.3209
3	1.272	3.86	97.14	2.860	0.040	0.00192	0.0690	0.1389
4	0.708	2.14	99.28	0.716	0.025	0.00151	0.0378	0.0838
5	0.144	0.44	99.72	0.281	0.020	0.00166	0.0265	0.0477
6	0.053	0.16	99.88	0.120	0.016	0.00222	0.0199	0.0370
7	0.034	0.10	99.98	0.017	0.008	0.00232	0.0092	0.0220
8	0.005	0.01	100.00	0.003	0.005	0.00522	0.0052	0.0060
9	0.001	0.00	100.00	0.000	0.000	0.00000	0.0000	0.0000
Varimax orthogonal rotation with 4 factors:								
0.057	0.473	0.378	0.072	0.037	0.243	0.158	1.586	2.792
0.100	1.468	0.460	0.175	0.058	1.030	0.261	1.368	1.356
0.061	0.515	0.371	0.177	0.039	0.287	0.222	2.474	1.376
0.040	0.597	1.272	0.136	0.079	0.390	0.164	1.262	1.542
Variances of rotated factors:			10.772	7.252	8.589	6.150		
% communalities (covar0) with 4 Varimax factors:								
72.4	98.4	100.0	68.1	91.2	93.8	77.9	100.0	100.0

the Malinowski Indicator function point to four or five significant factors. The Exner function does not give a clear indication of the number of factors in this case, but the 'satisfactory level' of XNR ~<0.1 is attained with four factors. Calculations with both four and five factors suggested that the fifth factor did not contribute to the final interpretation of the data, so only four factors were retained.

A Varimax rotation is also shown. The similar loadings on each rotated factor indicates that the variables have not really been separated into strong clusters associated with unique sources. Part of this is due to the magnitude of the NO_3^- and SO_4^{2-} concentrations which dominated the product-moment calculations. By deriving unique factors for each of these species through target rotation, their effects can, to some extent, be isolated from the other variables.

A number of hypothetical factors were devised for the target rotation phase. A crustal factor was assembled from the average relative abundances of elements in the earth's crust (Mason and Moore, 1982). A sea salt factor was taken from previous FA and CEB studies (Hopke, 1981; Kowalczyk et al., 1978); it differs from the chemical composition of bulk seawater principally by being depleted in chlorine. The remaining test factors were mostly binary vectors.

Four of these test vectors were found to be well matched with actual factors derived from the data. They were refined from the test vectors in, typically, 2-4 iterations. The initial and final vectors are compared in Table 4.4. Several other factors could also have been accepted, but on scrutiny it appeared that they were composites of two or more of the factors in Table 4.4. For instance, a 'vapour' factor was found which was equal to the sum of the sulphate and nitrate factors; it was dropped in favour of the two separate factors.

The third factor has been labelled 'soil', even though it was refined from a general test vector representing average crustal abundances. What is particularly notable about this factor is the deficiency in iron; this can also be seen in the raw concentration data of Table 4.2. This factor represents material originally derived from rocks but which has undergone considerable element fractionation by weathering. In highly simplified fashion (after Mason and

Table 4.4 Cloudwater target and final vectors.

Label	Ag	Na	Mg	Fe	Mn	K	Cl^-	NO_3^-	SO_4^{2-}
Crustal	0.000	0.570	0.420	1.000	0.020	0.520	0.003	0.000	0.000
	0.028	0.622	0.501	0.069	0.036	0.470	0.080	0.049	0.000
Nitrate NO_3^-	0.000	0.000	0.000	0.000	0.000	0.000	0.000	1.000	0.000
	0.013	0.017	0.000	0.068	0.004	-0.014	0.067	0.998	0.000
Sulphate SO_4^{2-}	0.000	0.000	0.000	0.000	0.000	0.000	0.000	0.000	1.000
	0.007	0.020	0.001	-0.028	0.002	-0.011	0.001	0.002	0.999
Magnesium Mg	0.000	0.000	0.000	0.000	0.000	0.000	0.000	1.000	0.000
	-0.014	-0.001	0.999	0.043	0.047	0.014	0.012	0.000	0.000

Correlation matrix of refined vectors:

1.000			
0.068	1.000		
0.007	0.001	1.000	
0.546	0.004	-0.000	1.000

Moore, 1982) the effects of weathering on the chemical composition of rocks might be illustrated as:

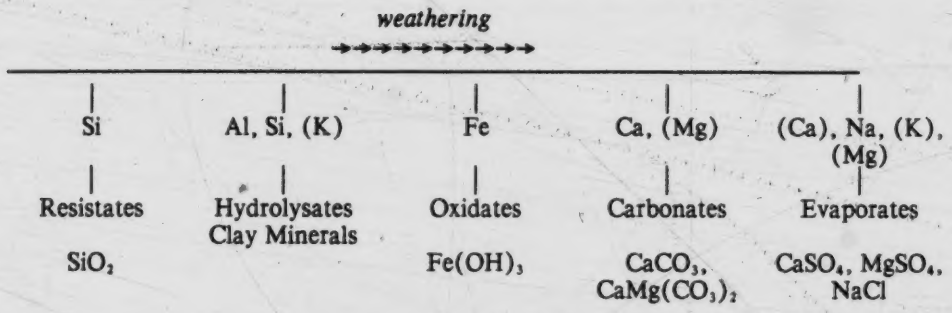

The soil factor thus represents the lighter, more friable material at the end of the weathering sequence. The relative concentrations in this factor are consistent with chemical analysis of glacial tills and soils in south-central Alberta. Glacial tills underlie most of the area east of the Rockies and form the parent material from which the soils are derived. Fe is present in concentrations of typically 2% - 3% and is correlated with minor elements such as B, Co, Cu, Zn, and Mb; the correlation reflects a common source, mainly associated with the clay-size fraction of the tills (Pawluk and Bayrock, 1969). On the other hand, the calcium content of tills (and the Mg and Na content, inferring from the data of Pawluk and Bayrock, 1969) is uncorrelated with Fe since Ca, Mg, and Na are mainly derived from silt-sized particles of sedimentary origin. As well, Ca, Mg, and Na can be found concentrated as soluble salts (Na_2SO_4, $CaSO_4$, $MgSO_4$, NaCl) on or near the surface in depressed areas because of leaching by rainwater. The concentration of Mg^{2+}, for example, is usually a few tenths of a percent or less in the surface layer of loams, but may reach 1% - 2% in salt crusts (Bowser et al., 1951).

The fourth factor derived, unique for magnesium, was necessary in order to explain the variability in the observed Mg concentrations. The data are too limited to permit a reasonable interpretation of this factor. It is tempting to say that the TFA procedure has differentiated

between a 'normal' soil component and a component from salt crusts or salt-enriched alkaline soils, but there is no support for this other than the presence of the weak magnesium factor. In addition, if the fourth factor is really indicative of such a source, it is surprising that there is not at least a small correlation with Na. The reliability of this analysis (and interpretability of the results) could have been greatly increased if the cloudwater samples had been analyzed for additional species, especially calcium. It has been observed in CANSAP samples that calcium and magnesium are both unrealistically high at sampling sites in the West, suggestive of sample contamination by basic salts (Barrie and Sirois, 1982). If true, then this source would also make a sizeable contribution to the total amount of SO_4^{2-} observed.

> "In the southern Prairies, central Alberta, and northeastern British Columbia, the acidity of precipitation is so low that a calcium correction estimate is meaningless. It suffices to point out that in these regions there is sufficient calcium present in CANSAP samples to neutralize rain with an acidity of pH 4.0, 4.5, and 4.7, respectively. If the calcium levels in these regions are indeed 50% or more contamination and originate from basic salts, the ability of the network to detect acid precipitation would be severely impaired. A study is needed to resolve this important question.
>
> ..... Insufficient evidence exists to do a comprehensive error assessment for data collected in western Canada. It is our opinion that in the Prairie region of western Canada SO_4^{2-} and NO_3^- concentrations in precipitation originate predominantly from the same sources as Ca^{2+}. Since CANSAP samples tend to have unrealistically high calcium levels, precipitation chemistry results in this region should be used with a great deal of caution." (Barrie and Sirois, 1982)

There is a need for further analysis of Alberta cloudwater samples, and an effort should be made to measure calcium concentrations. If cloudwater Mg and Ca are correlated and are both at levels comparable to those observed in ground-level precipitation collectors, then the latter cannot be explained solely by low-level contamination due to collector siting and sampling protocol. Rather, the high Ca and Mg concentrations are at least partially due to the

composition of the 'background' airborne particulates in this region. It is of interest to note that studies of airborne particles over the Great Plains of the United States (Hobbs et al., 1985) have shown that the ratio of the number of calcareous particles in a sample to the number of siliceous particles can vary widely, and appears to be dependent on the regional soil composition. A ratio of ~1 was observed over Texas, where the soil has a high calcium content, but decreased to ~0.2 over Montana and the Midwest.

Overall, the use of the TFA procedure with the cloudwater data must be judged a failure in the sense that the results were not definitive or unambiguous. The methods were unable to extract reliable chemical profiles of underlying factors from the data, although there was an indication of a soil-derived component and a separate (weak) component for magnesium. There was also evidence that the concentrations of the dominant chemical species (SO_4^{2-}, NO_3^-) were somewhat de-coupled from the other elements. During the target rotation of several hypothetical vectors, it was found that the SO_4^{2-} and NO_3^- loadings could be fixed independently of the other element loadings. The test vectors would converge to the same final factors regardless of the initial SO_4^{2-} and NO_3^- loadings, which were relatively unaffected by the rotations.

The reasons for this failure are mainly due to the nature of the data. The samples were taken under conditions which were subject to too many other variables and processes that would affect the chemical composition of the cloudwater, such as airmass origin, in-cloud scavenging of particles, absorption of gases, etc. The inadequacy of the simple model of chemical concentrations being equal to the sum of contributions from a small number of sources can be seen most easily in the correlation matrix calculated from the observed concentrations:

1.00								
-.02	1.00							
-.12	.13	1.00						
.09	.37	.16	1.00					
-.12	.30	.75	.29	1.00				
-.16	.75	.19	.44	.55	1.00			
.18	.00	.28	.34	.27	.09	1.00		
.38	.01	.26	.36	.29	.05	.79	1.00	
.07	.04	.61	.04	.54	.09	.33	.57	1.00

Only four of the cross-correlation terms are greater than 0.6; most indicate little or no

correlation between pairs of elements. Additional concentration data for major elements like Si and Ca, for trace elements such as Pb, Cu, Cr, Ni, and V, and cloud physics parameters would be necessary for a reasonable chance of success in interpreting cloudwater concentration data.

4.2 TFA of Urban Aerosol Data

These data were copied from a report by Klemm and Gray (1982), which summarized the results of an exploratory study of the chemical composition of atmospheric aerosols in the city of Edmonton. In three study periods (November, 1978; March/April, 1979; July/August, 1979), each of approximately 30 days duration, daily Hi-Vol samples were collected at a monitoring site within the city, supplemented by occasional Hi-Vol samples from WSE (Stony Plain), 15 km west of Edmonton, and routine data (Pb, CO, COH, TSP) from a monitoring network operated by Alberta Environment.

The November samples were collected at the site of the Edmonton Residential Monitoring Unit in the northwest part of the city (135 Avenue, 127 Street). During this period, the authors of the study realized that their data may be biased because of emissions from low-level stacks on nearby buildings. The sampling site was re-located to the Edmonton Industrial Monitoring Unit near the eastern outskirts of the city (105 Avenue, 17 Street) for the spring and summer sampling periods (Fig. 4.1).

The November 1978 data are used here, for three reasons. First, the data set was the most comprehensive of the three periods and contained concentrations for a number of chemical species useful for characterizing different sources. Second, these data are the most representative of the aerosol composition likely to be encountered in residential areas. Third, the possible sample bias due to a local source means that this data set is a rather stringent test of the TFA procedure. The data were copied directly from Table 6 and Table 7 in the final report of Klemm and Gray (1982). While the actual copying could be checked easily, there are numerous typographical errors throughout the final report which raise the possibility of similar errors in the data tables.

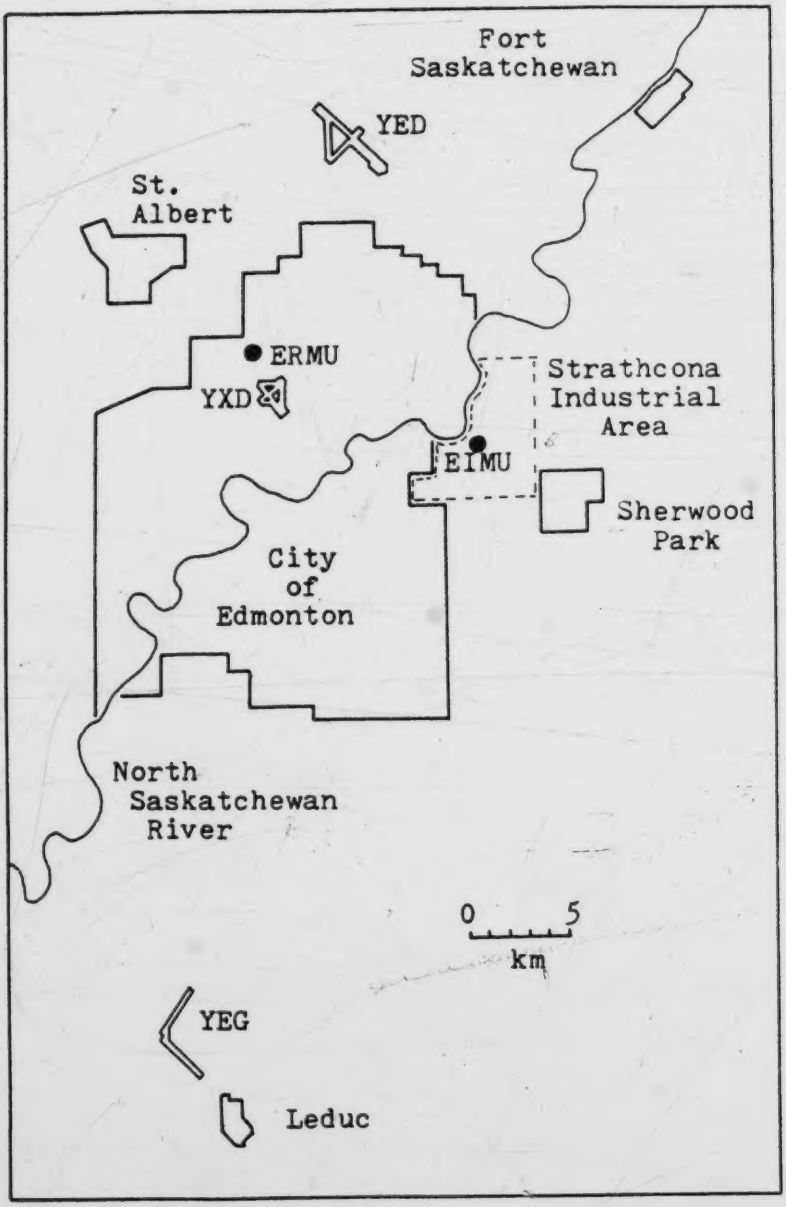

Fig. 4.1 Location map of the Edmonton area. The major airports (YED, YXD, YEG) are indicated. ERMU is the site of the Edmonton Residential Monitoring Unit, and EIMU is the site of the Edmonton Industrial Monitoring Unit.

Several analytical methods were used to determine the various species concentrations: X-ray fluorescence (XRF), ion chromatography (IAN), neutron activation analysis (NAA). A composite data set was formed from the XRF (Pb, Fe, Ca, K, Si, Al) and IAN (Na^+, Cl^-, NH_4^+, NO_3^-, SO_4^{2-}) concentrations; elements were selected which showed a reasonable degree of variability throughout the sampling period, and which have been found useful for characterizing aerosol sources in previous studies. The data are shown in Table 4.5. Klemm and Gray (1982) stated an accuracy of ±30% for the XRF data. The 'mdl', or minimum detectable levels (XRF), and the mean concentrations (IAN) in 15 blank filters were:

	Pb	Fe	Ca	K	Si	Al	Na^+	Cl^-	NH_4^+	NO_3^-	SO_4^{2-}
IAN							.02	.12	.05	.01	.02
XRF	.05	.01	.03	.08	.09	.30					

(all concentrations in ug-m^{-3} of air)

Weights were assigned on the basis of the magnitude of the element variances. Uniform weighting of all elements gave a product moment matrix completely dominated by the Si and SO_4^{2-} terms; weighting of these concentrations (and the concentrations of NH_4^+ and NO_3^-) by 0.2 gave a more reasonable matrix, without sacrificing the variability necessary for eigenvalue extraction.

The results of the eigenvalue calculations are displayed in Table 4.6. The minimum in the Malinowski Indicator function suggests only three significant factors, but the Scree test points to five or six factors. The Exner function decreases by about 0.03 when both the fourth and fifth factors are added, but the decrease is only ~0.01 with each additional factor after that. As well, the magnitude of the Exner function reaches the 'acceptable level' of 0.1 with five factors. Experiments with four, five, and six factors suggested that the set of four factors resulted in blurred profiles composed of more than one component, while the set of six factors indicated that the factors were beginning to describe individual variables. As a compromise, based mainly on the Scree and Exner tests, five significant factors were retained.

Table 4.5 Urban aerosol concentration data.

Date	Pb	Fe	Ca	K	Si	Al	Na^+	NH_4^+	Cl^-	NO_3^-	SO_4^{2-}
Nov. 3	0.60	4.80	3.80	1.80	36.00	3.00	0.20	0.50	0.10	0.70	1.20
4	0.70	1.90	2.40	9.20	17.00	1.40	0.10	0.70	0.50	0.90	1.30
5	0.10	0.60	0.50	0.20	5.00	0.70	0.20	0.50	0.50	0.90	1.20
6	0.90	3.10	2.50	1.20	3.00	2.30	0.10	0.50	0.20	0.50	0.60
7	1.10	2.90	2.50	1.20	30.00	2.80	0.10	0.60	0.20	0.50	0.80
8	0.20	2.30	0.90	0.50	13.00	0.80	0.10	0.20	0.20	0.20	0.50
9	0.20	1.20	0.80	0.50	12.00	1.00	0.20	0.50	0.30	0.10	0.80
10	0.80	2.30	2.40	0.90	21.00	1.90	0.70	1.50	0.70	1.20	1.70
11	0.40	1.70	1.10	0.60	14.00	1.40	0.50	0.90	0.90	1.60	1.60
12	0.40	1.20	2.20	0.60	12.00	1.10	0.40	0.60	1.00	1.70	2.50
13	0.70	1.80	1.40	0.70	19.00	1.80	0.30	1.10	0.90	0.90	1.80
14	0.60	3.00	3.00	1.20	29.00	2.60	0.40	0.80	0.60	0.80	1.80
15	0.50	2.00	2.10	0.80	15.00	1.30	0.20	0.60	1.10	1.70	3.50
16	0.30	1.70	1.10	0.20	14.00	1.30	0.30	0.60	1.30	1.80	4.30
17	0.30	0.80	0.50	0.30	6.00	0.70	1.10	2.30	0.50	0.30	1.10
18	0.40	0.50	0.90	0.30	4.00	0.40	1.00	1.90	0.70	0.70	1.70
19	0.50	0.40	0.40	0.10	4.00	0.40	2.80	4.90	0.90	1.30	2.00
20	1.20	1.40	1.30	0.60	15.00	1.20	4.70	7.60	1.50	2.70	2.20
21	2.30	3.40	4.00	1.30	32.00	2.80	5.20	9.50	3.40	5.40	3.80
22	1.20	2.50	4.20	1.10	24.00	1.70	4.80	7.20	1.80	3.60	3.30
23	1.00	1.00	1.50	0.40	7.00	0.80	0.70	1.60	1.00	1.30	1.40
24	1.60	0.90	0.80	0.20	4.00	0.50	0.30	1.70	2.10	1.80	3.20
25	0.90	0.80	2.20	0.30	6.00	0.80	1.00	2.00	0.90	2.60	1.50
26	0.20	0.10	0.20	0.10	1.00	0.40	0.20	0.50	1.50	0.90	3.40
27	0.60	0.80	1.10	0.40	6.00	0.90	1.30	2.70	3.20	2.80	6.70
28	0.10	0.20	0.20	0.10	1.00	0.30	0.30	0.30	1.00	0.30	2.70
29	0.30	0.20	0.40	0.10	1.00	0.30	0.30	0.70	3.80	1.80	13.60
30	0.90	0.20	0.30	0.10	1.00	0.10	0.30	1.40	1.00	4.00	16.20

Table 4.6 Urban aerosol eigenvalue calculations.

Data set dimensions: 28 11

Variable (column) weights:

Pb	Fe	Ca	K	Si	Al	Na^+	NH_4^+	Cl^-	NO_3^-	SO_4^{2-}
1.0	1.0	1.0	1.0	0.2	1.0	1.0	1.0	0.2	0.2	0.2

Initial product moment matrix:

0.835										
1.126	3.133									
1.252	2.823	3.070								
0.479	1.264	1.269	1.204							
1.577	4.485	4.198	1.891	7.432						
0.956	2.438	2.344	1.031	3.635	2.145					
0.720	1.120	1.362	0.470	1.823	1.060	1.530				
1.670	2.365	2.791	1.002	3.740	2.177	2.789	5.482			
0.316	0.409	0.482	0.180	0.601	0.466	0.380	0.774	0.276		
0.347	0.479	0.579	0.201	0.738	0.465	0.380	0.830	0.195	0.216	
0.852	1.001	1.181	0.447	1.450	1.137	0.921	1.976	0.750	0.625	2.677

Total variance (covar0):

0.835	3.133	3.070	1.204	7.432	2.145	1.530	5.482	0.276	0.216	2.677

Eigenvectors (columns):

0.742	-0.240	0.071	0.140	-0.267	-0.299	-0.171	0.079	0.060	-0.058	-0.015
1.632	0.544	0.066	0.034	-0.214	0.162	-0.247	-0.186	0.016	0.024	-0.009
1.651	0.225	0.009	0.247	-0.352	-0.040	0.323	-0.044	-0.002	0.010	0.018
0.716	0.263	0.064	0.690	0.376	-0.011	-0.035	0.004	0.001	0.000	-0.004
2.533	0.868	-0.054	-0.377	0.301	-0.161	0.044	0.017	0.013	-0.002	0.001
1.381	0.257	0.179	0.009	-0.111	0.253	-0.050	0.236	-0.056	-0.034	0.002
0.930	-0.667	-0.380	-0.044	0.107	0.185	0.109	-0.052	0.087	-0.064	-0.048
1.889	-1.255	-0.570	-0.002	0.041	-0.040	-0.082	0.007	-0.058	0.038	0.033
0.328	-0.244	0.255	-0.007	-0.004	0.052	0.004	0.121	0.134	0.093	-0.001
0.359	-0.189	0.154	-0.000	-0.043	-0.079	0.032	0.017	-0.078	0.049	-0.097
0.849	-0.808	1.130	-0.085	0.106	0.004	0.024	-0.074	-0.015	-0.023	0.015

Eigenvalues:

20.162	4.060	1.883	0.709	0.511	0.252	0.221	0.121	0.042	0.022	0.014

Significance tests for eigenvalues:

#	EIGEN	VAR	CPV	SCR	IME	IND	RSD	XNR
1	20.162	72.01	72.01	27.991	0.050	0.00167	0.1673	0.4395
2	4.060	14.50	86.51	13.489	0.052	0.00151	0.12	
3	1.883	6.72	93.23	6.765	0.048	0.00144	0.0920	0.1449
4	0.709	2.53	95.77	4.232	0.047	0.00159	0.0778	0.1058
5	0.511	1.83	97.59	2.405	0.043	0.00176	0.0633	0.0725
6	0.252	0.90	98.50	1.504	0.041	0.00219	0.0549	0.0638
7	0.221	0.79	99.28	0.717	0.034	0.00265	0.0423	0.0579
8	0.122	0.44	99.72	0.281	0.026	0.00340	0.3058	0.0400
9	0.042	0.15	99.87	0.129	0.023	0.00635	0.0254	0.0301
8	0.022	0.08	99.95	0.049	0.021	0.02210	0.0221	0.0158
9	0.014	0.05	100.00	0.000	0.000	0.00000	0.00000	0.0000

Varimax orthogonal rotation with 5 factors:

0.456	1.607	1.418	0.497	2.494	1.238	0.337	0.751	0.120	0.180	0.206
0.431	0.367	0.591	0.140	0.726	0.374	1.106	2.041	0.159	0.195	0.256
0.410	0.333	0.433	0.127	0.424	0.487	0.344	0.801	0.435	0.337	1.596
0.122	0.373	0.438	0.959	0.533	0.311	0.115	0.242	0.044	0.041	0.114
0.355	0.207	0.470	0.036	-0.437	0.125	0.007	0.194	0.036	0.069	-0.031

Variances of rotated factors: 13.572 6.873 4.505 1.733 0.643

% communalities (covar0) with 5 Varimax factors:

84.2	96.1	96.5	99.9	99.6	94.1	95.9	99.7	84.0	88.2	99.7

A Varimax rotation with these five factors is also shown.

As before, a number of hypothetical vectors were constructed which included both binary vectors and aerosol composition profiles derived from other FA and CEB studies reported in the literature. Specific information of the composition of major aerosol sources in the Edmonton area could not be located. General test vectors were used which consisted of the relative chemical profiles of aerosols from crustal material, sea salt, automobiles, burning of refuse (fugitive emissions and/or municipal incinerators), road salt, emissions from cement plants, and flyash from the combustion of coal and oil. The best five factors are shown in Table 4.7. There is considerable reason to be confident (in a qualitative sense) that the final factors are very similar to the true underlying factors. All test vectors, including the binary vectors, eventually converged to one of these factors, or a very similar one. The problem of interpretation of the factors remains, however.

The factor scores were calculated for each factor, and multiple linear regression with the observed TSP gave the appropriate scaling coefficients. (The regression model was $TSP = \sum_{i=1}^{5} a_i S_i$.) The coefficients and the scaled factors are shown in Table 4.8. The scaled source profiles are somewhat easier to discuss than the unscaled factors, since they should be close to the profiles which would be obtained if a separate analysis could be made of aerosols from each of these sources.

There is little doubt about the interpretation of the first three factors, although the Si content of the soil component is somewhat high. Assuming that all Si is present as the oxide SiO_2, then the maximum Si content possible would be $1000 \times (\frac{28}{28 + 2 \times 16}) = 467$ mg·g^{-1}. And this would be for a sample of quartz or, perhaps, sand. Nevertheless, given the accuracy of ±30% in the original data, the fact that Si was certainly the dominant mineral in most of the aerosol samples (an average of 15% of the total particulate mass), and the similarity between these element concentrations and those found in other cities (eg., Alpert and Hopke, 1981), this source profile seems quite reasonable. The sulphate component reflects the unusual behaviour of the major ions, which were present at relatively constant levels until the end of the month, when the concentrations rose abruptly. Reference to Table 11 in Klemm

Table 4.7 Urban aerosol factors.

	Soil	Sulphate	Traffic	Flyash	Refuse
Pb	-0.064	0.120	0.222	0.230	0.218
Fe	0.352	0.007	0.040	0.417	0.295
Ca	0.147	0.017	0.218	0.476	0.501
K	0.045	0.006	0.000	0.101	1.000
Si	0.952	0.002	0.000	0.272	0.001
Al	0.281	0.142	0.061	0.301	0.223
Na^+	0.088	-0.001	0.512	-0.036	-0.016
Cl^-	0.101	0.079	0.959	0.051	0.079
NH_4^+	0.004	0.247	0.057	0.038	0.030
NO_3^-	0.008	0.167	0.080	0.060	0.036
SO_4^{2-}	0.028	1.000	0.039	0.049	0.029

Correlation matrix of the rotated factors:

Soil	1.000				
Sulphate	0.068	1.000			
Traffic	0.158	0.150	1.000		
Flyash	0.645	0.182	0.252	1.000	
Refuse	0.217	0.096	0.187	0.613	1.000

Table 4.8 Urban aerosol source profiles.

	Soil	Sulphate	Traffic	Flyash	Refuse
Pb	0.0	5.7	27.4	12.7	19.1
Fe	37.8	0.3	4.9	23.0	25.9
Ca	15.8	0.8	26.9	26.2	44.0
K	4.8	0.2	0.1	5.6	87.8
Si	510.5	0.4	0.2	74.9	1.0
Al	30.2	6.8	7.5	16.6	19.6
Na^+	9.4	0.0	63.2	0.0	0.0
Cl^-	10.8	3.8	118.3	2.8	6.9
NH_4^+	1.9	58.9	35.4	10.4	13.2
NO_3^-	4.3	39.8	49.2	16.6	15.7
SO_4^{2-}	14.8	238.7	24.2	13.4	13.1
MLR coefficients:	9.34	20.95	8.10	18.13	11.40

and Gray (1982) will show that the concentrations of several heavy metals, such as cadmium, exhibited a similar trend. (Cd, and other metals, were not included in this analysis because the concentrations were 'bdl' in too many of the samples.)

The third component has been labelled 'traffic' rather than 'motor vehicles', as has been customary in FA and CEB studies. Lead is an excellent tracer of vehicle emissions, since minor elements such as Fe, Al, Ca, and Cl are only a small fraction of the Pb content of these particles. An even better method of identifying vehicle emissions in urban areas requires Pb and Br concentrations (Harrison and Sturges, 1983), but Klemm and Gray (1982) did not measure Br. The curious thing about the traffic component is the association of Na^+ and Cl^- with Pb. This is easily understood by noting that November 1978 was rather cold and had 12 days with 0.2 cm or more of snow (AES, 1978); road salting operations commenced in the second half of the month (Klemm and Gray, 1982). Thus the TFA procedure was unable to resolve a separate (predominantly Pb) component for vehicle emissions; only a mixed component consisting of the primary automotive emissions and road surface particles, enriched in salt, could be derived.

The fourth and fifth components are somewhat ambiguous, since they are similar to several of the test profiles. One of the uncertainties of TFA is the sensitivity of the methods: at what point can components which have very similar chemical profiles be separated into unique factors? An example is the composition of aerosols from a crustal or soil source, coal flyash, oil flyash, and cement plants. Typical relative composition profiles of these sources, based mostly on measured concentrations at the sources, are shown in Table 4.9.

Table 4.9 Relative composition profiles of particulate matter from similar sources.

	Soil†	Coal Flyash†	Oil Flyash†	Cement‡
Pb	0.00019	0.004	0.94	0.00
Fe	0.63	0.70	6.70	0.48
Ca	0.081	0.090	19.40	20.00
K	0.19	0.13	1.06	0.24
Si	•	•	•	4.60
Al	1.00	1.00	1.00	1.00
Na	0.053	0.016	29.40	0.20
Cl	0.0033	0.002	29.40	0.00
NH_4^+	•	•	•	•
NO_3^-	•	•	•	•
SO_4^{2-}	•	•	•	•

† From Kowalczyk et al. (1978).
‡ From Friedlander (1973).
• Not measured.

The sensitivity of TFA may depend ultimately on the variability of only one or two characteristic chemical elements. This is the situation here with factors four and five. The major differences are only in the Si and K loadings. A comparison with the profiles in Table 4.9 and with others (eg., Alpert and Hopke, 1981) led to the tentative label of 'flyash' for the fourth factor. The fifth factor is labelled 'refuse' principally because a source with this profile could not be identified. Interestingly, Alpert and Hopke (1981) derived a similar refuse component in aerosol samples from St. Louis, Missouri, which also had a high loading for potassium. Their identification of the refuse component was more reliable because their data set included zinc concentrations, often used as a marker element for incinerator emissions (Kowalczyk et al., 1978). Biomass burning and, possibly, combustion of fossil fuels, have been suggested as sources of particles with high potassium content (Andreae, 1983).

Direct confirmation of the source profiles for aerosols at the Edmonton Residential Monitoring Unit would be difficult. Some confidence in these components can be gained by

examining the time series of the corresponding scaled factor scores (Fig. 4.2) and simultaneous meteorological data (Fig. 4.3). As described by Klemm and Gray (1982), high sulphate and heavy metal concentrations were correlated with wind direction. This is clearly evident in the scores for the sulphate component which reached their highest values with the northeast winds at the end of the month. Hopper (1986a), extending the work of Hage (1972) and Robertson (1955), showed that reduced visibilities at the Edmonton Municipal Airport (YXD) during cold spells were also strongly correlated with northeast winds, and could be reasonably explained by advection of water vapour emissions from the Strathcona Industrial Area. The change in the visibility pattern at YXD over a number of years is shown in Fig. 4.4. Given the concentration of heavy industries in the east and northeast parts of the city, it is suggested that the correlation with northeast winds of both reduced visibilities (high water content), and high values of the sulphate component, is not a coincidence.

The traffic component usually contributed less than 10 ug-m^{-3} to the Hi-Vol samples. The amount increased rapidly to 60~70 ug-m^{-3} in the third week of November, when a cold Arctic High pressure system moved into Alberta. Precipitation amounted to only a few centimeters of snow, but daily maximum temperatures remained below -10°C from 17 November to 20 November, making roads slippery and leading to the application of road salt to the city streets. Light winds during this period helped to increase the particulate loading from local streets.

The flyash component contributed an average mass loading of 27 ug-m^{-3} at the monitoring site, compared to 22 ug-m^{-3} from the soil component. Klemm and Gray (1982) noted the high correlation ($r > 0.9$) between the crustal elements (Si, Al, K, Ca, Mn) and TSP; by assuming the normal crustal abundance of oxygen they calculated that 96% of the TSP could be accounted for by these elements. From that, they concluded that "most (95%) of Edmonton TSP originates from lithophilic material. In particular, the elements Si, Al, K, Fe, and Ti are essentially of crustal origin" (Klemm and Gray, 1982). The TFA results indicate that this estimate should be lowered. The soil component only accounts for an average of about 30% of the TSP, while the mean flyash contribution was 35%. Together,

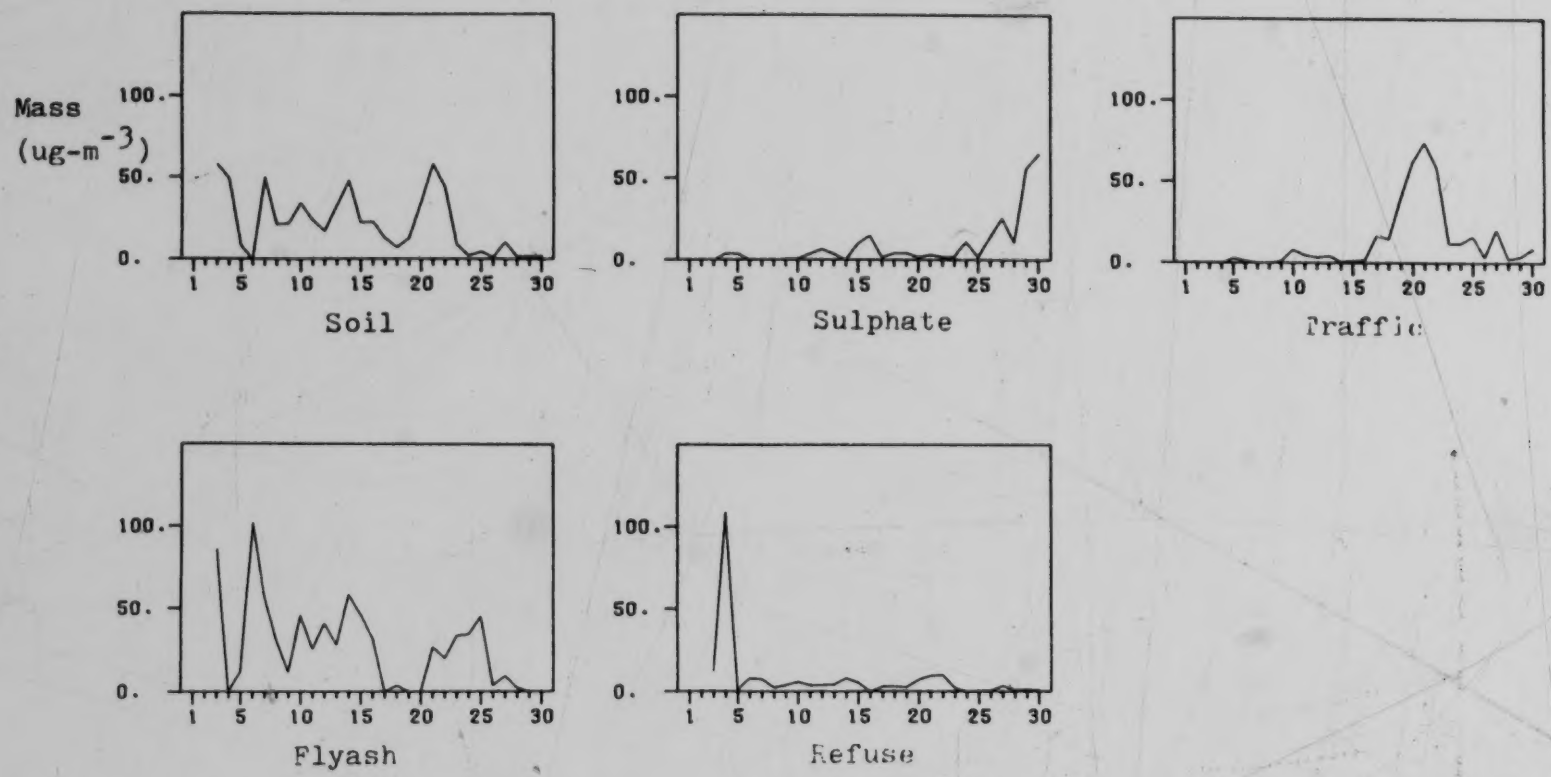

Fig. 4.2 Time series of aerosol source strengths. Five aerosol components were derived from Target Factor Analysis of Edmonton aerosol data. These graphs show how the total aerosol mass in each of the daily samples is distributed among the five components by TFA.

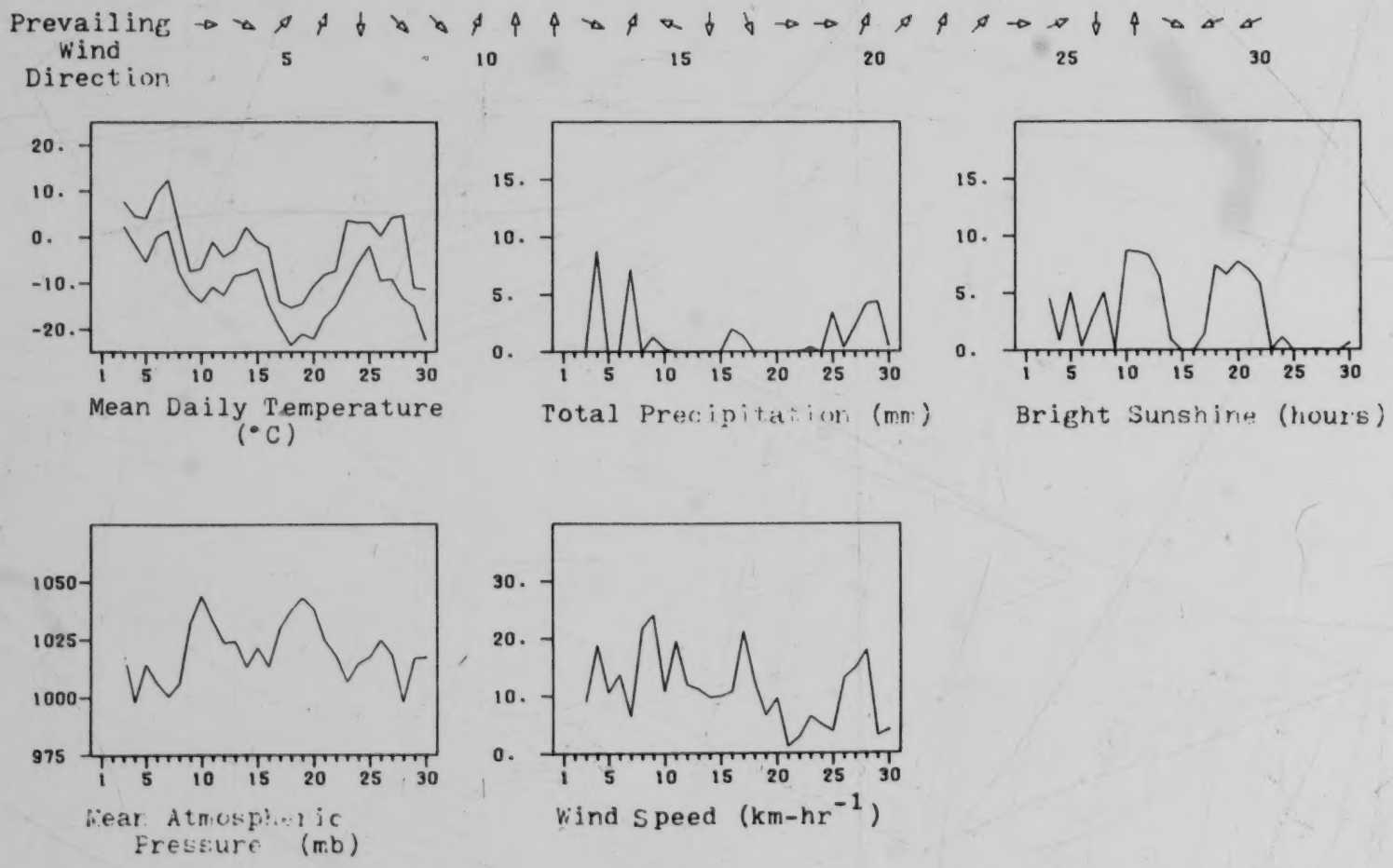

Fig. 4.3 Time series of related meteorological data. The data were abstracted from the monthly summary of synoptic observations at YXD for November 1978 (AES, 1978).

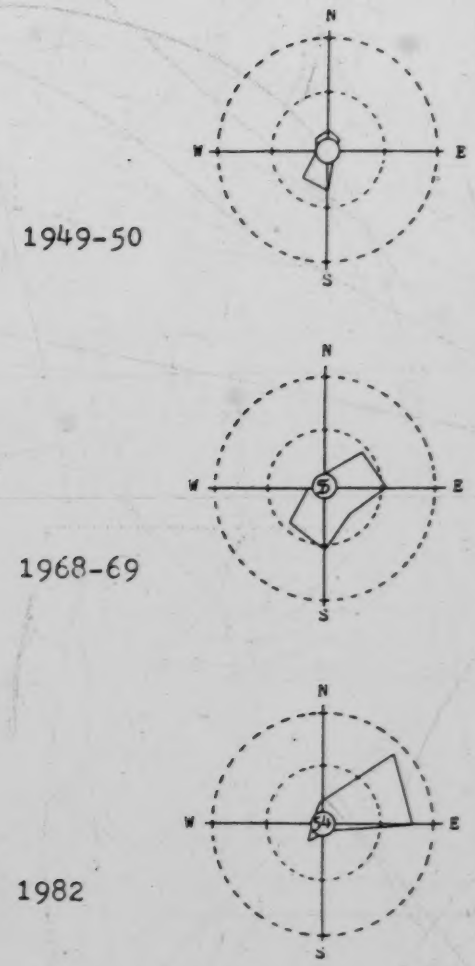

Fig. 4.4 Frequency of reduced visibilities at YXD during cold spells. The data were abstracted from hourly synoptic observations during cold spells (temperature less than -18 °C) in three winters. The percent frequency of visibilities of 3.2 km or less is indicated for each wind direction. Inner ring is 50%, outer ring is 100%.

these two components might be considered lithophilic material originally, but the remaining three components still accounted for an average of one-third of the TSP. As Fig. 4.2 shows, however, the relative contributions from each component in any sample can vary considerably. The meteorological controls on the soil and flyash components are more complicated than the others. Precipitation, wind speed, wind direction, and temperature all seem to be important, but these are not independent variables.

The final factor, refuse, makes only a small contribution to the TSP each day, with the exception of 4 November. The small amounts would normally be expected from fugitive emissions in a predominantly residential area. The sample of 4 November was dominated by the refuse component; the calculated mass contribution from this source alone was several times larger than the measured TSP. This is a direct consequence of setting all negative factor scores equal to zero. For this one sample, a large positive score for the refuse factor (necessary to account for the high K concentration observed in the sample) was offset by a large negative score for the flyash factor. When the offsetting negative score was neglected, the mass contribution from the refuse component was greatly exaggerated. It should be noted that this was the only case of a large negative factor score. There were 16 factor scores less than zero in the entire factor score matrix (out of a total of 5 x 28 = 140), 15 of which were small and assumed to be negligible. It is possible that this datum is incorrect, perhaps due to a typographical error, since the potassium concentration in this sample is three times greater than the largest concentration observed in any of the other samples. Or the sample may have been contaminated by emissions from a local incinerator; without further information, the reason for the high K concentrations cannot be determined. While the refuse component of 4 November could be adjusted accordingly, or omitted, this does illustrate a potential bias in the TFA procedure.[12] Table 4.10 compares the observed TSP with the predicted TSP from all factor scores, and with the predicted TSP after replacing negative factor scores by zero.

[12]Hopke and co-workers have managed to avoid this problem by not calculating the partial mass contributions for each sample, such as have been displayed in Fig. 4.2, but only calculated the averages at each site. To examine correlations with other data, however, it would seem that the sets of individual factor scores are really quite an important part of the research results.

Table 4.10 Observed and predicted TSP. Measured TSP refers to the aerosol mass actually measured in each sample. Preliminary TSP is the sample mass re-calculated from the initial factor scores, after scaling by the MLR coefficients. The Final Predicted TSP is the sample mass calculated from the scaled factor scores, after setting negative scores equal to 0.0. All units are $ug\text{-}m^{-3}$.

Measured TSP	Preliminary TSP	Final Predicted TSP
148.	147.	157.
45.	46.	162.
84.	28.	28.
116.	98.	111.
101.	109.	114.
66.	51.	54.
60.	39.	39.
93.	95.	95.
89.	61.	61.
67.	72.	72.
67.	73.	73.
108.	115.	115.
79.	86.	86.
86.	70.	72.
39.	30.	34.
36.	33.	33.
49.	28.	60.
88.	70.	106.
150.	172.	172.
125.	135.	135.
46.	58.	58.
61.	59.	60.
61.	69.	69.
33.	23.	23.
70.	69.	69.
18.	18.	18.
49.	63.	63.
77.	74.	75.

4.3 Summary

Before applying the TFA procedure to the primary data set, it is worthwhile to review its performance with the cloudwater data and with the Edmonton aerosol data. When the chemical species follow the additive model of Eqn. 2.1, reasonable source profiles can be derived by using target rotation with vectors which represent either abstract hypothesized sources, or real source profiles, even if the latter are known only approximately. By using methods based on the principal components model and covariance about the origin, the procedure is simply an attempt to align the eigenvectors describing the data set with the target profiles. A successful alignment is assumed to indicate that the source is a true contributor to the observed variance in the data.

More frequently, a rotated vector is similar to, but not identical with, the target vector. In this case, the target factor analysis gives the actual or 'realizable' source profile; that is, a profile which represents the source contribution at the monitoring site. Changes in the source composition may have occurred during transport of the aerosol from source to receptor, giving a different apparent chemical composition.

The procedure worked well with the urban aerosol data, although there are still a number of potential problems (number of significant factors, interpretation of ambiguous factors, negative source strengths). With care, these difficulties can be overcome and errors can be kept to a minimum. The advantages of TFA are significant, since both realistic profiles at the receptor (as opposed to idealized source composition profiles arbitrarily forced to fit the data) and the partial mass contributions from each source can be derived simultaneously. Accurate local source profile data need to be collected in order to perform a proper verification of the TFA results.

A more serious problem is presented by data sets where the variables do not follow Eqn. 2.1. The cloudwater data was one example, where heterogeneous chemical reactions, cloud physics, and synoptic parameters apparently had greater influence on the chemical composition than the variability caused by source fluctuations alone. With such data, TFA is not an effective way of analyzing the data. BFA or analysis of data correlations might be a

better, although less powerful, approach in this case.

5. Arctic Haze - Introduction

Arctic haze is a relatively new field of research, but one which has grown rapidly in the past decade. The term refers to a dramatic increase in gaseous and particulate air pollutants in the Arctic atmosphere during the late winter and early spring. This is, perhaps, the ultimate in long-range transport of air pollutants because it appears that transport over several thousand kilometers is involved. It is unlikely that Arctic haze has really become a household word as claimed by Rahn (1985), but the subject is of sufficient interest to have merited three special symposia in 1977, 1980, and 1984. There have also been three issues of scientific journals devoted largely to Arctic haze: Atmospheric Environment **15**(8), 1981; Geophysical Research Letters **11**(5), 1984; Atmospheric Environment **19**(12), 1985.

Reviews of Arctic haze, both expert and popular, have been written by Rahn (1978), Rahn (1981a), Rahn and Heidam (1981), Hileman (1983), Schnell (1984a), Schnell (1984b), Rahn (1984), Rahn (1985), and Barrie (1986). Some of the more important features of Arctic haze are:

1. It is a widespread phenomenon. Data from Alaska, the Canadian Arctic, Greenland, Norway, and Spitsbergen all show a pronounced annual cycle, with gas and aerosol concentrations lowest in the summer and highest in the late winter. There are no data from the Soviet Arctic.
2. During the winter maximum, concentrations of several species such as sulphate (~2.-3. ug-m^{-3}), organics (~1. ug-m^{-3}), and soot (~0.3 ug-m^{-3}) can reach levels as high as those found in rural mid-continental areas. These three species are the dominant materials in the aerosol, but there is a wide variety of other chemical species present (Rahn, 1985).
3. Arctic haze can often be detected by eye, and appears as layers, bands, or patches. Aircraft experiments (Schnell, 1984b) have shown that these layers can extend over large horizontal distances, or they may be rather spotty.

The annual cycle in $SO_4^{=}$ concentrations is displayed in Fig. 5.1 for three locations in the Canadian Arctic. Plotting the $SO_4^{=}$ concentrations on a logarithmic scale (Fig. 5.2) reveals

the interesting fact that the annual cycle is asymmetric; this is most noticeable at Alert, where the springtime weekly mean SO_4^{2-} concentrations decrease quite rapidly. That Arctic haze is indeed a widespread phenomenon is demonstrated in Fig. 5.3, which compares SO_4^{2-} concentrations at Igloolik and at Ny Alesund, Spitsbergen. (Some of the locations mentioned here are indicated in Fig. 5.4 and in Fig. 5.5.) The uniqueness of the annual cycle to high latitudes can be inferred from Fig. 5.6, which compares monthly mean TSP concentrations at several locations in Canada; if anything, the annual trend at places like Edmonton is 180° out of phase with the cycle displayed in Fig. 5.1. A comparison between sulphate and TSP is known to be incorrect because SO_4^{2-} in the Arctic is more closely related to the fine particle mass than the total mass (Barrie and Hoff, 1985; Barrie, 1986), but SO_4^{2-} is one of the predominant constituents of the Arctic aerosol and its annual variation gives a rough picture of the annual variation in TSP.

The simplest classification method for research papers on Arctic haze, and related topics, is by geographical area. Borys and Rahn (1981) observed high levels of cloud-condensation nuclei (CCN) transported from Europe to Iceland. Megaw (1982) reported that a "curious thin layer haze over the Greenland icecap" had been observed in the summer of 1973 but this may be a phenomenon unique to the icecap. Monitoring programs of several years duration in Greenland (Heidam, 1981, 1982, 1984, 1985; Davidson et al., 1981; Davidson, et al., 1985) do show, however, the late winter maximum in aerosol concentrations. This is significant because the Greenland icecap contains an excellent record of long-term atmospheric concentrations (Oeschger et al., 1966; Busenberg and Langway, 1979; Boutron and Delmas, 1980; Herron, 1982; Craig and Chou, 1982).

Numerous studies have been carried out in the Norwegian Arctic, both by Scandinavian groups (Heintzenberg, 1980; Rahn et al., 1980; Heintzenberg et al., 1981; Heintzenberg, 1982; Pacyna et al., 1984; Joranger and Ottar, 1984; Semb et al., 1984; Ottar and Pacyna, 1984; Pacyna et al., 1985; Pacyna and Ottar, 1985) and American groups (Raatz and Schnell, 1984; Winchester et al., 1984; Cahill and Eldred, 1984; Raatz et al., 1985b, 1985c). Rahn (1981d) attempted to estimate the deposition of the aerosol to the Arctic ocean,

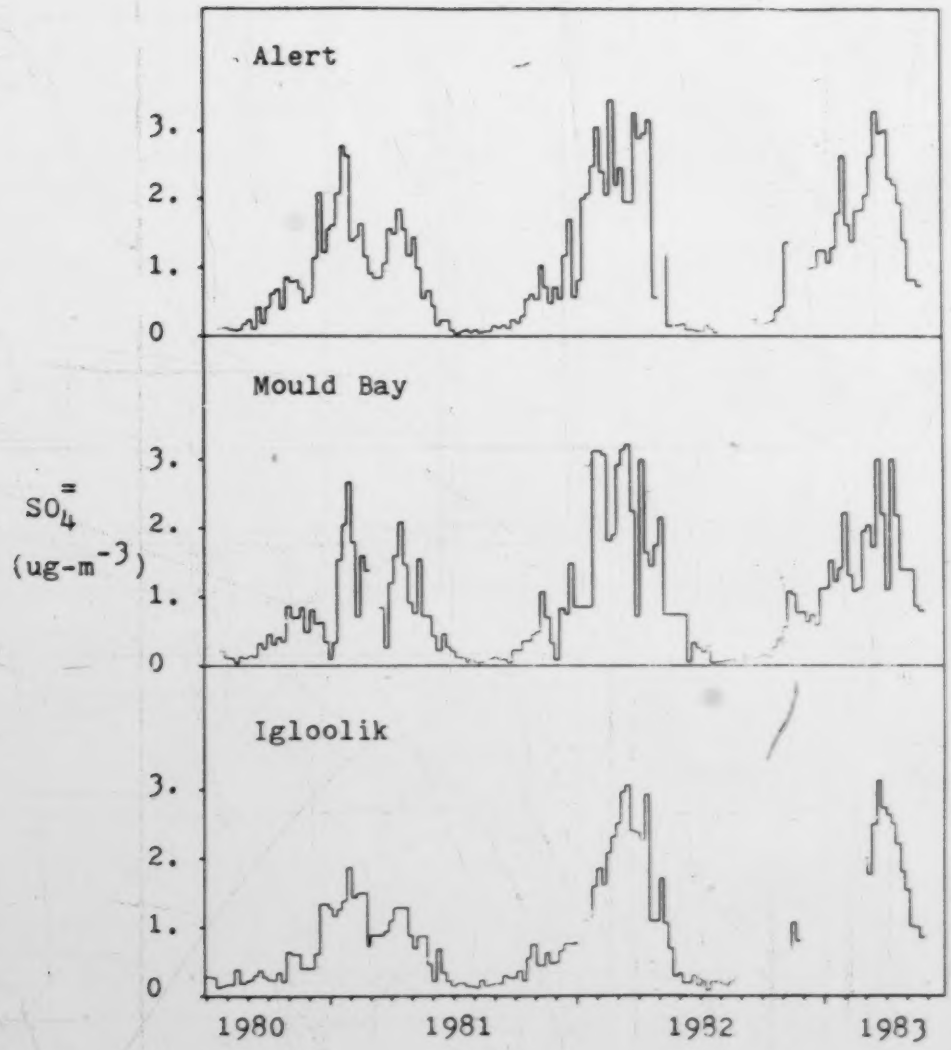

Fig. 5.1 Sulphate concentrations in the Canadian Arctic. These are the total $SO_4^=$ concentrations observed in approximately weekly Hi-Vol aerosol samples.

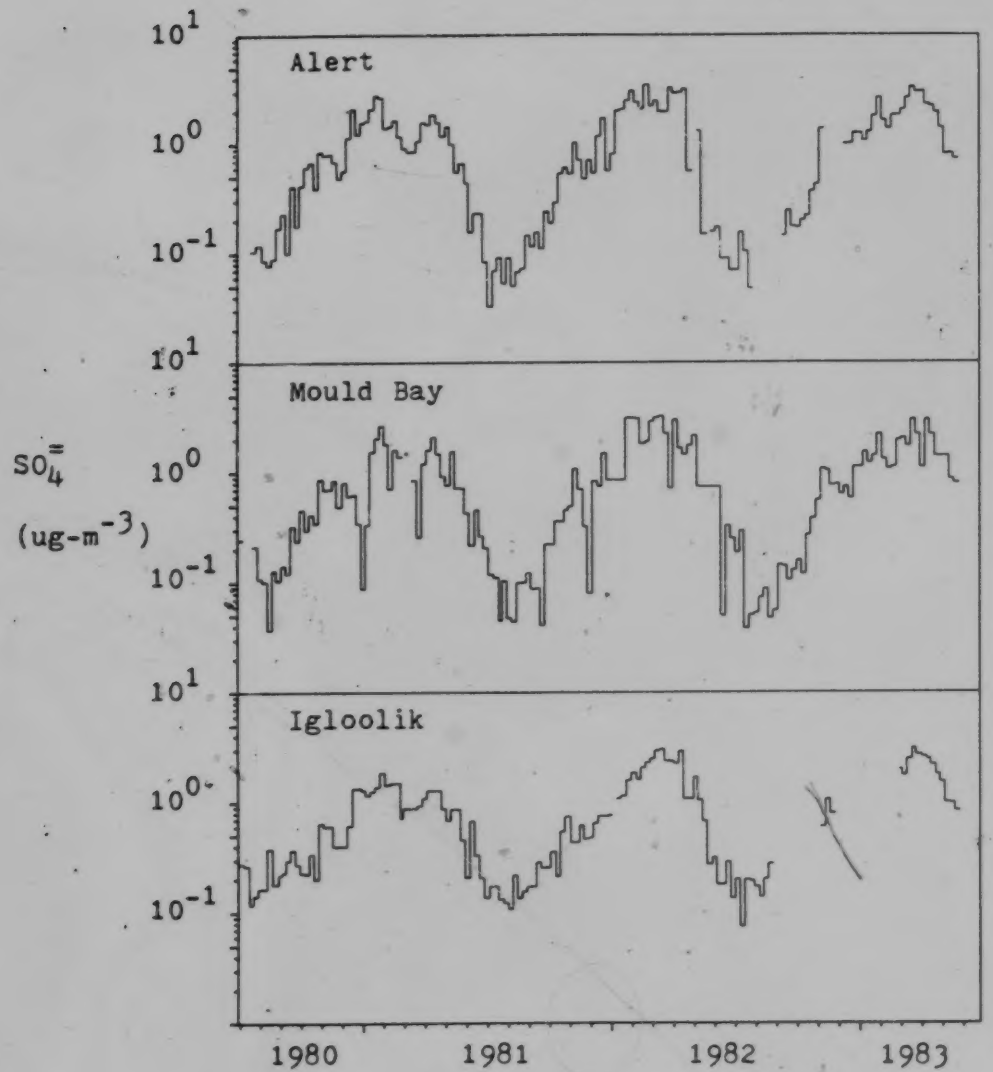

Fig. 5.2 Logarithms of sulphate concentrations. Same as Fig. 5.1, but plotted with a logarithmic vertical scale.

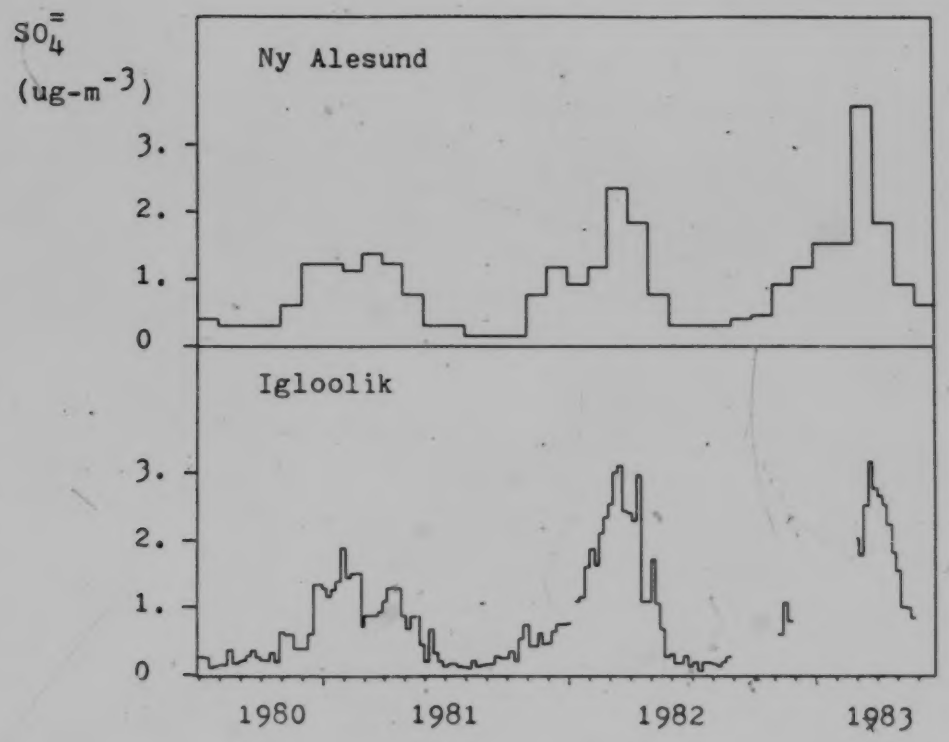

Fig. 5.3 Sulphate concentrations at Igloolik and Ny Alesund. The Spitsbergen data are based on calculations of the monthly mean of the sulphur concentration present as SO_4^{2-} (adapted from Iversen and Joranger, 1985).

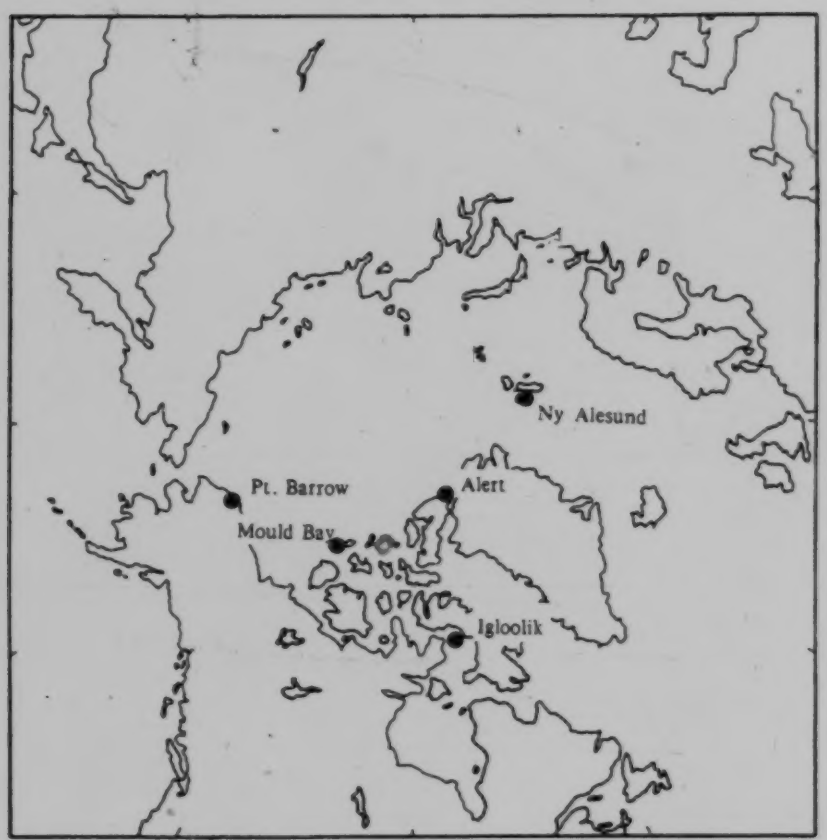

Fig. 5.4 Map of the Arctic region.

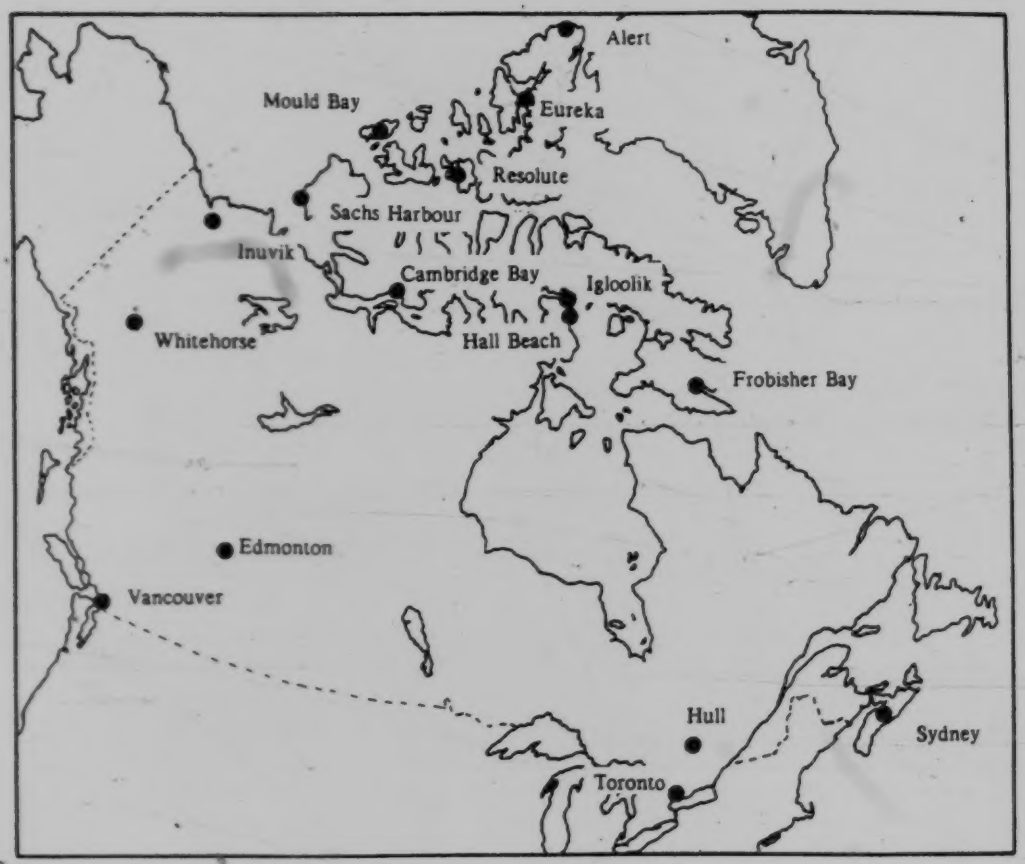

Fig. 5.5 Map of Canada and the Canadian Arctic.

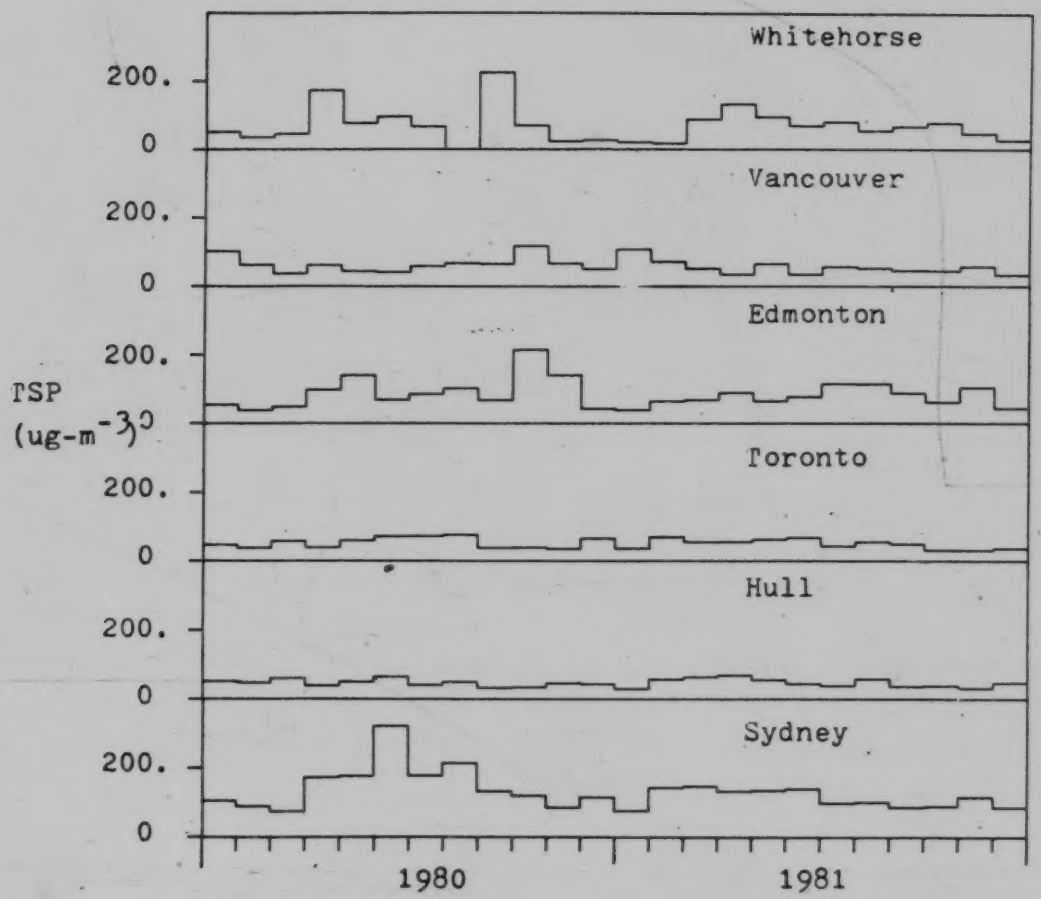

Fig. 5.6 Monthly TSP concentrations in Canadian cities. These are monthly averages, calculated from 24-hour Hi-Vol samples collected every six days (EPS, 1981; 1982).

and arrived at figures which showed that the atmospheric fluxes of Al, V, Mn, Cd, $SO_4^{=}$, and NO_3^- were probably insignificant compared to the fluxes of these species from rivers and inter-ocean exchange; only Pb may have a significant atmospheric component.

Studies from the Alaskan Arctic form a large fraction of the papers on Arctic haze: Rahn and McCaffrey (1979, 1980); Rahn (1981b, 1981c); Raatz (1981); Halter and Peterson (1981); Miller (1981); Bodhaine et al. (1981); Shaw (1982a); Raatz (1982); Peterson et al. (1982); Rahn et al. (1983); Raatz (1983); Khalil and Rasmussen (1983); Shaw (1983a, 1983b); Kienle et al. (1983); Schnell and Raatz (1984); Shine et al. (1984); Lazrus and Ferek (1984); Shaw (1984,1985); Wilkniss and Larson (1984); Radke et al. (1984a, 1984b); Bailey et al. (1984); Clarke et al. (1984); Bodhaine (1984); Hansen and Rosen (1984); Raatz and Shaw (1984); Rahn and Lowenthal (1984); Dayan et al. (1985); Raatz et al. (1985a,1985d); Halter and Harris (1985); Conway et al. (1985); Sheridan and Musselman (1985); Lowenthal and Rahn (1985).

Studies from the Canadian Arctic were reported by Barrie et al. (1981), Koerner and Fisher (1982), Hoff et al. (1983), Hoff and Trivett (1984), McNeely and Gummer (1984), Hogan et al. (1984b), Leaitch et al. (1984), Barrie and Hoff (1984), Higuchi and Daggupaty (1985), Barrie et al. (1985), and Barrie and Hoff (1985).

Much of the original interest in Arctic haze was stimulated by the calculations of Shaw and Stamnes (1980), who estimated that atmospheric heating rates of 1 °C-day^{-1} might result from absorption of visible solar radiation by the haze aerosol. Such high heating rates were, in a sense, alarming since they appeared to be the result of an anthropogenic perturbation of the radiation balance in a climatically-sensitive region. The Polar Group (1980) identified two reasons which make the polar regions important on a global scale. First, there are positive feedback mechanisms (higher temperatures ←→ lower albedo; higher temperatures ←→ higher moisture content) which might amplify small perturbations. Second, the polar regions respond more dramatically than lower latitudes, so indications of climatic change might be expected to be noticed first at high latitudes.

To pursue further the radiative effects of Arctic haze, a variety of different approaches have been used, ranging from more observations of the optical depth with sun photometers (Mendonca et al., 1982; Shaw, 1982b; Dutton et al., 1984), to application of radiative transfer models and analyses of broadband radiation data (Freund, 1983a, 1983b; Leighton, 1983; Blanchet and List, 1983; Cess, 1983; Wendling et al., 1985; McGuffie et al., 1985). A significant experiment during the AGASP[13] aircraft flights directly measured the radiative flux divergence at different altitudes in Arctic haze (Valero et al., 1983; Valero et al., 1984; Ackerman and Valero, 1984). Heating rates of 1.1 ° to 1.5 °C-day^{-1} were indeed found, confirming the estimates of Shaw and Stamnes (1980).

The more recent data, summarized by Rahn (1985), suggest that these heating rates can certainly be found in the Arctic during late winter and spring, but that the overall average for the Arctic is much less (0.01 ° - 0.1 °C-day^{-1}) and may not be of immediate importance. The lower estimates came about because of revised figures for the absorptivity per unit mass of aerosol, and the awareness that the haze is usually not distributed throughout a very thick layer of the Arctic atmosphere.

The high heating rates are the direct consequence of the relatively large amounts of soot in the Arctic aerosol. (Soot is also called graphitic carbon, elemental carbon, particulate elemental carbon.) This material is produced by combustion processes and is significant because it is a highly absorbing material. Fig. 5.7 compares the absorptivity of various materials (expressed by the imaginary part of the refractive index of the material), with estimates of the range of values for "typical" atmospheric aerosols, summarized from a number of observational studies. Soot is notable for having a high absorptivity throughout the visible and near infrared portions of the spectrum. The absorptivity of the "typical" atmospheric aerosol shown in Fig. 5.7 can be explained by only very small amounts of soot in the aerosol. It is not surprising, then, that soot in the Arctic has been examined in great detail (Rosen et al., 1981; Porch and MacCracken, 1982; Patterson et al., 1982; Hogan et al., 1984a; Rosen and Hansen, 1984; Rosen and Hansen, 1985; Hansen and Rosen, 1985). The effects of

[13]AGASP: Arctic Gas and Aerosol Sampling Project (spring, 1983)

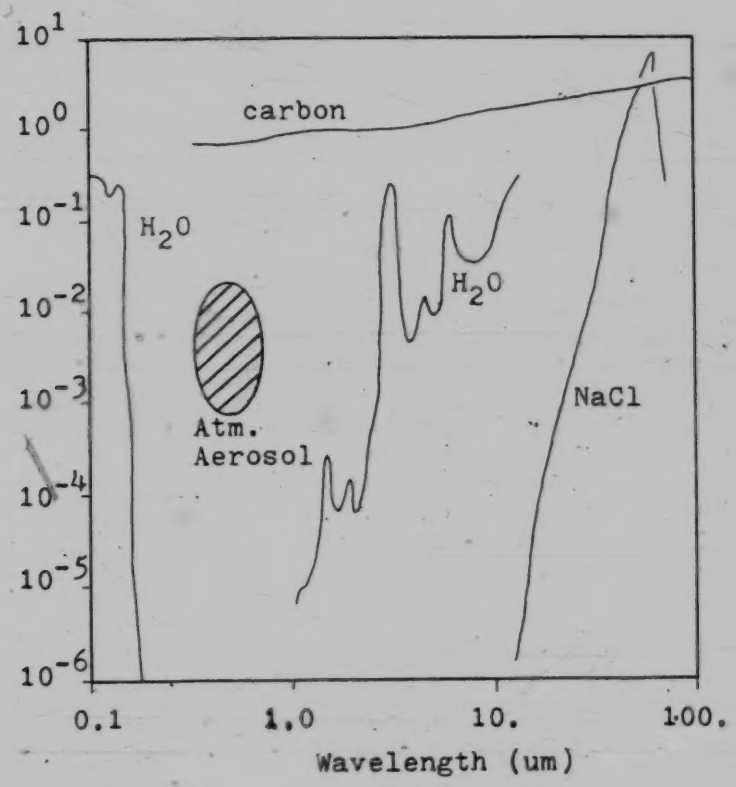

Fig. 5.7 Absorptivity of atmospheric aerosols. The graph shows the imaginary part of the refractive index of some aerosol component materials, as well as the range of observed values for typical atmospheric aerosols. (after Bohren and Huffman, 1983).

soot in the Arctic are not limited to airborne material, since the results of Clarke and Noone (1985) indicate that the absorption of shortwave radiation by the springtime snowpack may be 5%-10% greater than for soot-free snow.

There have also been investigations of Arctic concentrations of the same pollutants which are a source of concern in more populated areas, such as pesticides (Ottar, 1981), organics (Weschler, 1981; Daisey et al., 1981; Hov et al., 1984), and halocarbons (Berg et al., 1983; Oehme and Ottar, 1984; Khalil and Rasmussen, 1984; Rasmussen and Khalil, 1984; Berg et al., 1984; Winchester et al., 1985).

The meteorology of Arctic haze remains poorly understood. Trajectory calculations (Miller, 1981; Barrie et al., 1981; Patterson and Husar, 1981; Harris, 1984; Barrie and Hoff, 1985) have not been able to identify unequivocably the sources of Arctic haze, although there is much indirect evidence to support locations in Siberia and Eurasia as major sources of aerosols in the Alaskan and Canadian Arctic. There are several reasons why trajectory calculations have been, at best, only moderately successful. The main reason is the long time-scales involved, typically 10-20 days (Rahn, 1981b). Roughly 50% of the 10-day 85 kPa back trajectories from Mould Bay, calculated by Barrie et al. (1981) for December 1979 and January 1980, never left the Arctic. Similarly, the majority of the 5-day back trajectories from Mould Bay (calculated with a three-dimensional trajectory model) had endpoints over the polar basin (Barrie and Hoff, 1985); however, there was a tendency for trajectories associated with high values of aerosol light scattering at Mould Bay to have originated on the Eurasian side of the Arctic Ocean. The relative scarcity of reliable synoptic data for the Arctic is also a significant cause of the poor performance of trajectory programs.

Attempts to identify the sources of Arctic haze have prompted investigations of the meteorological transport processes involved. Reiter (1981) tried to relate planetary-wave behaviour to aerosol tracer concentrations at Point Barrow, Alaska. Carlson (1981) suggested the transport process might, in a first approximation, be considered adiabatic so that a quasi-conservative hydrodynamic variable like potential temperature[14] could serve as a tracer

[14]Potential temperature: $\theta = T \times \{ 100 / p \}^{.287}$

of Arctic haze, although a correction for radiative cooling may be necessary if transport times are very long.

The idea of an isentropic process re-appears in the papers by Iversen (1984) and Raatz (1985). These same authors have also attempted to describe the meteorology of Arctic haze from more of a synoptic point of view. Iversen and Joranger (1985) showed that blocking over the Laptev Sea and the Kara Sea, accompanied by deep troughs over the Barents Sea and Scandinavia, respectively, could create a direct pathway from northern Eurasia into the polar basin; they substantiated this with two examples of enhanced sulphur dioxide concentrations at Spitsbergen under these conditions. The work of Raatz and Shaw (1984), Raatz (1984), and Raatz (1985) emphasized the Alaskan Arctic (Pt. Barrow), but the same mechanism was later used to explain some of the conditions encountered during the AGASP flights. The scheme involved several stages, the first of which was an accumulation of atmospheric aerosols and gases in a stationary High pressure area (stagnation), such as might be found in Siberia during winter. In the second stage, the stagnation conditions were disrupted by an approaching Low pressure system; the increasing pressure gradient led to strong winds around the periphery of the High. These winds caused a surge or pulse of pollutants into the Arctic which were then advected across the polar basin.

One of the problems in studying Arctic haze is that it is a phenomenon associated with several time- and space-scales. Many of the more detailed measurements of the haze aerosol (chemical composition, size distributions, physical and optical properties) are isolated spot measurements. Arctic haze is a widespread phenomenon, involving distances on the order of 10^4 km, and has a pronounced annual cycle (Fig. 5.1), yet there can be orders of magnitude differences in aerosol concentrations over as small a distance as 100 m (Rahn, 1985). Shaw (1981) tried to look at the large-scale problem and devised an eddy diffusion model to explain the observed sulphur concentrations at Point Barrow. While there were many approximations and simplifications involved, the model did give a mean sulphur concentration within a factor of 2 of the observed value. The most serious difficulty with this approach is that it assumes a fairly uniform distribution of pollutants within the Arctic

atmosphere, and the later studies have shown that there is actually considerable variability.

One of the highlights of the AGASP flights in 1983 was a traverse of a tropopause fold (Staley, 1960; Danielson, 1968). The tropopause was found to descend from 20 kPa outside of the polar vortex, to 40 kPa within the vortex; the transition zone was marked by lobes where the tropopause descended even further. Within this area, Shapiro et al. (1984) measured high ozone concentrations typical of the lower stratosphere, as well as an order of magnitude increase in condensation nuclei concentrations above the perturbed tropopause. Analysis of aerosol samples showed a population consisting of small spherical sulphur-containing particles, most likely H_2SO_4 droplets, and larger irregularly-shaped particles, mostly composed of crustal elements. It was concluded that the latter type was volcanic debris from the eruption of El Chichon the previous year. In a related aircraft experiment, Chuan and Woods (1984) measured small amounts of carbon in some of their samples of stratospheric aerosols; however, they suggested that, since no mechanism is known which relates carbonaceous particles to volcanic activity, their samples may have contained debris from meteorites.

5.1 Data

The aerosol data used here are from the Canadian Arctic Aerosol Sampling Network and have been described in detail by Barrie et al. (1981), and Barrie and Hoff (1985). Weekly Hi-vol samples were collected at Mould Bay, Igloolik, and Alert. The samples were analyzed for ions and trace elements, using ion chromatography (IAN), inductively-coupled plasma emission spectroscopy (ICP), and neutron activation analysis (NAA). Detection limits (taken from Barrie and Hoff, 1985) for the various species are shown in Table 5.1. Barrie and Hoff (1985) give confidence limits of 20% - 30% in the measured absolute concentrations. Several species were measured by more than one analytical method; with one exception (Al), linear regression of the paired concentrations showed good agreement. That is, the regression gave a slope of about 1.0 and a squared correlation coefficient of 0.8 or greater (Table 2 of Barrie and Hoff, 1985). When a choice had to be made, the NAA concentrations were

Table 5.1 Arctic aerosol composition data.

Code #	Chemical Species	Analysis Technique	Detection Limit ($ng \cdot m^{-3}$)
1	F^-	IAN	1.4 - 3.7
2	Cl^-	IAN	12 - 20
3	Br^-	IAN	(large)
4	NO_3^-	IAN	1.0 - 1.5
5	SO_4^{2-}	IAN	1.0 - 3.0
6	H^+	IAN	?
7	Na^+	IAN	4 - 6
8	$NH4^+$	IAN	7 - 10
9	K^+	IAN	2 - 25
10	I	NAA	.05 - .09
11	Br	NAA	0.5 - 1.9
12	Mn	NAA	.05 - .15
13	Na	NAA	4 - 6
14	V	NAA	.003 - .01
15	Al	NAA	1 - 4
16	Cl	NAA	12 - 20
17	Cu	ICP	.1 - .3
18	Cr	ICP	.05 - .2
19	Al	ICP	1 - 4
20	Ba	ICP	.04 - .07
21	S	ICP	?
22	Ni	ICP	.01 - .10
23	Ca	ICP	5 - 7
24	Zn	ICP	.9 - 1.7
25	Pb	ICP	.2 - .5
26	Mg	ICP	5 - 8
27	Sr	ICP	.01 - .03
28	Fe	ICP	2 - 5
29	V	ICP	.003 - .01
30	Ti	ICP	.2 - .5
31	Mn	ICP	.05 - .15
32	P	ICP	1.0 - 1.4

assumed to be the most reliable because the method gave the total elemental concentrations with a minimum of sample pre-treatment (which might lead to species fractionation).

The primary data period studied here was between 01 July 1980 and 30 June 1983. Except for the final month, all three sampling sites were in operation during this period. Some aerosol data were also available for late 1979 and early 1980 as the sampling programs began at each site, but these data were used mostly for checking the results of the primary data analysis. These early data were discussed by Barrie et al. (1981), while Barrie and Hoff (1985) analyzed all of the available aerosol data.

Meteorological data consisted of two series (surface; constant upper pressure levels) of microfilm weather maps for North America and the Northern Hemisphere, obtained from the National Oceanic and Atmospheric Administration in Asheville, North Carolina. In addition, magnetic tapes with standard and significant level observations from 00Z and 12Z upper air soundings were obtained from the Atmospheric Environment Service of Canada, Downsview, Ontario, for nine Arctic stations (Alert, Eureka, Mould Bay, Resolute, Inuvik, Sachs Harbour, Cambridge Bay, Hall Beach, Frobisher Bay). Both the microfilm weather maps and the upper air soundings covered the complete primary analysis period, 80/07/01 to 83/06/30.

The aerosol sampling program places limits on the types of analyses which might be done, and on any conclusions which might be drawn. The data were weekly averages, so they can be related only to the larger-scale meteorological systems and cycles. It is not possible, for instance, to identify pulses of high pollutant levels which are only a couple of days duration, even though such rapid events are known to occur (Iversen and Joranger, 1985). Daily or even hourly measurements would be necessary for a study of the higher frequency variability. An example of the variability in aerosol concentrations which might be observed with hourly averages, albeit from a mid-continental location at only 53°N and close to large aerosol sources, is shown in Fig. 5.8.

All three of the Arctic aerosol samplers were located at ground-level. While

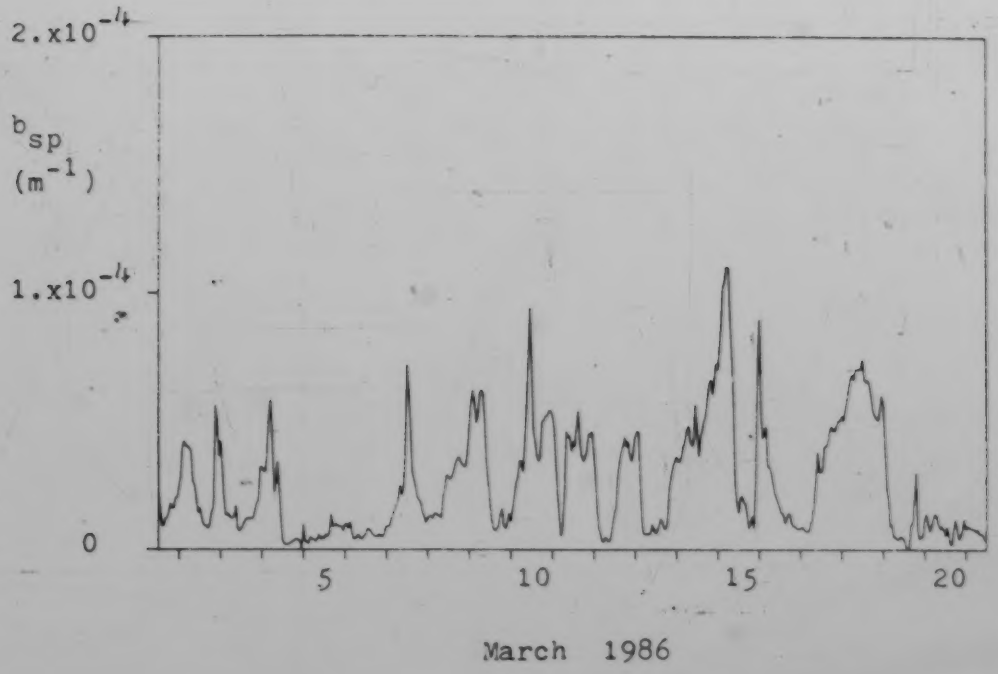

Fig. 5.8 Hourly averages of the aerosol scattering coefficient. The sampling location was the University of Alberta Ellerslie farm, on the southern outskirts of Edmonton AB. Aerosol scattering was measured by a Model 1591 MRI Integrating Nephelometer during the period 86/03/01 to 86/03/22.

considerable care was taken to avoid contamination from local aerosol sources[15] (Barrie and Hoff, 1985), there may be some sample bias under certain conditions. As an example, higher concentrations of crustal material might be found in summer samples than in samples from winter months due to wind-blown dust from the area immediately around the sampler. The samples also give concentrations representative of the boundary layer. Given the frequently-reported laminar structure of Arctic haze, detected at altitudes up to several kilometers on occasion, one should not expect to be able to do a comprehensive study of Arctic haze with ground-level data only. This problem was recognized and, in conjunction with the continuous ground-level sampling program, several short-term aircraft experiments have been carried out by the Atmospheric Environment Serice of Canada (Hoff et al., 1983; Hoff and Trivett, 1984; Leaitch et al., 1984).

[15]For instance, the sampler at Alert was located on a plateau 10 km from the camp.

6. TFA of Arctic Aerosol Data

There are numerous ways of analyzing the Arctic data. The approach here was to try to use the data as efficiently as possible, particularly with regard to the variables (chemical species) to include in the analysis. The major control on this was the availability of concentration data for each variable, since many concentrations were 'bdl' during the summer months.

Data availability is shown in Fig. 6.1 (Alert), Fig. 6.2 (Mould Bay), and Fig. 6.3 (Igloolik). Line segments indicate variable concentrations above the detection limits; gaps indicate either 'bdl' concentrations or missing samples (data missing for all variables). To examine trends over the entire three-year period, a data set (Arctic1) was formed of twelve species: Cl^-, NO_3^-, SO_4^{2-}, Na^+, NH_4^+, Mn (NAA), V (NAA), Al (ICP), Ca, Mg, Sr, and Fe. This data set was weak in the sense that few trace metals were included, but it was relatively complete throughout the entire three-year period (ie., a tolerable number of 'bdl' values). Descriptive statistics for this data set are summarized in Table 6.1. Statistics for both the original data and the data after a logarithmic transformation are shown; the concentrations of many of the chemical species have an approximate log-normal distribution, which was also noted by Heidam (1981, 1982).

A second data set (Arctic2) was formed from samples collected in the period December - March of each winter. The three winters were combined in order to have an adequate number of samples for the analysis. These four months were assumed to be most representative of Arctic haze, although there is certainly some year-to-year variability. The chemical species included in Arctic2 were the same as those in Arctic1, with an additional six elements: Br, Cu, Ba, Ni, Zn, Pb. A minor improvement in Arctic2 was the use of the Al (NAA) concentrations instead of the Al concentrations determined by ICP; when necessary, the results of a linear regression between these two sets of Al concentrations (Barrie and Hoff, 1985) were used to supplement the Al (NAA) data. Descriptive statistics for Arctic2 are shown in Table 6.2.

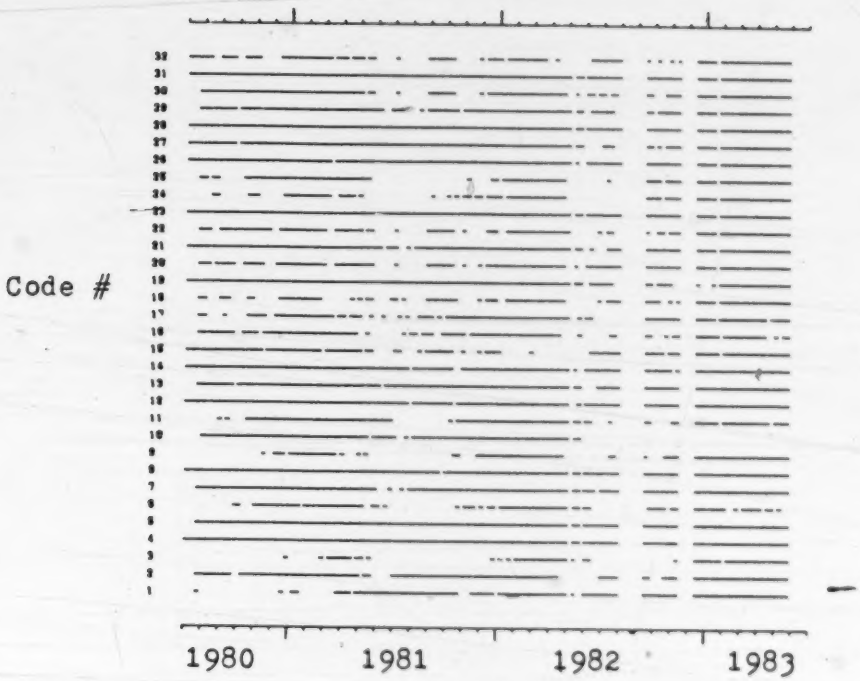

Fig. 6.1 Availability of concentration data at Alert. A line segment indicates a concentration for a chemical species which is above the analytical detection limits. A gap indicates 'bdl' concentrations or missing samples. The chemical species are coded the same as in Table 5.1.

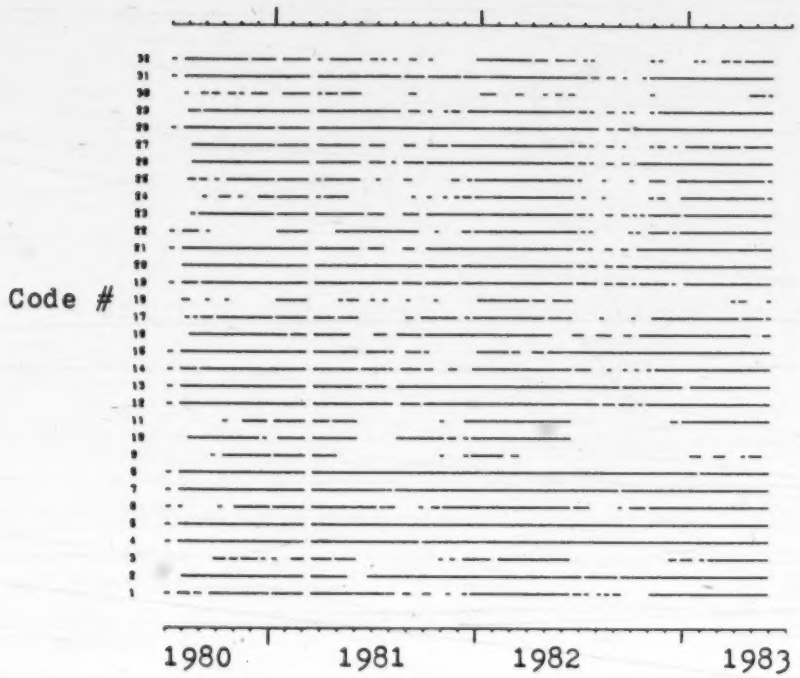

Fig. 6.2 Availability of concentration data at Mould Bay. Same as Fig. 6.1.

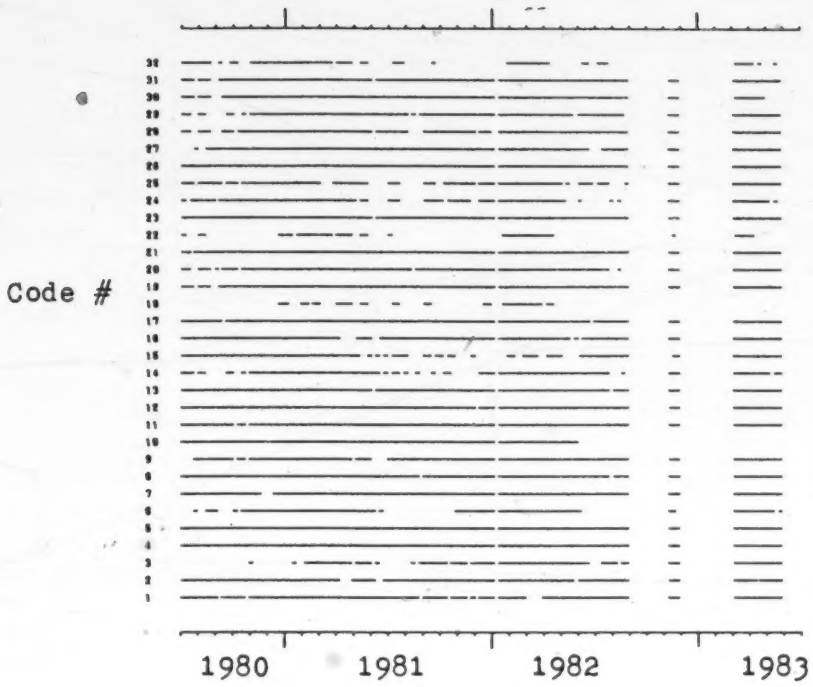

Fig. 6.3 Availability of concentration data at Igloolik. Same as Fig. 6.1.

Table 6.1 Arctic1 variable statistics.

Alert ID #	Arctic1 Species	Linear N	Min	Max	Mean	std dev	Skew	Kurt
1	Cl^-	137	0.00	1338.90	184.25	255.24	2.13	4.77
2	NO_3^-	137	7.04	642.61	67.64	69.34	4.50	32.88
3	SO_4^{2-}	137	0.00	3451.70	1030.20	934.13	0.83	-.37
4	Na^+	137	0.00	656.08	162.06	158.25	1.06	.47
5	NH_4^+	137	0.00	517.17	96.40	98.48	1.61	2.53
6	Mn	137	0.00	10.16	1.63	1.70	1.99	4.98
7	V	137	0.00	3.07	0.57	.62	1.64	2.97
8	Al	137	0.00	442.34	65.67	85.61	2.24	4.94
9	Ca	137	7.34	1712.50	205.95	276.21	2.47	7.21
10	Mg	137	0.00	657.47	113.59	116.90	1.84	3.90
11	Sr	137	0.00	2.00	0.47	0.43	1.06	0.84
12	Fe	137	5.26	544.46	96.01	116.09	1.86	2.77

Alert ID #	Arctic1 Species	Log10 N > 0	Min	Max	Mean	std dev	Skew	Kurt
101	Cl^-	117	1.03	3.13	2.02	0.56	-0.05	-0.96
102	NO_3^-	137	0.85	2.81	1.68	0.38	-0.07	-0.47
103	SO_4^{2-}	136	1.51	3.54	2.76	0.54	-0.45	-1.04
104	Na^+	129	0.62	2.82	1.97	0.57	-0.67	-0.55
105	NH_4^+	136	0.97	2.71	1.77	0.44	0.13	-1.10
106	Mn	134	-0.89	1.01	0.01	0.45	-0.10	-0.85
107	V	132	-1.70	0.49	-0.51	0.56	-0.35	-0.90
108	Al	129	0.57	2.65	1.59	0.47	0.28	-0.49
109	Ca	137	0.87	3.23	2.01	0.51	0.27	-0.59
110	Mg	135	-0.39	2.82	1.83	0.51	-0.76	1.47
111	Sr	124	-2.00	0.30	-0.47	0.47	-0.94	0.74
112	Fe	137	0.72	2.74	1.71	0.49	0.19	-0.72

Table 6.1 (continued).

Mould Bay ID #	Arctic1 Species	Linear N	Min	Max	Mean	std dev	Skew	Kurt
1	Cl^-	138	0.00	2661.80	317.02	451.14	2.75	8.45
2	NO_3^-	138	0.00	270.90	62.12	59.16	1.66	2.41
3	SO_4^{2-}	138	36.74	3217.50	873.08	862.85	1.18	0.51
4	Na^+	138	0.00	1401.60	217.05	233.09	2.28	6.74
5	NH_4^+	138	0.00	539.28	87.45	98.39	2.39	6.36
6	Mn	138	0.00	4.15	0.79	0.86	2.17	4.66
7	V	138	0.00	4.17	0.38	0.61	3.50	14.78
8	Al	138	0.00	297.61	32.23	43.16	3.58	16.42
9	Ca	138	0.00	159.34	34.52	33.82	1.49	2.38
10	Mg	138	0.00	701.20	78.32	102.22	2.85	11.22
11	Sr	138	0.00	2.94	0.39	0.48	2.07	5.63
12	Fe	138	0.00	245.67	33.69	38.03	2.88	10.58

Mould Bay ID #	Arctic1 Species	Log10 N > 0	Min	Max	Mean	std dev	Skew	Kurt
101	Cl^-	130	0.94	3.43	2.24	0.51	0.08	-0.28
102	NO_3^-	137	0.71	2.43	1.62	0.40	0.07	-0.78
103	SO_4^{2-}	138	1.57	3.51	2.67	0.54	-0.34	-0.98
104	Na^+	135	0.77	3.15	2.11	0.50	-0.58	0.02
105	NH_4^+	137	0.81	2.73	1.74	0.42	0.16	-0.42
106	Mn	131	-1.30	0.62	-0.26	0.41	-0.04	-0.34
107	V	111	-1.70	0.62	-0.59	0.47	0.21	-0.29
108	Al	125	0.55	2.47	1.36	0.39	0.40	-0.10
109	Ca	114	0.86	2.20	1.49	0.34	-0.06	-0.84
110	Mg	119	0.78	2.85	1.75	0.43	0.22	-0.58
111	Sr	103	-1.40	0.47	-0.45	0.39	0.04	-0.54
112	Fe	133	0.18	2.39	1.36	0.41	-0.07	-0.08

Table 6.1 (continued).

Igloolik ID #	Arctic1 Species	Linear N	Min	Max	Mean	std dev	Skew	Kurt
1	Cl^-	111	0.00	3244.60	485.72	557.13	2.19	5.82
2	NO_3^-	111	10.66	202.87	70.58	45.10	0.95	0.34
3	SO_4^{2-}	111	75.15	3121.00	912.05	824.88	1.07	0.07
4	Na^+	111	0.00	1760.50	298.47	263.11	2.23	7.86
5	NH_4^+	111	0.00	340.98	90.95	74.64	1.11	0.39
6	Mn	111	0.00	2.46	0.66	0.51	1.01	0.46
7	V	111	0.00	2.34	0.33	0.49	2.0	3.74
8	Al	111	0.00	100.46	19.21	14.73	2.11	7.85
9	Ca	111	0.00	808.76	101.90	129.56	3.06	10.64
10	Mg	111	9.32	559.02	129.87	103.10	1.64	3.10
11	Sr	111	0.00	2.44	0.52	0.49	1.47	2.10
12	Fe	111	0.00	82.06	21.17	15.62	0.97	1.37

Igloolik ID #	Arctic1 Species	Log10 N > 0	Min	Max	Mean	std dev	Skew	Kurt
101	Cl^-	107	1.03	3.51	2.45	0.51	-0.33	-.38
102	NO_3^-	111	1.03	2.31	1.76	0.30	-0.29	-0.63
103	SO_4^{2-}	111	1.88	3.49	2.77	0.43	0.43	-0.02
104	Na^+	110	0.98	3.25	2.31	0.43	-0.84	0.87
105	NH_4^+	109	0.86	2.53	1.82	0.37	-0.02	-0.74
106	Mn	110	-1.30	0.39	-0.32	0.38	-0.41	-0.48
107	V	83	-2.00	0.37	-0.67	0.55	0.04	-0.90
108	Al	108	0.32	2.00	1.19	0.32	-0.31	-0.01
109	Ca	110	1.02	2.91	1.82	0.38	0.65	0.25
110	Mg	111	0.97	2.75	1.98	0.36	-0.32	-0.20
111	Sr	104	-1.52	0.39	-0.42	0.42	-0.40	-0.37
112	Fe	98	0.40	1.91	1.30	0.27	-0.39	0.10

Table 6.2 Arctic2 variable statistics.

Alert ID #	Arctic2 Species	Linear N > 0	Min	Max	Mean	std dev	Skew	Kurt
1	Cl^-	47	31.75	1338.90	362.61	291.05	1.31	1.89
2	NO_3^-	47	43.80	642.61	124.20	88.81	4.37	22.96
3	SO_4^{2-}	47	537.75	3451.70	1709.70	734.92	0.41	-0.53
4	Na^+	47	47.76	656.08	296.59	141.73	0.59	-0.07
5	NH_4^+	47	22.14	517.17	172.10	109.00	1.02	0.90
6	Br	47	0.00	72.11	10.80	13.41	2.89	8.83
7	Mn	47	0.21	10.16	1.99	1.80	2.62	8.37
8	V	47	0.02	3.07	0.97	0.75	1.00	0.57
9	Al	47	7.56	1338.80	102.38	201.54	5.17	28.64
10	Cu	47	0.00	4.92	2.27	1.24	0.24	-0.92
11	Ba	47	0.00	3.04	0.64	0.54	2.28	6.80
12	Ni	47	0.00	1.74	0.70	0.50	0.53	-0.62
13	Ca	47	20.90	1712.50	197.99	311.72	3.16	10.89
14	Zn	47	0.00	256.68	12.92	36.64	6.46	40.51
15	Pb	47	0.00	10.59	3.85	2.50	0.71	0.31
16	Mg	47	0.00	657.47	163.82	129.73	1.54	2.81
17	Sr	47	0.10	2.00	0.76	0.44	0.75	0.39
18	Fe	47	8.53	544.46	88.56	110.90	2.66	6.88

Alert ID #	Arctic2 Species	Log10 N > 0	Min	Max	Mean	std dev	Skew	Kurt
101	Cl^-	47	1.50	3.13	2.41	0.40	-0.46	-0.51
102	NO_3^-	47	1.64	2.81	2.04	0.20	0.99	2.73
103	SO_4^{2-}	47	2.73	3.54	3.19	0.20	-0.45	-0.47
104	Na^+	47	1.68	2.82	2.42	0.24	-0.82	0.85
105	NH_4^+	47	1.35	2.71	2.14	0.31	-0.51	-0.13
106	Br	46	0.19	1.86	0.86	0.37	0.66	0.41
107	Mn	47	-0.68	1.01	0.16	0.35	-0.15	-0.00
108	V	47	-1.70	0.49	-0.19	0.48	-1.16	1.33
109	Al	47	0.88	3.13	1.73	0.44	0.65	0.91
110	Cu	46	-0.37	0.69	0.29	0.27	-0.69	-0.21
111	Ba	45	-0.80	0.48	-0.27	0.29	0.30	-0.13
112	Ni	42	-0.82	0.24	-0.20	0.30	-0.43	-0.66
113	Ca	47	1.32	3.23	2.01	0.45	0.82	0.16
114	Zn	42	0.40	2.41	0.91	0.32	2.15	8.98
115	Pb	45	-0.25	1.02	0.51	0.31	-0.70	-0.03
116	Mg	46	1.36	2.82	2.11	0.33	-0.09	-0.51
117	Sr	47	-1.00	0.30	-0.20	0.30	-0.81	0.25
118	Fe	47	0.93	2.74	1.74	0.41	0.44	0.05

Table 6.2 (continued).

Mould Bay	Arctic2	Linear						
ID #	Species	N > 0	Min	Max	Mean	std dev	Skew	Kurt
1	Cl^-	43	47.50	2183.30	580.32	558.62	1.36	1.11
2	NO_3^-	43	23.40	270.90	113.18	64.65	0.96	0.15
3	SO_4^{2-}	43	256.93	3217.50	1543.60	890.21	0.53	-0.86
4	Na^+	43	40.85	1149.40	358.42	262.73	1.22	1.53
5	NH_4^+	43	0.00	539.28	162.71	133.44	1.28	0.94
6	Br	43	0.00	97.82	19.21	22.72	1.94	3.02
7	Mn	43	0.20	4.15	1.13	0.97	1.67	2.03
8	V	43	0.00	4.17	0.84	0.91	1.97	3.76
9	Al	43	2.92	55.06	21.52	14.01	0.82	-0.22
10	Cu	43	0.00	8.38	1.91	1.57	2.15	5.73
11	Ba	43	0.08	5.18	0.52	0.79	4.96	26.21
12	Ni	43	0.00	1.79	0.56	0.50	0.85	-0.09
13	Ca	43	0.00	159.34	47.84	31.59	1.14	2.19
14	Zn	43	0.00	25.54	6.88	5.58	1.30	1.55
15	Pb	43	0.00	25.60	5.00	5.04	2.06	4.99
16	Mg	43	11.79	701.20	154.01	137.10	1.97	4.81
17	Sr	43	0.00	2.94	0.75	0.60	1.30	2.51
18	Fe	43	4.48	73.10	26.42	17.37	1.10	0.44

Mould Bay	Arctic2	Log10						
ID #	Species	N > 0	Min	Max	Mean	std dev	Skew	Kurt
101	Cl^-	43	1.68	3.34	2.56	0.45	-0.08	-0.95
102	NO_3^-	43	1.37	2.43	1.98	0.26	-0.29	-0.11
103	SO_4^{2-}	43	2.41	3.51	3.11	0.29	-0.47	-0.45
104	Na^+	43	1.61	3.06	2.43	0.36	-0.40	-0.66
105	NH_4^+	42	1.45	2.73	2.09	0.35	-0.01	-0.85
106	Br	41	0.19	1.99	1.10	0.42	0.42	-0.34
107	Mn	43	-0.70	0.62	-0.08	0.33	0.26	-0.47
108	V	41	-1.22	0.62	-0.25	0.43	-0.05	-0.39
109	Al	43	0.47	1.74	1.23	0.31	-0.40	-0.44
110	Cu	42	-0.51	0.92	0.19	0.30	0.17	-0.14
111	Ba	43	-1.10	0.71	-0.47	0.36	0.68	1.53
112	Ni	35	-1.05	0.25	-0.26	0.32	-0.45	-0.31
113	Ca	42	0.86	2.20	1.59	0.32	-0.68	-0.12
114	Zn	39	0.31	1.41	0.79	0.28	0.32	-0.83
115	Pb	40	-0.04	1.41	0.59	0.35	0.35	-0.58
116	Mg	43	1.07	2.85	2.03	0.40	-0.33	-0.42
117	Sr	40	-1.40	0.47	-0.22	0.38	-0.87	0.82
118	Fe	43	0.65	1.86	1.33	0.29	-0.16	-0.44

Table 6.2 (continued).

Igloolik ID #	Arctic2 Species	Linear N > 0	Min	Max	Mean	std dev	Skew	Kurt
1	Cl^-	32	10.70	2281.90	698.20	550.30	1.25	1.19
2	NO_3^-	32	37.01	202.87	111.70	43.98	0.22	-0.77
3	SO_4^{2-}	32	480.10	3121.00	1574.80	738.29	0.55	-0.59
4	Na^+	32	75.02	949.15	425.72	218.71	0.74	-0.04
5	NH_4^+	32	20.06	340.98	152.13	80.16	0.36	-0.74
6	Br	32	3.19	62.35	21.67	18.45	0.93	-0.44
7	Mn	32	0.00	2.46	1.03	0.60	0.19	-0.68
8	V	32	0.00	2.34	0.83	0.62	0.64	-0.38
9	Al	32	0.00	49.99	18.87	14.16	0.44	-0.74
10	Cu	32	0.30	5.03	1.74	1.08	1.26	1.34
11	Ba	32	0.05	0.73	0.32	0.18	0.63	-0.42
12	Ni	32	0.00	1.18	0.44	0.37	0.23	-1.09
13	Ca	32	24.32	123.22	61.38	27.20	0.67	-0.18
14	Zn	32	0.00	16.21	7.53	3.93	0.11	-0.51
15	Pb	32	0.00	18.64	7.21	4.49	1.04	0.95
16	Mg	32	38.99	423.21	176.42	101.01	0.98	0.42
17	Sr	32	0.26	2.44	0.97	0.53	0.82	0.31
18	Fe	32	0.00	52.20	23.51	13.31	0.41	-0.44

Igloolik ID #	Arctic2 Species	Log10 N > 0	Min	Max	Mean	std dev	Skew	Kurt
101	Cl^-	32	1.03	3.36	2.67	0.48	-1.47	2.90
102	NO_3^-	32	1.57	2.31	2.01	0.19	-0.56	-0.38
103	SO_4^{2-}	32	2.68	3.49	3.15	0.22	-0.28	-0.73
104	Na^+	32	1.88	2.98	2.57	0.25	-0.62	0.44
105	NH_4^+	32	1.30	2.53	2.11	0.28	-0.83	0.51
106	Br	32	0.50	1.79	1.17	0.41	-0.04	-1.24
107	Mn	31	-0.60	0.39	-0.05	0.29	-0.59	-0.92
108	V	31	-0.96	0.37	-0.20	0.39	-0.52	-0.92
109	Al	30	0.10	1.70	1.15	0.44	-0.94	-0.16
110	Cu	32	-0.52	0.70	0.16	0.27	-0.24	-0.05
111	Ba	32	-1.30	-0.14	-0.57	0.29	-0.54	-0.27
112	Ni	22	-0.92	0.07	-0.25	0.23	-1.15	1.70
113	Ca	32	1.39	2.09	1.75	0.20	-0.15	-0.80
114	Zn	31	0.11	1.21	0.83	0.27	-1.03	0.66
115	Pb	30	0.50	1.27	0.83	0.22	0.36	-0.50
116	Mg	32	1.59	2.63	2.18	0.26	-0.29	-0.35
117	Sr	32	-0.59	0.39	-0.08	0.25	-0.28	-0.71
118	Fe	30	1.02	1.72	1.35	0.21	0.05	-1.19

Concentration data for F^-, H^+, K^+, Cr, Ti, and P were judged to be too frequently 'bdl' at one or more stations to be included in the analysis, and were ignored. For the twelve species in Arctic1 and the eighteen species in Arctic2, any 'bdl' concentrations were replaced by zero. These two data sets were further sub-divided by station, and the data from Alert, Mould Bay, and Igloolik were analyzed separately.

One of the advantages of TFA is the ease with which the results of one analysis can be used as a starting point for another analysis. Thus, while the construction and testing of possible source profile vectors is the most time-consuming part of the TFA procedure, this step could be shortened considerably by using the final refined factors from one station as target vectors for the other two stations. This does not assume that the factors are common to each station. Rather, it is a testing of the hypothesis that the factors are the same, since the target rotation will produce a rotated vector different from the test vector if the factor is not common. Data from Alert, the most northerly station, were the first to be analyzed, followed by Mould Bay and Igloolik.

As with the analyses of Chapter 4, weights were assigned to each chemical species. The selection of weights was only an attempt to keep the variance at roughly (order of magnitude) the same level and, by doing so, equalize the significance of each variable. Weights for variables common to Arctic1 and Arctic2 were the same for each data set, and the same weights were used with the data from each of the stations.

6.1 Arctic1 - Factors

The results of the eigenvalue calculations are shown in Tables 6.3-6.5 for Alert, Mould Bay, and Igloolik, respectively. The Malinowski Indicator function and the Scree test suggest only three significant factors at Alert, and the value of the Exner function is acceptable with only these three factors. The 'eigenvalue-one' criteria would require keeping at least five factors; however, if this criteria were used it would be difficult to ignore the sixth factor which is associated with an eigenvalue only marginally less than 1.0. And then the seventh factor has an eigenvalue of 0.740, not much smaller that the sixth eigenvalue. One of

Table 6.3 Arctic1 eigenvalue calculations for Alert.

Alert Arctic1 M,N; Data set dimensions: 137 12

Variable (column) weights:

Cl^-	NO_3^-	SO_4^{2-}	Na^+	NH_4^+	Mn	V	Al	Ca	Mg	Sr	Fe
1.0	1.0	0.100	1.0	1.0	100.0	100.0	1.0	1.0	1.0	100.0	1.0

Total variance (covar0):

21.328	5.841	13.786	18.606	11.606	15.793	2.650	3.058	30.779	5.699	1.272	6.580

Eigenvectors (columns):

-3.333	2.390	2.043	0.396	-0.206	-0.323	-0.087	0.050	-0.139	0.012	0.030	0.001
-1.983	0.389	-0.680	0.968	0.137	0.506	0.064	-0.260	-0.086	-0.006	0.042	0.0
-2.936	1.048	-1.885	-0.456	0.326	-0.276	-0.207	-0.107	-0.254	-0.017	0.050	-0.005
-3.587	2.203	0.335	-0.604	0.345	0.480	0.156	0.082	0.154	0.070	-0.052	0.002
-2.792	0.658	-1.677	0.560	-0.114	-0.304	0.046	0.277	0.256	0.007	-0.029	-0.003
-3.690	-1.185	-0.229	-0.212	-0.679	0.327	-0.015	0.215	-0.146	-0.206	-0.006	0.030
-1.259	0.117	-0.445	-0.243	-0.630	-0.170	0.517	-0.253	-0.009	0.190	0.009	0.004
-1.475	-0.772	0.076	-0.040	-0.135	0.061	-0.402	-0.055	0.093	0.228	0.069	0.163
-4.679	-2.801	0.764	0.087	0.580	-0.206	0.255	0.016	-0.041	0.022	-0.063	0.021
-2.273	-0.229	0.401	-0.201	-0.047	-0.136	-0.086	-0.302	0.266	-0.258	0.154	-0.017
-0.990	0.101	-0.009	0.005	-0.186	-0.054	-0.262	-0.237	0.048	-0.043	-0.340	-0.010
-2.208	-1.207	0.168	-0.050	-0.176	0.115	-0.299	0.023	0.030	0.208	0.058	-0.178

Eigenvalues:

94.609	23.632	12.143	2.137	1.580	0.975	0.740	0.427	0.286	0.248	0.161	0.060

Significance tests for eigenvalues:

#	EIGEN	VAR	CPV	SCR	IME	IND	RSD	XNR
1.000	94.609	69.060	69.060	30.942	0.048	0.0014	0.168	0.478
2.000	23.632	17.250	86.310	13.692	0.048	0.0012	0.117	0.368
3.000	12.143	8.860	95.170	4.828	0.037	0.0009	0.073	0.087
4.000	2.137	1.560	96.730	3.268	0.037	0.0010	0.064	0.068
5.000	1.580	1.150	97.890	2.115	0.035	0.0011	0.055	0.061
6.000	0.975	0.710	98.600	1.403	0.034	0.0013	0.048	0.043
7.000	0.740	0.540	99.140	0.863	0.032	0.0017	0.042	0.032
8.000	0.427	0.310	99.450	0.551	0.030	0.0023	0.037	0.017
9.000	0.286	0.210	99.660	0.342	0.029	0.0038	0.034	0.007
10.000	0.248	0.180	99.840	0.161	0.026	0.0071	0.028	0.006
11.000	0.161	0.120	99.960	0.044	0.020	0.0209	0.021	0.005
12.000	0.060	0.040	100.000	0.0	-0.0	-0.0	-0.0	0.000

Varimax orthogonal rotation with 3 factors :

0.959	0.924	0.857	0.920	1.079	3.284	0.676	1.559	5.299	1.776	0.594	2.381
4.359	0.791	0.935	3.326	0.745	0.897	0.412	0.272	0.959	1.198	0.536	0.408
1.038	1.751	3.416	2.434	3.053	1.865	1.082	0.524	1.149	0.889	0.591	0.726

Variances of factors:

				55.446	35.972	38.965					

% communalities (covar0):

98.400	77.900	96.300	95.800	95.100	95.400	67.800	90.800	98.500	94.400	77.800	96.700

Table 6.4 Arctic1 eigenvalue calculations for Mould Bay.

Mould Bay Arctic1 M,N; Data set dimensions: 138 12

Variable (column) weights:

Cl^-	NO_3^-	SO_4^{2-}	Na^+	NH_4^+	Mn	V	Al	Ca	Mg	Sr	Fe
1.0	1.0	0.100	1.0	1.0	100.0	100.0	1.0	1.0	1.0	100.0	1.0

Total variance (covar0):

53.528	5.076	11.274	30.539	14.290	8.976	1.771	3.591	1.388	3.502	0.900	3.163

Eigenvectors (columns):

-6.818	-2.491	-0.271	-0.856	0.165	-0.0	0.062	-0.075	0.014	0.016	0.004	0.002
-1.886	0.847	0.111	-0.240	-0.383	-0.212	-0.653	-0.317	-0.043	0.094	0.021	0.011
-2.568	1.776	0.978	0.032	0.541	0.054	0.276	-0.440	0.016	-0.002	0.013	0.010
-5.269	-0.205	0.688	1.404	-0.520	0.027	0.064	0.133	0.021	-0.017	-0.003	-0.005
-2.827	2.161	0.375	-1.076	-0.302	0.311	0.028	0.366	-0.046	-0.048	-0.013	-0.012
-2.311	1.297	-1.180	0.145	0.013	-0.664	0.207	0.030	-0.225	-0.050	0.009	-0.015
-0.881	0.649	0.100	-0.092	0.232	-0.510	-0.036	0.221	0.418	0.124	-0.017	-0.008
-1.141	0.717	-1.203	0.245	-0.055	0.420	-0.022	-0.156	0.200	-0.056	0.083	-0.115
-0.865	0.281	-0.269	0.321	0.349	0.266	-0.021	0.139	-0.165	0.380	-0.024	-0.037
-1.592	0.136	-0.028	0.409	0.725	0.074	-0.414	0.158	-0.052	-0.197	-0.103	-0.031
-0.751	0.160	-0.066	0.215	0.369	0.072	-0.141	0.210	-0.023	-0.024	0.210	0.099
-1.157	0.714	-1.059	0.201	-0.087	0.295	0.037	-0.092	0.113	0.017	-0.104	0.153

Eigenvalues:

104.991	18.040	5.706	4.367	1.676	1.191	0.749	0.623	0.314	0.217	0.075	0.049

Significance tests for eigenvalues:

#	EIGEN	VAR	CPV	SCR	IME	IND	RSD	XNR
1.000	104.990	76.080	76.080	23.918	0.043	0.0012	0.147	0.631
2.000	18.040	13.070	89.150	10.846	0.043	0.0010	0.104	0.128
3.000	5.706	4.140	93.290	6.711	0.043	0.0011	0.086	0.105
4.000	4.367	3.160	96.450	3.546	0.038	0.0010	0.067	0.081
5.000	1.676	1.210	97.670	2.332	0.037	0.0012	0.058	0.051
6.000	1.191	0.860	98.530	1.468	0.035	0.0014	0.049	0.046
7.000	0.749	0.540	99.070	0.926	0.033	0.0017	0.043	0.021
8.000	0.623	0.450	99.530	0.474	0.028	0.0022	0.034	0.014
9.000	0.314	0.230	99.750	0.247	0.025	0.0032	0.029	0.004
10.000	0.217	0.160	99.910	0.090	0.019	0.0053	0.021	0.003
11.000	0.075	0.050	99.960	0.036	0.018	0.0189	0.019	0.000
12.000	0.049	0.040	100.000	0.0	-0.0	-0.0	-0.0	0.000

Varimax orthogonal rotation with 4 factors :

6.674	1.014	1.202	4.672	0.927	1.005	0.342	0.404	0.558	1.269	0.542	0.429
1.715	1.618	2.874	2.232	3.363	1.451	0.945	0.446	0.390	0.714	0.373	0.528
1.552	0.835	0.733	1.445	1.274	2.307	0.446	1.721	0.690	0.705	0.416	1.596
-1.899	-0.045	0.683	1.161	-0.412	0.029	0.082	0.011	0.249	0.323	0.183	0.012

Variances of factors:

				73.386	34.391	19.527	5.800				

% communalities (covar0):

99.900	85.600	95.000	99.000	97.700	94.000	68.600	92.500	72.200	77.700	71.100	95.200

Table 6.5 Arcticl eigenvalue calculations for Igloolik.

Igloolik Arcticl M,N; Data set dimensions: 111 12

Variable (column) weights:

Cl^-	NO_3^-	SO_4^{2-}	Na^+	NH_4^+	Mn	V	Al	Ca	Mg	Sr	Fe
1.0	1.0	0.100	1.0	1.0	100.0	100.0	1.0	1.0	1.0	100.0	1.0

Total variance (covar0):

47.184	3.488	7.025	24.608	7.457	2.669	0.938	0.321	10.074	5.935	0.898	0.401

Eigenvectors (columns):

-6.451	2.280	-0.281	0.532	0.032	-0.033	0.041	0.005	-0.007	0.006	0.0	-0.0
-1.436	-0.836	0.210	0.005	0.752	0.319	0.064	-0.016	-0.091	0.016	0.0	0.015
-1.832	-1.558	0.971	0.286	-0.315	-0.114	0.283	-0.111	-0.102	0.042	0.005	0.016
-4.731	-0.344	0.953	-1.087	-0.056	-0.070	-0.097	0.039	-0.001	-0.001	-0.001	-0.002
-1.906	-1.743	0.475	0.601	0.241	-0.276	-0.230	-0.058	0.082	-0.041	-0.014	-0.014
-1.230	-0.975	0.066	0.239	-0.123	0.155	0.015	0.266	0.142	0.098	0.051	0.043
-0.539	-0.428	0.279	0.329	-0.344	0.246	-0.217	0.125	-0.185	-0.013	-0.019	-0.042
-0.393	-0.325	-0.026	-0.036	0.086	0.011	0.151	0.060	0.060	-0.005	0.051	-0.137
-1.741	-1.247	-2.324	-0.184	0.005	-0.185	0.024	0.072	-0.096	-0.026	0.030	0.012
-2.017	-0.797	-0.991	-0.074	-0.249	0.324	-0.046	-0.241	0.109	0.043	-0.046	-0.015
-0.810	-0.265	0.228	0.056	-0.143	0.195	0.060	-0.011	0.049	-0.215	0.070	0.029
-0.418	-0.366	-0.096	0.003	0.010	0.003	0.148	0.166	0.046	-0.073	-0.164	-0.004

Eigenvalues:

82.938	15.118	8.730	2.116	0.951	0.459	0.247	0.199	0.109	0.068	0.041	0.024

Significance tests for eigenvalues:

#	EIGEN	VAR	CPV	SCR	IME	IND	RSD	XNR
1.000	82.938	74.720	74.720	25.280	0.044	0.0013	0.152	0.774
2.000	15.118	13.620	88.340	11.660	0.044	0.0011	0.108	0.203
3.000	8.730	7.860	96.200	3.796	0.032	0.0008	0.065	0.102
4.000	2.116	1.910	98.110	1.889	0.028	0.0008	0.049	0.057
5.000	0.951	0.860	98.970	1.032	0.025	0.0008	0.038	0.038
6.000	0.459	0.410	99.380	0.619	0.023	0.0009	0.032	0.025
7.000	0.247	0.220	99.600	0.397	0.022	0.0011	0.028	0.011
8.000	0.199	0.180	99.780	0.218	0.019	0.0015	0.023	0.008
9.000	0.109	0.100	99.880	0.120	0.017	0.0022	0.020	0.002
10.000	0.068	0.060	99.940	0.059	0.016	0.0043	0.017	0.002
11.000	0.041	0.040	99.980	0.022	0.014	0.0148	0.015	0.001
12.000	0.024	0.020	100.000	0.0	-0.0	-0.0	-0.0	0.001

Varimax orthogonal rotation with 4 factors :

6.490	0.702	0.667	3.776	0.559	0.431	0.202	0.131	0.476	1.083	0.524	0.119
1.368	1.315	2.440	2.449	2.466	1.326	0.774	0.374	0.466	0.952	0.670	0.392
1.683	0.683	0.445	1.210	0.925	0.756	0.098	0.298	3.059	1.896	0.208	0.377
-0.592	0.342	0.463	1.694	0.087	0.100	-0.102	0.128	-0.019	0.142	0.125	0.085

Variances of factors:

				59.562	25.857	19.841	3.641				

% communalities (covar0):

100.000	80.500	96.900	99.900	97.300	94.600	70.300	81.600	99.500	95.900	87.000	79.100

the difficulties with the 'eigenvalue-one' criteria is that it does not include the possible effects of errors in the observations on the magnitude of the eigenvalues. If all experimental error could somehow be removed from the data, then an analysis of the error-free data might very well give a different number of factors with eigenvalues greater than 1.0.

Experiments with three, four, and five factors showed that three factors were readily identifiable and were sufficient to account for most of the observed variance in the data. Four significant factors were retained for both Mould Bay and Igloolik, a decision based mainly on the XNR, IND, and Scree tests. This meant, again, ignoring two factors with eigenvalues greater than 1.0 at Mould Bay.

Test vectors for the three factors at Alert were relatively easy to devise. From data tables in Mason and Moore (1982), relative composition profiles were assembled for seawater and for crustal rocks. These test vectors are shown in Table 6.6, along with the refined profiles (concentrations have been multiplied by the weight appropriate for each chemical species). Also shown is a binary vector (Al, Fe) and the profile refined from this test vector. This was a check of the derived crustal component profile; the crustal test vector and the binary (Al, Fe) vector gave approximately the same final vector, within a constant scaling parameter.

Test vectors for the third factor at Alert, and the third and fourth factors at Mould Bay and Igloolik, were more difficult to devise, since a source composition could only be guessed at. The procedure in this case (and for similar cases later) was to compare the vectors already derived with the unrotated vectors comprising the raw factor loading matrix. Binary vectors were then constructed with elements corresponding to chemical species which were not yet explained by rotated vectors. For example, the refined crustal and seawater factors at Alert were 'weak' (small loadings) for species such as NO_3^-, SO_4^{2-}, NH_4^+, and V. If there are only three significant factors, then the third factor must account for most of the observed variance in the concentrations of these species.

The refined profile for the third factor at Alert is shown in Table 6.7. It is labelled 'Anthro' to suggest a man-caused or anthropogenic source, but this may be a misnomer. The

Table 6.6 Arctic1 test and refined vectors for Alert.

	Seawater			Crustal	Al,Fe -	Binary
	Test	Final	Test	Final	Test	Final
Cl^-	1.000	0.960	0.001	0.052	0.000	0.040
NO_3^-	0.000	0.076	0.000	0.118	0.000	0.091
SO_4^{2-}	0.014	0.027	0.000	0.001	0.000	0.002
Na^+	0.600	0.645	0.100	-0.004	0.000	-0.003
NH_4^+	0.000	-0.005	0.000	0.086	0.000	0.067
Mn	0.000	0.035	0.300	0.729	0.000	0.561
V	0.000	0.026	0.050	0.103	0.000	0.080
Al	0.000	-0.001	0.300	0.372	1.000	0.286
Ca	0.020	0.035	0.130	1.299	0.000	0.999
Mg	0.070	0.195	0.080	0.378	0.000	0.291
Sr	0.400	0.083	0.100	0.105	0.000	0.081
Fe	0.000	0.000	0.180	0.572	1.000	0.440

problem is that factor analysis, and other statistical methods based on the analysis of variance in a data set, can only resolve factors which have at least a little independent variability. As an example, consider an Arctic aerosol monitoring site, and assume that there are two aerosol source types in mid-latitude continental areas. One source may be a true anthropogenic source (industrial and/or urban area emissions), while the other is a biogenic source (emissions from vegetation, forested areas, etc.). If the transport of aerosols to the Arctic from both sources is governed by large-scale meteorological systems, then most of the variance in the observed concentrations is independent of the variability in the source strengths. Statistical analysis of the observed variability would not be able to resolve these separate sources, but would give a single pseudo-source with a profile which was a composite of the two true sources.

The way to overcome this problem is to try to incorporate outside or independent knowledge of the sources and variables into the analysis. Target rotation of known or likely source profile vectors is one method to do this, but to extract weak factors (or to resolve multiple factors which are similar) requires better and better knowledge of the dominant source profiles. Without this knowledge, it was deemed better to accept a single general component at Alert to represent the fraction of aerosol material from non-crustal, non-seawater sources.

The refined vectors for Alert, Mould Bay, and Igloolik are summarized in Table 6.7. Negative loadings were small and were assumed to be insignificant (resulting from round-off errors); they have been replaced by zero. Binary test vectors were used to refine the fourth factors at Mould Bay and Igloolik. This appears to be a factor common to these two stations. The general composition of this factor is apparent in the fourth row of the orthogonally-rotated (Varimax) factor loading matrix; the factor has high loadings for Na^+ and SO_4^{2-}, but a large negative loading for Cl^-. The adaptation of the PCA model to atmospheric aerosol composition data does not admit negative source elements, so the target rotations were carried out by testing binary vectors with high Na^+ and SO_4^{2-} loadings while forcing the Cl^- loadings to zero.

Table 6.7 Refined Arctic1 aerosol source profiles.

Alert	Sea Salt	Crustal	Anthro	
Cl^-	0.960	0.052	-0.001	
NO_3^-	0.076	0.118	0.492	
SO_4^{2-}	0.027	0.001	1.061	
Na^+	0.645	-0.004	0.554	
NH_4^+	-0.005	0.086	0.935	
Mn	0.035	0.729	0.377	
V	0.026	0.103	0.303	
Al	-0.001	0.372	0.065	
Ca	0.035	1.299	0.000	
Mg	0.195	0.378	0.114	
Sr	0.083	0.105	0.130	
Fe	0.000	0.572	0.074	—
Mould Bay	**Sea Salt**	**Crustal**	**Anthro**	**Na/SO_4^{2-}**
Cl^-	0.971	-0.001	-0.001	0.000
NO_3^-	0.084	0.123	0.473	0.145
SO_4^{2-}	0.075	0.006	0.874	0.588
Na^+	0.637	0.116	0.080	1.243
NH_4^+	-0.003	0.151	1.201	0.006
Mn	0.046	0.658	0.288	0.091
V	0.010	0.074	0.296	0.105
Al	0.000	0.556	0.001	-0.014
Ca	0.057	0.192	0.007	0.179
Mg	0.160	0.135	0.041	0.328
Sr	0.063	0.095	0.031	0.159
Fe	0.005	0.504	0.041	0.001
Igloolik	**Sea Salt**	**Crustal**	**Anthro**	**Na/SO_4^{2-}**
Cl^-	0.971	0.026	0.001	0.006
NO_3^-	0.089	0.202	0.362	0.267
SO_4^{2-}	0.052	0.098	0.831	0.348
Na^+	0.640	0.008	0.107	1.219
NH_4^+	0.008	0.341	0.940	-0.132
Mn	0.029	0.278	0.462	0.117
V	-0.001	0.027	0.340	-0.039
Al	0.016	0.109	0.096	0.095
Ca	0.054	1.301	-0.002	0.119
Mg	0.149	0.699	0.160	0.204
Sr	0.070	0.025	0.189	0.110
Fe	0.010	0.148	0.114	0.071

Again, there was a degree of subjective judgement involved. The eigenvalue calculations are indeterminate as to the major orientation of the factor axes. A 180° rotation of the fourth factors at Mould Bay and Igloolik would give large positive loadings for Cl^-, and large negative loadings for Na^+ and SO_4^{2-}. This is just as valid as the original vector.

Comparison of the sea salt factor at each station shows that the ratio of Na^+ to Cl^- is about 0.66, sufficiently close to the ratio of the molecular weights of these elements (0.65) in bulk seawater to demonstrate that a reasonable marine component can be derived which does not show significant loss of Cl^-. The major differences between the derived sea salt composition and the composition of bulk seawater lie in the relative amounts of the trace elements. The amount of strontium associated with sea salt is lower by a factor of 5-10, while NO_3^-, Mn, V, Ca, and Mg are all larger than expected. These results agree roughly with the results of Heidam (1981, 1984) and Hopper (1984), but they contradict the results of Shaw (1983a)[16].

Shaw (1983a) had found that marine particles in the Alaskan Arctic were characterized by high levels of Na, Mg, Ca, and K, but Cu and Cl behaved anomalously. He suggested that Cu and Cl might be due to biogenic activity instead of sea salt. It is possible to reconcile his results at least partially with the Canadian and Greenland studies, assuming of course that there is not a significant difference in the behaviour of chlorine in these different regions. The TFA results in Table 6.7 show that a marine component can be readily extracted at all three Canadian stations with the expected Na^+/Cl^- ratio. The fourth factors at Mould Bay and Igloolik indicate that there is additional variability in Cl^-, Na^+, and SO_4^{2-} concentrations not explained by the sea salt component; in particular, the opposite signs on the loadings for Cl^- and Na^+ in this factor suggest that these elements are inversely related. Sea salt is the dominant source of Cl^- for the Arctic aerosol, but there is an additional minor

[16]Any comparison with BFA studies must be a rather qualitative one. The usual BFA prodedure uses a Varimax rotation to calculate a final factor loading matrix, and retains only those factor loadings which are larger than some 'significant' level, say 0.5; smaller loadings are assumed to be insignificant. The analogous procedure in TFA would be to ignore all the species concentrations in the sea salt factor except for Na^+ and Cl^-.

control on the Na^+, SO_4^{2-}, and Cl^- concentrations from another component.

The relative composition profiles for the sea salt component can also be compared to a frequently-made assumption regarding sulphate. It has became customary to correct the total amount of SO_4^{2-} observed in samples for the amount of SO_4^{2-} contributed by sea salt particles (see Atmospheric Environment **19**(12) for examples). The weight ratio of SO_4^{2-} to Na^+ in bulk seawater is 0.25 (Mason and Moore, 1982), so that the non-marine or 'excess' sulphate is given by:

$$[XSO_4^{2-}] = [SO_4^{2-}] - 0.25 \times [Na^+] \qquad (6.1)$$

This correction assumes that the SO_4^{2-}/Na^+ ratio is constant for all atmospheric particles originally derived from sea salt. The sea salt components here seem to challenge that assumption, since the ratio is 0.42 at Alert, 1.18 at Mould Bay, and 0.81 at Igloolik.

What these ratios mean is that marine aerosols in the samples are accompanied by more sulphate than can be accounted for by sea salt alone, even if the sea salt particles are chemically conservative and do not undergo any changes in composition during transport in the atmosphere. The correction expressed by Eqn. 6.1 could still be valid in terms of individual particles, but it may not be suitable for apportioning aerosol mass in a bulk sample (depending on how the higher levels of SO_4^{2-} are to be interpreted). The ratios only indicate that the appearance of particles of marine origin at each receptor site coincided with higher levels of SO_4^{2-} than can be explained by simply assuming chemically-conservative particles.

The composition of the crustal components at each station is also interesting. It is well-known that chemical fractionation and enrichment processes can occur which will change the relative amounts of some elements compared to the original crustal material; Shaw (1983a) lists some possible mechanisms. There are some significant differences between the crustal components derived here for the three Arctic stations. Calcium is the dominant crustal element at Alert and Igloolik, but it is only a minor element at Mould Bay. Al and Fe are relatively strong at Alert and Mould Bay, but they are weak at Igloolik.

There does not appear to be a common crustal factor for all three stations. On the other hand, the anthropogenic factor is relatively similar at Alert, Mould Bay, and Igloolik.

This is not too surprising because the crustal component should be influenced by the soil and rock composition of the region around the sampling site, while the anthropogenic factor (based on the limited number of elemental tracers included in Arctic1) would be expected to be more widespread and have a rather uniform composition.

No errors or confidence limits have been placed on any of the loadings of the refined source profiles, because the method described in Section 3.6 could not be applied to these data. The reason for this will be discussed shortly, in connection with the calculation of the factor scores. A crude upper-limit on the uncertainty associated with each element can be estimated by assuming the confidence limits in the raw concentration data (~±30%) also applies to each factor loading. This estimate is a little higher than might be inferred from some observations during the tests of the stability of the factors: after a change of ~±10% in any major element, a target rotation would usually produce the original vector again. These uncertainty estimates are really only valid for the larger factor loadings. A bias was introduced when it was assumed that small negative elements were insignificant, resulting from numerical round-off, and could be ignored. Some of the small positive elements are also likely to be the result of similar errors and should be ignored.

6.2 Arctic1 - Scores

Factor scores for the refined source profiles were also calculated. Unfortunately, the final step of the TFA procedure (source scaling; Section 3.5) could not be carried out. TSP, or the total mass in each sample, was not measured for these Arctic samples. This prevented the conversion from relative source compositions and source strengths to absolute units, and the assessment of errors in the factor loadings and scores by the method of Section 3.6. The omission of TSP from the data set is most regrettable. This parameter is not an independent variable, although Heidam (1982) argued that it was such and used TSP as just another variable for his factor analyses. While one can appreciate the practical difficulties in obtaining an accurate TSP measurement for samples collected in remote areas[17], the total particulate

[17]Among the potential problems is contamination by on-site handling, since "everyone up there smokes like a chimney" (personal communication, R. Hoff, 1984).

mass is a necessary parameter for mass apportionment studies of this sort[18].

An attempt was made to estimate the TSP for each sample based on the observation by Leaitch et al. (1984) that the ratio of soluble to total particle mass was typically 0.15-0.35. An approximate soluble mass for each sample was calculated by summing the concentrations of all of the measured ionic species. This sum was multiplied by 3.0. Linear regression between these "TSP" values and the factor scores (S_k) at the three stations gave:

Alert
$r^2 = 0.999$
$$\text{"TSP"} = 0.51S_1 + 6.12S_2 + 38.4S_3 \quad (6.2)$$

Mould Bay
$r^2 = 0.963$
$$\text{"TSP"} = 4.87S_1 + 0.81S_2 + 33.9S_3 + 22.6S_4 \quad (6.3)$$

Igloolik
$r^2 = 0.939$
$$\text{"TSP"} = 4.73S_1 + 1.38S_2 + 29.0S_3 + 18.2S_4 \quad (6.4)$$

The partial mass contributions for each source are plotted along with the "TSP" at each station in Figures 6.4-6.6.

The source contributions in these figures are incorrect, as are the regression results in Equations 6.2-6.4. The approximate "TSP" is predominantly Na^+, Cl^-, SO_4^{2-}, and NO_3^-. The linear regression over-estimated the contributions from the components which have relatively large amounts of these species (such as sea salt) and, at each station, under-estimated the contribution from the crustal component which had only small amounts of the elements used to devise "TSP".

In order to examine the trends and cycles in the components, the factor scores were normalized by the largest score for each component. These normalized scores are plotted in Figures 6.7-6.9. Typical source profiles, after removing the variable weights and scaling by an arbitrary constant, are shown in Table 6.8[19]. It should be emphasized that the elements of the

[18] An alternative approach avoids the need for TSP data by using ratios of elemental concentrations to identify trends (Barrie and Hoff, 1985) or as tracers of significant aerosol sources (Rahn, 1981c; Rahn and Lowenthal, 1984; Lowenthal and Rahn, 1985), but these could be used for mass apportionment only if a number of additional assumptions are made.

[19] The scaling constant for each component was selected only to give a reasonable-looking source profile, so that major elements were on the order of 100 $mg \cdot g^{-1}$ and the sum of the elements was less than 1000 $mg \cdot g^{-1}$.

Table 6.8 Arctic1 scaled source profiles.

Alert Arctic1 M, N, LP:				
	137	12	3	
MLR score coeffs:	0.51	6.12	38.38	
Weighting coeffs:	10.00	1.00	1.00	
Scaled source profiles (mg/g):				
	Crustal	Sea Salt	Anthro	
Cl^-	10.40	157.30	0.00	
NO_3^-	23.20	12.40	12.80	
SO_4^{2-}	1.40	44.80	276.00	
Na^+	0.00	105.60	14.40	
NH_4^+	16.90	0.00	24.30	
Mn	1.40	0.06	0.10	
V	0.20	0.04	0.10	
Al	73.00	0.00	1.70	
Ca	255.20	6.40	0.00	
Mg	74.40	32.00	2.90	
Sr	0.20	0.20	0.03	
Fe	112.60	0.20	1.90	
Mould Bay Arctic1 M, N, LP:				
	138	12	4	
MLR score coeffs:	4.87	0.81	33.89	22.65
Weighting coeffs:	1.00	5.00	1.00	1.00
Scaled source profiles (mg/g):				
	Sea Salt	Crustal	Anthro	Na/SO_4^{2-}
Cl^-	199.90	0.00	0.00	0.00
NO_3^-	17.30	30.20	13.90	6.40
SO_4^{2-}	153.50	12.40	257.40	260.10
Na^+	131.10	28.80	2.30	54.90
NH_4^+	0.00	37.20	35.40	0.30
Mn	0.09	1.70	0.10	0.04
V	0.02	0.20	0.10	0.05
Al	0.20	137.60	0.10	0.00
Ca	11.70	47.60	0.20	7.90
Mg	33.10	33.50	1.20	14.50
Sr	0.20	0.20	0.01	0.10
Fe	1.20	125.00	1.20	0.04
Igloolik Arctic1 M, N, LP:				
	111	12	4	
MLR score coeffs:	4.73	1.38	29.79	18.22
Weighting coeffs:	1.00	5.00	1.00	1.00
Scaled source profiles (mg/g):				
	Sea Salt	Crustal	Anthro	Na/SO_4^{2-}
Cl^-	206.80	3.60	0.00	0.30
NO_3^-	19.20	29.20	12.20	14.70
SO_4^{2-}	115.10	140.60	278.60	186.90
Na^+	136.20	1.00	3.60	66.90
NH_4^+	2.10	49.20	31.50	7.30
Mn	0.06	0.40	0.20	0.10
V	0.00	0.04	0.10	0.00
Al	3.40	15.80	3.20	5.20
Ca	11.40	188.20	0.00	6.60
Mg	31.70	101.10	5.40	11.20
Sr	0.20	0.04	0.10	0.10
Fe	2.30	21.40	3.80	4.00

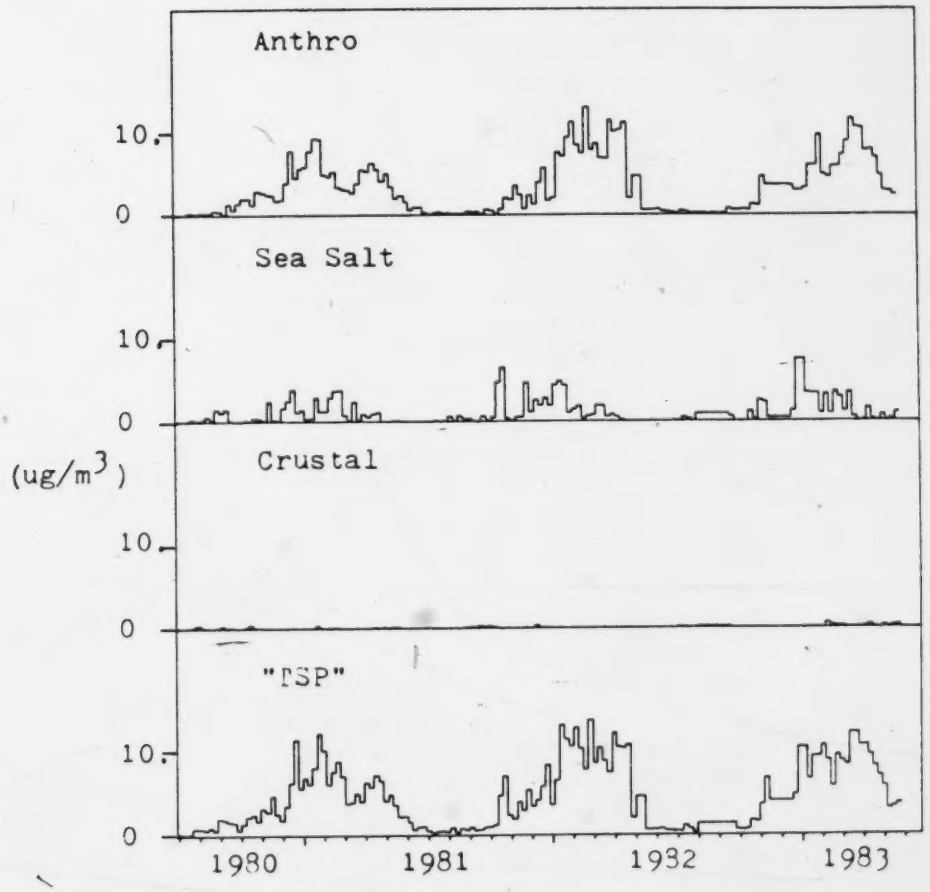

Fig. 6.4 Source strengths for the Alert factors (Arctic1). Also shown is the pseudo-"TSP", based on a constant ratio of soluble to total mass. The source strengths were scaled by the coefficients obtained from a multiple linear regression between "TSP" and the factor scores.

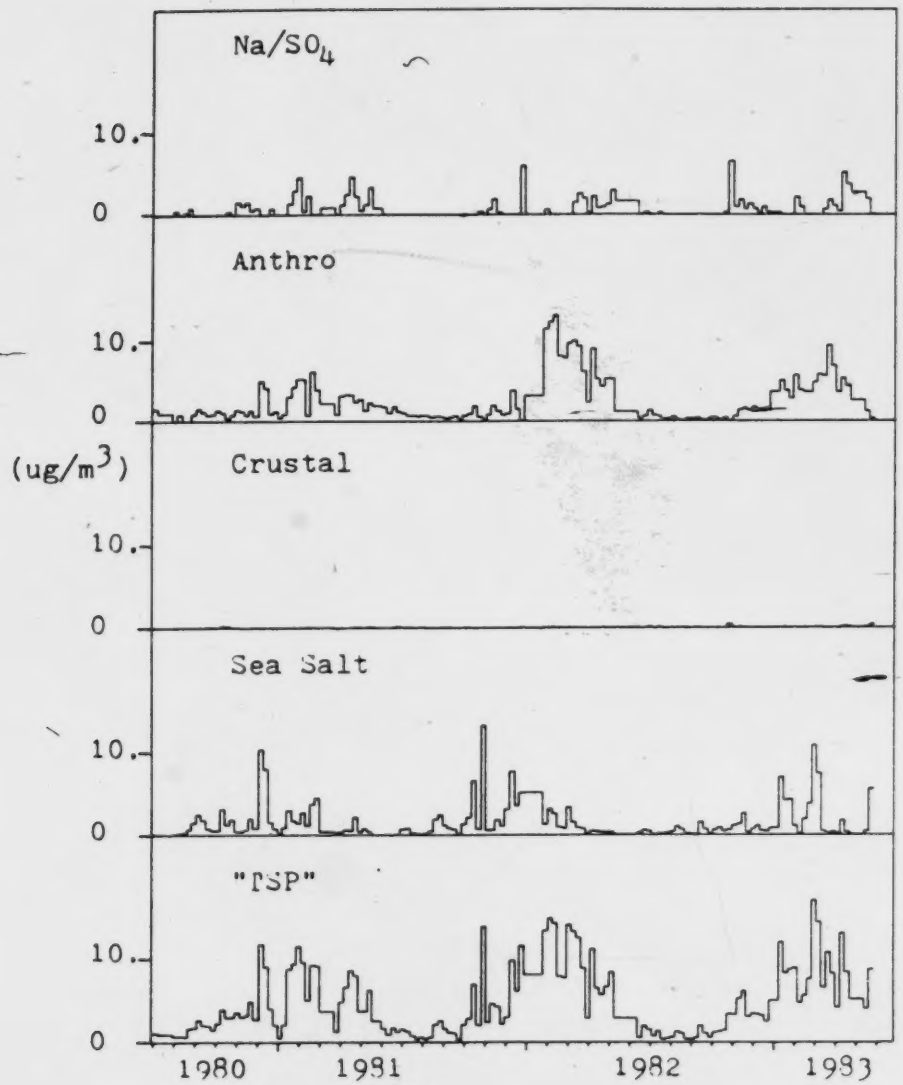

Fig. 6.5 Source strengths for the Mould Bay factors (Arctic1). Same as Fig. 6.4.

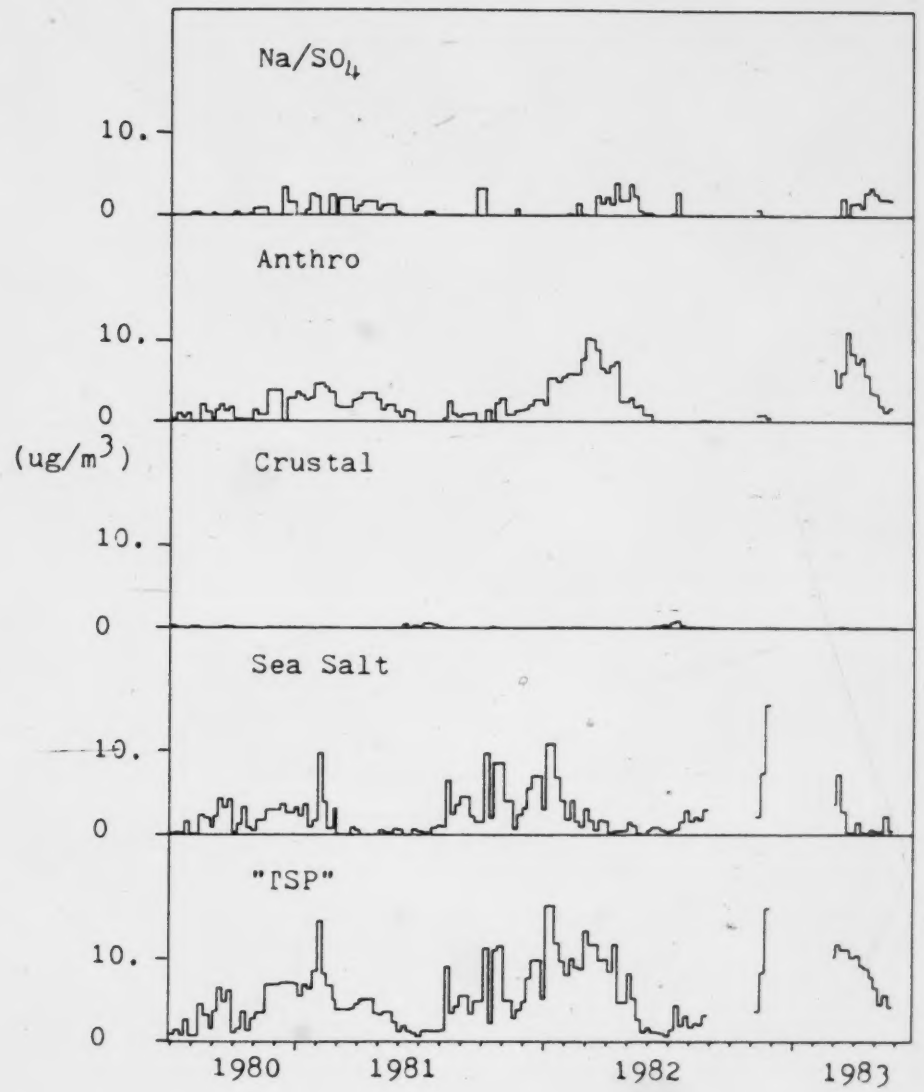

Fig. 6.6 Source strengths for the Igloolik factors (Arctic1). Same as Fig. 6.4.

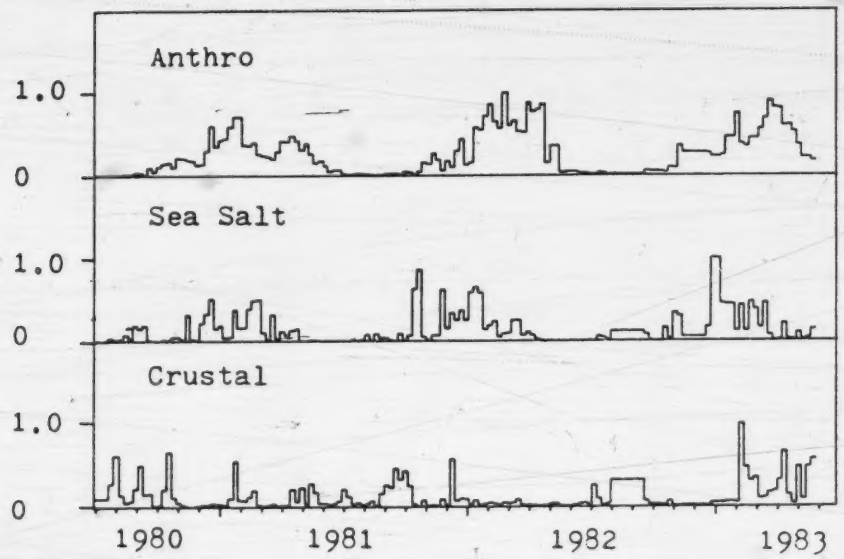

Fig. 6.7 Normalized factor scores at Alert (Arctic1).

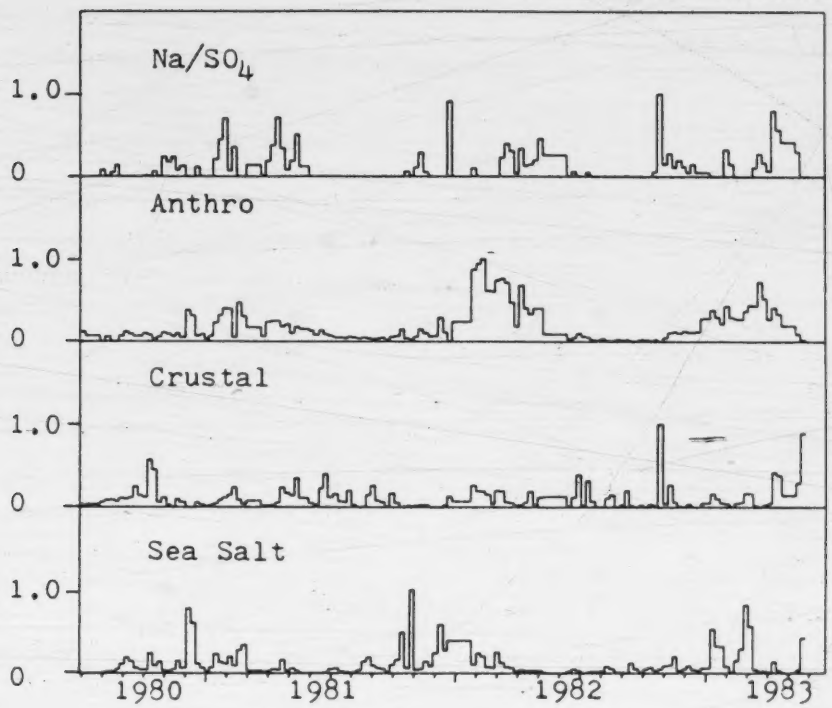

Fig. 6.8 Normalized factor scores at Mould Bay (Arctic1).

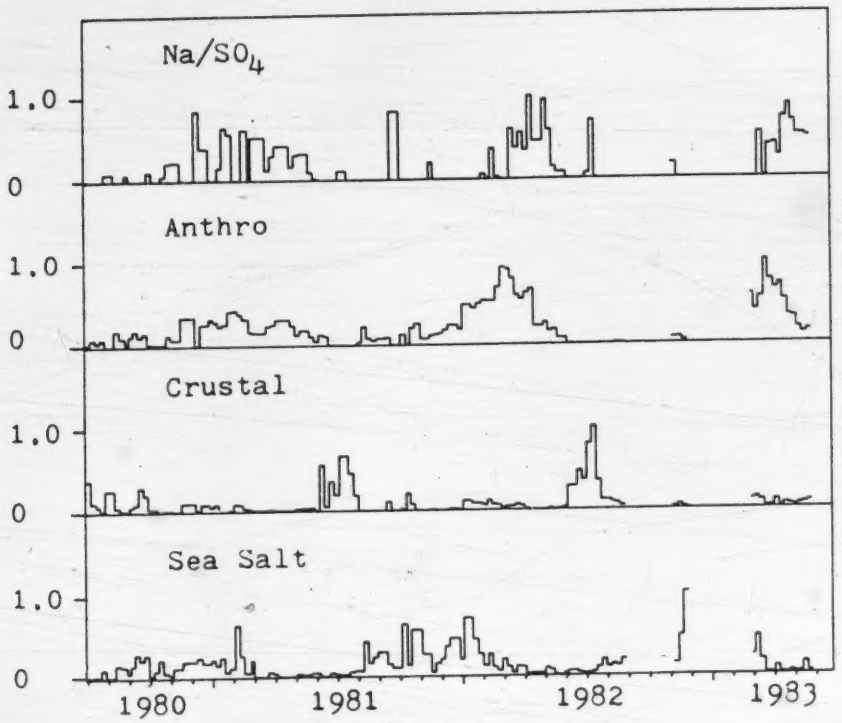

Fig. 6.9 Normalized factor scores at Igloolik (Arctic1).

components and scores are accurate on a relative basis; they have been scaled and normalized, respectively, solely for convenience. Without a true TSP estimate for each sample, scaling to absolute units cannot be done.

Some generalizations can be made from the plots of the normalized factor scores. Trends in the components are similar at Alert, Mould Bay, and Igloolik. The sea salt, anthro, and Na/SO_4^{2-} components all show an annual cycle, but the times of their maxima are different. The sea salt component appears first, usually in September or late August, and peaks in January-February. Sea salt is at a minimum in May-June. The mean data for the complete freeze-over of seawater ranges from early November in the Igloolik area, to mid-September at Mould Bay and early September at Alert (Maxwell, 1980). The mean date for seawater clear of ice is late July at Igloolik; Maxwell (1980) shows the sea surface around Mould Bay and Alert as never being completely clear of ice. Comparison of these dates with the behaviour of the sea salt component suggests that the presence of an ice-free sea surface in the immediate area may account for the first appearance of marine aerosols in late summer or fall, but sea-ice cover by itself is insufficient to explain the winter maximum and the May-June minimum.

The anthropogenic components are at a minimum from July to October, and their increase in the autumn lags sea salt by 1-2 months. They also peak later than sea salt, typically in February or March. The Na/SO_4^{2-} components at Mould Bay and Igloolik are more episodic, but their annual cycle tends to reach a maximum in late winter (March-April). The winter maximum in these components reflects the seasonal variation in particle residence time in the Arctic atmosphere.

The crustal component at Igloolik also has an obvious annual cycle, but it peaks during the summer and is negligible much of the remaining time. Maxwell (1980) gives the mean dates of snow-cover loss and formation as early July and mid-September, respectively, for the Igloolik area, which agrees well with the cycle of the crustal component (allowing for some year-to-year variability). By contrast, the crustal components at Alert and Mould Bay have a less definable pattern, although one might try to argue that high values of this component at Mould Bay are more likely during the summer months.

The strong summer maximum for the crustal component at Igloolik agrees well with the discussion of nephelometer data by Barrie and Hoff (1985). The sampling site was on the edge of the town of Igloolik, and Barrie and Hoff (1985) noted that contamination of nephelometer data by vehicular dust was evident during the summer months. The crustal component at Igloolik is probably dominated by this source and reflects the composition of the local soil. The crustal components at Mould Bay and Alert are more likely an average of local soil-derived dust and dust transported from other sources.

Cross-correlations between similar factors at Alert and Mould Bay are shown in Fig. 6.10. They were calculated using 59 factor scores for samples from the period mid-March 1981 to May 1982. These represented approximately weekly samples, but two of the Mould Bay samples were from longer periods[20]. The original concentration data are known to be from non-normal and non-randomly sampled populations, and the distributions of the scores have been further distorted by transforming negative scores to zero; thus the cross-correlation functions should be interpreted rather cautiously. There is no evidence of a significant correlation at any large lag, although there seems to be a tendency for the sea salt and anthro components at Alert to lead the corresponding components at Mould Bay by ~1 week. The crustal component scores do not appear to be correlated at all, which agrees with the rather random nature of the scores depicted in Fig. 6.7 and Fig. 6.8.

6.3 Arctic2 - Factors

The second data set was processed in a manner similar to that used for Arctic1. Selection of the number of significant factors was considerably more difficult, however, because it was unusual for two or more tests to indicate the same number of factors. In general, the Scree, Exner, and Malinowski Indicator tests pointed to between three and five significant factors. Results of the eigenvalue calculations for Alert, Mould Bay, and Igloolik are displayed in Tables 6.9-6.11. In the end, five factors were retained at each station, a decision which also took into account the 'identifiability' of factors. That meant, for instance,

[20]The Mould Bay series was adjusted by assuming that the results for the two long samples would be the same for shorter periods in the same sampling interval.

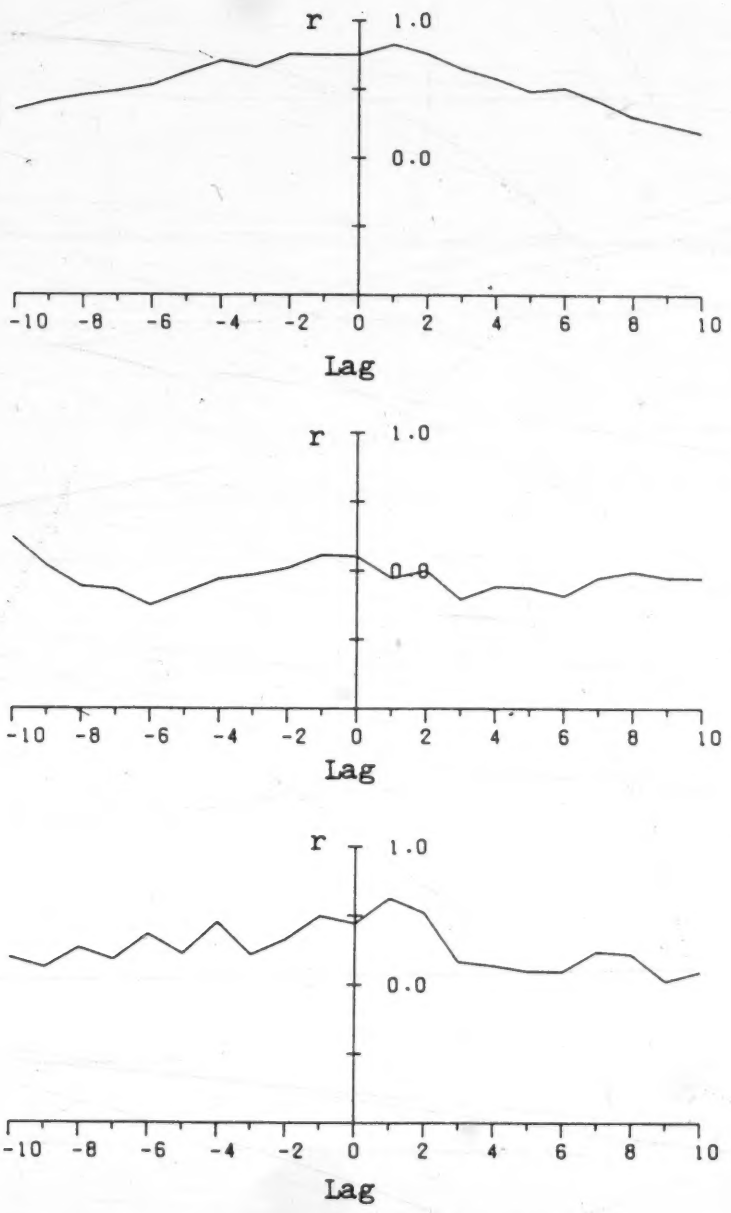

Fig. 6.10 Cross-correlations for Arctic1 scores. The normalized factor scores at Alert and Mould Bay were used for these calculations. The abscissa gives the number of samples (~weeks) by which the scores for Mould Bay lag behind the Alert scores.

trying to include factors similar to the factors derived from Arctic1, since these are present in the winter but the selected time intervals may have been too short for these factors to show substantial variability.

Table 6.9 Arctic2 eigenvalue calculations for Alert.

Alert Arctic2 M,N; Data set dimensions: 47 18

Variable (column) weights:

Cl^-	NO_3^-	SO_4^{2-}	Na^+	NH_4^+	Br	Mn	V	Al	Cu	Ba	Ni	Ca	Zn	Pb	Mg	Sr	Fe
1.0	1.0	0.100	1.0	1.0	10.0	100.0	100.0	1.0	50.0	100.0	100.0	1.0	10.0	20.0	1.0	100.0	1.0
Total variance (covar0):																	
11.007	1.708	3.618	8.207	3.758	2.489	3.188	1.174	0.930	1.545	0.335	0.548	3.191	1.618	0.775	1.819	0.422	0.667
Eigenvectors (columns):																	
-2.967	1.446	-0.169	-0.082	-0.078	-0.230	-0.081	-0.020	-0.031	-0.091	-0.001	0.036	-0.009	0.027	-0.0	-0.005	-0.002	-0.001
-1.204	-0.119	-0.223	0.114	0.130	0.023	-0.013	-0.191	0.346	-0.022	0.072	-0.038	-0.004	0.003	-0.010	0.002	-0.0	0.001
-1.736	-0.650	-0.283	-0.005	0.130	0.083	0.123	-0.044	-0.122	-0.032	0.162	0.100	-0.080	0.016	-0.021	-0.004	0.010	0.0
-2.770	0.441	-0.346	0.147	0.101	0.348	0.186	0.130	0.011	0.097	-0.081	-0.022	0.024	-0.007	0.003	0.002	0.005	-0.004
-1.694	-0.794	-0.315	0.193	0.166	-0.208	0.107	-0.006	-0.103	-0.104	-0.004	-0.090	0.108	-0.019	-0.004	0.006	-0.004	-0.001
-0.965	-0.492	-0.348	-1.086	-0.088	0.008	-0.045	0.045	0.040	0.010	-0.030	-0.012	0.011	-0.0	-0.002	0.0	-0.004	-0.0
-1.615	-0.511	0.454	0.139	0.079	-0.028	-0.122	0.208	0.069	-0.090	-0.066	0.008	-0.089	-0.043	-0.007	0.036	-0.024	-0.001
-0.916	-0.431	-0.110	0.175	0.063	-0.148	-0.139	0.102	0.070	0.145	0.009	0.131	0.077	-0.003	0.020	-0.023	-0.020	0.008
-0.695	-0.203	0.476	-0.101	0.073	-0.137	0.262	-0.207	0.014	0.022	-0.158	0.065	-0.032	-0.045	0.006	-0.017	0.007	-0.003
-1.084	-0.318	-0.002	0.098	-0.065	0.263	-0.325	-0.240	-0.102	-0.057	-0.081	0.025	0.028	-0.004	0.006	-0.001	-0.005	0.003
-0.518	-0.146	0.142	0.060	0.004	-0.035	-0.042	0.040	-0.006	0.031	-0.056	-0.048	-0.024	0.043	-0.069	-0.034	0.011	0.043
-0.612	-0.316	-0.021	0.102	-0.0	-0.135	-0.133	-0.012	-0.010	0.123	-0.051	-0.013	-0.015	0.059	-0.038	0.022	0.042	-0.036
-1.314	-0.047	1.185	-0.171	0.005	0.077	0.069	-0.007	0.007	0.0	0.070	0.002	0.070	0.079	0.014	0.020	0.002	0.005
-0.804	-0.414	-0.091	0.210	-0.857	-0.004	0.103	0.013	0.044	-0.019	0.003	0.008	0.002	0.003	0.001	0.0	0.001	0.0
-0.759	-0.361	-0.149	0.081	0.038	-0.072	-0.016	-0.026	-0.033	0.054	-0.021	-0.082	-0.088	0.079	0.081	-0.019	-0.012	0.004
-1.256	0.219	0.318	-0.055	-0.101	-0.052	-0.051	-0.101	-0.088	0.174	0.097	-0.083	-0.023	-0.082	-0.019	0.003	-0.031	-0.003
-0.629	0.028	0.020	-0.020	-0.012	-0.051	-0.079	0.015	-0.0	0.028	0.035	-0.005	-0.003	-0.071	0.045	0.023	0.067	0.026
-0.652	-0.107	0.437	-0.014	-0.001	0.062	-0.088	0.106	0.027	-0.070	0.040	-0.035	0.0	-0.040	0.006	-0.073	0.024	-0.025
Eigenvalues:																	
35.838	4.667	2.693	1.426	0.851	0.375	0.330	0.237	0.180	0.118	0.098	0.061	0.049	0.037	0.016	0.011	0.009	0.005

Table 6.9 (continued).

Significance tests for eigenvalues:

#	EIGEN	VAR	CPV	SCR	IME	IND	RSD	XNR
1.000	35.838	76.250	76.250	23.749	0.028	0.00041	0.118	0.412
2.000	4.667	9.930	86.180	13.819	0.031	0.00036	0.093	0.237
3.000	2.693	5.730	91.910	8.089	0.030	0.00033	0.073	0.098
4.000	1.426	3.030	94.940	5.056	0.028	0.00031	0.060	0.090
5.000	0.851	1.810	96.760	3.245	0.026	0.00030	0.050	0.086
6.000	0.375	0.800	97.550	2.446	0.026	0.00031	0.045	0.073
7.000	0.330	0.700	98.260	1.744	0.025	0.00033	0.040	0.055
8.000	0.237	0.500	98.760	1.240	0.023	0.00035	0.035	0.045
9.000	0.180	0.380	99.140	0.858	0.022	0.00038	0.031	0.024
10.000	0.118	0.250	99.390	0.606	0.021	0.00043	0.028	0.015
11.000	0.098	0.210	99.600	0.398	0.019	0.00049	0.024	0.011
12.000	0.061	0.130	99.730	0.268	0.017	0.00059	0.021	0.009
13.000	0.049	0.100	99.840	0.165	0.015	0.00073	0.018	0.003
14.000	0.037	0.080	99.910	0.087	0.013	0.00092	0.015	0.001
15.000	0.016	0.030	99.950	0.052	0.012	0.00146	0.013	0.001
16.000	0.011	0.020	99.970	0.029	0.011	0.00304	0.012	0.000
17.000	0.009	0.020	99.990	0.010	0.010	0.00989	0.010	0.000
18.000	0.005	0.010	100.000	0.0	-0.0	-0.0	-0.0	0.0

Varimax orthogonal rotation with 5 factors :

2.985	0.723	0.678	2.157	0.554	0.312	0.541	0.287	0.180	0.452	0.188	0.159	0.526	0.235	0.247	0.885	0.414	0.234
0.853	0.915	1.517	1.527	1.666	0.569	1.148	0.898	0.345	0.828	0.358	0.582	0.324	0.563	0.740	0.436	0.328	0.285
1.017	0.346	0.598	0.866	0.548	0.280	1.162	0.341	0.764	0.500	0.365	0.276	1.652	0.253	0.238	0.814	0.296	0.688
0.394	0.212	0.569	0.404	0.416	1.398	0.210	0.148	0.167	0.212	0.052	0.110	0.161	0.153	0.197	0.190	0.137	0.070
0.329	0.135	0.305	0.348	0.324	0.169	0.309	0.211	0.057	0.326	0.119	0.182	0.168	1.070	0.180	0.258	0.113	0.119

Variances of factors:

						17.025	14.040	9.224	3.116	2.070							

% communalities (covar0):

99.400	90.400	97.700	97.700	97.400	99.700	97.200	91.300	82.400	83.500	93.600	88.500	99.100	99.200	95.100	95.700	94.300	94.100

Table 6.10 Arctic2 eigenvalue calculations for Mould Bay.

Mould Bay Arctic2 M,N; Data set dimensions: 43 18

Variable (column) weights:

Cl^-	NO_3^-	SO_4^{2-}	Na^+	NH_4^+	Br	Mn	V	Al	Cu	Ba	Ni	Ca	Zn	Pb	Mg	Sr	Fe
1.0	1.0	0.100	1.0	1.0	10.0	100.0	100.0	1.0	50.0	100.0	100.0	1.0	10.0	20.0	1.0	100.0	1.0
Total variance (covar0):																	
16.409	1.156	2.523	7.412	2.784	4.772	1.196	0.734	0.065	1.638	0.290	0.458	0.134	0.466	1.251	1.370	0.279	0.061
Eigenvectors (columns):																	
-3.811	-1.311	0.193	-0.218	0.275	-0.073	-0.042	-0.034	0.020	-0.020	-0.003	0.003	-0.004	0.0	-0.003	-0.001	0.0	0.0
-0.978	0.259	-0.250	0.090	0.037	-0.067	-0.030	0.117	-0.122	0.038	-0.115	0.101	-0.030	-0.035	0.012	-0.002	0.0	0.0
-1.342	0.726	-0.134	0.098	-0.029	-0.334	0.179	-0.128	0.023	0.039	-0.044	-0.056	-0.017	0.017	0.008	-0.002	-0.0	-0.001
-2.621	-0.297	-0.152	0.337	-0.545	0.116	-0.061	-0.065	-0.0	-0.020	0.001	-0.006	0.004	-0.003	-0.0	0.002	-0.0	-0.0
-1.351	0.861	-0.325	-0.221	-0.059	-0.162	-0.079	0.037	0.029	0.001	0.141	0.061	0.035	-0.022	0.0	0.002	0.001	0.0
-1.451	1.202	1.101	-0.040	-0.012	0.069	-0.035	0.013	-0.015	-0.029	-0.014	0.003	-0.008	-0.002	-0.002	0.003	-0.001	-0.0
-0.904	0.446	-0.349	-0.129	0.016	0.020	-0.109	0.140	-0.009	-0.038	-0.058	-0.019	0.028	0.063	-0.006	0.025	-0.007	-0.005
-0.636	0.411	-0.301	-0.165	-0.003	0.031	-0.073	0.112	0.023	-0.068	-0.038	-0.124	-0.013	-0.037	-0.011	-0.027	0.006	0.002
-0.210	0.066	0.012	0.077	-0.007	-0.019	0.017	0.007	-0.031	0.022	0.0	0.052	0.012	0.032	-0.045	-0.047	-0.008	-0.001
-0.914	0.426	-0.181	0.632	0.420	0.082	-0.046	-0.008	-0.0	-0.024	0.041	-0.020	0.021	-0.004	0.005	-0.001	-0.001	-0.0
-0.387	0.198	-0.023	0.007	0.031	0.091	-0.074	0.021	0.232	0.171	-0.050	0.014	0.002	-0.006	-0.004	0.0	0.002	-0.0
-0.471	0.249	-0.214	-0.054	0.034	0.129	0.245	-0.007	0.140	-0.148	-0.032	0.068	-0.004	-0.010	-0.005	0.003	-0.002	-0.0
-0.348	0.008	0.039	0.007	-0.021	0.040	0.032	0.059	0.002	-0.008	0.008	0.026	0.006	0.040	0.026	-0.020	0.032	0.001
-0.546	0.277	-0.235	-0.036	0.049	0.104	-0.004	-0.004	-0.020	0.027	0.072	0.001	-0.121	0.019	-0.015	0.010	0.003	-0.0
-0.782	0.548	-0.323	-0.309	0.102	0.255	0.026	-0.218	-0.105	0.057	-0.024	-0.006	0.031	-0.002	0.006	-0.005	0.001	0.0
-1.096	-0.180	0.068	0.024	-0.023	0.082	0.269	0.176	-0.073	0.101	0.039	-0.039	0.029	-0.012	-0.017	0.014	0.003	0.001
-0.492	-0.060	0.023	-0.068	-0.031	0.085	0.060	0.096	0.019	0.024	0.044	-0.013	-0.016	0.012	0.049	-0.026	-0.022	-0.003
-0.217	0.104	-0.047	0.0	0.002	-0.006	0.001	0.017	0.007	-0.0	-0.009	0.002	0.003	0.018	0.003	0.002	-0.005	0.026
Eigenvalues:																	
33.071	5.666	1.919	0.783	0.572	0.290	0.206	0.162	0.109	0.078	0.055	0.043	0.021	0.011	0.006	0.005	0.002	0.001

Table 6.10 (continued).

Significance tests for eigenvalues:

#	EIGEN	VAR	CPV	SCR	IME	IND	RSD	XNR
1.000	33.071	76.910	76.910	23.089	0.027	0.00040	0.117	0.582
2.000	5.666	13.180	90.090	9.912	0.026	0.00031	0.079	0.098
3.000	1.919	4.460	94.550	5.448	0.025	0.00027	0.060	0.088
4.000	0.783	1.820	96.370	3.627	0.024	0.00026	0.051	0.071
5.000	0.572	1.330	97.700	2.297	0.022	0.00025	0.042	0.048
6.000	0.290	0.680	98.380	1.621	0.021	0.00026	0.037	0.034
7.000	0.206	0.480	98.860	1.141	0.020	0.00027	0.032	0.016
8.000	0.162	0.380	99.230	0.765	0.018	0.00028	0.028	0.010
9.000	0.109	0.250	99.490	0.513	0.017	0.00029	0.024	0.009
10.000	0.078	0.180	99.670	0.332	0.015	0.00032	0.020	0.008
11.000	0.055	0.130	99.790	0.205	0.013	0.00035	0.017	0.006
12.000	0.043	0.100	99.890	0.105	0.011	0.00037	0.013	0.003
13.000	0.021	0.050	99.940	0.057	0.009	0.00043	0.011	0.003
14.000	0.011	0.030	99.970	0.031	0.008	0.00056	0.009	0.002
15.000	0.006	0.010	99.980	0.017	0.007	0.00084	0.008	0.001
16.000	0.005	0.010	99.990	0.005	0.005	0.00131	0.005	0.001
17.000	0.002	0.0	100.000	0.002	0.004	0.00400	0.004	0.000
18.000	0.001	0.0	100.000	0.0	-0.0	-0.0	-0.0	0.000

Varimax orthogonal rotation with 5 factors :

3.812	0.596	0.644	2.294	0.570	0.625	0.432	0.246	0.129	0.389	0.192	0.208	0.282	0.247	0.279	0.993	0.439	0.108
1.041	0.726	1.101	1.040	1.402	0.786	0.931	0.768	0.105	0.568	0.310	0.509	0.147	0.566	0.982	0.374	0.212	0.190
0.369	0.177	0.618	0.389	0.557	1.893	0.192	0.148	0.095	0.258	0.182	0.081	0.123	0.097	0.240	0.227	0.112	0.072
0.656	0.417	0.557	0.689	0.325	0.414	0.249	0.131	0.125	1.041	0.156	0.159	0.083	0.207	0.119	0.251	0.042	0.080
0.464	-0.084	-0.190	-0.648	-0.134	0.002	-0.050	-0.038	-0.047	0.031	-0.008	-0.015	-0.022	-0.017	0.092	-0.015	0.003	-0.021

Variances of factors:

						23.185	10.162	4.920	3.031	0.714							

% communalities (covar0):

99.900	94.700	93.400	99.700	97.800	99.800	96.600	94.100	84.100	99.300	65.700	73.000	92.100	93.100	89.700	90.500	90.300	97.600

Table 6.11 Arctic2 eigenvalue calculations for Igloolik.

Igloolik Arctic2 M,N; Data set dimensions: 32 18

Variable (column) weights:

Cl^-	NO_3^-	SO_4^{2-}	Na^+	NH_4^+	Br	Mn	V	Al	Cu	Ba	Ni	Ca	Zn	Pb	Mg	Sr	Fe
1.0	1.0	0.100	1.0	1.0	10.0	100.0	100.0	1.0	50.0	100.0	100.0	1.0	10.0	20.0	1.0	100.0	1.0

Total variance (covar0):

13.962	0.571	1.493	6.416	1.515	3.427	0.617	0.487	0.028	0.412	0.065	0.148	0.140	0.340	0.982	1.049	0.315	0.033

Eigenvectors (columns):

-3.544	-1.129	-0.351	-0.046	0.033	0.042	0.006	0.003	-0.006	0.002	-0.001	-0.0	-0.001	0.002	0.0	0.0	0.0	0.0
-0.697	0.122	0.165	-0.031	0.092	-0.096	0.056	0.067	-0.127	-0.009	-0.008	-0.012	0.0	0.004	0.001	0.0	0.001	-0.0
-1.016	0.643	0.061	-0.104	0.062	0.109	-0.065	-0.076	-0.058	0.037	-0.027	0.018	-0.013	-0.007	-0.001	-0.001	0.002	-0.0
-2.444	-0.094	0.624	0.190	-0.061	0.025	0.039	-0.012	0.036	-0.005	-0.0	0.003	0.002	-0.002	0.0	-0.001	0.0	-0.0
-0.996	0.651	0.075	-0.222	0.161	0.107	-0.046	0.019	0.018	-0.024	0.046	-0.022	0.002	0.003	0.003	0.003	-0.002	0.0
-1.340	1.161	-0.328	0.417	-0.037	0.022	0.023	0.015	-0.001	-0.018	-0.002	-0.001	-0.001	0.003	0.001	0.001	0.0	0.0
-0.646	0.399	-0.052	-0.160	0.053	-0.044	0.032	0.053	0.043	0.016	-0.018	0.011	0.028	-0.019	0.018	-0.003	0.004	-0.0
-0.527	0.375	-0.042	-0.193	0.094	-0.081	0.100	-0.025	0.029	-0.024	0.001	0.042	-0.009	0.005	-0.011	0.005	-0.003	0.001
-0.123	0.054	0.032	0.003	0.004	0.020	-0.067	0.036	-0.004	0.008	0.003	0.027	0.032	0.027	-0.006	-0.010	0.002	0.001
-0.526	0.304	-0.069	-0.068	-0.116	-0.057	0.080	-0.056	-0.018	0.063	0.041	-0.012	0.017	0.005	0.0	-0.001	-0.001	0.0
-0.204	0.134	-0.006	-0.041	0.016	0.011	-0.001	-0.007	0.012	0.004	-0.039	-0.023	0.022	-0.002	-0.007	0.001	-0.010	0.005
-0.277	0.211	-0.013	-0.121	0.037	-0.045	0.035	-0.052	0.038	-0.009	-0.032	-0.032	-0.009	0.022	0.003	-0.003	0.008	-0.0
-0.358	0.073	0.025	0.009	-0.007	-0.034	-0.050	0.029	0.014	0.019	-0.004	-0.006	0.021	-0.002	-0.017	0.016	0.008	-0.0
-0.481	0.285	0.005	-0.094	-0.053	-0.001	0.0	0.101	0.038	0.045	-0.005	-0.006	-0.038	0.001	-0.010	-0.005	-0.001	-0.0
-0.831	0.322	-0.022	-0.281	-0.322	-0.003	-0.035	0.007	-0.024	-0.042	-0.005	0.002	0.001	-0.001	0.001	0.001	0.0	0.0
-0.987	0.087	0.028	0.052	0.027	-0.215	-0.128	-0.018	0.014	0.009	0.005	0.004	-0.013	0.005	0.011	0.003	-0.004	0.0
-0.537	0.091	-0.039	0.006	0.045	-0.105	-0.033	-0.035	0.0	-0.023	0.012	-0.013	0.007	-0.020	-0.018	-0.013	0.003	-0.001
-0.147	0.096	-0.010	-0.032	0.005	0.005	-0.0	-0.001	0.010	0.004	-0.020	-0.006	0.015	0.005	-0.003	0.0	-0.007	-0.008

Eigenvalues:

26.280	4.159	0.670	0.449	0.180	0.108	0.056	0.034	0.028	0.012	0.008	0.006	0.005	0.002	0.001	0.001	0.0	0.0

Table 6.11 (continued).

Significance tests for eigenvalues:

#	EIGEN	VAR	CPV	SCR	IME	IND	RSD	XNR
1.000	26.280	82.120	82.120	17.875	0.024	0.00035	0.103	0.608
2.000	4.159	13.000	95.120	4.877	0.018	0.00022	0.055	0.085
3.000	0.670	2.090	97.220	2.784	0.018	0.00019	0.043	0.044
4.000	0.449	1.400	98.620	1.382	0.015	0.00016	0.031	0.039
5.000	0.180	0.560	99.180	0.819	0.013	0.00015	0.025	0.032
6.000	0.108	0.340	99.520	0.481	0.012	0.00014	0.020	0.022
7.000	0.056	0.170	99.690	0.306	0.010	0.00014	0.017	0.018
8.000	0.034	0.110	99.800	0.199	0.009	0.00014	0.014	0.013
9.000	0.028	0.090	99.890	0.111	0.008	0.00014	0.011	0.005
10.000	0.012	0.040	99.930	0.073	0.007	0.00015	0.010	0.004
11.000	0.008	0.020	99.950	0.048	0.006	0.00017	0.008	0.003
12.000	0.006	0.020	99.970	0.031	0.006	0.00020	0.007	0.002
13.000	0.005	0.020	99.990	0.014	0.005	0.00022	0.005	0.001
14.000	0.002	0.010	99.990	0.008	0.004	0.00027	0.004	0.000
15.000	0.001	0.0	100.000	0.003	0.003	0.00037	0.003	0.000
16.000	0.001	0.0	100.000	0.001	0.002	0.00065	0.003	0.000
17.000	0.0	0.0	100.000	0.0	0.002	0.00154	0.002	0.000
18.000	0.0	0.0	100.000	0.0	-0.0	-0.0	-0.0	0.000

Varimax orthogonal rotation with 5 factors :

3.543	0.562	0.565	2.229	0.539	0.609	0.344	0.253	0.084	0.281	0.107	0.124	0.276	0.262	0.495	0.818	0.418	0.076
0.865	0.432	0.997	0.916	1.066	1.309	0.678	0.628	0.094	0.480	0.215	0.346	0.212	0.463	0.682	0.501	0.325	0.155
-0.616	0.174	0.200	0.619	0.179	0.098	0.018	0.009	0.045	0.013	0.020	0.014	0.047	0.065	0.034	0.063	-0.012	0.008
0.193	0.068	0.309	0.324	0.191	1.143	0.143	0.076	0.033	0.194	0.053	0.028	0.088	0.123	0.097	0.225	0.135	0.039
0.492	0.018	0.125	0.342	0.057	0.160	0.094	0.045	0.013	0.213	0.028	0.041	0.057	0.149	0.507	0.106	0.038	0.027

Variances of factors:

						20.352	7.983	0.889	1.755	0.758							

% communalities (covar0):

100.000	94.200	98.100	99.900	98.800	100.000	98.400	95.700	68.400	95.300	95.400	93.100	95.600	95.500	99.600	93.900	95.200	97.000

The relative source profiles refined by target rotation are shown in Table 6.12. These are compared to the profiles for Arctic1 in Table 6.13. Common to all stations is the appearance of a factor unique for Br. There is also a small amount of sulphate associated with this factor. After removal of the variable weights, the mass ratio of Br to SO_4^{2-} is about 0.05, twice the ratio for bulk seawater. Moreover, there are only small (probably insignificant) amounts of Na^+ and Cl^- associated with the bromine factor, which argues against a direct seawater source for the observed Br.

Another new factor also appears at Alert. This is mainly a copper-zinc factor, although there are small amounts of Mg, Ni, and Mn associated with it. This factor is most likely an artifact. Inspection of the factor scores showed that this factor contributed only small amounts in all but one sample (collected from 14 March to 21 March, 1983). The reported Zn concentration in this sample was 256 $ng\text{-}m^{-3}$, two orders of magnitude larger than the average level, and an order of magnitude greater than the largest Zn concentration in any other sample.

The sea salt, crustal, and anthro factors derived from Arctic2 at Alert are quite similar to the corresponding components from Arctic1. The addition of Zn and Pb in the second data set shows that these metals are clearly associated with the anthro factor. By contrast, Cu, Ba, and Ni are grouped similarly to Mn, V, Al, Mg, and Sr; that is, they are associated with both the crustal and anthro factors. A possible explanation for this would attribute the anthro factor to relatively 'fresh' atmospheric aerosols transported in a short time from their sources, while the crustal factor at Alert is an aged aerosol mixture of true crustal material and anthropogenic particles.

At Mould Bay and Igloolik, there are some differences between the sea salt and Na/SO_4^{2-} factors derived from the two data sets, but these are fairly small for most of the chemical elements. More significant are the changes in the crustal and anthro factors. These are easily explained at Igloolik since the Arctic1 crustal factor was a fairly clear representation of local road dust, and was present mostly during the summer months so that it would not be a major component for the Arctic2 samples. A similar explanation may be valid at Mould Bay, but the omission of the samples with a strong identifiable crustal component is not as obvious.

Table 6.12 Refined Arctic2 aerosol source profiles.

Alert	Sea Salt	Crustal	Anthro	Cu/Zn	Br
Cl^-	0.953	0.071	0.008	0.045	0.028
NO_3^-	0.160	0.001	0.476	-0.027	0.011
SO_4^{2-}	0.067	0.122	0.865	0.051	0.200
Na^+	0.597	0.033	0.613	0.024	0.002
NH_4^+	0.014	0.091	0.992	0.065	0.078
Br	0.020	0.030	0.303	0.015	0.930
Mn	0.024	0.705	0.594	0.105	-0.008
V	0.001	0.092	0.531	0.075	-0.013
Al	-0.001	0.568	0.146	-0.022	0.075
Cu	0.056	0.190	0.438	0.184	0.030
Ba	0.014	0.216	0.181	0.055	-0.014
Ni	-0.013	0.109	0.342	0.093	0.002
Ca	0.068	1.255	0.002	0.052	0.056
Zn	0.001	-0.002	0.271	0.984	0.006
Pb	0.006	0.032	0.439	0.065	0.043
Mg	0.234	0.426	0.080	0.135	0.040
Sr	0.103	0.107	0.129	0.041	0.039
Fe	0.020	0.496	0.099	0.052	0.006

Mould Bay	Sea Salt	Crustal	Anthro	Na/SO_4^{2-}	Br
Cl^-	0.962	0.000	0.197	0.099	0.013
NO_3^-	0.104	0.222	0.463	0.244	0.000
SO_4^{2-}	0.070	0.313	0.594	0.382	0.206
Na^+	0.596	0.139	0.034	1.296	0.023
NH_4^+	0.047	0.457	0.726	0.336	0.167
Br	0.002	0.002	0.042	-0.001	0.961
Mn	0.052	0.324	0.558	0.195	0.009
V	0.016	0.280	0.451	0.142	0.009
Al	0.022	0.017	0.051	0.079	0.033
Cu	-0.003	0.170	0.804	-0.003	0.024
Ba	0.019	0.087	0.185	0.047	0.064
Ni	0.019	0.183	0.338	0.086	-0.009
Ca	0.064	0.015	0.023	0.078	0.045
Zn	0.024	0.202	0.388	0.096	-0.009
Pb	0.000	0.356	0.615	-0.014	0.048
Mg	0.242	0.023	0.057	0.199	0.060
Sr	0.108	0.028	0.018	0.082	0.034
Fe	0.014	0.059	0.110	0.053	0.018

Igloolik	Sea Salt	Crustal	Anthro	Na/SO_4^{2-}	Br
Cl^-	0.969	0.983	0.097	0.011	0.013
NO_3^-	0.138	0.085	0.190	0.310	-0.008
SO_4^{2-}	0.056	0.155	0.328	0.270	0.172
Na^+	0.610	0.923	0.138	10.227	0.054
NH_4^+	0.047	0.025	0.459	0.232	0.068
Br	0.023	0.064	0.105	0.115	0.916
Mn	0.018	0.081	0.251	0.024	0.071
V	0.000	-0.005	0.282	-0.002	0.021
Al	0.017	0.030	0.028	0.066	0.015
Cu	0.007	0.308	0.049	0.022	0.127
Ba	0.007	0.026	0.077	0.025	0.028
Ni	-0.007	0.026	0.152	0.005	-0.001
Ca	0.060	0.108	0.041	0.102	0.048
Zn	0.013	0.222	0.108	0.087	0.061
Pb	0.017	0.822	0.032	0.068	0.002
Mg	0.197	0.212	0.107	0.224	0.127
Sr	0.092	0.050	0.095	0.050	0.084
Fe	0.003	0.029	0.051	0.010	0.021

Table 6.13 Comparison of Arctic1 and Arctic2 components.

Alert		Sea Salt		Crustal		Anthro		Cu/Zn		Br
Cl^-	0.960	0.953	0.052	0.071	-0.001	0.008	•	0.045	•	0.028
NO_3^-	0.076	0.160	0.118	0.001	0.492	0.476	•	-0.027	•	0.011
SO_4^{2-}	0.027	0.067	0.001	0.122	1.061	0.865	•	0.051	•	0.200
Na^+	0.645	0.597	-0.004	0.033	0.554	0.613	•	0.024	•	0.002
NH_4^+	-0.005	0.014	0.086	0.091	0.935	0.992	•	0.065	•	0.078
Br	•	0.020	•	0.030	•	0.303	•	0.015	•	0.930
Mn	0.035	0.024	0.729	0.705	0.377	0.594	•	0.105	•	-0.008
V	0.026	0.001	0.103	0.092	0.303	0.531	•	0.075	•	-0.013
Al	-0.001	-0.001	0.372	0.568	0.065	0.146	•	-0.022	•	0.075
Cu	•	0.056	•	0.190	•	0.438	•	0.184	•	0.030
Ba	•	0.014	•	0.216	•	0.181	•	0.055	•	-0.014
Ni	•	-0.013	•	0.109	•	0.342	•	0.093	•	0.002
Ca	0.035	0.068	1.299	1.255	0.000	0.002	•	0.052	•	0.056
Zn	•	0.001	•	-0.002	•	0.271	•	0.984	•	0.006
Pb	•	0.006	•	-0.032	•	0.439	•	0.065	•	0.043
Mg	0.195	0.234	0.378	0.426	0.114	0.080	•	0.135	•	0.040
Sr	0.083	0.103	0.105	0.107	0.130	0.129	•	0.041	•	0.039
Fe	0.000	0.020	0.572	0.496	0.074	0.099	•	0.052	•	0.006

Mould Bay		Sea Salt		Crustal		Anthro		Na/SO_4^{2-}		Br
Cl^-	0.971	0.962	-0.001	0.000	-0.001	0.197	0.000	0.099	•	0.013
NO_3^-	0.084	0.104	0.123	0.222	0.473	0.463	0.145	0.244	•	0.000
SO_4^{2-}	0.075	0.070	0.006	0.313	0.874	0.594	0.588	0.382	•	0.206
Na^+	0.637	0.596	0.116	0.139	0.080	0.034	1.243	1.296	•	0.023
NH_4^+	-0.003	0.047	0.151	0.457	1.201	0.726	0.006	0.336	•	0.167
Br	•	0.002	•	0.002	•	0.042	•	-0.001	•	0.961
Mn	0.046	0.052	0.658	0.324	0.288	0.558	0.091	0.195	•	0.009
V	0.010	0.016	0.074	0.280	0.296	0.451	0.105	0.142	•	0.009
Al	0.000	0.022	0.556	0.017	0.001	0.051	-0.014	0.079	•	0.033
Cu	•	-0.003	•	0.170	•	0.804	•	-0.003	•	0.024
Ba	•	0.019	•	0.087	•	0.185	•	0.047	•	0.064
Ni	•	0.019	•	0.183	•	0.338	•	0.086	•	-0.009
Ca	0.057	0.064	0.192	0.015	0.007	0.023	0.179	0.078	•	0.045
Zn	•	0.024	•	0.202	•	0.388	•	0.096	•	-0.009
Pb	•	0.000	•	0.356	•	0.615	•	-0.014	•	0.048
Mg	0.160	0.242	0.135	0.023	0.041	0.057	0.328	0.199	•	0.060
Sr	0.063	0.108	0.095	0.028	0.031	0.018	0.159	0.082	•	0.034
Fe	0.005	0.014	0.504	0.059	0.041	0.110	0.001	0.053	•	0.018

Igloolik		Sea Salt		Crustal		Anthro		Na/SO_4^{2-}		Br
Cl^-	0.971	0.969	0.026	0.985	0.001	0.097	0.006	0.011	•	0.013
NO_3^-	0.089	0.138	0.202	0.085	0.362	0.190	0.267	0.310	•	-0.008
SO_4^{2-}	0.052	0.056	0.098	0.155	0.831	0.328	0.340	0.270	•	0.172
Na^+	0.640	0.610	0.008	0.923	0.107	0.138	1.219	1.227	•	0.054
NH_4^+	0.008	0.047	0.341	0.025	0.940	0.459	0.132	0.232	•	0.068
Br	•	0.023	•	0.064	•	0.105	•	0.115	•	0.916
Mn	0.029	0.018	0.278	0.081	0.462	0.251	0.117	0.024	•	0.071
V	-0.001	0.000	0.027	-0.005	0.340	0.282	-0.039	-0.002	•	0.021
Al	0.016	0.017	0.109	0.030	0.096	0.028	0.095	0.066	•	0.015
Cu	•	0.007	•	0.308	•	0.049	•	0.022	•	0.127
Ba	•	0.007	•	0.026	•	0.077	•	0.025	•	0.028
Ni	•	-0.007	•	0.026	•	0.152	•	0.005	•	-0.001
Ca	0.054	0.060	1.301	0.108	-0.002	0.041	0.119	0.102	•	0.048
Zn	•	0.013	•	0.222	•	0.108	•	0.087	•	0.061
Pb	•	0.017	•	0.822	•	0.032	•	0.068	•	0.002
Mg	0.149	0.197	0.699	0.212	0.160	0.107	0.204	0.224	•	0.127
Sr	0.070	0.092	0.025	0.050	0.189	0.095	0.110	0.050	•	0.084
Fe	0.010	0.003	0.148	0.029	0.114	0.051	0.071	0.010	•	0.021

There is a high correlation between the Arctic2 crustal and anthro factors at Mould Bay and at Igloolik. Were it not for the behaviour of some of the trace metals (Cu, Ni, Zn, Pb), which are associated with one factor and not the other, these factors might have been judged to be the same. Whether the Arctic2 crustal factor still deserves this label is questionable. The crustal and anthro factors derived from the winter concentration data may, again, represent two different combinations of 'fresh' and 'aged' aerosols, rather than distinct source types. For convenience, the crustal and anthro labels will be retained.

6.4 Arctic2 - Scores

The normalized factor scores are displayed in Figures 6.11-6.13. Source scaling was not attempted. The rather unique behaviour of the bromine factor at each station, rising from a minimum in December to a peak in March (or possibly April), suggests that this is a fairly reliable factor. Barrie and Hoff (1985) pointed out that the particulate Br observed in the samples may be an artifact, due to the conversion of gaseous Br species as air is drawn through the filtering medium. These authors also describe the differences in the mean winter Br concentrations at the three stations, ranging from 13 $ng\text{-}m^{-3}$ at Alert to 26 $ng\text{-}m^{-3}$ at Mould Bay, which may be the result of the effects of different amounts of solar radiation on photochemical reactions involving Br.

The scores for the Arctic2 sea salt factor at all three stations are very similar to the Arctic1 scores, and the similarity suggests that this factor is also reliable. The same comment also applies to the Na/SO_4^{2-} factors at Mould Bay and Igloolik, and to the crustal and anthro factors at Alert. The remaining factors are somewhat dubious. Inspection of the unrotated factor loading matrix for Alert and the original data suggests that copper and zinc do exhibit some variability not completely explained by the other factors, but this is rather small and, without the unusual sample of 14-21 March 1983, would not justify a unique factor for these metals. Comparison of the scores for the anthro and crustal factors at Mould Bay shows that these factors are inversely related; that is, when the scores for one of these are large, the scores for the other factor are small or zero. These factors are associated with source profiles which

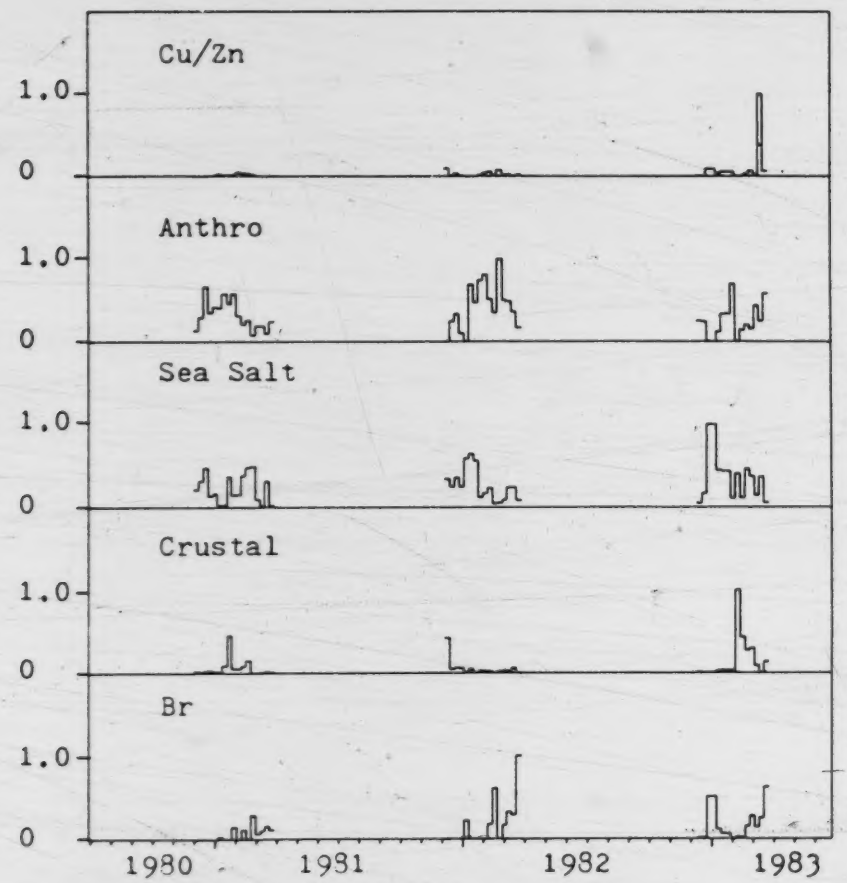

Fig. 6.11 Normalized factor scores at Alert (Arctic2).

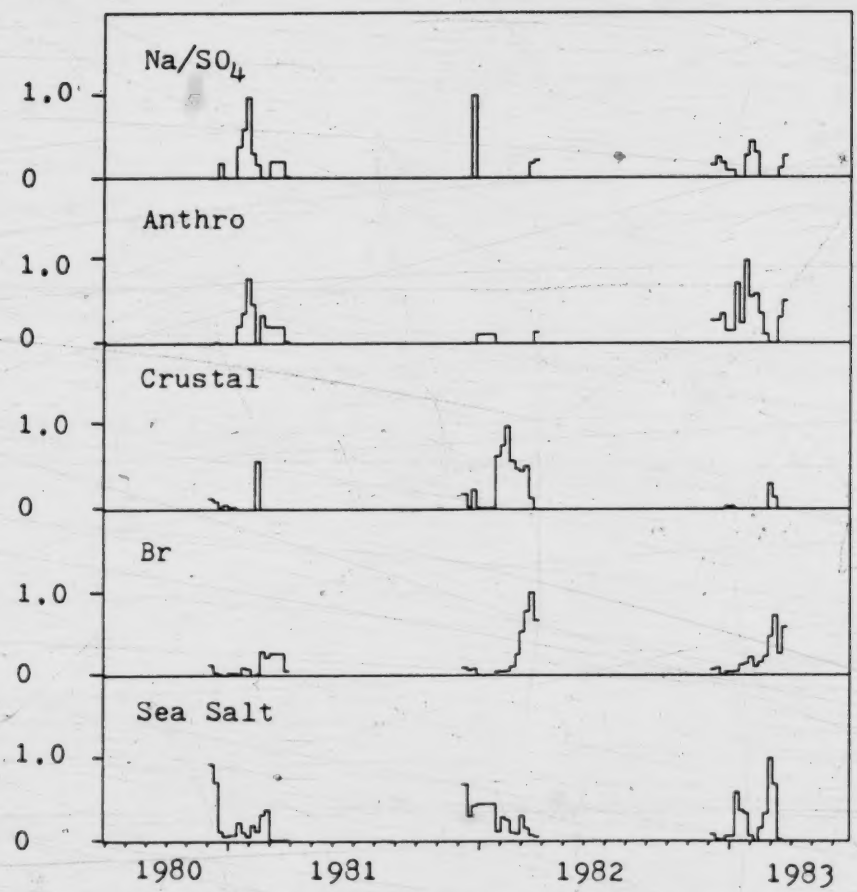

Fig. 6.12 Normalized factor scores at Mould Bay (Arctic2).

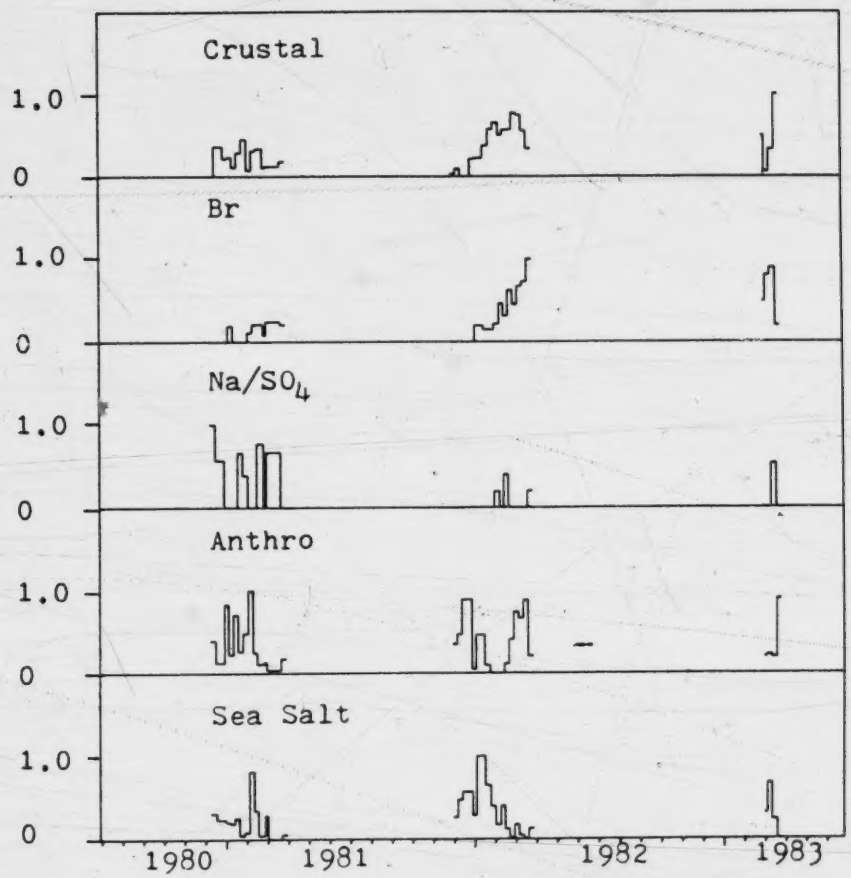

Fig. 6.13 Normalized factor scores at Igloolik (Arctic2).

appear to be too similar to fully separate the source contributions and, instead, they swing from one extreme to the other according to the magnitude of some trace metal concentrations. There is at least one reliable component in the Mould Bay Arctic2 data set with a profile similar to the crustal or anthro factors of Table 6.12, but a division into two separate factors does not seem to be justified.

6.5 Element Ratios

Various methods have been devised to derive more information from aerosol composition data, than is possible by a simple inspection of the raw data. Calculation of Enrichment Factors (Milford and Davidson, 1985) was one of the earliest:

$$EFQ = \frac{[Q_a] / [R_a]}{[Q_{cr}] / [R_{cr}]} \qquad (6.5)$$

This is a 'ratio of ratios'. A reference element R characteristic of crustal material is selected, and ratios of the concentration of the element of interest Q to the concentration of R in an aerosol sample (subscript a) and in background crustal material (subscript cr) are calculated. EF's around 1.0 are assumed to indicate crustal weathering as the predominant source of Q, while larger values suggest non-crustal or enriched sources. There are difficulties in interpretation of enrichment factors because of uncertainties in the relative composition of background material in the atmosphere and because of uncertainty in deciding at what level Enrichment Factors become significantly larger than background. A simple error analysis of Eqn. 6.5[21] (Bevington, 1969) shows that the uncertainty in the EF equals twice the uncertainty in the elemental concentrations. For instance, confidence levels for the Arctic aerosol data used here were ±30%; assuming an equal confidence level for the concentration of true crustal material (or for the applicability of data like those of Mason and Moore, 1982), then the EF of 'true' aerosol crustal material would be 1.0±0.6.

[21]Assumes that all errors are uncorrelated, that there are no systematic errors, and that each parameter on the right-hand side of Eqn. 6.5 is independently measured with the same accuracy.

Another method calculates the amount of an element in an aerosol sample which exceeds the crustal contribution; that is, the measured concentration of Q is adjusted by subtracting the portion from crustal material:

$$XQ = [Q_a] - [R_a] \times \frac{[Q_{cr}]}{[R_{cr}]} \qquad (6.6)$$

The excess amounts can be used by themselves (eg., Raatz and Shaw, 1984), or ratios of excess amounts of two elements can be formed. The ratio of excess Mn (XMn) to excess V (XV) was once advocated as a discriminator between European, Eurasian, and North American aerosol sources (Rahn, 1981c; Raatz and Shaw, 1984), but more recent attempts have used a set of seven ratios (Rahn and Lowenthal, 1984; Lowenthal and Rahn, 1985).

The use of such ratios raises many questions, ranging from the theoretical justification[22] to the statistical independence of the ratios[23], none of which can be seriously examined here. A practicable tracer scheme using such ratios would be invaluable; it would be a 'smoking gun' capable of identifying the dominant source regions or countries for large-scale air quality problems such as Arctic haze and acidic precipitation.

It is of interest to compare elemental ratios with the TFA results. The available data limit the comparison to the XMn/XV ratio. An immediate problem is the selection of an appropriate reference element for calculating the crustal fraction. Al, Fe, Si, and Ti have all been used by various groups. Fig. 6.14 shows the ratios of Al (ICP) to Fe (ICP) in the samples from all three stations. There is considerable variability in this ratio, suggesting that the concentrations of one or both of these elements are affected by a non-crustal source.

---

[22]If the ratio is a function of the type of industry prevalent in a region, or reflects the composition of oil used for heating and power production (Rahn, 1981c), or depends on the relative efficiency of industrial processes in different countries, then can observed regional differences in elemental ratios form a stable and reliable set of tracers in a volatile world economy?

[23]If a number of samples are used to calculate a mean element ratio characteristic for a region, is this result a unique signature for the region or is it a composite from a mixture of aerosols transported from other regions during the sampling periods?

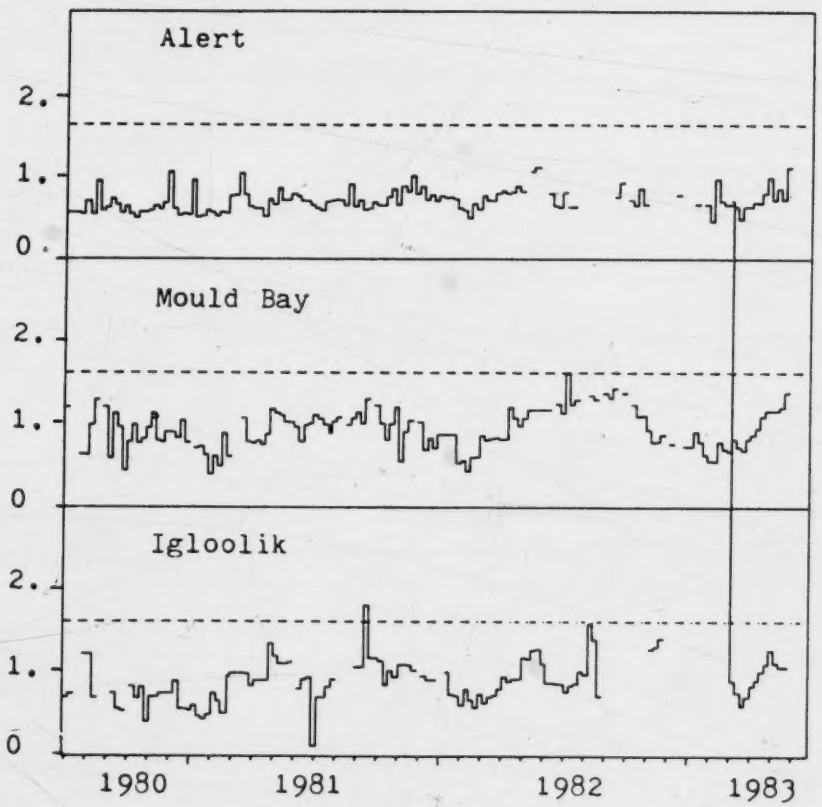

Fig. 6.14 The Al(ICP)/Fe(ICP) ratio. A value of 1.626 (dashed line) would be expected from the average crustal abundances of these elements.

Moreover, even in the Alert series which seems to have the least variability, the mean value (indicated by the dashed line in Fig. 6.14) is much less than the ratio of Al to Fe in the average crustal material of Mason and Moore (1982):

Average crustal Al/Fe ratio:	1.626
Alert Al/Fe ratio: (n=129)	mean = 0.705 std dev = 0.137 range = (0.454,1.11)

The aluminum content of the Arctic samples was also measured by neutron activation analysis. Barrie and Hoff (1985) have already described an analytical problem involving the Al measurements, which shows up in the results of a linear regression between the two sets of Al concentrations. A slope of 2.43, not 1.0, was found which was attributed to loss of Al during the chemical pretreatment of samples for ICP analysis. Fig. 6.15 suggests that the problem may not have been so simple. This graph is identical to Fig. 6.14, but Al (NAA) has been substituted for Al (ICP). While the mean values are closer to the expected value of 1.626, the fluctuations are much larger and there is evidence of a problem with the Al (ICP) concentrations in 1981-82.

Not enough is known of the original data to be able to explain Fig. 6.14 and Fig. 6.15. Certainly the Al concentrations should not be used as a normalizing or reference element. If it is assumed that the Fe concentrations are accurate and that Fe is a reliable reference for crustal material in atmospheric aerosols, then Enrichment Factors (Fig. 6.16), XV, XMn, and XMn/XV (Fig. 6.17) can still be calculated. Comparison with figures presented by Raatz and Shaw (1984) will show that these results are quite reasonable. Comparison with the factor scores of Fig. 6.7 (Arctic1) and Fig. 6.11 (Arctic2) will show that XMn and XV are well correlated with trends in the anthro component at Alert.

Fig. 6.18 is a scatter plot of XMn versus XV for the Alert data. This is similar to Fig. 3 of Rahn (1981c), and areas on this plot with values characteristic of certain regions are indicated (adapted from Rahn, 1981c). The comparison may not be entirely justified because

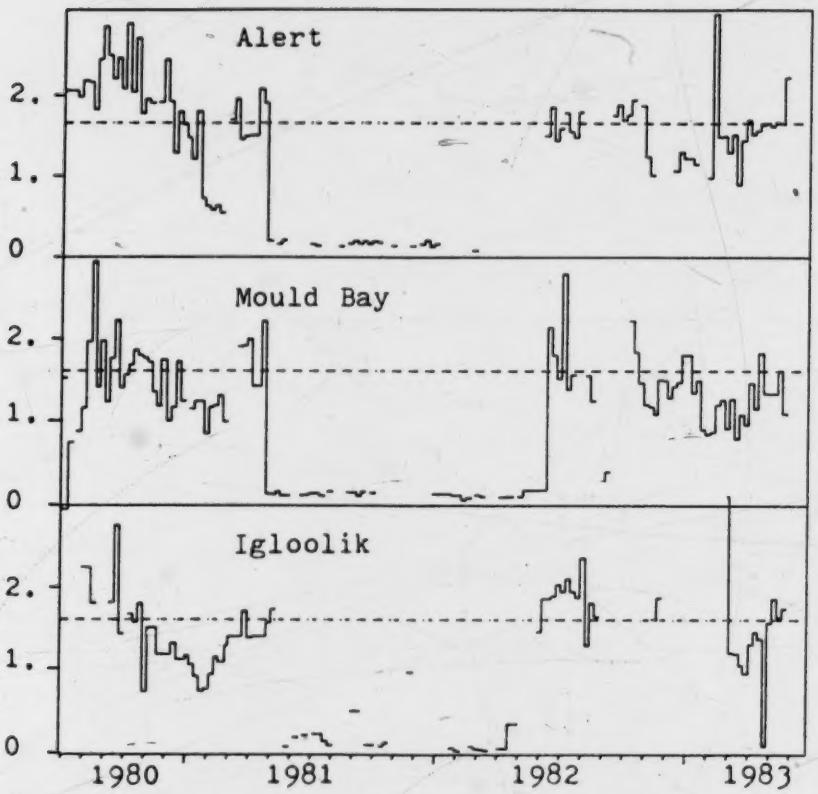

Fig. 6.15 The Al(NAA)/Fe(ICP) ratio. A value of 1.626 (dashed line) would be expected from the average crustal abundances of these elements.

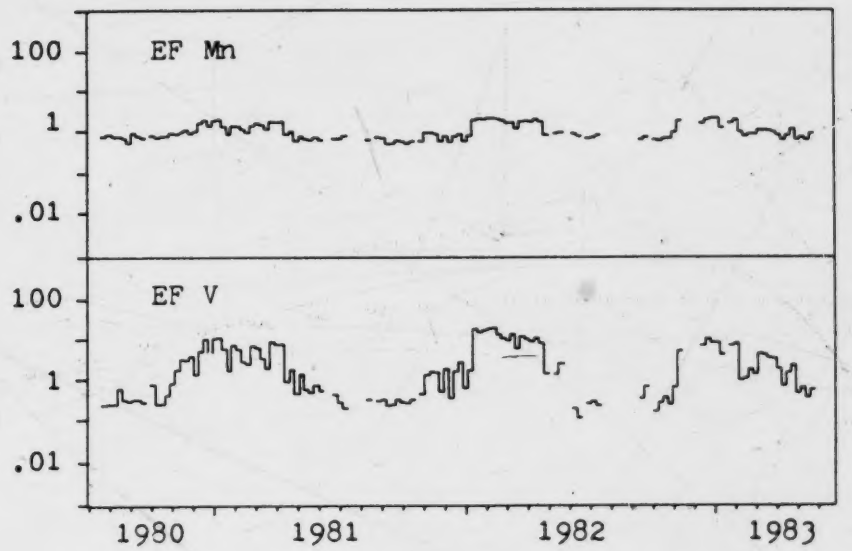

Fig. 6.16 Enrichment factors for Mn and V at Alert. Based on an Fe(ICP) reference.

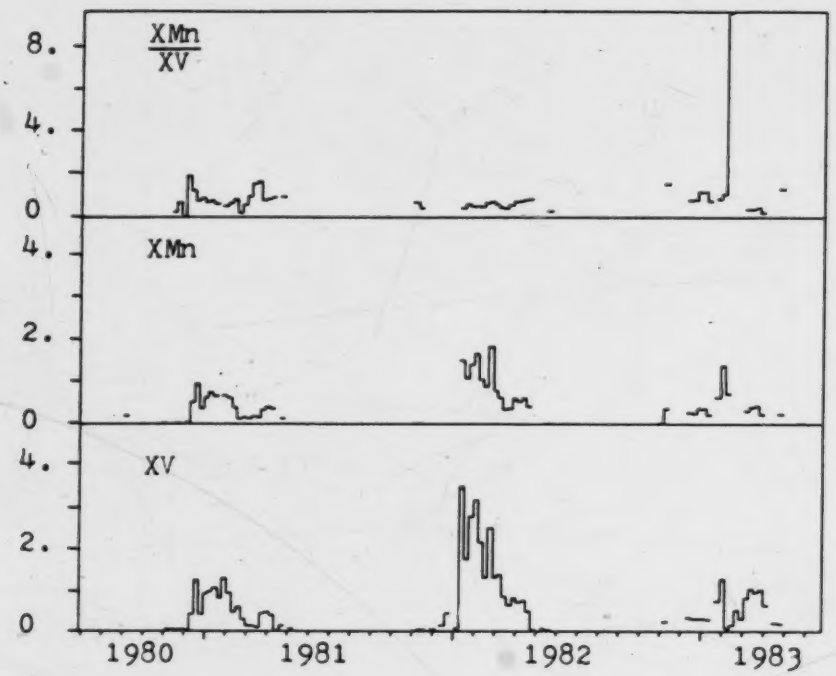

Fig. 6.17 XMn, XV, and XMn/XV at Alert. The excess amounts of Mn and V were calculated by subtracting the crustal amount based on an Fe(ICP) reference.

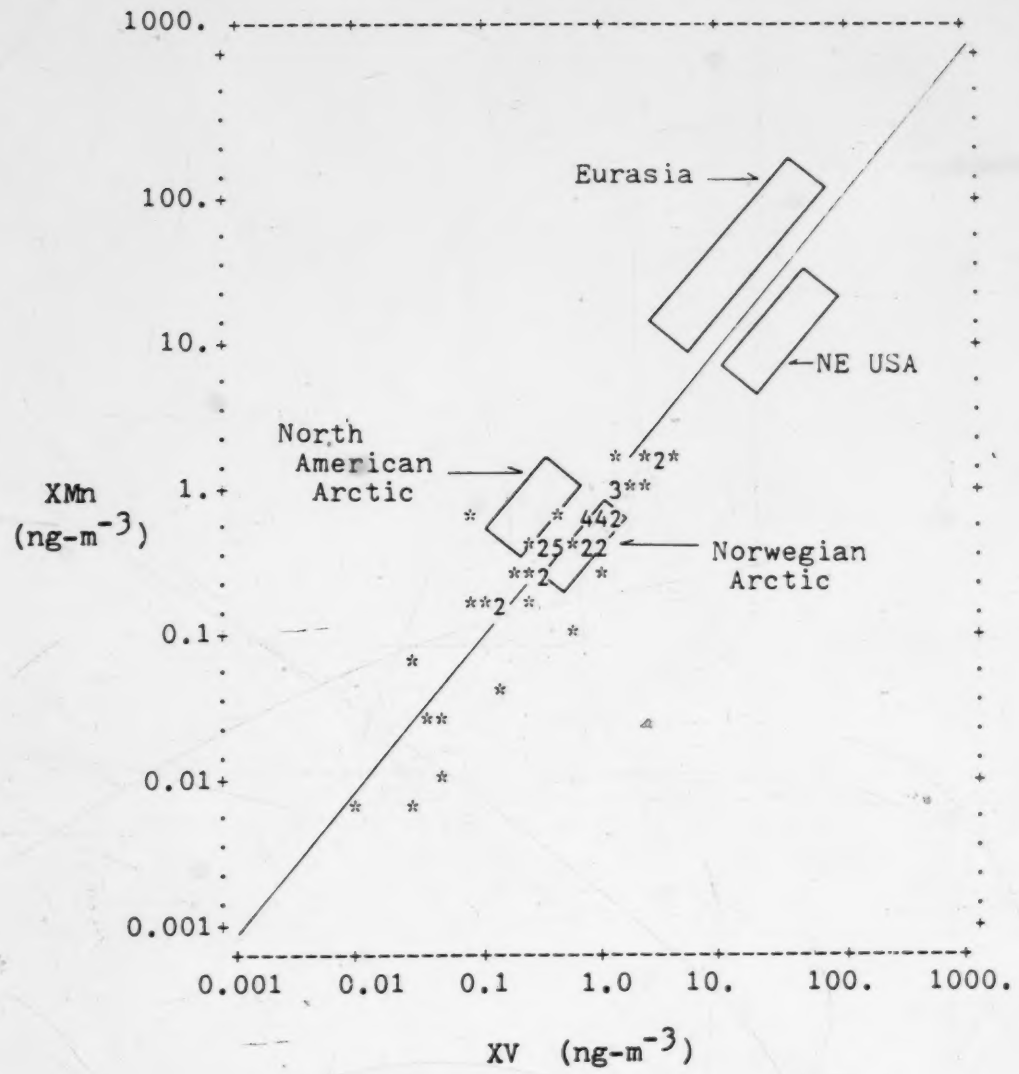

Fig. 6.18 XMn versus XV at Alert. This plot is similar to Fig. 3 of Rahn (1981c), who attempted to characterize aerosol source regions by these values.

the Alert data were calculated from weekly average samples, and it seems likely that the length of the sample averaging (collection) time could have an important effect on calculation of 'average excesses' (a point not discussed by Rahn, 1981c, or by Raatz and Shaw, 1984). If one does accept the validity of Fig. 6.18, then one must conclude either that Alert shares a greater similarity with the Norwegian Arctic than Rahn's North American Arctic (ie., Point Barrow), or else one must begin to question the simple interpretations of XMn, XV, XMn/XV, and similar ratios.

Finally, it is noted that Heidam (1985) has attempted to normalize aerosol composition data with respect to a crustal reference (Ti), and then applied FA techniques.

7. Arctic Aerosols and Meteorology

A simple view of the Arctic atmosphere might describe the winter months as cold, dark, and dry, the summer months as cool, bright, and (relatively) moist, and spring and fall as transition periods. Closer examination reveals considerable variability within any season, although the fluctuations may not be as large or as dramatic as in lower latitudes.

Many of the meteorological quantities to be discussed are presented in the form of time series plots. For upper air parameters, the original data were taken from twice-daily radiosonde ascents at stations in the Canadian Arctic. A 15-point rectangular filter was used to smooth these series and remove the high frequency components. Fig. 7.1 is an example of the difference between an unfiltered time series of 12-hour data and the same series after calculating approximately weekly moving averages.

The amount of solar radiation received at ground level is a function of both time of year and cloud cover. Fig. 7.2 reveals that insolation is not a smoothly-varying parameter in the Arctic. In spring and early summer, insolation increases fairly constantly each day but by June, the daily totals begin to fluctuate from day to day, due to the effects of varying cloud cover. This agrees well with figures presented by Maxwell (1980) portraying the mean monthly cloud amount (all types) at high Arctic stations. From December to April, the mean cloud amount is about 4/10, but rises quickly to 8/10 during the June-August period. This difference between the insolation in spring and in late summer could be significant when modelling the behaviour of photochemical species in the Arctic atmosphere.

Fig. 7.3 displays the Liquid Water Equivalent (LWE) calculated from the radiosonde data. This parameter gives the equivalent depth of liquid water which would be produced by condensation of all of the water vapour in a column of air. Of particular note are the very low values during winter (February monthly means range from 1.1 $kg\text{-}m^{-2}$ at Alert to 2.4 $kg\text{-}m^{-2}$ at Inuvik) and the large, rather abrupt changes during the summer. A spectral analysis of the summer and winter portions of these time series revealed a broad peak with a period of 5 - 10 days (Fig. 7.4). Hopper (1986b) attributed this peak to the passage of large-scale synoptic systems, although the frequency is somewhat less than the 4-day synoptic maximum

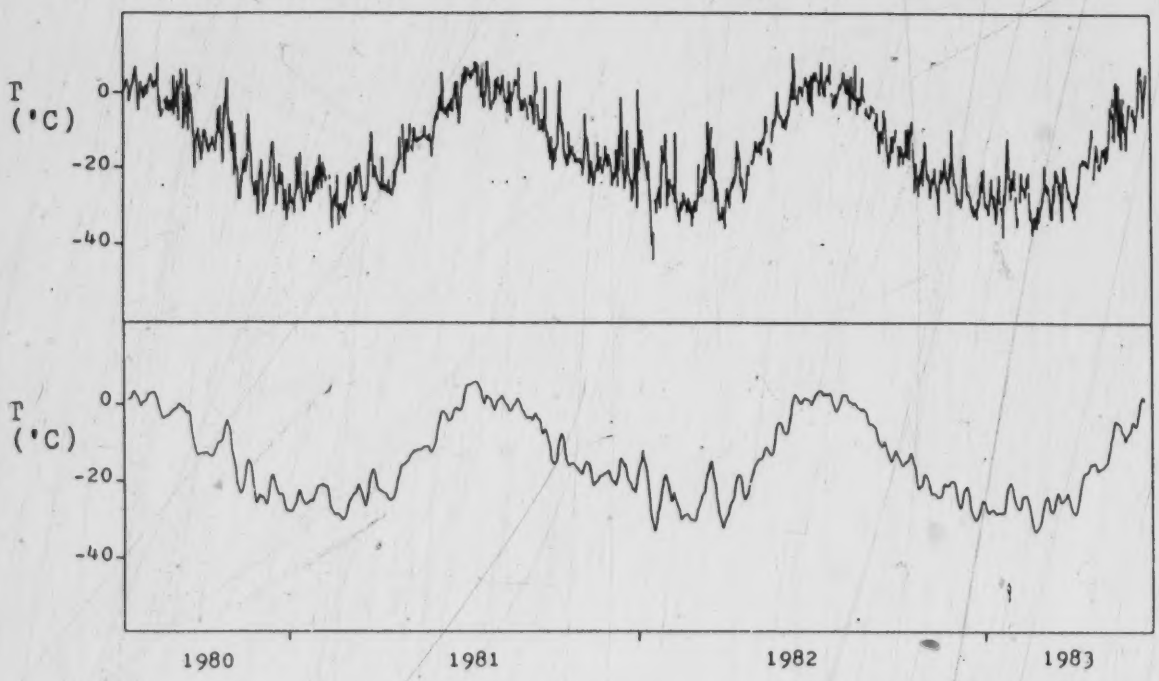

Fig. 7.1 Temperatures at the 90 kPa level at Alert. The upper series is composed of the raw observations from the twice-daily radiosonde ascents; the lower series are 15-point (~weekly) moving averages.

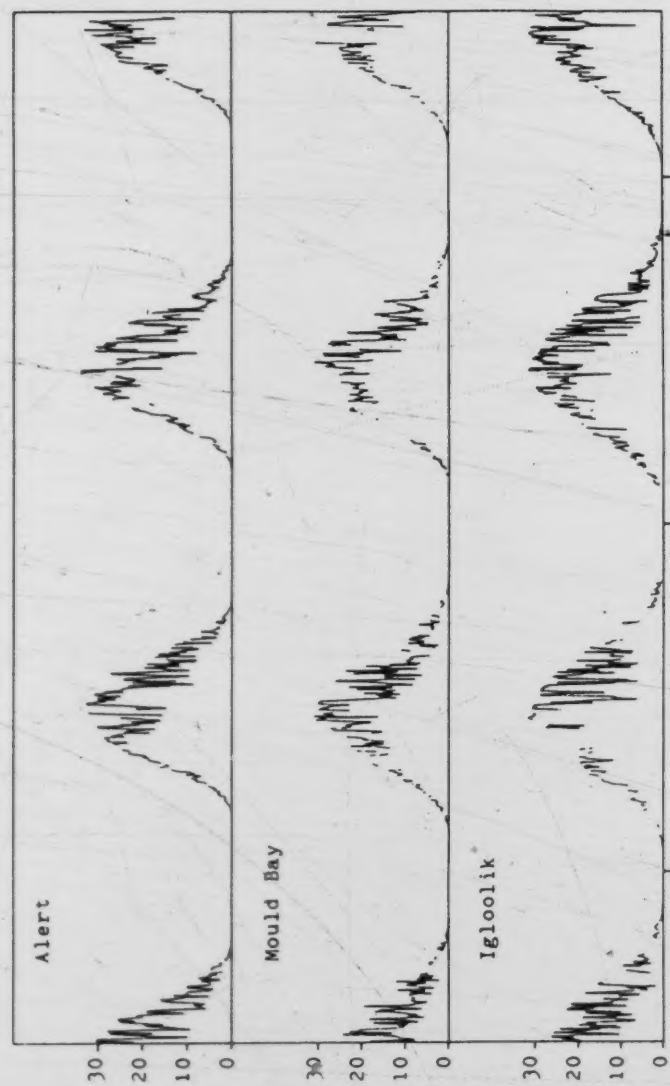

Fig. 7.2 Daily totals of global solar radiation (RF1).

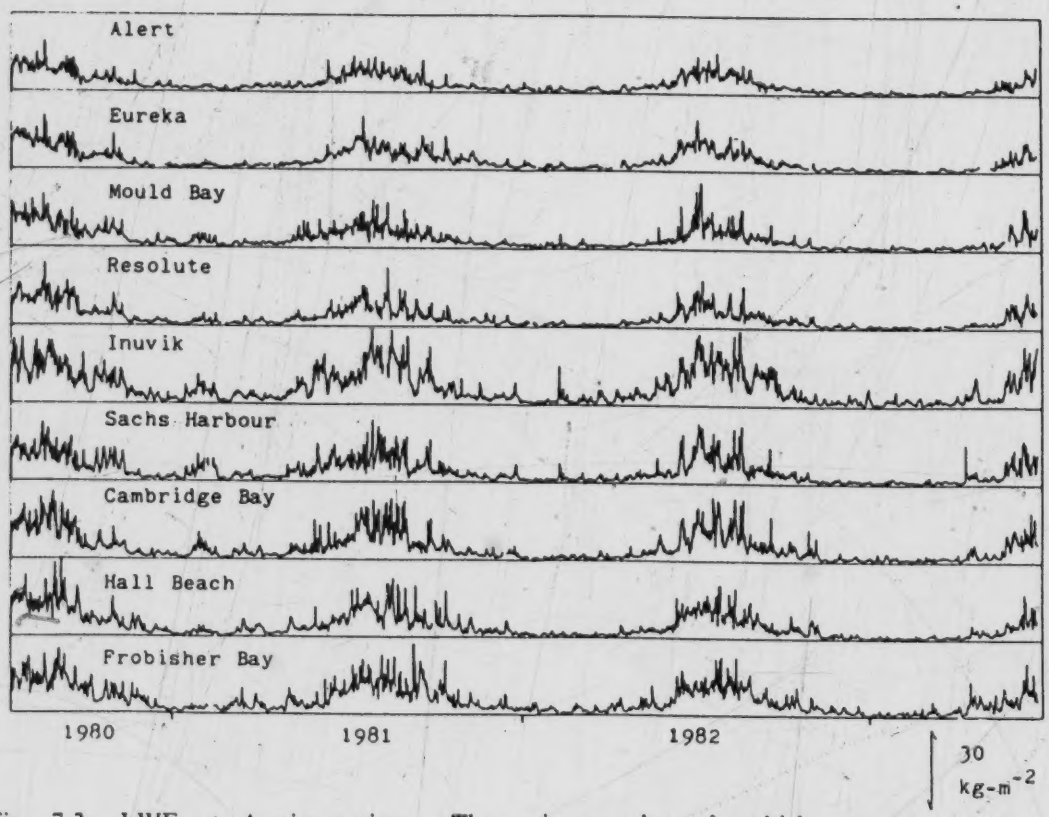

Fig. 7.3 LWE at Arctic stations. The units are $kg\text{-}m^{-2}$, which are equivalent to millimeters of liquid water.

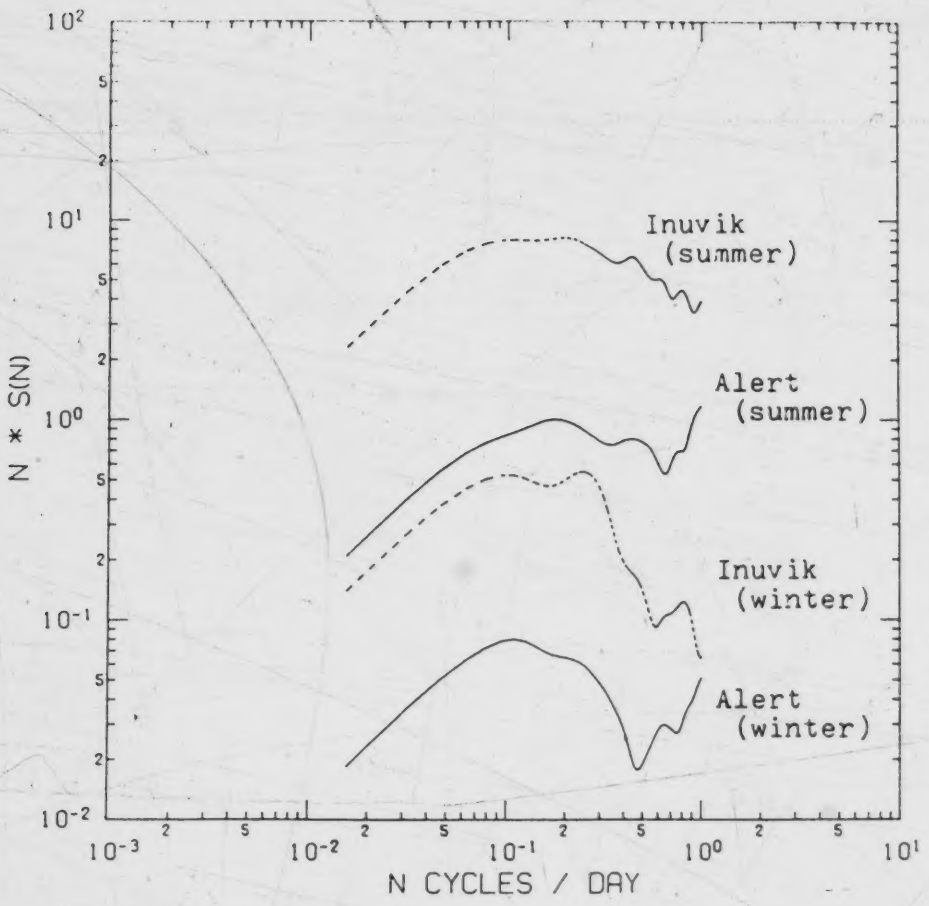

Fig. 7.4 LWE spectra. A Fast Fourier Transform provided spectral estimates from portions of the time series representing summer and winter at Inuvik and Alert. The spectral estimates were heavily smoothed in order to enhance their reliability.

reported by Van der Hoven (1957). The shape of the spectrum is remarkably similar for summer and winter, and for such disparate stations as Inuvik and Alert.

Rahn (1981b), Barrie et al. (1981), and Raatz (1981) have all described the inverse correlation between the annual cycle of cloud cover and aerosol concentrations in the Arctic, and a similar correlation is revealed by a comparison of sulphate concentrations and simultaneous average LWE values (Fig. 7.5). Unfortunately, such good agreement does not necessarily establish a cause and effect relationship. The correlation is best on a time-scale of a year or more, but fails to explain some of the larger variations in sulphate concentration (and other aerosol parameters) during the winter months. Time series of atmospheric data in the Arctic are dominated by the annual cycle, which is a common climatological feature. To identify the significant meteorological controls on the Arctic aerosol requires a more detailed consideration of the data.

One approach involves the use of hydrodynamic tracers. Reiter (1969) discussed the basis for such tracers and reviewed much of the older work. The primary difficulty is in the selection of an appropriate hydrodynamic parameter because no single parameter is strictly conserved for all thermodynamic processes in the atmosphere. For instance, potential temperature has been discussed as a tracer of Arctic haze by Carlson (1981), Iversen (1984), and Raatz (1985), but potential temperature is not conserved during saturated adiabatic expansion or during isobaric warming and cooling; the latter is particularly important because of the strong radiative cooling which takes place during the polar night.

Meteorological data from Alert only were studied in detail. An examination of mean monthly profiles of temperature, wind speed, and the horizontal fluxes of sensible and latent heat (Fig. 7.6 - Fig. 7.10) suggested that the boundary layer ($\sim< 90$ kPa) was somewhat de-coupled from the mid-troposphere and stratosphere during the winter months. Heat flux was defined as

$$H = 1005. \times V \times (T + 273.15) \qquad (7.1)$$

where V and T are the wind speed and temperature at each pressure level; latent heat flux was defined similarly. The aerosol data from ground-level samples might, then, be compared to the

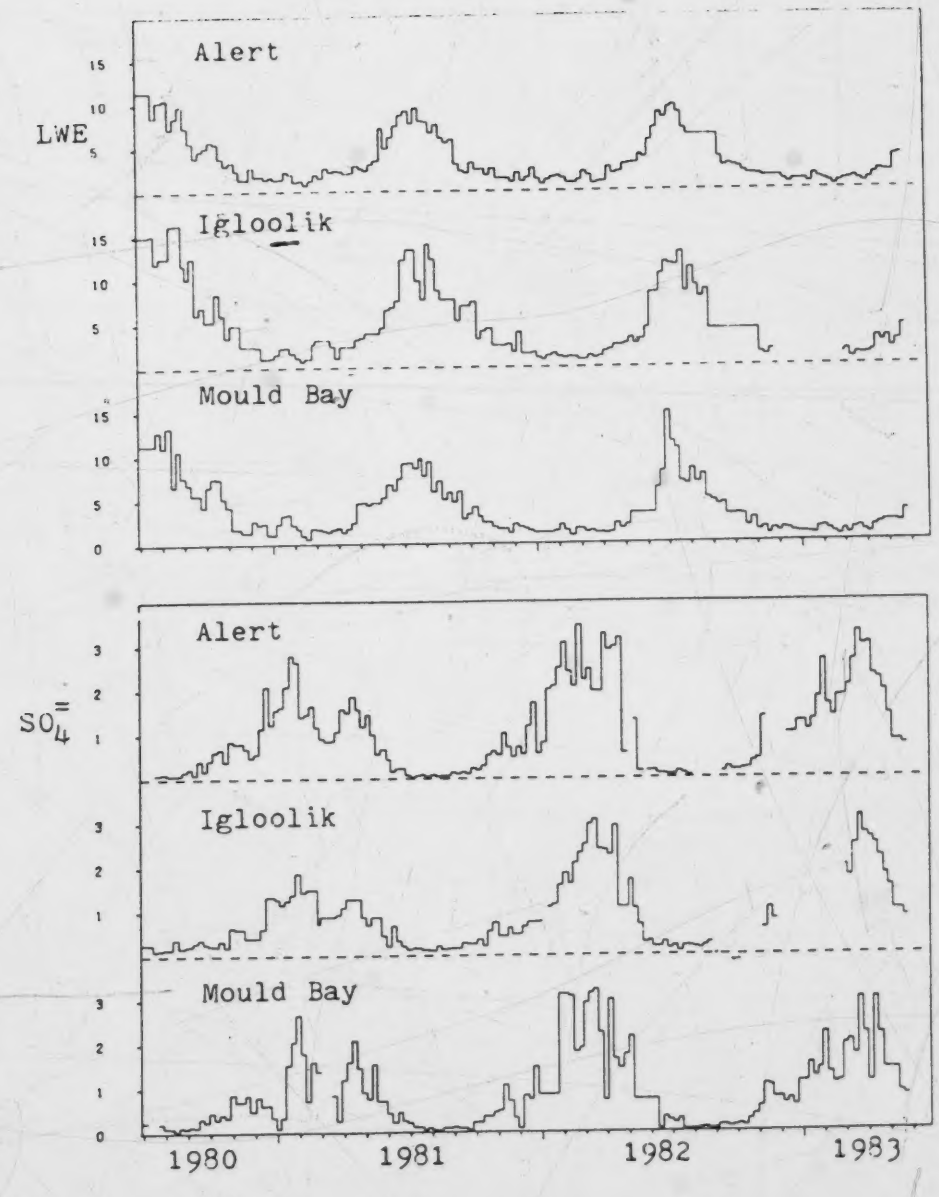

Fig. 7.5 LWE and sulphate concentrations.

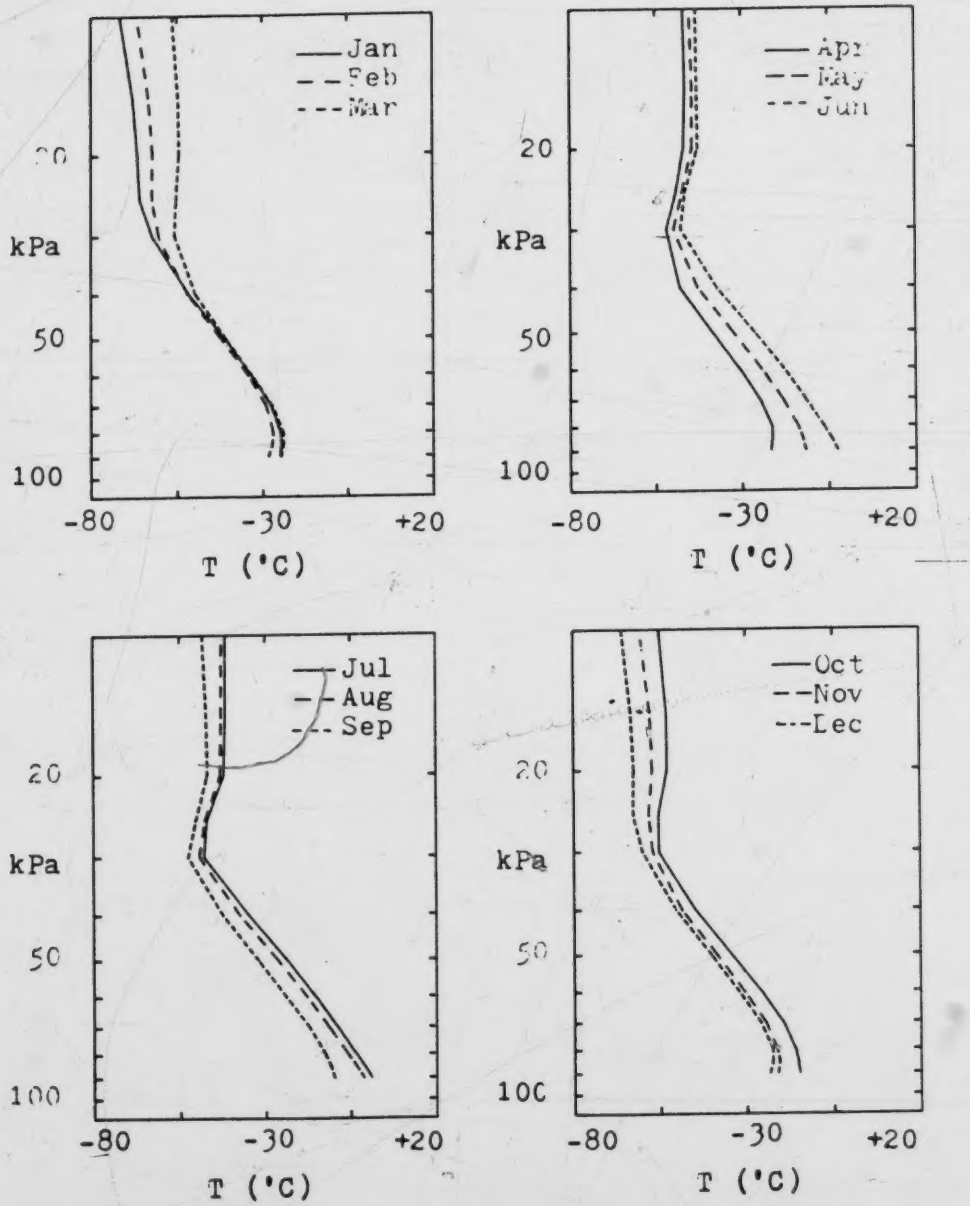

Fig. 7.6 Mean monthly vertical profiles of temperature. These are averages from Alert radiosonde data (90 kPa to 10 kPa).

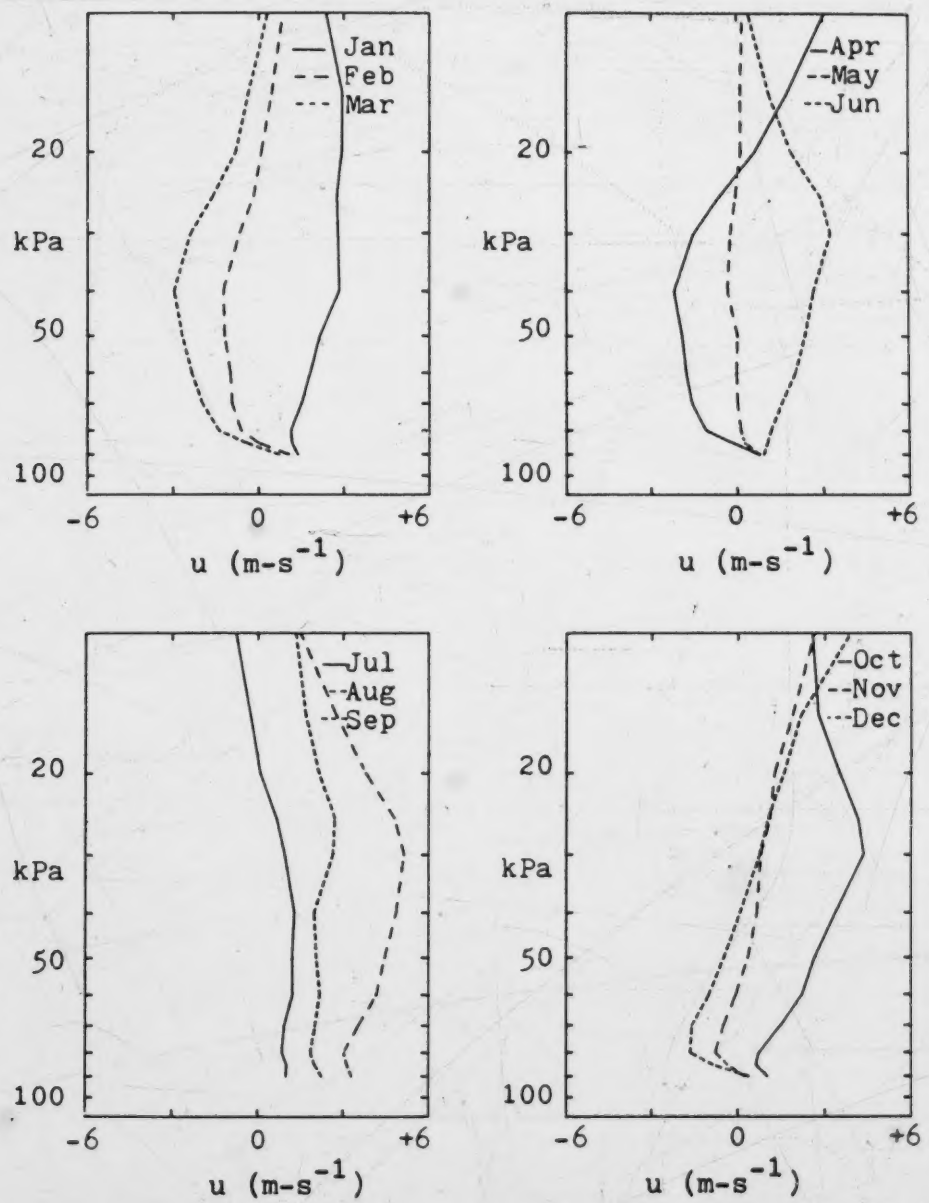

Fig. 7.7 Mean monthly vertical profiles of zonal wind speed. Same as Fig. 7.6.

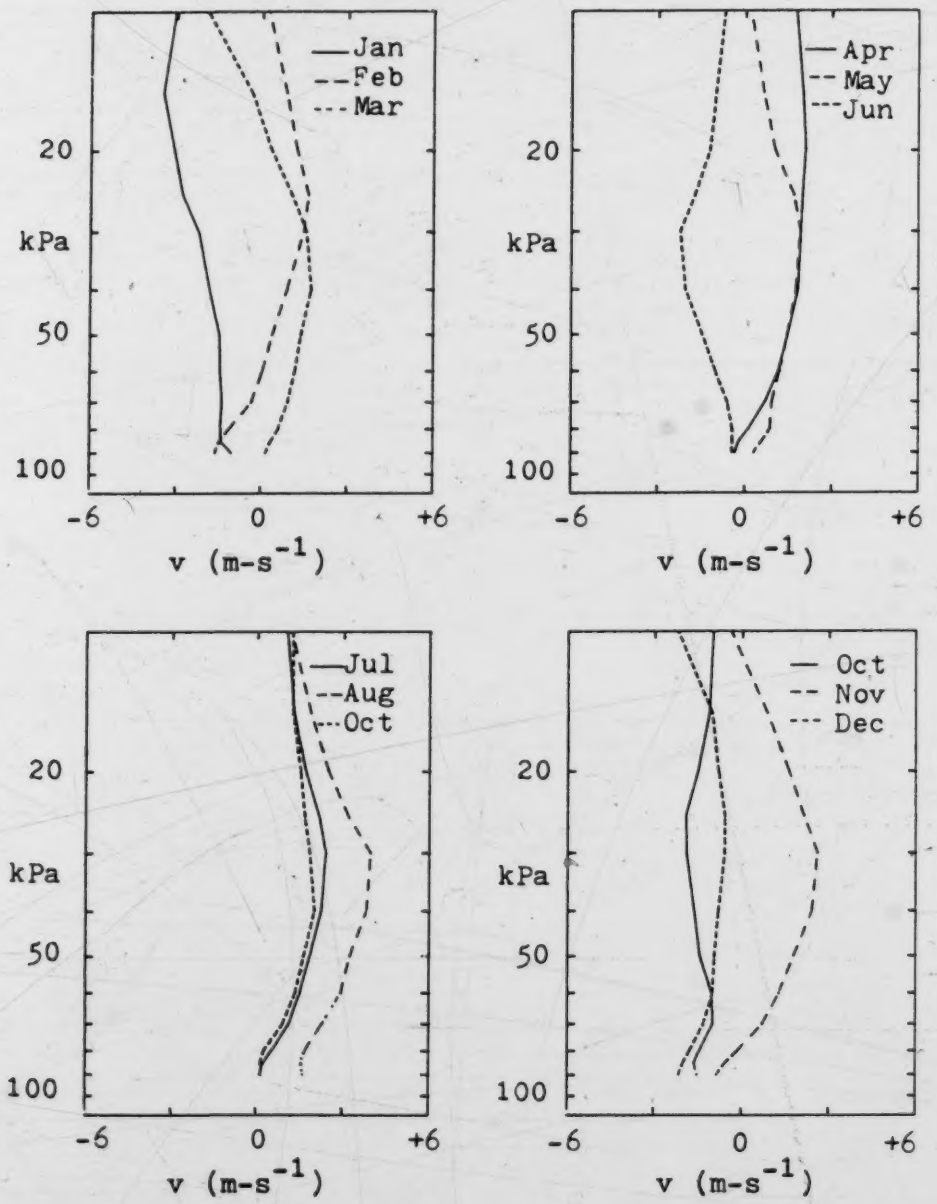

Fig. 7.8 Mean monthly vertical profiles meridional wind speed. Same as Fig. 7.6.

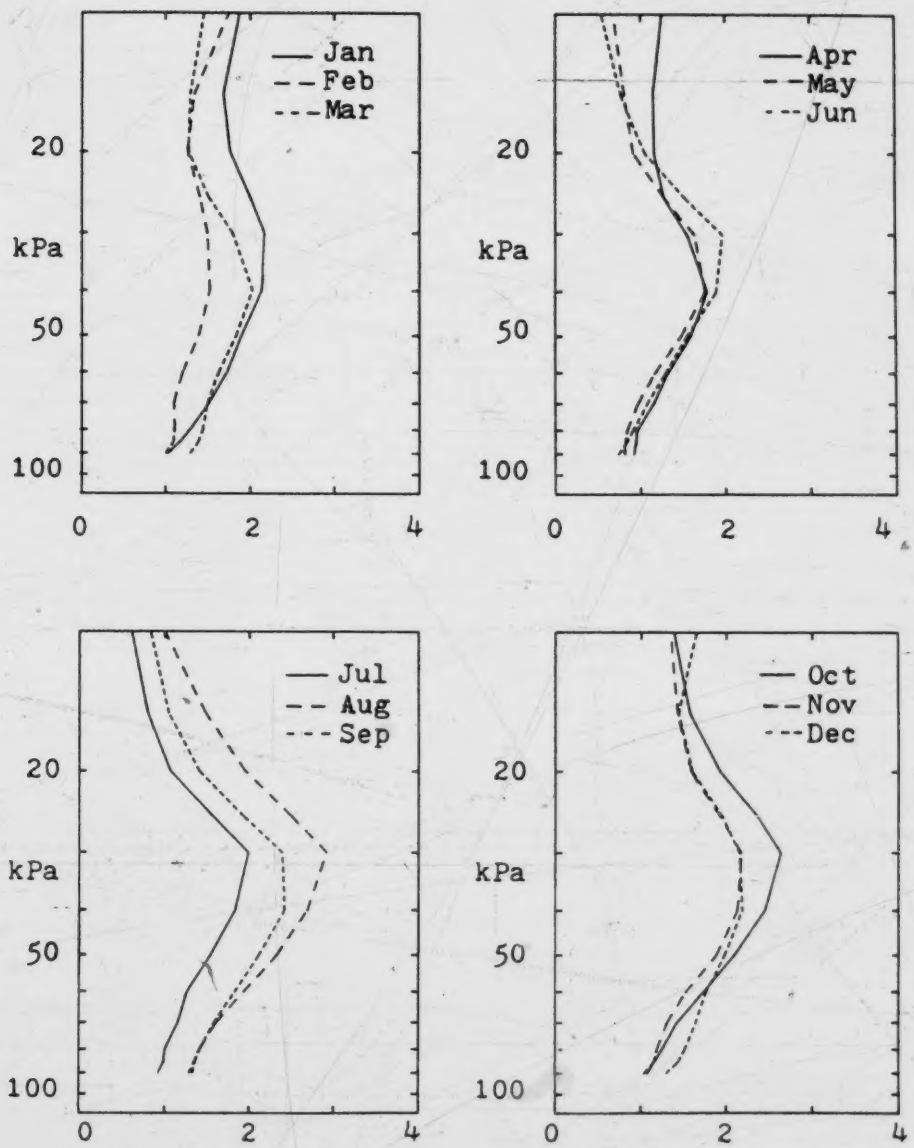

Fig. 7.9 Mean monthly vertical profiles of horizontal sensible heat flux H. Units are 10^6 J - m - kg^{-1} - s^{-1}. Same as Fig. 7.6.

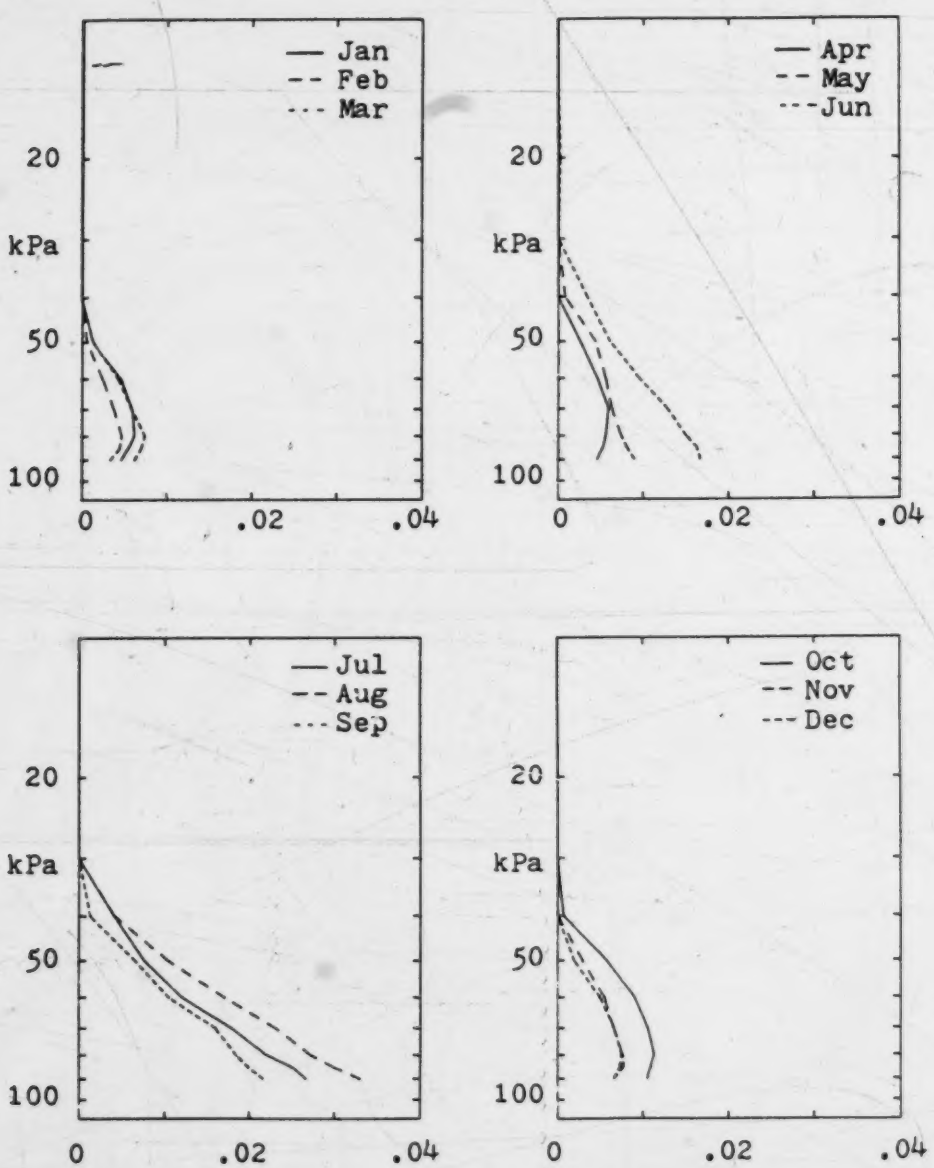

Fig. 7.10 Mean monthly vertical profiles of horizontal latent heat flux. Units are 10^4 J · m · kg^{-1} · s^{-1}. Same as Fig. 7.6.

characteristics of the surface - 90 kPa layer. This was a crude but necessary simplification.

Pressure-weighted mean values of four parameters in the surface - 90 kPa layer were calculated from each radiosonde ascent: temperature, potential temperature, specific humidity, and static potential vorticity. The latter is given by (Hoskins et al., 1985):

$$PVS = -fg \times (\partial\theta / \partial p) \qquad (7.2)$$

That is, PVS is the same as the isentropic potential vorticity (eg., Reiter, 1969) without the relative vorticity term. It does not seem quite appropriate to refer to the quantity expressed by Eqn. 7.2 as any sort of vorticity when the relative vorticity term has been left out, but the 'PVS' label will be retained here. PVS was interpreted as an indicator of the lapse rate in the surface - 90 kPa layer since the fg term becomes important only for PVS calculations at different latitudes.

Time series plots of these parameters, such as displayed in Fig. 7.11, show sufficient variability on time-scales of a week or month to encourage further examination of these parameters. This cannot be done here because of the coarseness of the aerosol data. When averages of these parameters were calculated so as to coincide with the sampling periods of the aerosol data, much of the fine-scale structure disappeared, especially during the winter months, and the annual cycle is predominant (Fig. 7.12).

Correlations with temperature or temperature-based tracers appeared to have the most likely chance of success. A more detailed comparison of PVS with the normalized scores for the anthro factor (Arctic1) at Alert was encouraging at first (Fig. 7.13). During the winter of 1980-81, these two series were inversely related, that is, the largest increases in the anthro component were accompanied by large decreases in PVS. This relationship was not true for the next two winters, when it appeared more likely that increases and decreases occurred at the same time in PVS and in the anthro component. Some sort of temperature-based parameter may indeed be correlated with the anthropogenic component of Arctic aerosols, but potential temperature and PVS do not seem to be reliably correlated with the anthro factor on a time-scale of a week. The question of a temperature-based or thermal hydrodynamic tracer will be taken up again shortly.

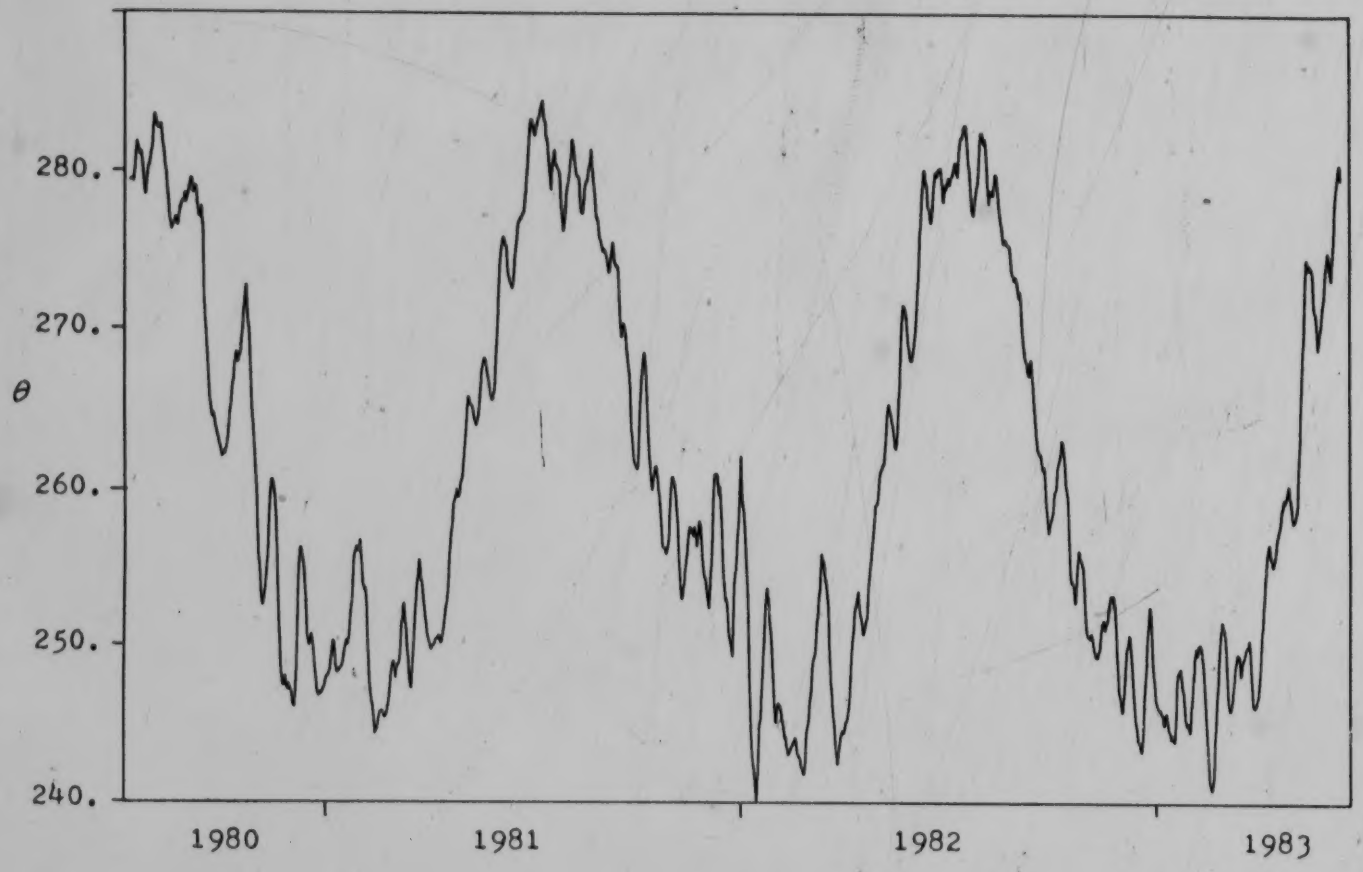

Fig. 7.11 Time series of potential temperature at Alert. These are 15-point (~weekly) moving averages of the pressure-weighted mean values for the surface - 90 kPa layer.

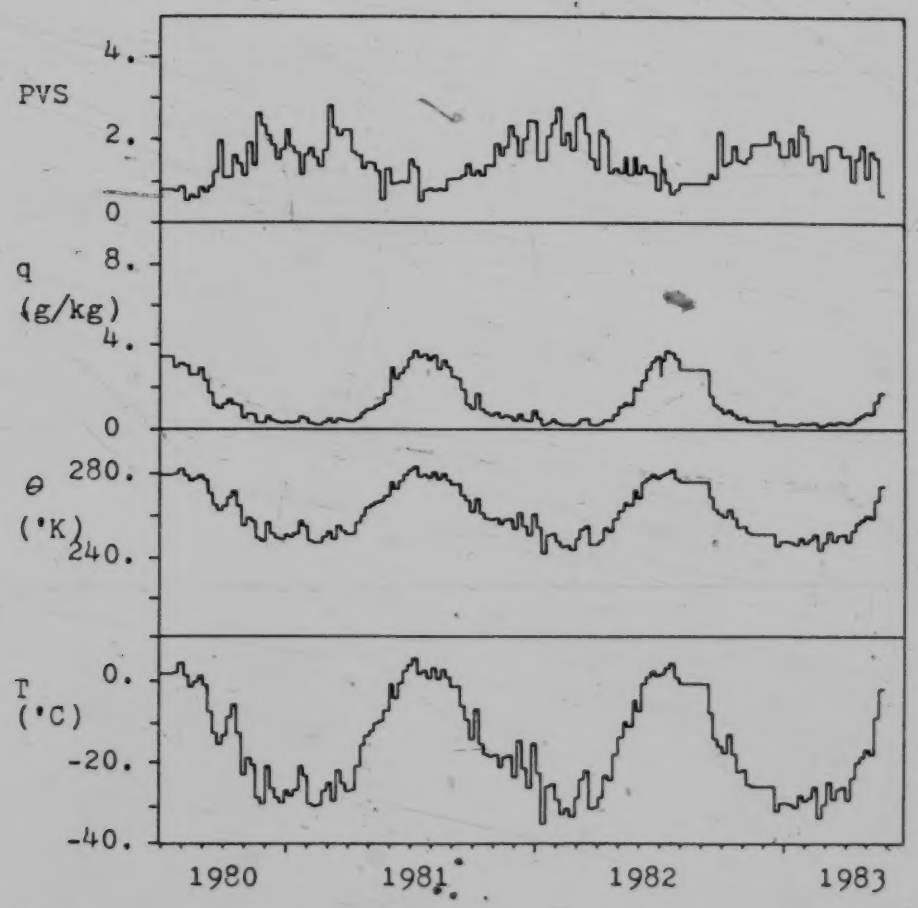

Fig. 7.12 Boundary layer characteristics at Alert. The surface - 90 kPa layer was assumed to be representative of the boundary layer. Pressure-weighted mean values of (from bottom to top) temperature, potential temperature, specific humidity, and static potential vorticity were calculated from radiosonde ascents, and averaged over the same time periods as the aerosol samples. Units of PVS are 10^{-6} K · m^2 · kg^{-1} · s^{-1}.

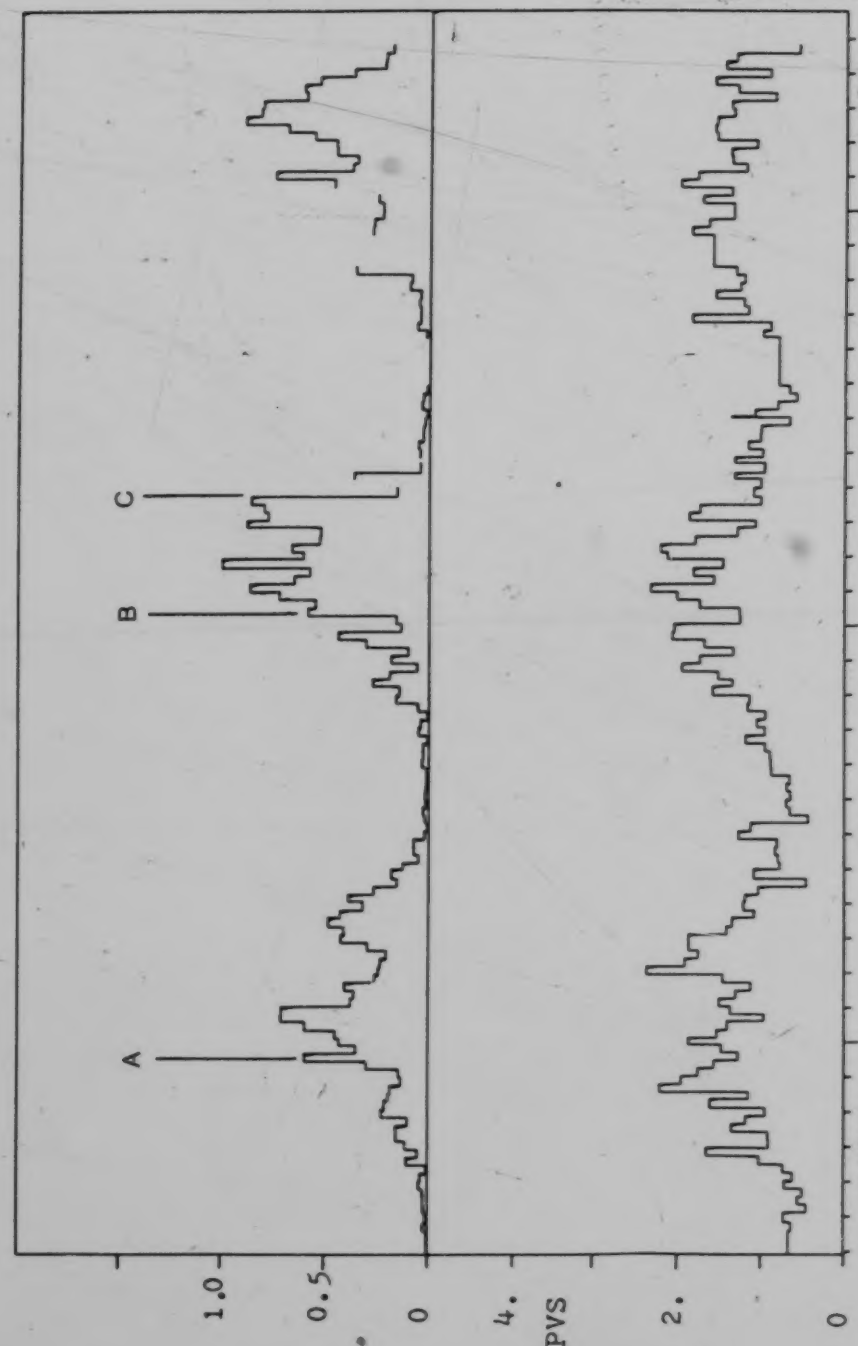

Fig. 7.13 PVS and the anthro factor scores at Alert.

Two periods have been noted as being especially interesting; these are marked 'A' and 'B' in Fig. 7.13. The early part of the haze season (December - January) is somewhat easier to study because the appearance of new aerosol material is more conspicuous. 'A' and 'B' were characterized by an abrupt increase in the scores for the anthro component at Alert. For 'A', the scores for the samples were[24]:

Sampling Period	Anthro Factor Scores
80/12/02 - 80/12/09	0.14
80/19/09 - 80/12/16	0.30
80/12/16 - 80/12/22	0.60
80/12/22 - 80/12/29	0.35
80/12/29 - 81/01/04	0.43

The surface weather map[25] for 80/12/08 (Fig. 7.14) showed little organized flow in the central polar basin, although major storms were located south of Novaya Zemlya and over the Norwegian Sea. By 80/12/15 (Fig. 7.15), these two Low centers had pivoted slightly and substantially increased the pressure gradient across the polar basin, providing almost direct transpolar flow from north-central USSR to northern Greenland and northern Ellesmere Island. The intensity of the pressure gradient was enhanced by a large Siberian High pressure center which was moving only slowly. The transpolar surface flow continued for several days (Fig. 7.16) until the Siberian High had moved into Alaska and western Canada (Fig. 7.17). The anthro factor score decreased by half in the sample from the following week, as Alert was no longer in a direct transpolar flow but came under the influence of a large Icelandic Low linked to a secondary center over Axel Heiberg Island (Fig. 7.18). The anthro factor score remained about the same for the next week.

'B' represents a similar sequence of events but the changes were more dramatic. The

---

[24]These are the normalized scores from Arctic1, and range from 0.0 to 1.0.

[25]All maps are for 00Z. These maps are only rough sketches of the actual NOAA surface maps, to show the main Low and High centers and the general trends of the isobars. A particular shortcoming is the inability to depict regions where there was a strong pressure gradient. It is assumed that the flow in the surface - 90 kPa layer was, in general, parallel to the isobars although this is yet another approximation.

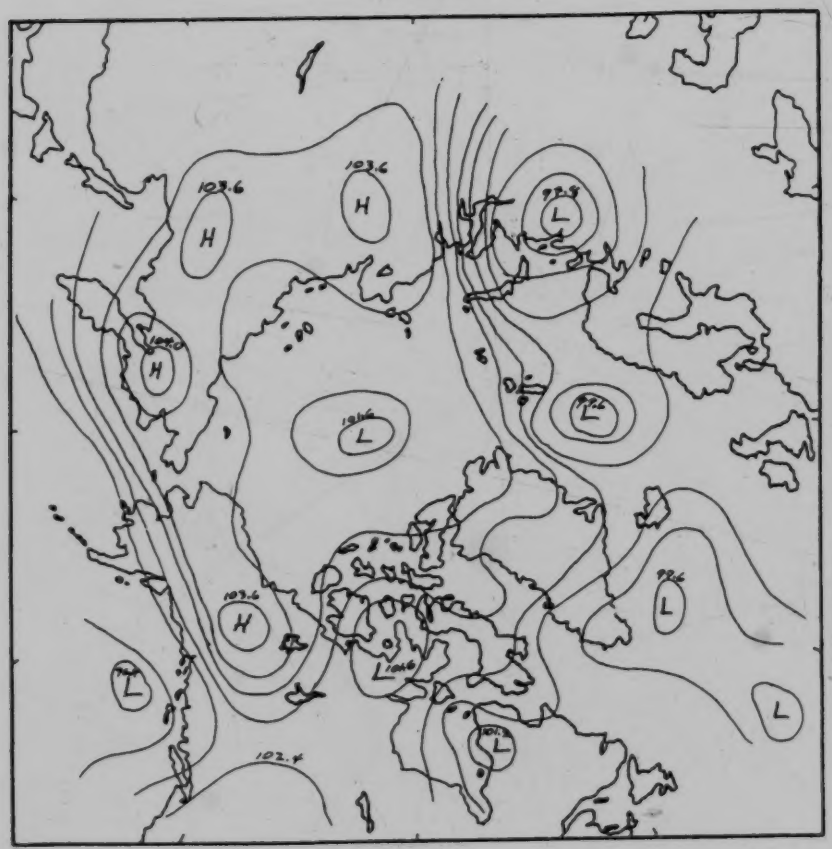

Fig. 7.14 Surface weather map for 80/12/08.

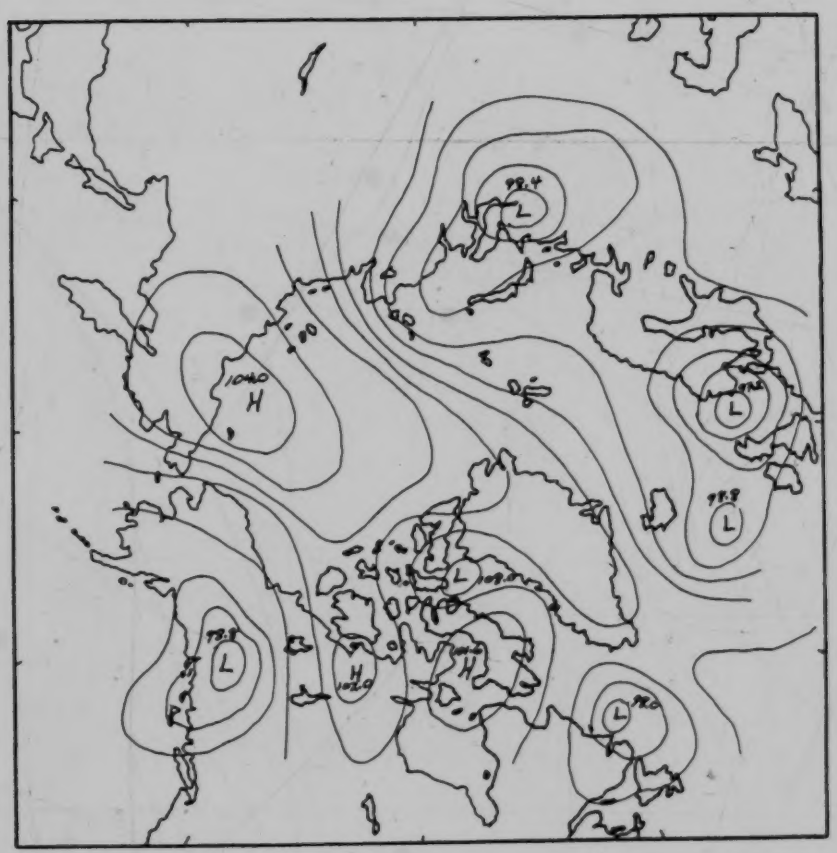

Fig. 7.15 Surface weather map for 80/12/15.

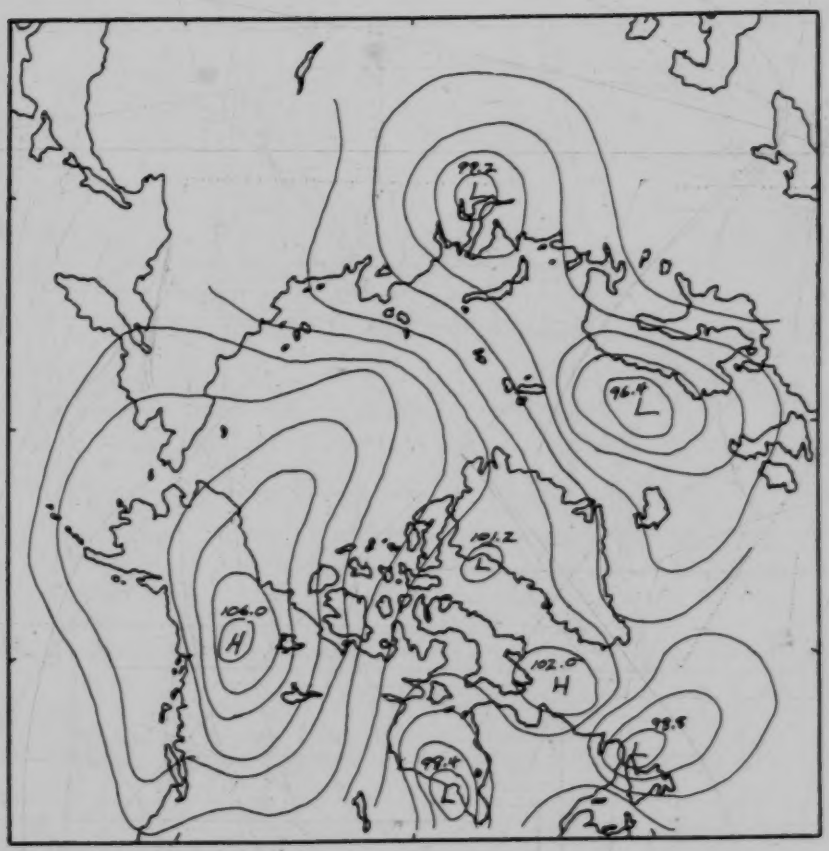

Fig. 7.16 Surface weather map for 80/12/18.

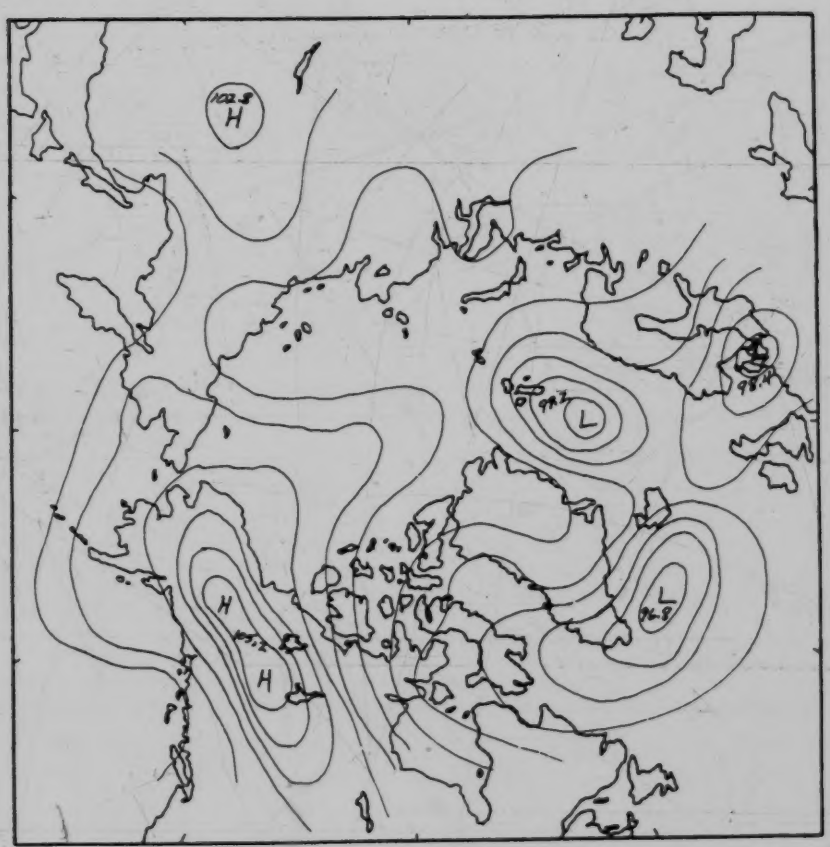

Fig. 7.17 Surface weather map for 80/12/21.

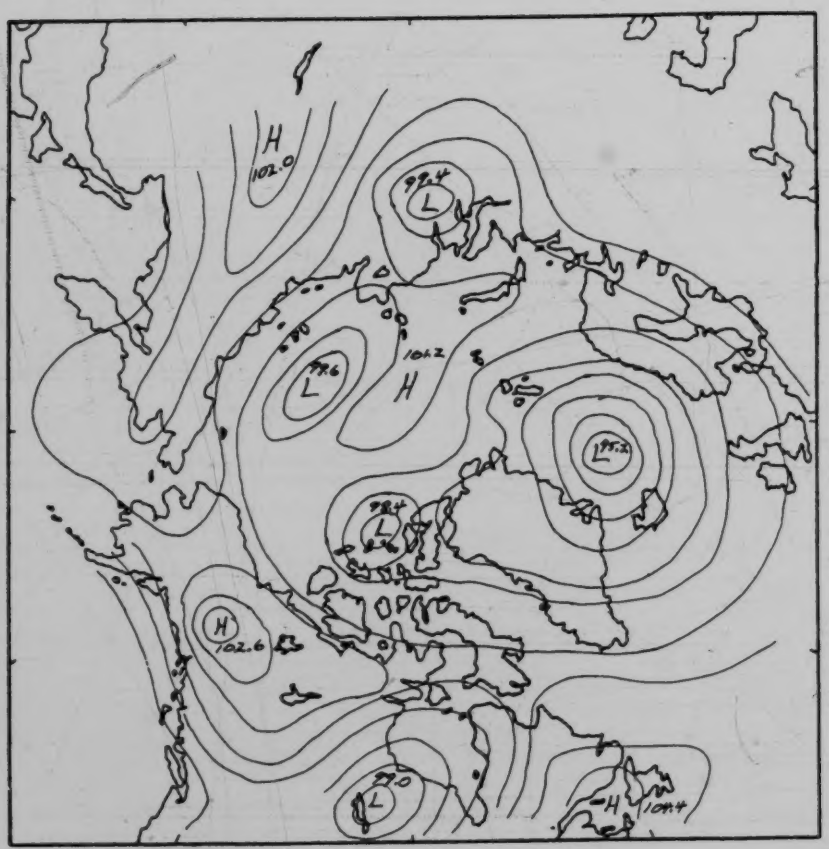

Fig. 7.18 Surface weather map for 80/12/28.

normalized scores for the anthro component at Alert were:

Sampling Period	Anthro Factor Scores
82/01/04 - 82/01/11	0.16
82/01/11 - 82/01/18	0.58
82/01/18 - 82/01/25	0.55
82/01/25 - 82/02/01	0.72

During the last week of 1981 and the first week of 1982, a Low pressure center dominated the surface flow over the Arctic islands (Fig. 7.19). This situation changed rapidly and by 82/01/12 (Fig. 7.20), the Canadian Arctic was again in a direct transpolar surface flow. The driving stimulus for this situation was the same: a deep Low center over the Barents Sea and a Siberian anticyclone extending into Alaska and northeastern Canada. This time, however, a storm system was approaching Cape Farewell on the southern tip of Greenland and soon split into two centers. Berry et al. (1953) describe storms along this track as having "a rather high frequency during the cold season". As is typical for cyclones following this storm track, the smaller center moved north into Davis Strait and Baffin Bay while the main system continued towards Iceland. By 82/01/14 (Fig. 7.21), the Icelandic Low center was well established and a secondary Low was located over Melville Peninsula. Between these systems and the old Siberian anticyclone, the center of which was moving northeastwards into the East Siberian Sea, a strong pressure gradient continued to exist across the polar basin for some time, and the anthro component at Alert also remained high.

A comparison with the anthro factor scores from Mould Bay is not possible because the aerosol sample was not changed regularly during this period. There is only a single average sample collected from 81/12/28 to 82/01/25. However, the normalized score for the anthro factor at Mould Bay was low (~0.0) preceding this period, and was quite large (0.87) in the following sample (82/01/25 - 82/02/01). The anthro factor scores at Igloolik were relatively constant (~0.5) throughout January 1982.

These two examples do not prove anything by themselves, but they are consistent with the surge hypothesis of Raatz and Shaw (1984). An important part of this idea is the combination of two meteorological systems leading to rapid transpolar advection of aerosols.

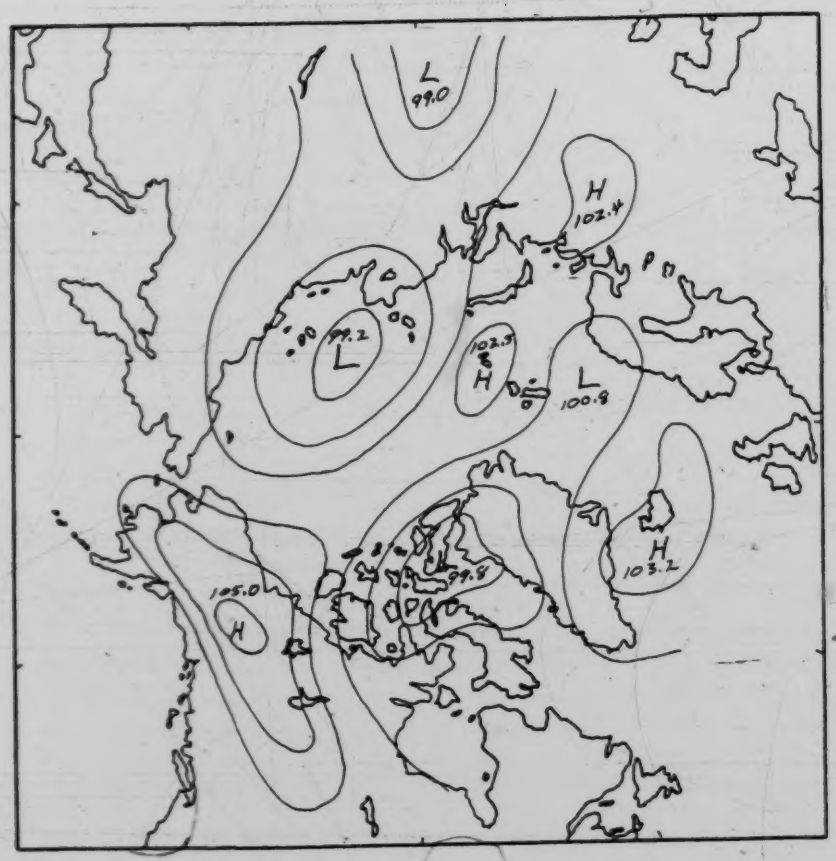

Fig. 7.19 Surface weather map for 82/01/08.

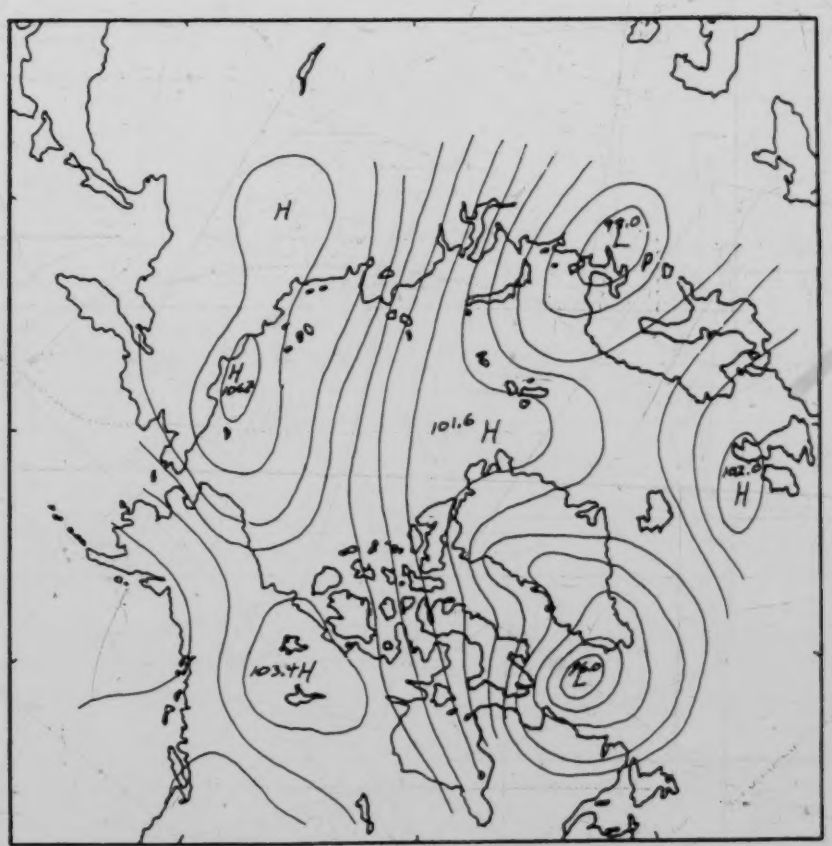

Fig. 7.20 Surface weather map for 82/01/12.

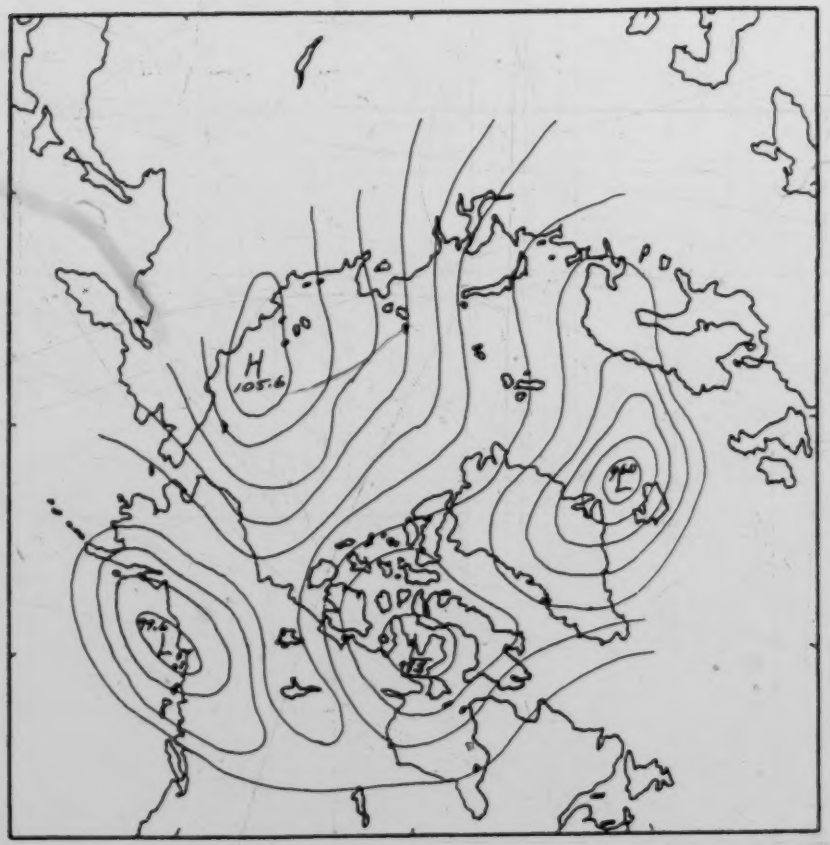

Fig. 7.21 Surface weather map for 82/01/14.

The interaction of a Barents Sea Low with a Siberian High provides both the necessary pressure gradient, and the east-west direction of the flow.

The fate of aerosols transported to the Arctic has received very little attention. An example of a rapid decrease in the anthro component at Alert (indicated by 'C' in Fig. 7.13) will be discussed in the same qualitative fashion as 'A' and 'B'. The normalized scores for the anthro factor at Alert during the period were:

Sampling Period	Anthro Factor Scores	Mean Temp (° C)	Total Precip (mm)
82/04/11 - 82/04/18	0.80	-28.9	1.9
82/04/18 - 82/04/25	0.86	-27.8	6.3
82/04/25 - 82/05/04	0.15	-22.1	3.2

The surface weather map for 82/04/23 (Fig. 22) is similar to the rapid transport scenario of 'A' and 'B', although the centers of action are further to the west. This would suggest that the high anthro score at Alert was due to an aerosol source region in western USSR or northeastern Europe, instead of central USSR as in the two previous cases. Once more, the situation changed rapidly and, three days later (Fig. 7.23), northern Ellesmere Island was under the influence of an Arctic anticyclone. This High intensified and remained over Greenland and the northern Arctic islands for the next week (Fig. 7.24), coinciding with the aerosol sample of 82/04/25 - 82/04/09. The Low center near Cape Farewell on 82/04/09 split as before, with the main Low carrying on towards Iceland and the smaller center tracking northwards along the west coast of Greenland (Fig. 7.25). However, this secondary center did not reach Alert, which remained under the anticyclone for several more days (Fig. 7.26).

Temperatures at Alert were beginning to moderate a little by the first week of May. Still, the air mass was cool and absolute humidities were low. The rapid decrease in the anthro factor scores is not explained by increased precipitation scavenging, because the recorded total precipitation from 82/04/25 - 82/05/04 was only one-half of the total precipitation during the previous week. Rather, the abrupt decrease was the result of a different air mass over Alert as the spring Arctic anticyclone became established and blocked any direct advection of aerosols from outside the region.

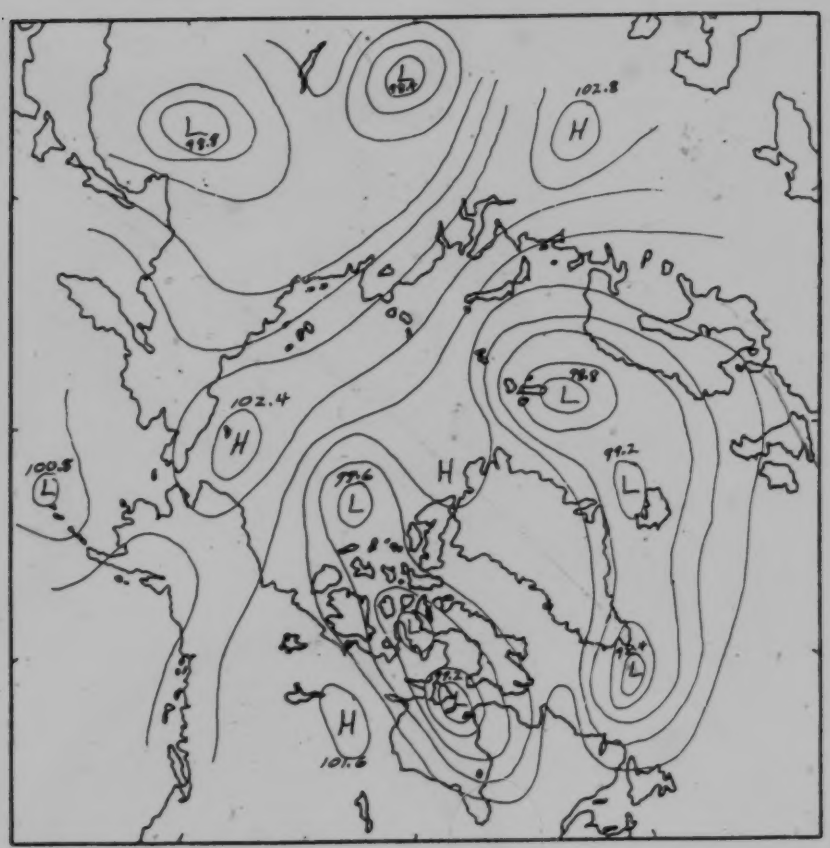

Fig. 7.22 Surface weather map for 82/04/23.

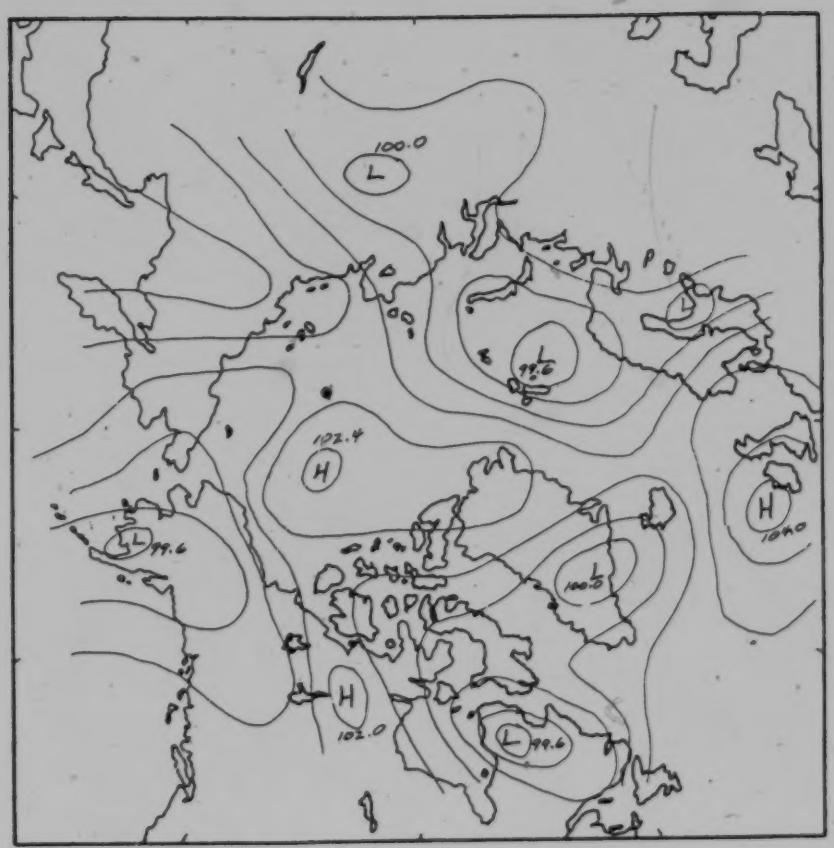

Fig. 7.23 Surface weather map for 82/04/26.

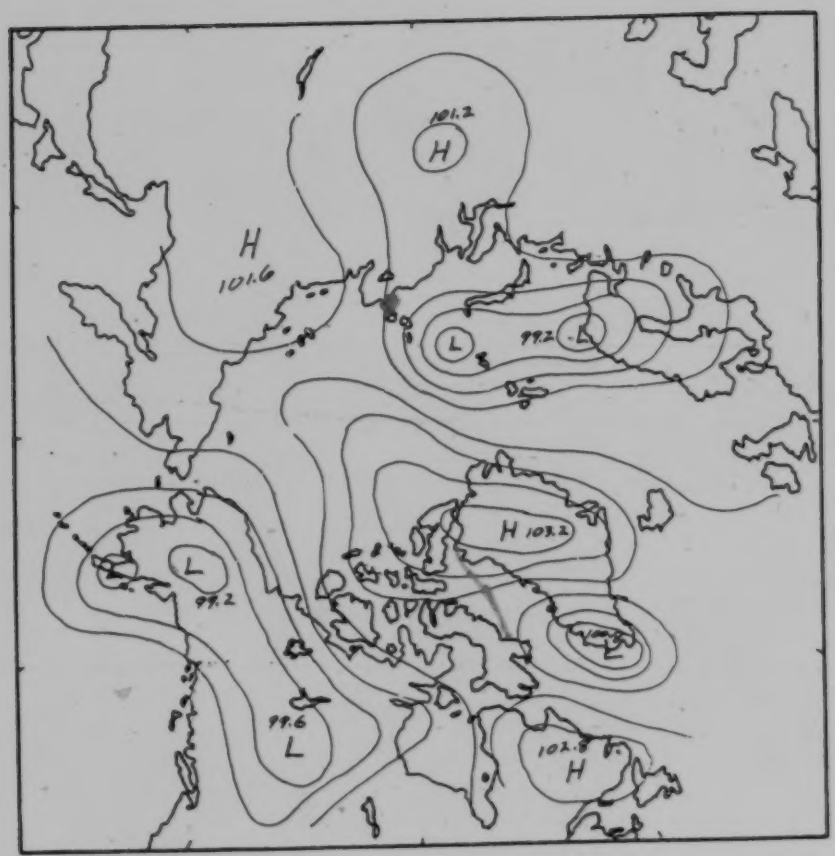

Fig. 7.24 Surface weather map for 82/04/29.

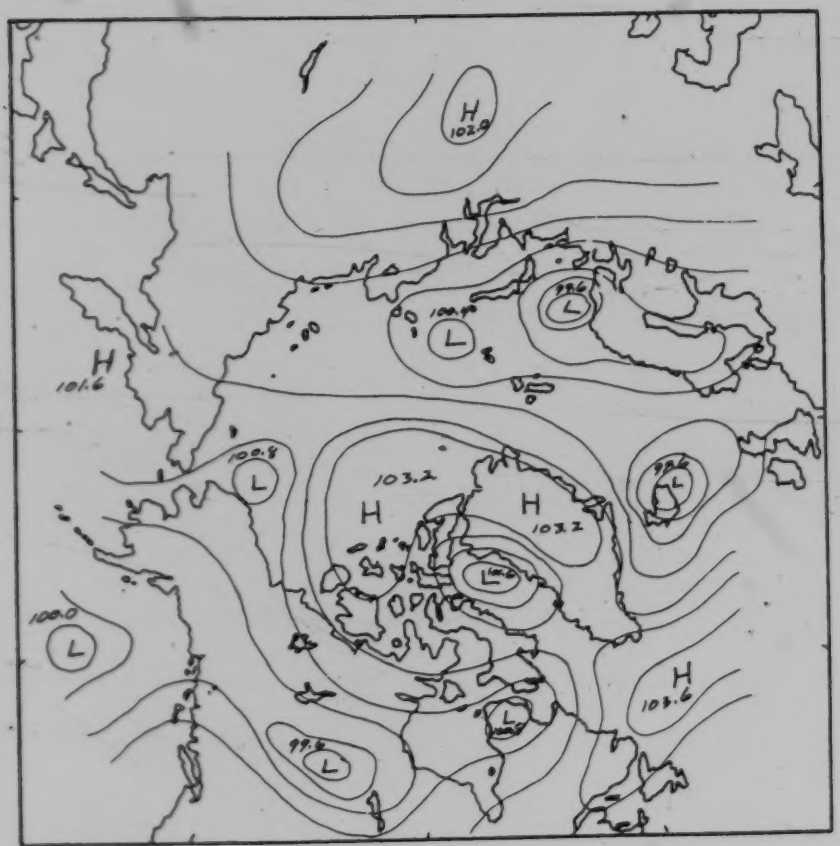

Fig. 7.25 Surface weather map for 82/04/30.

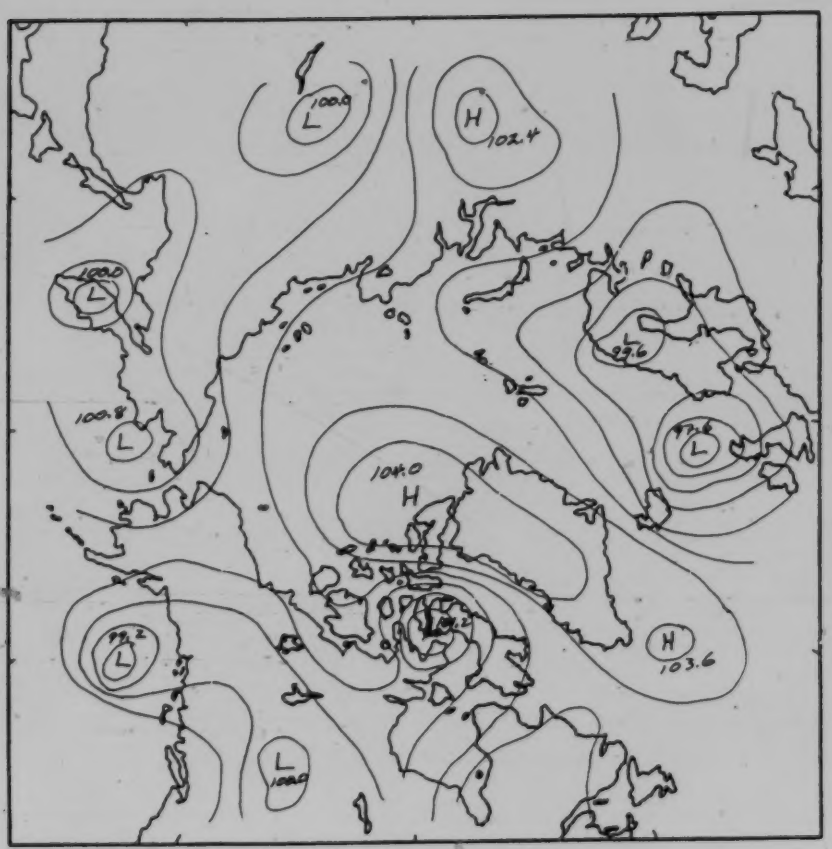

Fig. 7.26 Surface weather map for 82/05/03.

The earlier inference regarding an imperfect link between the anthro scores at Alert and a temperature-based meteorological parameter seems a little more credible after reviewing 'A' and 'B'. The important role of the Barents Sea Low suggested that an examination of the heat flux might be in order. There is a little previous work which implies that aerosol and energy transport in polar regions might be correlated. Hogan et al. (1982) and Hogan et al. (1984b) found that surface ozone and aerosol concentrations at the South Pole were correlated with heat and moisture fluxes, and explained this with an uncomplicated synoptic model. Sizeable heat fluxes in the mid-winter Arctic atmosphere also occur, as described by Jackson (1960; quoted by Maxwell, 1980):

> "A significant source area for warm air arriving over northern Ellesmere Island in mid-winter appears to be the Norwegian Sea (between Greenland and Norway). Three main features characteristic of this air are:
>
> (a) The advection appears to take place above 1500 m and especially between 1500 m and 2000 m suggesting that north Greenland forms an orographic barrier to the intrusion of warm air at lower levels.
> (b) Partly because of this feature, the warmth from such air appears to be transmitted to the ground more often by long-wave radiation from clouds or snowfall than by surface winds.
> (c) The snowfall associated with this warm air possibly accounts for the major part of mid-winter precipitation."

From the Alert radiosonde data, the time series of the sensible heat flux H at 95 kPa was calculated, and then averaged over the same periods as the aerosol samples[24]. (Heat flux H was defined in Eqn. 7.1). This level was chosen as a compromise between the constraints of

Jackson (1960), which suggested warm air advection occurred around 90 - 80 kPa, and the ground-level aerosol data. Fig. 7.27 is a simultaneous plot of the normalized scores for the anthro factor and the heat flux at Alert. 'A' is a remarkably good confirmation of this idea, but 'B' seems to contradict it. The good agreement for 'A' is a little fortuitous. Conditions were such that the heat flux was maximized, with a strong pressure gradient and correspondingly strong winds impacting directly onto northern Ellesmere Island. This wasn't the case for 'B', when surface temperatures remained very low and the strongest pressure gradient was further to the west, giving rather light winds and small values for H.

An examination of similar rapid increases in the anthro factor scores at Alert in Fig. 7.27 revealed the same erratic correlation. For instance, the end of March 1982 and late January 1983 were both occasions of strong direct transpolar flow arriving at Alert, and the anthro score and the heat flux both increased. On the other hand, the highest score for the anthro factor occurred at the end of February 1982, but the heat flux increased by only a small amount. This was a different synoptic situation, with a large anticyclone over eastern Siberia which eventually moved into the Beaufort Sea area. In general, the correlation between heat flux and the anthropogenic aerosol component at Alert arises from a special set of circumstances which seems most likely to occur in December or January.

The prolonged periods of a high anthro factor score during late winter and early spring are more difficult to explain. A common feature in most of these cases is a large anticyclone extending northeastwards from Siberia and/or occupying the western polar basin. Advection of aerosols along the periphery of a High may again be the predominant pathway but the route for aerosols reaching Alert would be much more circuitous. Aerosol sources in central or northeastern Siberia could be inferred in such cases, but this may be a simplistic interpretation because levels of aerosols in the spring are generally high and the high scores for the anthropogenic component may just be old material re-circulating through, or persisting in, the polar basin.

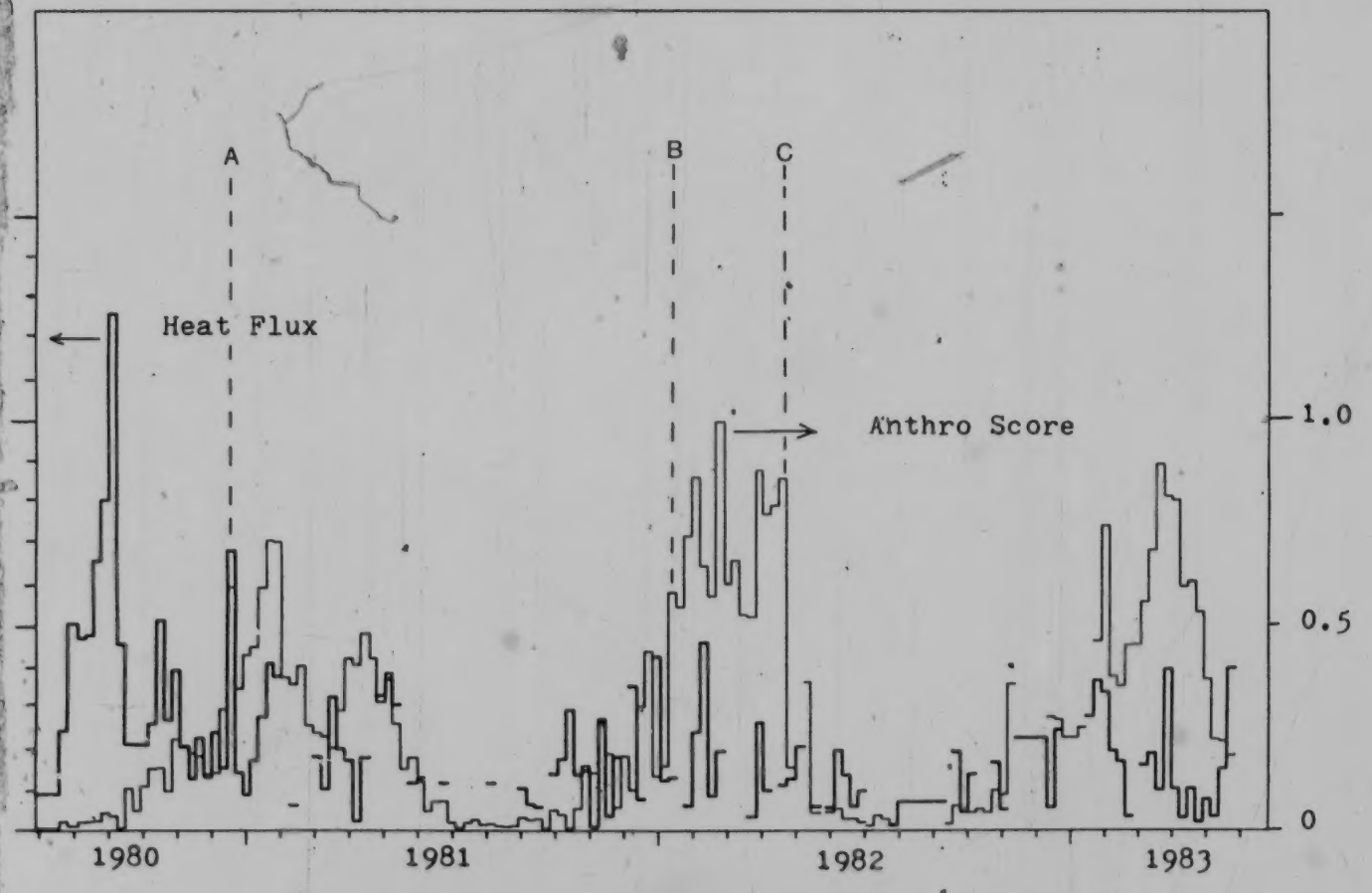

Fig. 7.27 Anthro factor scores and the 95 kPa heat flux at Alert. The heat flux was calculated from individual radiosonde ascents and then averaged over the same time periods as the aerosol samples. Units of heat flux are 10^4 J - m - kg^{-1} - s^{-1}.

7.1 Conjectures

Once more, these examples are too few and insufficiently detailed to "prove" anything. But it is possible to combine the larger trends in the aerosol and meteorological data into a consistent picture. When discussing the annual cycles of the three Arcticl factors at Alert (Fig. 6.7), it was noted that the sea salt factor tended to lead the anthro factor. That is, sea salt appeared earlier (~September) and peaked in January-February, while the anthro factor reached its highest levels in February to March or April. These trends can be explained by combining the discussion of synoptic conditions with maps of the mean surface pressure for January and April (Fig. 7.28 and Fig. 7.29, respectively; adapted from Vowinckel and Orvig, 1970).

The Icelandic Low and the Siberian High are the dominant features in the high latitude eastern hemisphere in January. It is suggested that the elongated trough extending from Iceland to Novaya Zemlya in Fig. 7.28 is only partly due to the quasi-stationary Icelandic Low. The frequency of cyclones in the White Sea and Barents Sea regions is sufficiently high so as to appear on the mean monthly map as an extension of the Icelandic Low. On most days, the transpolar flow is probably more variable in both speed and direction than might be inferred from the isobars of Fig. 7.28. The weak transpolar flow on the mean monthly map is partly due to averaging of the strong pressure gradients between the Siberian High and an approaching Barents Sea Low, which create occasional surges of aerosol-rich (relatively speaking) air from east to west. Vowinckel and Orvig (1970) present data which show that the percentage of open water within the pack ice of the Barents Sea continues to decrease through December and January, reaching a minimum in February and March. The sea salt may have been added from the open water in this region, or it may have been carried from areas further south (such as the North Sea). It is sufficient to point out that this means there are two possible source regions for the observed sea salt.

By March, however, the sea ice cover is at a maximum while the frequency of occurrence of deep cyclones over the Barents Sea is decreasing. The results of Berry

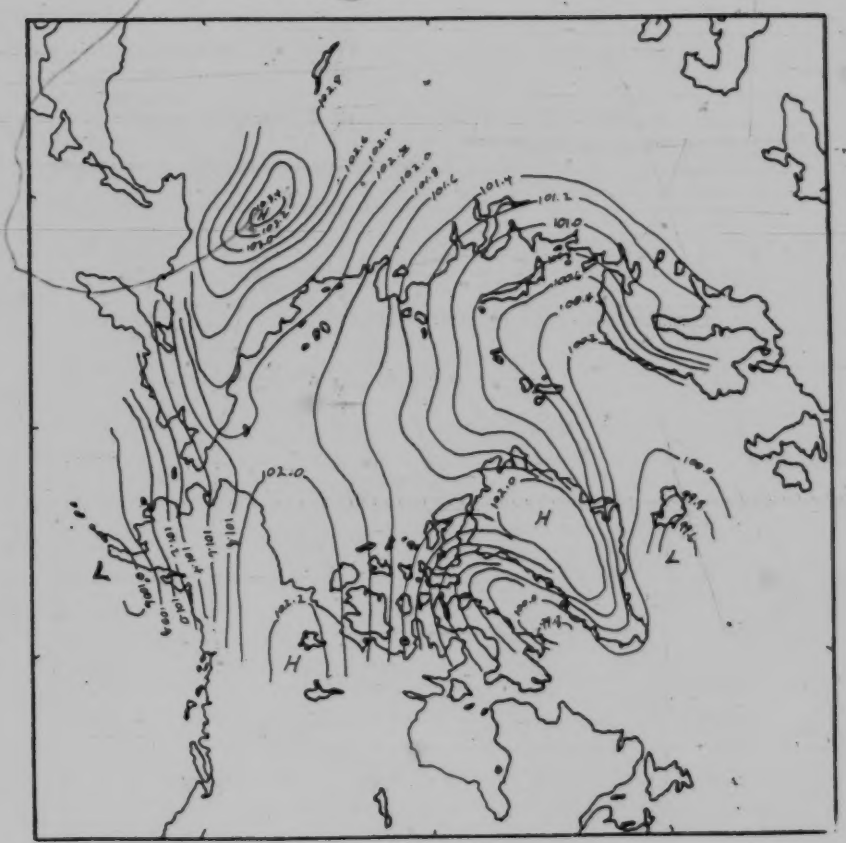

Fig. 7.28 Mean surface pressure (kPa) in January (adapted from Vowinckel and Orvig, 1970).

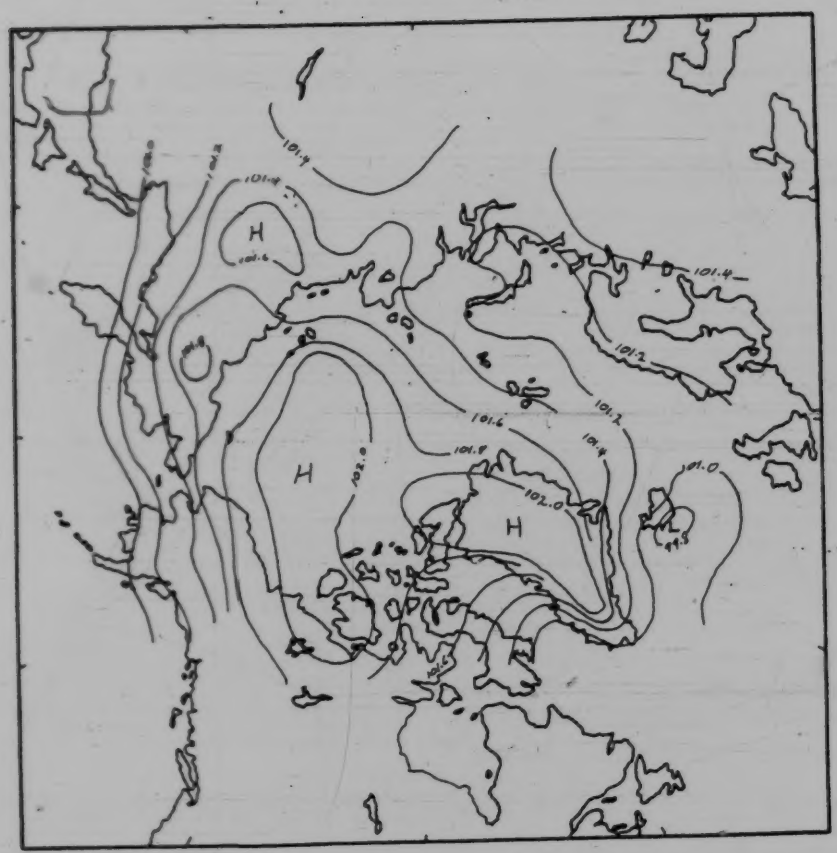

Fig. 7.29 Mean surface pressure (kPa) in April (adapted from Vowinckel and Orvig, 1970).

slightly smaller in April-June than in January-March (a total of 15 in January-March, 1944-1951, versus 13 in April-June) but, perhaps more significantly, the mean track of the systems is about 5° of latitude further south (that is, from a little south of Spitsbergen to a track along the Scandinavian coastline). This was expressed a little more clearly by Hare and Orvig (1958):

> "The Norwegian-Barents-Kara Seas maximum is also well-known, though we have recently learned that its summer behaviour is more vigorous than formerly supposed. In the cooler months the area is frequently invaded by fast-moving Atlantic cyclones, with strong southwesterly advection of warmth and humidity over Scandinavia and along the Siberian coast. Again there is warm open water to favor the maintenance of intensity. At times, however - and especially in summer - the path may lie directly across Scandinavia. Figs. 7-10[17], showing five-day mean pressures for periods in January, 1955, show that cyclonic activity of the greatest intensity may occur well inland, proving that the warmth of the Norwegian Sea water is not a necessary condition for this activity - though it is possible that the Baltic plays a similar role. For prolonged periods, this sector may be the scene of the most vigorous cyclones of the whole hemisphere, replacing the Icelandic low as the principal "graveyard area". There is some evidence that Atlantic blocking tends to be accompanied by active cyclonic activity in this area, whose locus shifts westwards as the blocking high retrogresses."

The sea salt component at Alert decreases steadily from January to March. The anthro component either remains at fairly constant levels or may increase to slightly higher levels; if the latter, then the anthro component is likely to remain high for 3 - 4 weeks, instead of the short (~< 1 week) surges of December-January. This would seem to be the result of a change in the average synoptic conditions as the Arctic anticyclone becomes established over the

western Arctic Ocean (Fig. 7.29). These are cold, dry air masses which would account for the lack of significant levels of sea salt, and also for the steady, unbroken increase each spring in RF1 at Alert (as shown in Fig. 7.2).

If this simple model is correct, it has rather significant implications. The anthro component at Alert is not one annual cycle, but is composed of two over-lapping cycles. During December-January, the Arctic atmosphere is being 'charged up' with aerosols pumped fairly quickly across the polar basin. As the synoptic conditions responsible for this become less frequent, a new regime starts to dominate in March and April. Whether the anthro component is high at this time because of a mixed reservoir of aerosols in the Arctic anticyclone, or because these slow-moving, almost quasi-stationary, systems establish a long-lived route for advection of aerosols along their periphery, cannot be determined from the data available here.

There is one other small bit of evidence, however, which may support the two-mode cycle for the anthropogenic component of the Arctic aerosols. The Na/SO_4^{2-} factor derived at Mould Bay and Igloolik tended to have high values coinciding with the latter part of the peak in the anthro component at these stations (Fig. 6.8 and Fig. 6.9). A discussion of this factor as an aerosol source was avoided because of uncertainties about its interpretation; this may not be a 'true' source component, but a 'spoiler' factor. This was the fourth factor derived from the aerosol data at Mould Bay and Igloolik, and it may have represented an adjustment during the eigenvalue calculations to balance the variance removed during extraction of the first three factors. The question of the physical significance of the Na/SO_4^{2-} factor (a 'true' component or a 'spoiler' factor?) probably isn't important at this stage; what is important is that the scores for this factor show that something different was occurring in late March and April, during the latter part of the annual cycle in the anthro component. Whether this was the appearance of a new aerosol component with the arrival of the spring Arctic anticyclone, or a slight shift in the composition of the anthro and sea salt components, will have to be left unanswered.

8. References

Ackerman, T.; Valero, F. (1984)
The Vertical Structure of Arctic Haze as Determined from Airborne Net-Flux Radiometer Measurements.
Geo. Res. Lett., **11**(5), p.469-472.

AES (1978)
Monthly Meteorological Summary. Edmonton Municipal Airport, November 1978.
Atmospheric Environment Service, Environment Canada.

AES (1978-1983)
CANSAP Data Summary.
Air Quality and Inter-Environmental Branch, Atmospheric Environment Service, Environment Canada.

Alpert, D.; Hopke, P. (1980)
A Quantitative Determination of Sources in the Boston Urban Aerosol.
Atm. Env., **14**, p.1137-1146.

Alpert, D.; Hopke, P. (1981)
A Determination of the Sources of Airborne Particles Collected During the Regional Air Pollution Study.
Atm. Env., **15**, p.675-687.

Andreae, M. (1983)
Soot Carbon and Excess Fine Potassium: Long-Range Transport of Combustion-Derived Aerosols.
Science, **220**, p.1148-1151.

Anon. (1979)
IMSL Library Reference Manual, Version 7.
IMSL Inc., Houston TX. (3 volumes).

Anon. (1986)
SPSSx User's Guide, Second Edition.
McGraw-Hill, New York NY.

Bailey, I.; Radke, L.; Lyons, J.; Hobbs, P. (1984)
Airborne Observations of Arctic Aerosols II: Giant Particles.
Geo. Res. Lett., **11**(5), p.397-400.

Barrie, L.; Hoff, R.; Daggupaty, S. (1981)
The Influence of Mid-Latitudinal Pollution Sources on Haze in the Canadian Arctic.
Atm. Env., **15**(8), p.1407-1449.

Barrie, L.; Sirois, A. (1982)
An Analysis and Assessment of Precipitation Chemistry Measurements made by CANSAP (The Canadian Network for Sampling Precipitation): 1977-1980.
Report AQRB-82-003-T, Atmospheric Envronment Service, Environment Canada.

Barrie, L.; Hoff, R. (1984)
The Oxidation Rate and Residence Time of Sulphur Dioxide in the Arctic Atmosphere.
Atm. Env., **18**(12), p.2711-2722.

Barrie, L.; Hoff, R. (1985)
Five Years of Air Chemistry Observations in the Canadian Arctic.
Atm. Env., **19**(12), p.1995-2010.

Barrie, L.; Fisher, D.; Koerner, R. (1985)
Twentieth Century Trends in Arctic Air Pollution Revealed By Conductivity and Acidity Observations in Snow and Ice in the Canadian High Arctic.
Atm. Env., **19**(12), p.2055-2063.

Barry, R.; Perry, A. (1973)
Synoptic Climatology.
Methuen and Co., London. 555 pp.

Berg, W.; Sperry, P.; Rahn, K.; Gladney, E. (1983)
Atmospheric Bromine in the Arctic.
J. Geo. Res., **88**(C11), p.6719-6736.

Berg, W.; Heidt, L.; Pollock, W.; Sperry, P.; Cicerone, R.; Gladney, E. (1984)
Brominated Organic Species in the Arctic Atmosphere.
Geo. Res. Lett., **11**(5), p.429-432.

Berry, F.; Owens, G.; Wilson, H. (1953)
Arctic Weather Maps.
Project AROWA, TED-UNL-MA-501. US Navy, Norfolk VA.

Bevington, P. (1969)
Data Reduction and Error Analysis for the Physical Sciences.
McGraw-Hill, New York NY. 336pp.

Blanchet, J.; List, R. (1983)
Estimation of Optical Properties of Arctic Haze Using a Numerical Model.
Atm.-Ocean, **21**(4), p.444-465.

Blasing, T. (1975)
A Comparison of Map-Pattern Correlation and Principal Component Eigenvector Methods for Analyzing Climatic Anomaly Patterns.
Preprints, Fourth Conf. on Prob. and Stat. in Atm. Sciences, AMS (Tallahassee), p.96-101.

Blifford, I.; Meeker, G. (1967)
A Factor Analysis Model of Large Scale Pollution.
Atm. Env., **1**, p.147-157.

Bodhaine, B.; Harris, J.; Herbert, G. (1981)
Aerosol Light Scattering and Condensation Nuclei Measurements at Barrow, Alaska.
Atm. Env., **15**(8), p.1375-1389.

Bodhaine, B.; Dutton, E.; DeLuisi, J. (1984)
Surface Aerosol Measurements at Barrow During AGASP.
Geo. Res. Lett., **11**(5), p.377-380.

Bohren, C.; Huffman, D. (1983)
Absorption and Scattering of Light by Small Particles.
J. Wiley, New York NY. 530pp.

Boutron, C.; Delmas, R. (1980)
Historical Record of Global Atmospheric Pollution Revealed in Polar Ice Cores.
Ambio, 9(5), p.210-215.

Boutron, C.; Martin, S. (1980)
Sources of Twelve Trace Metals in Antarctic Snows Determined by Principal Component Analysis.
J. Geo. Res., 85(C10), p.5631-5638.

Bowser, W; Peters, T.; Newton, J. (1951)
Soil Survey of Red Deer Sheet.
Alberta Soil Survey Report No. 16, 86pp.

Borys, R.; Rahn, K. (1981)
Long-Range Atmospheric Transport of Cloud-Active Aerosol to Iceland.
Atm. Env., 15(8), p.1491-1501.

Buell, E. (1975)
The Topography of the Empirical Orthogonal Functions.
Preprints, Fourth Conf. on Prob. and Stat. in Atm. Sciences. AMS (Tallahassee) p.188-193.

Busenberg, E.; Langway, C. (1979)
Levels of Ammonium, Sulfate, Chloride, Calcium, and Sodium in Snow and Ice From Southern Greenland.
J. Geo. Res., 84(C4), p.1705-1709.

Cahill, T.; Eldred, R. (1984)
Elemental Composition of Arctic Particulate Matter.
Geo. Res. Lett., 11(5), p.413-416.

Carlson, T. (1981)
Speculations on the Movement of Polluted Air to the Arctic.
Atm. Env., 15(8), p.1473-1477.

Cattell, R. (1952)
Factor Analysis: An Introduction and Manual for the Psychologist and Social Scientist.
Harper and Row, New York NY.

Cess, R. (1983)
Arctic Aerosols: Model Estimates of Interactive Influences Upon the Surface-Atmosphere Clear-Sky Radiation Budget.
Atm. Env., 17(12), p.2555-2564.

Chuan, R.; Woods, D. (1984)
The Appearance of Carbon Aerosol Particles in the Lower Stratosphere.
Geo. Res. Lett., 11(5), p.553-556.

Clarke, A.; Charlson, R.; Radke, L. (1984)
Airborne Observations of Arctic Aerosols IV: Optical Properties of Arctic Haze.
Geo. Res. Lett., 11(5), p.405-408.

Clarke, A.; Noone, K. (1985)
Soot in the Arctic Snowpack: A Cause for Perturbations in Radiative Transfer.
Atm. Env., 19(12), p.2045-2053.

Conway, T.; Raatz, W.; Gammon, R. (1985)
Airborne CO_2 Measurements in the Arctic During Spring 1983.
Atm. Env., **19**(12), p.2195-2201.

Craddock, J.; Flintoff, S. (1970)
Eigenvector Representations of Northern Hemisphere Fields.
Quart. J. Roy. Met. Soc., **96**, p.124-129.

Craig, H.; Chou, C. (1982)
Methane: The Record in Polar Ice Cores.
Geo. Res. Lett., **9**(11), p.1221-1224.

Daisey, J.; McCaffrey, R.; Gallagher, R. (1981)
Polycyclic Aromatic Hydrocarbons and Total Extractable Particulate Organic Matter in the Arctic Aerosol.
Atm. Env., **15**(8), p.1353-1363.

Danielson, E. (1968)
Stratospheric-Tropospheric Exchange Based Upon Radioactivity, Ozone and Potential Vorticity.
J. Atm. Sci., **25**, p.502-516.

Davidson, C.; Chu, L.; Grimm, T.; Nasta, M.; Qamoos, M. (1981)
Wet and Dry Deposition of Trace Elements onto the Greenland Ice Sheet.
Atm. Env., **15**(8), p.1429-1437.

Davidson, C.; Santhanam, S.; Fortmann, R.; Olson, M. (1985)
Atmospheric Transport and Deposition of Trace Elements onto the Greenland Ice Sheet.
Atm. Env., **19**(12), p.2065-2081.

Dayan, U.; Miller, J.; Keene, W.; Galloway, J. (1985)
An Analysis of Precipitation Chemistry Data from Alaska.
Atm. Env., **19**(4), p.651-657.

Dixon, W. (1983)
BMDP Statistical Software.
Univ. of California Press, Los Angeles CA. 733pp.

Dutton, E.; DeLuisi, J.; Bodhaine, B. (1984)
Features of Aerosol Optical Depth Observed at Barrow, March 10-20, 1983.
Geo. Res. Lett., **11**(5), p.385-388.

Eckart, C.; Young, G. (1936)
The Approximation of One Matrix by Another of Lower Rank.
Psychometrika, **1**, p.211-218.

EPS (1981)
National Air Pollution Surveillance: 1980 Annual Summary.
Air Pollution Control Directorate, Environmental Protection Service, Environment Canada. Surveillance Report EPS 5-AP-81-13 (Oct. 1981).

EPS (1982)
National Air Pollution Surveillance: 1981 Annual Summary.
Air Pollution Control Directorate, Environmental Protection Service, Environment Canada. Surveillance Report EPS 5-AP-82-13 (Nov. 1982).

Essenwanger, O. (1975)
Eigenvector Representation of Wind Profiles.
Preprints, Fourth Conf. on Prob. and Stat. in Atm. Sciences. AMS (Tallahasse), p.206-210.

Essenwanger, O. (1976)
Applied Statistics in Atmospheric Science, Part A.
Developments in Atm. Sci., Vol. 4A, Elsevier, New York NY. 412pp.

Exner, O. (1966)
Additive Properties. I. General Relationships and Problems of Statistical Nature.
Coll. Czech. Chem. Comm., **31**, p.3222-3251.

Freund, J. (1983a)
Aerosol Optical Depth in the Canadian Arctic.
Atm.-Ocean, **21**(2), p.158-167.

Freund, J. (1983b)
Aerosol Single-Scattering Albedo in the Arctic, Determined from Ground-Based Nonspectral Solar Irradiance Measurements.
J. Atm. Sci., **40**(11), p.2724-2731.

Friedlander, S. (1973)
Chemical Element Balances and Identification of Air Pollution Sources.
Env. Sci. Tech., **7**, p.235-240.

Gaarenstroom, P.; Perone, S.; Moyers, J. (1977)
Applications of Pattern Recognition and Factor Analysis for Characterization of Atmospheric Particulate Composition in Southwest Desert Atmosphere.
Env. Sci. Tech., **11**(8), p.795-800.

Gatz, D. (1975)
Relative Contributions of Different Sources of Urban Aerosols: Application of a New Estimation Method to Multiple Sites in Chicago.
Atm. Env., **9**, p.1-18.

Gatz, D. (1978)
Identification of Aerosol Sources in the St. Louis Area Using Factor Analysis.
J. Appl. Met., **17**, p.600-608.

Guttman, L. (1953)
Image Theory for the Structure of Quantitative Variates.
Psychometrika, **18**, p.277-296.

Hage, K. (1972)
Urban Growth Effects on Low Temperature Fog in Edmonton.
Bound. Layer Met., **2**, p.334-347.

Halter, B.; Peterson, J. (1981)
On the Variability of Atmospheric Carbon Dioxide Concentration at Barrow, Alaska During Summer.
Atm. Env., **15**(8), p.1391-1399.

Halter, B.; Harris, J. (1985)
A Study of Winter Variability in Carbon Dioxide and Arctic Haze Aerosols at Barrow, Alaska.
Atm. Env., **19**(12), p.2033-2037.

Hansen, A.; Rosen, H. (1984)
Vertical Distributions of Particulate Carbon, Sulfur, and Bromine in the Arctic Haze and Comparison with Ground-Level Measurements at Barrow, Alaska.
Geo. Res. Lett., **11**(5), p.381-384.

Hansen, A.; Rosen, H. (1985)
Horizontal Inhomogeneities in the Particulate Carbon Component of the Arctic Haze.
Atm. Env., **19**(12), p.2175-2180.

Hare, K.; Orvig, S. (1958)
The Arctic Circulation.
Arctic Meteor. Res. Group, Publ. No. 12, McGill Univ., Montreal. 211pp.

Harman, H. (1967)
Modern Factor Analysis.
Univ. of Chicago Press, Chicago IL. 474pp.

Harris, J. (1984)
Trajectories During AGASP.
Geo. Res. Lett., **11**(5), p.453-456.

Harrison, R.; Sturges, W. (1983)
The Measurement and Interpretation of Br/Pb Ratios in Airborne Particles.
Atm. Env., **17**(2), p.311-328.

Heidam, N. (1981)
On the Origin of the Arctic Aerosol: A Statistical Approach.
Atm. Env., **15**(8), p.1421-1427.

Heidam, N. (1982)
Atmospheric Aerosol Factor Models, Mass and Missing Data.
Atm. Env., **16**(8), p.1923-1931.

Heidam, N. (1984)
The Components of the Arctic Aerosol.
Atm. Env., **18**(2), p.329-343.

Heidam, N. (1985)
Crustal Enrichments in the Arctic Aerosol.
Atm. Env., **19**(12), p.2083-2097.

Heidam, N.; Kronberg, D. (1985)
Discussion: A Comparison of R- and Q-modes in Target Transformation Factor Analysis for Resolving Environmental Data.
Atm. Env., **19**(9), p.1549-1553.

Heintzenberg, J. (1980)
Particle Size Distribution and Optical Properties of Arctic Haze.
Tellus, **32**, p.251-260.

Heintzenberg, J.; Hansson, H.; Lannefors, H. (1981)
The Chemical Composition of Arctic Haze at Ny-Alesund, Spitsbergen.
Tellus, **33**, p.162-171.

Heintzenberg, J. (1982)
Size-Segregated Measurements of Particulate Elemental Carbon and Aerosol Light Absorption at Remote Arctic Locations.
Atm. Env., **16**(10), p.2461-2469.

Henry, R. (1977)
The Application of Factor Analysis to Urban Aerosol Source Identification.
Preprints, Fifth Conf. Prob. and Stat. in Atm. Science. AMS (Las Vegas). p.134-138.

Herron, M. (1982)
Impurity Sources of F^-, Cl^-, NO_3^-, and SO_4^{2-} in Greenland and Antarctic Precipitation.
J. Geo. Res., **87**(C4), p.3052-3060.

Higuchi, K.; Daggupaty, S (1985)
On Variability of Atmospheric CO_2 at Station Alert.
Atm. Env., **19**(12), p.2039-2044.

Hileman, B. (1983)
Arctic Haze.
Env. Sci. Tech., **17**(6), p.232-236.

Hobbs, P.; Bowdle, D.; Radke, L. (1985)
Particles in the Lower Troposphere Over the High Plains of the United States. Part I: Size Distributions, Elemental Compositions and Morphologies.
J. Clim. and Appl. Met., **24**(12), p.1344-1356.

Hoff, R.; Leaitch, R.; Fellin, P.; Barrie, L. (1983)
Mass Size Distributions of Chemical Constituents of the Winter Arctic Aerosol.
J. Geo. Res., **88**, p.10947-10956.

Hoff, R.; Trivett, N. (1984)
Ground-Based Measurements of Arctic Haze Made at Alert, NWT, Canada, During the Arctic Gas and Aerosol Sampling Project (AGASP).
Geo. Res. Lett., **11**(5), p.389-392.

Hogan, A.; Barnard, S.; Samson, J.; Winters, W. (1982)
The Transport of Heat, Water Vapor, and Particulate Material to the South Polar Plateau.
J. Geo. Res., **87**(C6), p.4287-4292.

Hogan, A.; Barnard, S.; Mossl, B.; Loiseaux, M. (1984a)
A Preliminary Climatology of Aerosol Blackness.
J. Aer. Sci., **15**(1), p.1-12.

Hogan, A.; Barnard, S.; Kebschull, K.; Townsend, R.; Samson, J. (1984b)
Aerosol Variation in the Western Hemisphere Arctic.
J. Aer. Sci., **15**(1), p.13-33.

Hogan, A.; Kebschull, K.; Townsend, R.; Murphey, M.; Samson, J.; Barnard, S. (1984c)
Particle Concentrations at the South Pole, On Meteorological and Climatological Time Scales; Is the Difference Important?
Geo. Res. Lett., **11**(9), p.850-853.

Hopke, P. (1981)
The Application of Factor Analysis to Urban Aerosol Source Resolution.
In: Atmospheric Aerosol; Source/Air Quality Relationships (ed. by E. Macias and P. Hopke), ACS Symposium Series No. 167, Amer. Chem. Soc., p.21-49.

Hopke, P. (1982)
Discussions: Trace Element Concentrations in Summer Aerosols, at Rural Sites in New York State and Their Possible Sources; Seasonal Variations in the Composition of Ambient Sulfate-Containing Aerosols in the New York Area.
Atm. Env., **16**(5), p.1279-1280.

Hopke, P.; Gladney, E.; Gordon, G.; Zoller, W. Jones, A. (1976)
The Use of Multivariate Analysis to Identify Sources of Selected Elements in the Boston Urban Aerosol.
Atm. Env., **10**, p.1015-1025.

Hopke, P.; Lamb, R.; Natusch, D. (1980)
Multielemental Characterization of Urban Roadway Dust.
Env. Sci. Tech., **14**(2), p.164-172.

Hopper, F. (1984)
Factor Analysis of Aerosol Composition Data from the Canadian Arctic.
Extended Abstracts, Third Symposium on Arctic Air Chemistry, Downsview ON.

Hopper, F. (1986a)
Urban Visibilities at Low Temperatures.
Accepted for publication in Atmospheric Environment (10 February 1986).

Hopper, F. (1986b)
On the Variability of Water Vapour in the Arctic Atmosphere.
Submitted to Atmosphere-Ocean (March 1986).

Horst, P. (1965)
Factor Analysis of Data Matrices.
Holt, Rinehart and Winston Inc., New York NY. 730pp.

Hoskins, B.; McIntyre, M.; Robertson, A. (1955)
On the Use and Significance of Isentropic Potential Vorticity Maps.
Q. J. Roy. Met. Soc., **111**, p.877-946.

Hov, O.; Penkett, S.; Isaksen, I.; Semb, A. (1984)
Organic Gases in the Norwegian Arctic.
Geo. Res. Lett., **11**(5), p.425-428.

Hurley, J.; Cattell, R. (1962)
The Procrustes Program: Producing Direct Rotation to Test a Hypothesized Factor Structure.
Behavioural Sci., 7, p.258-262.

Hwang, C.; Severin, K.; Hopke, P. (1984)
A Comparision of R- and Q-modes in Target Transformation Factor Analysis for Resolving Environmental Data.
Atm. Env., **18**(2), p.345-352.

Imbrie, J.; Purdy, E. (1962)
Classification of Modern Bahamian Carbonate Sediments.
Classification of Carbonate Rocks: A Symposium (ed. by W. Ham), Mem. 1, Amer. Assoc. Petr. Geol., p.253-272.

Iversen, T. (1984)
On the Atmosphere Transport of Pollution to the Arctic.
Geo. Res. Lett., **11**(5), p.457-460.

Iversen, T.; Joranger, E. (1985)
Arctic Air Pollution and Large Scale Atmospheric Flows.
Atm. Env., **19**(12), p.2099-2108.

Jackson, C. (1960)
The Meteorology of Lake Hazen, NWT. Parts II,III,IV - Synoptic Influences, Local Forecasting, Bibliography.
Arctic Met. Res. Group, Publ. Meteor. No. 16, McGill University. 295pp.

Johnson, R. (1963)
On a Theorem Stated by Eckart and Young.
Psychometrika, **28**, p.259-263.

Joranger, E.; Ottar, B. (1984)
Air Pollution Studies in the Norwegian Arctic.
Geo. Res. Lett., **11**(5), p.365-368.

Joreskog, K.; Klovan, J.; Reyment, R. (1976)
Geological Factor Analysis.
Methods in Geomathematics 1, Elsevier, New York NY. 178pp.

Kaiser, H. (1958)
The Varimax Criterion for Analytic Rotation in Factor Analysis.
Psychometrika, **23**, p.187-200.

Kaiser, H.; Caffrey, J. (1965)
Alpha Factor Analysis.
Psychometrica, **30**, p.1-14.

Khalil, M; Rasmussen, R. (1983)
Gaseous Tracers of Arctic Haze.
Env. Sci. Tech., **17**(3), p.157-164.

Khalil, M; Rasmussen, R (1984)
Statistical Analysis of Trace Gases in Arctic Haze.
Geo. Res. Lett., **11**(5), p.437-440.

Kienle, J.; Roederer, J.; Shaw, G. (1983)
Volcanic Event in Soviet Arctic?
EOS, Trans. Amer. Geo. Union, **64**(20).

Klemm, R.; Gray, J. (1982)
A Study of the Chemical Composition of Particulate Matter and Aerosols over Edmonton.
RMD 82/9, Research Management Division, Alberta Environment, Edmonton AB.

Koerner, R.; Fisher, D. (1982)
Acid Snow in the Canadian High Arctic.
Nature, **295**, p.137-140.

Kowalczyk, G.; Choquette, C.; Gordon, G. (1978)
Chemical Element Balances and Identification of Air Pollution Sources in Washington DC.
Atm. Env., **12**, p.1143-1153.

Lawley, D. (1943)
The Application of the Maximum Likelihood Method to Factor Analysis.
British J. of Psych., **33**, p.172-175.

Lazrus A.; Ferek, R. (1984)
Acidic Sulfate Paricles in the Winter Arctic Atmosphere.
Geo. Res. Lett., **11**(5), p.417-419.

Leaitch, R.; Hoff, R.; Melnichuk, S.; Hogan, A. (1984)
Some Physical and Chemical Properties of the Arctic Winter Aerosol in Northeastern Canada.
J. Cl. and Appl. Met., **23**(6), p.916-928.

LeDrew, E. (1980)
Eigenvector Analysis of the Vertical Velocity Field Over the Eastern Canadian Arctic.
Mon. Wea. Rev., **108**(12), p.1992-2005.

Leighton, H. (1983)
Influence of Arctic Haze on the Solar Radiation Budget.
Atm. Env., **17**(10), p.2065-2068.

Liu, C.; Roscoe, B.; Severin, K.; Hopke, P. (1982)
The Application of Factor Analysis to Source Apportionment of Aerosol Mass.
Am. Ind. Hyg. Assoc. J., **43**, p.314-318.

Lorenz, E. (1956)
Empirical Orthogonal Functions and Statistical Weather Prediction.
Sci. Rep. No. 1, Met. Dept., MIT. 49pp.

Lowenthal, D.; Rahn, K. (1985)
Regional Sources of Pollution Aerosol at Barrow, Alaska During Winter 1979-80 As Deduced from Elemental Tracers.
Atm. Env., **19**(12), p.2011-2024.

Macias, E.; Hopke, P. (eds.) (1981)
Atmospheric Aerosol: Source/Air Quality Relationships.
ACS Symposium Series No. 167, Amer. Chem. Soc. 359pp.

Malinowski, E.; Howery, D. (1980)
Factor Analysis in Chemistry.
J. Wiley and Sons, New York NY.

Mason, B.; Moore, C. (1982)
Principles of Geochemistry, Fourth Edition.
J. Wiley and Sons, New York NY. 344pp.

Matalas, N.; Reiher, B. (1967)
Some Comments on the Use of Factor Analysis.
Water Resources Research, 3(1), p.213-223.

Maxwell, J. (1980)
The Climate of the Canadian Arctic Islands and Adjacent Waters. Volumes 1 and 2.
Climatological Studies No. 30. Atmospheric Environment Service, Environment Canada.

McGuffie, K.; Cogley, J.; Henderson-Sellers, A. (1985)
Climatological Analysis of Arctic Aerosol Quantity and Optical Properties at Resolute, NWT.
Atm. Env., **19**(5), p.707-714.

McNeely, R.; Gummer, W. (1984)
A Reconnaissance Survey of the Environmental Chemistry in East-Central Ellesmere Island, NWT.
Arctic, 37(3), p.210-223.

Megaw, W. (1982)
Summer Tropospheric Aerosols Over Greenland.
In: Atmospheric Aerosols; Their Formation, Optical Properties and Effects.
Spectrum Press, Hampton VA, p.39-50.

Mendonca, B.; DeLuisi, J.; Schroeder, J. (1982)
Arctic Haze and Solar Irradiance Measurements at Barrow, Alaska.
Preprints, Second Symp. Composition of the Nonurban Troposphere, AMS (Williamsburg), p.176-178.

Milford, J.; Davidson, C. (1985)
The Sizes of Particulate Trace Elements in the Atmosphere - A Review.
J. Air Poll. Contr. Assoc., 35(12), p.1249-1260.

Miller, J. (1981)
A Five-Year Climatology of Five-Day Back Trajectories from Barrow, Alaska.
Atm. Env., **15**(8), p.1401-1405.

Mulaik, S. (1972)
The Foundations of Factor Analysis.
McGraw-Hill, New York NY. 453pp.

Oehme, M.; Ottar, B. (1984)
The Long Range Transport of Polychlorinated Hydrocarbons to the Arctic.
Geo. Res. Lett., **11**(11), p.1133-1136.

Oeschger, H.; Alder, B.; Loosli, H.; Langway, C.; Renaud, A. (1966)
Radiocarbon Dating of Ice.
Earth and Plan. Sci. Lett., 1, p.49-54.

Ottar, B. (1981)
The Transfer of Airborne Pollutants to the Arctic Region.
Atm. Env., **15**(8), p.1439-1445.

Ottar, B.; Pacyna, J. (1984)
Sources of Ni, Pb, and Zn During the Arctic Episode in March 1983.
Geo. Res. Lett., **11**(5), p.441-444.

Pacyna, J.; Vitols, V.; Hanssen, J. (1984)
Size-Differentiated Composition of the Arctic Aerosol at Ny-Alesund, Spitsbergen.
Atm. Env., **18**(11), p.2447-2459.

Pacyna, J.; Ottar, B. (1985)
Transport and Chemical Composition of the Summer Aerosol in the Norwegian Arctic.
Atm. Env., **19**(12), p.2109-2120.

Pacyna, J.; Ottar, B.; Tomza, U.; Maenhaut, W. (1985)
Long-Range Transport of Trace Elements to Ny-Alesund, Spitsbergen.
Atm. Env., **19**(6), p.857-865.

Parekh, P.; Husain, L. (1981)
Trace Element Concentrations in Summer Aerosols at Rural Sites in New York State and Their Possible Sources.
Atm. Env., **15**, p.1717-1725.

Patterson, D.; Husar, R. (1981)
A Direct Simulation of Hemispherical Transport of Pollutants.
Atm. Env., **15**(8), p.1479-1482.

Patterson, E.; Marshall, B.; Rahn, K. (1982)
Radiative Properties of the Arctic Aerosol.
Atm. Env., **16**(12), p.2967-2977.

Pawluk, S.; Bayrock, L. (1969)
Some Characteristics and Physical Properties of Alberta Tills.
Research Council of Alberta, Bull. No. 26. 72pp.

Peterson, J.; Komhyr, W.; Harris, T.; Waterman, L. (1982)
Atmospheric Carbon Dioxide Measurements at Barrow, Alaska, 1973-1979.
Tellus, **34**, p.166-175.

Pierce, R.; Whelpdale, D.; Sheffer, M. (1982)
Pollutants in Air.
Proceedings of a Symposium of Monitoring and Assessment of Airborne Pollutants with Special Emphasis on Long-Range Transport and Deposition of Acidic Materials. Nat. Res. Council of Canada. 502pp.

Pitchford, M.; Pitchford, A. (1985)
Analysis of Regional Visibility in the Southwest Using Principal Component and Back Trajectory Techniques.
Atm. Env., **19**(8), p.1301-1316.

Polar Group (1980)
Polar Atmosphere-Ice-Ocean Processes: A Review of Polar Problems in Climate Research.
Rev. Geophys. and Space Phys., **18**(2), p.525-543.

Porch, W.; MacCracken, M. (1982)
Parametric Study of the Effects of Arctic Soot on Solar Radiation.
Atm. Env., **16**(6), p.1365-1371.

Preisendorfer, R.; Barnett, T. (1977)
Significance Tests for Empirical Orthogonal Functions.
Preprints, Fifth Conf. on Prob. and Stat. in Atm. Sci. AMS (Las Vegas), p.169-172.

Prospero, J.; Charlson, R.; Mohnen, V.; Jaenicke, R.; Delany, A.; Moyers, J.; Zoller, W.; Rahn, K. (1983)
The Atmospheric Aerosol System: An Overview.
Rev. Geophys. and Space Phys., **21**(7), p.1607-1629.

Raatz, W. (1981)
Trends in Cloudiness in the Arctic Since 1920.
Atm. Env., **15**(8), p.1503-1506.

Raatz, W. (1982)
On the Meteorological Characteristics of Polluted Air Masses at Barrow, Alaska.
Pageophysics, **120**, p.662-672.

Raatz, W. (1983)
Spectrum and Cross-Spectrum Analysis of Daily Meteorological and Chemical Data at BRW.
In: Geophysical Monitoring for Climatic Change, No. 11, p.140-142.

Raatz, W. (1984)
Tropospheric Circulation Patterns During the Arctic Gas and Aerosol Sampling Program (AGASP), March/April 1983.
Geo. Res. Lett., **11**(5), p.449-452.

Raatz, W. (1985)
Meteorological Conditions Over Eurasia and The Arctic Contributing to the March 1983 Arctic Haze Episode.
Atm. Env., **19**(12), p.2121-2126.

Raatz, W.; Shaw, G. (1984)
Long-Range Tropospheric Transport of Pollution Aerosols into the Alaskan Arctic.
J. Cl. and App. Met., **23**(7), p.1052-1064.

Raatz, W.; Schnell, R. (1984)
Aerosol Distributions and an Arctic Aerosol Front During AGASP: Norwegian Arctic.
Geo. Res. Lett., **11**(5), p.373-376.

Raatz, W.; Schnell, R.; Bodhaine, B.; Oltmans, S.; Gammon, R. (1985a)
Air Mass Characteristics in the Vicinity of Barrow, Alaska, 9-19 March 1983.
Atm. Env., **19**(12), p.2127-2134.

Raatz, W.; Schnell, R.; Bodhaine, B. (1985b)
The Distribution and Transport of Pollution Aerosols Over the Norwegian Arctic on 31 March and 4 April 1983.
Atm. Env., **19**(12), p.2135-2142.

Raatz, W.; Schnell, R.; Bodhaine, B.; Oltmans, S. (1985c)
Observations of Arctic Haze During Polar Flights from Alaska to Norway.
Atm. Env., **19**(12), p.2143-2151.

Raatz, W.; Schnell, R.; Shapiro, M.; Oltmans, S.; Bodhaine, B. (1985d)
Intrusions of Stratospheric Air into Alaska's Troposphere, March 1983.
Atm. Env., **19**(12), p.2153-2158.

Radke, L.; Lyons, J.; Hegg, D.; Hobbs, P. (1984a)
Airborne Observations of Arctic Aerosols. I: Characteristics of Arctic Haze.
Geo. Res. Lett., **11**(5), p.393-396.

Radke, L.; Hobbs, P.; Bailey, I. (1984b)
Airborne Observations of Arctic Aerosols. III: Origins and Effects of Airmasses.
Geo. Res. Lett., **11**(5), p.401-404.

Rahn, K. (1978)
Arctic Air-Sampling Network.
Arctic Bulletin, **2**, p.343-346.

Rahn, K. (1981a)
The Arctic Air-Sampling Network in 1980.
Atm. Env., **15**(8), p.1349-1352.

Rahn, K. (1981b)
Relative Importances of North America and Eurasia as Sources of Arctic Aerosol.
Atm. Env., **15**(8), p.1447-1455.

Rahn, K. (1981c)
The Mn/V Ratio as a Tracer of Large-Scale Sources of Pollution Aerosol for the Arctic.
Atm. Env., **15**(8), p.1457-1464.

Rahn, K. (1981d)
Atmospheric, Riverine and Oceanic Sources of Seven Trace Constituents to the Arctic Ocean.
Atm. Env., **15**(8), p.1507-1516.

Rahn, K. (1984)
Who's Polluting the Arctic?
Natural History, **93**.

Rahn, K. (1985)
Progress in Arctic Air Chemistry, 1980-1984.
Atm. Env., **19**(12), p.1987-1994.

Rahn, K.; McCaffrey, R. (1979)
Compositional Differences Between Arctic Aerosol and Snow.
Nature, **280**, p.479-480.

Rahn, K.; McCaffrey, R. (1980)
On the Origin and Transport of the Winter Arctic Aerosol.
Ann. New York Acad. Sci., 338, p.486-503.

Rahn, K.; Joranger, E.; Semb, A.; Conway, T. (1980)
High Winter Concentrations of SO_2 in the Norwegian Arctic and Transport from Eurasia.
Nature, 287, p.824-826.

Rahn, K.; Heidam, N. (1981)
Progress in Arctic Air Chemistry, 1977-1980: A Comparison of the First and Second Symposia.
Atm. Env., 15(8), p.1345-1348.

Rahn, K.; Lewis, N.; Lowenthal, D.; Smith, D. (1983)
Norilsk Only a Minor Contributor to Arctic Haze.
Nature, 306, p.459-461.

Rahn, K.; Lowenthal, D. (1984)
Elemental Tracers of Distant Regional Pollution Aerosols.
Science, 223, p.132-139.

Rao, C. (1955)
Estimation and Tests of Significance in Factor Analysis.
Psychometrica, 20, p.93-111.

Rasmussen, R.; Khalil, M. (1984)
Gaseous Bromine in the Arctic and Arctic Haze.
Geo. Res. Lett., 11(5), p.433-436.

Redman, T.; Zinsmeister, A. (1982)
Discussions: A Quantitative Determination of Sources in the Boston Urban Aerosol.
Atm. Env., 16(6), p.1567.

Reiter, E. (1969)
Atmospheric Transport Processes. Part 3: Hydrodynamic Tracers.
AEC Critical Review Series, TID-25314.

Reiter, E. (1981)
Planetary-Wave Behaviour and Arctic Air Pollution.
Atm. Env., 15(8), p.1465-1471.

Robertson, G. (1955)
Low-Temperature Fog at the Edmonton Airport as Influenced by Moisture from the Combustion of Natural Gas.
Quart. J. Roy. Met. Soc., 81, p.190-197.

Roscoe, B.; Hopke, P. (1981a)
Comparison of Weighted and Unweighted Target Transformation Rotations in Factor Analysis.
Comput. Chem., 5, p.1-7.

Roscoe, B.; Hopke, P. (1981b)
Error Estimation for Factor Loadings and Scores Obtained with Target Transformation Factor Analysis.
Analyt. Chim. Acta., 132, p.89-97.

Rosen, H.; Novakov, T.; Bodhaine, B. (1981)
Soot in the Arctic.
Atm. Env., **15**(8), p.1371-1374.

Rosen, H.; Hansen, A. (1984)
Role of Combustion-Generated Particles in the Absorption of Solar Radiation in the Arctic Haze.
Geo. Res. Lett., **11**(5), p.461-464.

Rosen, H.; Hansen, A. (1985)
Estimates of Springtime Soot and Sulfur Fluxes Entering the Arctic Troposphere: Implications to Source Regions.
Atm. Env., **19**(12), p.2203-2207.

Rozett, R.; Petersen, E. (1975)
Methods of Factor Analysis of Mass Spectra.
Analyt. Chem., **47**, p.1301-1308.

Rummel, R. (1970)
Applied Factor Analysis.
Northwestern Univ. Press, Evanston IL. 617pp.

Schickedanz, P. (1977)
Applications of Factor Analysis in Weather Modification Research.
Preprints, Fifth Conf. on Prob. and Stat. in Atm. Sci., AMS (Las Vegas), p.190-195.

Schnell, R. (1984a)
Arctic Haze: Editorial.
Geo. Res. Lett., **11**(5), p.359.

Schnell, R. (1984b)
Arctic Haze and the Arctic Gas and Aerosol Sampling Program (AGASP).
Geo. Res. Lett., **11**(5), p.361-364.

Schnell, R.; Raatz, W. (1984)
Vertical and Horizontal Characteristics of Arctic Haze During AGASP: Alaskan Arctic.
Geo. Res. Lett., **11**(5), p.369-372.

Semb, A.; Braekken, R.; Joranger, E. (1984)
Major Ions in Spitsbergen Snow Samples.
Geo. Res. Lett., **11**(5), p.445-448.

Shapiro, M.; Schnell, R.; Parungo, F.; Oltmans, S.; Bodhaine, B. (1984)
El Chichon Volcanic Debris in an Arctic Tropopause Fold.
Geo. Res. Lett., **11**(5), p.421-424.

Shaw, G. (1981)
Eddy Diffusion Transport of Arctic Pollution From the Mid-Latitudes: A Preliminary Model.
Atm. Env., **15**(8), p.1483-1490.

Shaw, G. (1982a)
Evidence for a Central European Source Area of Arctic Haze in Alaska.
Nature, **299**, p.815-818.

Shaw, G. (1982b)
Atmospheric Turbidity in the Polar Regions.
J. App. Met., **21**(8), p.1080-1088.

Shaw, G. (1983a)
X-Ray Spectrometry of Polar Aerosols.
Atm. Env., **17**(2), p.329-339.

Shaw, G. (1983b)
On the Aerosol Particle Size Distribution Spectrum in Alaskan Air Mass Systems: Arctic Haze and Non-Haze Episodes.
J. Atm. Sci., **40**(5), p.1313-1320.

Shaw, G. (1984)
Microparticle Size Spectrum of Arctic Haze.
Geo. Res. Lett., **11**(5), p.409-412.

Shaw, G. (1985)
Aerosol Measurements in Central Alaska, 1982-1984.
Atm. Env., **19**(12), p.2025-2031.

Shaw, G.; Stamnes, K. (1980)
Arctic Haze: Perturbation of the Polar Radiation Budget.
Ann. New York Acad. Sci., **338**, p.533-539.

Shaw, R. (1986)
A Proposed Strategy for Reducing Sulphate Deposition in North America - II. Methodology for Minimizing Costs.
Atm. Env., **20**(1), p.201-206.

Sheridan, P.; Musselman, I. (1985)
Characterization of Aircraft-Collected Particles Present in the Arctic Aerosol; Alaskan Arctic, Spring 1983.
Atm. Env., **19**(12), p.2159-2166.

Shine, K.; Robinson, D.; Henderson-Sellers, A.; Kukla, G. (1984)
Evidence of Arctic-Wide Atmospheric Aerosols From DMSP Visible Imagery.
J. Cl. and App. Met., **23**(10), p.1459-1464.

Staley, D. (1960)
Evaluation of Potential-Vorticity Changes Near the Tropopause and the Related Vertical Motions, Vertical Advection of Vorticity, and Transfer of Radioactive Debris from Stratosphere to Troposphere.
J. Met., **17**, p.591-620.

Stone, R.; Warburton, J. (1984)
Final Report: 1983 Alberta Cloud Particulate Chemistry Program.
Atm. Sci. Center, Desert Research Inst., Univ. of Nevada.

Tanner, R.; Leaderer, B. (1982)
Seasonal Variation in the Composition of Ambient Sulfate-Containing Aerosols in the New York Area.
Atm. Env., **16**, p.569-580.

Valero, F.; Ackerman, T.; Gore, W. (1983)
Radiative Effects of the Arctic Haze.
Geo. Res. Lett., **10**(12), p.1184-1187.

Valero, F.; Ackerman, T.; Gore, W. (1984)
The Absorption of Solar Radiation by the Arctic Atmosphere During the Haze Season and Its Effects on the Radiation Balance.
Geo. Res. Lett., **11**(5), p.465-468.

Van der Hoven, I. (1957)
Power Spectrum of Horizontal Wind Speed in the Frequency Range from 0.0007 to 900 Cycles per Hour.
J. Met., **14**, p.160-164.

Vowinckel, E.; Orvig, S. (1970)
The Climate of the North Polar Basin.
In: Climates of the Polar Regions (ed. by S. Orvig), World Survey of Climatology, Vol. 14. Elsevier, New York NY. 370 pp.

Wendling, P.; Wendling, R.; Renger, W.; Covert, D.; Heintzenberg, J.; Moerl, P. (1985)
Calculated Radiative Effects of Arctic Haze During a Pollution Episode in Spring 1983 Based on Ground-Based and Airborne Measurements.
Atm. Env., **19**(12), p.2181-2193.

Weschler, C. (1981)
Identification of Selected Organics in the Arctic Aerosol.
Atm. Env., **15**(8), p.1365-1369.

Wilkniss, P.; Larson, R. (1984)
Atmospheric Radon Measurements in the Arctic; Fronts, Seasonal Observations, and Transport of Continental Air to Polar Regions.
J. Atm. Sci., **41**(15), p.2347-2358.

Winchester, J.; Li, S.; Fan, S.; Schnell, R.; Bodhaine, B.; Nagele, S. (1984)
Coarse Particle Soil Dust in Arctic Aerosols, Spring 1983.
Geo. Res. Lett., **11**(10), p.995-998.

Winchester, J.; Schnell, R.; Fan, S.M Li, S.; Bodhaine, B.; Nagele, S.; Hansen, A.; Rosen, H. (1985)
Particulate Sulfur and Chlorine in Arctic Aerosols, Spring 1983.
Atm. Env., **19**(12), p.2167-2173.

Young, J.; Shaw, R. (1986)
A Proposed Strategy for Reducing Sulphate Deposition in North America - I. Methodology for Minimizing Sulphur Removal.
Atm. Env., **20**(1), p.189-199.

9. Appendix A

The following is a listing of a *Fortranvs program to calculate the factor loading and factor score matrices by a direct algorithm, without first calculating a product-moment matrix. The calling routine is:

```
      REAL*4 D(500,50),S(500,50),F(50,50),
     1       EIGVL(50),CONVG,CUVAR,FVLEV
      COMMON /BLK1/D
      COMMON /BLK2/S
      COMMON /BLK3/F
      INTEGER*4 I,IRC,J,K,L,M,MAXIT,N
      DO 10 I=1,500
      DO 10 J=1,50
      D(I,J)=0.0
   10 S(I,J)=0.0
      DO 20 I=1,50
      DO 20 J=1,50
   20 F(I,J)=0.0
      READ(5,*) M,N,MAXIT,CONVG,CUVAR,LPFAC,FVLEV
      WRITE(6,800) M,N,MAXIT,CONVG,CUVAR,LPFAC,FVLEV
  800 FORMAT('*** Program DFA ***',//,
     1       'Data matrix read with',I4,' rows and',I3,' columns',/,
     2       'Subroutine control parameters (IP):',/,
     3       5X,'Maxm iterations =',I10,/,
     4       5X,'Convergence level =',F10.4,/,
     5       5X,'Requested total variance =',F10.4,/,
     6       5X,'Requested number of factors =',I10,/,
     7       5X,'Requested minimum significant variance =',F10.3,//)
      READ(7,*) ((D(I,J),J=1,N),I=1,M)
      DO 100 I=1,M
  100 WRITE(8,810) (D(I,J),J=1,N)
  810 FORMAT(50F10.3)
      WRITE(8,820)
  820 FORMAT(//)
      IRC=-99
      CALL DFA(M,N,MAXIT,CONVG,CUVAR,LPFAC,FVLEV,IRC,LP,EIGVL)
      DO 200 I=1,M
  200 WRITE(8,810) (D(I,J),J=1,N)
      WRITE(8,820)
      DO 300 I=1,M
  300 WRITE(8,810) (S(I,J),J=1,LP)
      WRITE(8,820)
      DO 400 I=1,N
  400 WRITE(8,810) (F(I,J),J=1,LP)
  999 STOP
      END
```

The subroutine 'DFA' contains the actual implementation of the algorithm:

```
C Subroutine'DFA'
C
C Routine to factor a data matrix using a direct method (iterative).
C No product-moment calculations required. The method finds the
C factor loading matrix and factor score matrix simultaneously.
C Refer to Horst (ch. 12), Basic Structure Single Factoring Method.
C
C   N          = number of rows in the data matrix (IP)
C   M          = number of columns in the data matrix (IP)
C   MAXIT      = maximum allowable number of iterations for each factor (IP)
C   CONVG      = iterative convergence criterion for successive
C                factor estimates
C   CUVAR      = requested total variance to be explained (IP)
C                by factors; factoring halted after sum of factor
C                variances exceeds 'CUVAR'
C   LPFAC      = requested maximum number of factors to be derived (IP)
C   FVLEV      = minimum variance of a factor which is (IP)
C                to be significant; factors with variance less
C                than 'FVLEV' are considered to be insignificant
C   IRC        = result code (OP)
C                 IRC=-1: no convergence for current factor
C                   maximum allowable iterations
C                 IRC= 0: maximum number of factors derived
C                   without exceeding any other criterion
C                 IRC= 1: next factor has variance less than
C                   individual significant amount
C                 IRC= 2: sum of variance of derived factors
C                   exceeds cumulative variance level
C   LP         = number of valid factors derived (OP)
C   EIGVL      = vector containing variances of factors (OP)
C                 (variances = eigenvalues)
C
      SUBROUTINE DFA(M,N,MAXIT,CONVG,CUVAR,
     1           LPFAC,FVLEV,IRC,LP,EIGVL)
      REAL*4 D(500,50),S(500,50),F(50,50),
     1           DD(500,50),FLV(50),FSV(50),EIGVL(50),
     1           ALPH,ALPH0,ALPH1,CONVG,CUVAR,FTVAR,FVLEV
      INTEGER*4 I,IER,IRC,J,K,L,LP,LPFAC,MAXIT,M,N
      COMMON /BLK1/D
      COMMON /BLK2/S
      COMMON /BLK3/F
      DO 700 I=1,M
      DO 700 J=1,N
  700 DD(I,J)=D(I,J)
      DO 740 LP=1,LPFAC
      EIGVL(LP)=0.0
      ALPH0=0.0
      ALPH=0.0
      DO 701 J=1,N
  701 FLV(J)=1.0
      DO 710 K=1,MAXIT
      DO 702 I=1,M
      FSV(I)=0.0
```

```
      DO 702 J=1,N
  702 FSV(I)=FSV(I)+DD(I,J)*FLV(J)
      DO 704 I=1,M
  704 ALPH=ALPH+FSV(I)*FSV(I)
      ALPH=SQRT(ALPH/M)
      DO 706 I=1,M
  706 FSV(I)=FSV(I)/ALPH
      ALPH0=EIGVL(LP)
      EIGVL(LP)=ALPH
      DO 708 J=1,N
      FLV(J)=0.0
      DO 708 I=1,M
  708 FLV(J)=FLV(J)+FSV(I)*DD(I,J)
      DO 709 J=1,N
  709 FLV(J)=FLV(J)/M
      IF(ABS(ALPH-ALPH0).LE.CONVG) GO TO 720
  710 CONTINUE
      IRC=-1
      WRITE(6,781) LP,MAXIT
  781 FORMAT('Factor',I3,' failed to converge after',/,I6,' iterations')
      GOTO 770
  720 IF(EIGVL(LP).LT.FVLEV) THEN
        IRC=1
        WRITE(6,782) LP,EIGVL(LP),FVLEV
  782   FORMAT('Next factor (',I2,') has variance of',F10.3,/,
     1          5X,' which is less the significance level of',F10.3)
        GOTO 770
      ENDIF
      DO 722 I=1,M
  722 S(I,LP)=FSV(I)
      DO 724 J=1,N
  724 F(J,LP)=FLV(J)
      IF(LP.EQ.1) THEN
        FTVAR=EIGVL(1)
      ELSE
        FTVAR=0.0
        DO 726 L=1,LP
  726   FTVAR=FTVAR+EIGVL(L)
      ENDIF
      IF(FTVAR.GT.CUVAR) THEN
        IRC=2
        WRITE(6,783) FTVAR,CUVAR
  783   FORMAT('Total variance of factors is',F10.3,/,
     1          5X,'which exceeds the requested variance of',G15.6)
        GOTO 770
      ENDIF
      DO 730 I=1,M
      DO 730 J=1,N
  730 DD(I,J)=DD(I,J)-FSV(I)*FLV(J)
  740 CONTINUE
      IRC=0
      WRITE(6,784) LPFAC
  784 FORMAT('Maximum number of requested factors (',I2,
     1 ')found without meeting any other criteria')
  770 IF(IRC.NE.2) LP=LP-1
      WRITE(6,785) LP,FTVAR
```

```
785 FORMAT(//,'Number of derived factors = ',I10,/,
   1        'Cumulative variance = ',F10.3,//)
    WRITE(6,786)
786 FORMAT(' Factor Variance %Total Cu.Var %Total',/)
    ALPH0=0.0
    DO 788 L=1,LP
    ALPH=100.*EIGVL(L)/FTVAR
    ALPH0=ALPH0+EIGVL(L)
    ALPH1=100.*ALPH0/FTVAR
    WRITE(6,787) L,EIGVL(L),ALPH,ALPH0,ALPH1
787 FORMAT(I6,F14.3,F10.3,F10.2,F10.2)
788 CONTINUE
799 RETURN
    END
```

10. Appendix B

This proof of the least square nature of the column rotation was adapted from that shown in the Appendix of Alpert and Hopke (1980). Let e_n be the difference between a target vector y_n and a rotation of the initial factor loading matrix F_{n^*p}. If t_p is the corresponding rotation vector for this transformation, then:

$$e_n = F_{n^*p}t_p - y_n$$

For a least squares fit, it is desirable to minimize e_n^2:

$$e_n^2 = (F_{n^*p}t_p - y_n)^\dagger(F_{n^*p}t_p - y_n)$$

$$e_n^2 = (t_p^\dagger F_{p^*n}^\dagger - y_n^\dagger)(F_{n^*p}t_p - y_n)$$

$$e_n^2 = t_p^\dagger F_{p^*n}^\dagger F_{n^*p}t_p - t_p^\dagger F_{p^*n}^\dagger y_n - y_n^\dagger F_{n^*p}t_p + y_n^\dagger y_n$$

Because the third term is a scalar quantity, it is equal to its transpose. Thus:

$$e_n^2 = t_p^\dagger F_{p^*n}^\dagger F_{n^*p}t_p - 2t_p^\dagger F_{p^*n}^\dagger y_n + y_n^\dagger y_n$$

Differentiating with respect to t_p and setting equal to zero gives:

$$(\partial e_n^2 / \partial t_p) = 2F_{p^*n}^\dagger F_{n^*p}t_p - 2F_{p^*n}^\dagger y_n = 0$$

Solving for t_p:

$$t_p = (F_{p^*n}^\dagger F_{n^*p})^{-1}F_{p^*n}^\dagger y_n$$

From Eqn. 2.11, $F_{p^*n}^\dagger F_{n^*p} = L_{p^*p}$ and $L_{p^*p}^{-1}$ is a diagonal matrix with elements equal to the reciprocals of the significant eigenvalues of the unrotated factor loading matrix. Thus:

$$t_p = L_{p^*p}^{-1}F_{p^*n}^\dagger y_n$$